9-2012

Mechanics and Energetics of Footfall Patterns in Running

Allison H. Gruber
University of Massachusetts Amherst, ahg0215@gmail.com

MECHANICS AND ENERGETICS OF FOOTFALL PATTERNS IN RUNNING

A Dissertation Presented

by

ALLISON H. GRUBER

Submitted to the Graduate School of the
University of Massachusetts Amherst in Partial fulfillment
of the requirements for the degree of

DOCTOR OF PHILOSOPHY

September 2012

Department of Kinesiology

MECHANICS AND ENERGETICS OF FOOTFALL PATTERNS IN RUNNING

A Dissertation Presented

by

ALLISON H. GRUBER

Approved as to style and content by:

_____
Joseph Hamill, Chair

_____
Brian Umberger, Member

_____
Richard E.A. van Emmerik, Member

_____
Ian Grosse, Member

_____
Patty S. Freedson, Department Head
Department of Kinesiology

DEDICATION

To Mom and Kevin

ACKNOWLEDGEMENTS

Thank you to my committee for providing your expertise, your support, and guidance through this process. Many people have helped and supported me through this journey. I would like to specifically thank:

…Joe Hamill for his endless patience, giving me this invaluable experience and opportunity, and for the many doors he has opened for me. …Carl Jewell, Sam del Pilar II for their hard work and assistance. I couldn't have done it without their help. …Brian Umberger for taking me under his wing and going above and beyond mentoring and tutoring me while learning the modeling process and much more. …Barry Braun, Rich Viskochil for your endless assistance and brain storming. Richard van Emmerik for exposing me to a "dynamical" way of thinking. …Paul Devita and Tibor Hortobagyi for teaching me much more than I realized after leaving East Carolina. …Graham Caldwell for being my first academic advisor and making sure I stayed on the right path. …Kirsten Granados for help with pilot data collection. …the participants: I know the protocol wasn't fun or easy but I appreciate your help (especially those who I made be a subject twice). …Brian Moscicki, Gixxer, Stryder, Kitty & Pete for sticking with me under less than ideal circumstances and for your unconditional love and support. …and all the people who have helped get me through this experience: Joe Seay, Patrick Rider, Ross Miller, Lex Gidley, Tim Derrick, Steve Malin, Elizabeth Russell, Mike Busa, Jen Baird, and others in the KIN family who have given me their support, and the Moscicki Family. …and a special thanks to Florrie Blackbird. I wouldn't be here today if you didn't give me the opportunity to work for you. Thank you for everything you've done for me.

ABSTRACT

.MECHANICS AND ENERGETICS OF FOOTFALL PATTERNS IN RUNNING

SEPTEMBER 2012

ALLISON H. GRUBER

B.S., EXERCISE SCIENCE, UNIVERSITY OF MASSACHUSETTS AMHERST

M.A., EXERCISE & SPORT SCIENCE, EAST CAROLINA UNIVERSITY

P.h.D., KINESIOLOGY, UNIVERSITY OF MASSACHUSETTS AMHERST

Directed by: Professor Joseph Hamill

The forefoot (FF) running pattern has been recently advocated to improve running economy and prevent overuse injuries compared to the rearfoot (RF) pattern. However, these claims have not been supported by empirical evidence. The purpose of this dissertation was to investigate the potential advantages of RF and FF patterns to improve running economy and reduce injury risk in 20 natural RF and 20 natural FF runners.

The first study found that the RF group was more economical when performing the RF pattern at a slow, medium, and fast speed vs. FF running. Only running at the fast speed resulted in a difference in economy between footfall patterns in the FF group in which RF running was more economical. Therefore, there is no advantage of FF running for improving running economy.

The results of the second study indicated that there was a weak to moderate relationship between Achilles tendon (AT) moment arm length and running with either RF or FF patterns. AT force was greater during FF running, which may increase the risk of developing tendon injury.

The third study used a modeling approach to find that FF running resulted in greater elastic energy recoil in the gastrocnemius (GA) and the soleus (SO). However, greater mechanical work overall with FF running resulted in no difference in metabolic cost of the GA between footfall patterns but greater metabolic cost of the SO compared to RF running.

The fourth study found that shock attenuation was greater during RF running compared to FF running. Greater shock attenuation during RF running was a result of an increased load imposed on the system. Decomposing the vertical ground reaction force in the frequency domain revealed that RF running may have a greater reliance on passive shock attenuation mechanism whereas the FF pattern may have a greater reliance on active shock attenuation mechanisms.

These results suggest that previous speculation that the FF running pattern is more economical was not substantiated. It is likely that each footfall pattern exposes a runner to different types of injuries, rather than one footfall pattern being more injurious than another.

TABLE OF CONTENTS

LIST OF TABLES

Table **Page**

LIST OF FIGURES

Figure **Page**

LIST OF EQUATIONS

Equation **Page**

CHAPTER 1

INTRODUCTION

General Introduction

Runners employ one of three distinct footfall patterns: forefoot (FF), midfoot (MF), or rearfoot (RF). The patterns are named by the location of the center of pressure at the instant of ground contact. The whole foot ultimately contacts the ground in both the RF and MF patterns whereas the heel does not make contact with the FF pattern. The MF pattern may be an intermediate between the RF and FF patterns in that initial contact is made on the anterior portion of the foot but the rest of the foot makes contact nearly at the same time. Recreational and competitive runners predominately employ the RF pattern whereas only about 25% use the MF or FF pattern (Hasegawa et al., 2007).

Since the fastest runners in short, middle, and long distance events are FF or MF runners (Hasegawa et al., 2007; Kerr et al., 1983; Payne, 1983), it is easy to suggest that these footfall patterns may enhance performance by improving running economy or running speed (Bonacci et al., 2010; Hasegawa et al., 2007). Additionally, the FF pattern has been advocated to reduce the risk of running injuries because of the absence of the initial impact peak of the vertical ground reaction force (GRF) component (Cavanagh and Lafortune, 1980; Daoud et al., 2012; Davis et al., 2010; Lieberman et al., 2010; Oakley and Pratt, 1988). However, these claims have not been substantiated in the literature and the mechanisms of these benefits are currently speculative.

Relationship Between Running Mechanics and Economy

The relationship between running mechanics and performance is typically assessed by measuring running economy, or sub-maximal rate of oxygen consumption ($\dot{V}O_2$) (Williams and Cavanagh, 1987). An improvement in running economy, and thereby performance, will be accomplished if some physiological or biomechanical change results in a reduction of $\dot{V}O_2$ over a range of running speeds (Williams, 1990).

Several biomechanical features of running have been identified in more economical runners including longer ground contact time, lower vertical GRF peaks, decreased vertical oscillation, greater trunk angle, greater maximum knee flexion in the stance phase and a more extended leg at touchdown (Williams and Cavanagh, 1987). Interestingly, several of these features are characteristic of those who run with the RF pattern. However, only one previous study found RF running to require a lower rate of oxygen consumption, but this relationship was not found at all speeds examined or for all metabolic variables (Slavin, 1992). Other studies have not found a difference in oxygen consumption between footfall patterns but only assessed runners of one habitual footfall type performing both the RF and FF patterns (Ardigo et al., 1995; Cunningham et al., 2010; Perl et al., 2012). However, a forward dynamics modeling study found RF running required a lower metabolic rate than FF running (Miller and Hamill, 2012).

Not assessing running economy in both natural RF and natural FF runners, in addition to small sample sizes may have contributed to the lack of significant differences between footfall patterns in previous studies. The addition of a natural FF runners group would allow for a direct comparison of running economy between patterns. Comparing both groups performing their natural footfall pattern will eliminate the potential for

differences to be masked due to the novelty of performing the alternate pattern. Additionally, a natural FF runners group can represent the effect of long term training of the FF pattern in natural RF runners.

Since running economy is dependent on biomechanics, physiology and anthropometry (Daniels, 1985; Morgan et al., 1994a), it is possible that each footfall pattern incorporates a combination of factors that do not bring about a net reduction in metabolic cost. Therefore, the possible factors that may affect running economy within each footfall pattern need to be identified in order to determine the advantage of altering footfall pattern to improve performance.

Achilles Tendon Moment Arm and Running Economy

An anthropometric factor that has been shown to affect running economy is the length of the Achilles tendon moment arm. Runners with shorter Achilles tendon moment arms tend to have greater economy than those with longer Achilles tendon moment arms (Scholz et al., 2008). A shorter Achilles tendon moment arm may increase the storage and release of elastic energy due to the increased force required to maintain a given joint moment. Despite the increased force necessary to produce a given joint moment, an increase in the storage and release of elastic energy has been suggested to be an energy saving mechanism (Albracht and Arampatzis, 2006; Biewener and Roberts, 2000; Roberts, 2002). Although muscle moment arm length is an anthropometric measure, it does change with joint position and it may be possible to manipulate joint position during running to improve economy. Magnetic resonance imaging studies have indicated the Achilles tendon moment arm is shorter in dorsiflexion positions compared

to plantar flexion positions (Maganaris et al., 1998; Maganaris et al., 2000). These findings suggest the RF running pattern may involve a shorter Achilles tendon moment arm during early stance which may result in greater economy over FF running.

A consequence of using an ankle joint position that decreases the Achilles tendon moment arm is that larger muscle forces would be required to produce a given joint moment. Therefore, larger muscle forces may be produced during RF running if a shorter Achilles tendon moment arm results from a dorsiflexed position at impact. However, the FF pattern results in greater plantar flexion ankle joint moments compared to RF running which may result in larger triceps surae muscle forces (Williams et al., 2000). The larger muscle forces required to maintain a plantar flexed position throughout the stance phase in FF running may be large enough to counteract the effect of having a longer Achilles tendon moment arm. Together, the combined effects of having a longer moment arm during stance and producing greater triceps surae muscle forces provide support for FF running being less economical than RF running.

In addition to negatively effecting running economy (Biewener and Roberts, 2000; Roberts et al., 1998), greater muscle forces will increase the stress placed on the Achilles tendon which may increase the risk of injury. Previous studies have also suggested that FF running may increase the risk of AT injury as a result of increased eccentric work of the plantar flexors and greater dorsiflexion velocity compared to RF running (Nilsson and Thorstensson, 1989; Oakley and Pratt, 1988; Williams et al., 2000). However, if RF running decreases the Achilles tendon moment arm, RF running may also cause high Achilles tendon stress due to the greater force required to generate a given joint moment. The combination of high muscle forces with a small moment arm may

compromise the safety factor of the tendon, increasing the risk of a tendon overuse injury or rupture (Biewener, 2005; Scholz et al., 2008). Therefore, a trade-off may exist between performance and injury concerning the potential differences of Achilles tendon moment arm length between running patterns.

Muscle Function and Elastic Energy Utilization in Running

As previously mentioned, the economical benefit of a shorter Achilles tendon moment arm may result from an increase of elastic energy storage and release (Scholz et al., 2008) which may be a mechanism for greater running economy with RF running. However, those that argue FF running is more economical speculate the improvement is due to increased elastic energy utilization compared to RF running (Ardigo et al., 1995; Hasegawa et al., 2007; Perl et al., 2012). Increased storage and release of elastic energy decreases the metabolic cost of running by contributing positive mechanical work that does not need to be produced by the muscle fibers (Cavagna, 1977a; Cavagna et al., 1977b; Lichtwark and Wilson, 2005b; Roberts, 2002; Williams and Cavanagh, 1987). RF running has been shown to utilize this mechanism by maintaining small changes in muscle fascicle length at near optimal shortening velocities while the elastic elements are responsible for producing the majority of positive work (Biewener and Roberts, 2000; Fenn, 1924; Huxley, 1974; Rall, 1985; Roberts et al., 1997).

Although not explicitly comparing footfall patterns, Hof et al. (2002) showed that a MF runner generated triceps surae muscle force when the fibers remained isometric at near optimum length of the force-length relationship. This allowed the shortening and lengthening of the whole muscle-tendon complex of the gastrocnemius and soleus to be

accomplished by passive elements. Since the MF runner produced substantially less positive work by the muscle fibers than a RF runner, MF running may require less muscle energy expenditure than RF running. If the MF running pattern is a true intermediate, the metabolic benefits of FF running may result from isometric muscle force development and utilization of elastic energy. However, a forward dynamics running simulation by Miller and Hamill (2012) exhibited a distinct RF running pattern when optimizing for minimal muscle energy expenditure. This finding suggests other mechanisms may be involved which counteract any possible energy savings mechanisms of FF running. Alternatively, the cumulative effects of requiring a shorter Achilles tendon moment arm and other biomechanical factors of RF running may result in greater energy savings over FF running.

The difference in elastic energy storage and release between footfall patterns was investigated by Ardigo et al. (1995). Elastic energy was estimated by calculating a ratio between external work and deceleration time to external work and acceleration time ($W_{ext}\ t_{dec}^{-1}/W_{ext}\ t_{acc}^{-1}$). Calculating this ratio revealed FF running resulted in greater elastic energy contribution although no difference in oxygen consumption between RF and FF running was detected. The authors suggested FF running generated more negative work which must be overcome by a combination of elastic energy and additional positive work, which did not result in energy savings. Therefore, it is possible that FF running utilizes more elastic energy than RF running, but the additional negative work generated to maintain a plantar flexed position during stance may negate any energy savings.

Impact Parameters in Running

The different segment orientations and force requirements of each footfall pattern will not only change how the muscles function, but may also affect the impact characteristics during landing and how those impacts are attenuated (Bobbert et al., 1992; Boyer and Nigg, 2004; Gerritsen et al., 1995; Wakeling et al., 2001b). Compared to FF running, RF running results in lower vertical active force peak but increased vertical GRF loading rate and tibial acceleration; however, there are conflicting reports on these findings (Cavanagh and Lafortune, 1980; Laughton et al., 2003; McClay and Manal, 1995b; Oakley and Pratt, 1988). Vertical GRF loading rate and the magnitude of the initial impact peak have been suggested to cause overuse injuries from running (Davis et al., 2010; Dickinson et al., 1985; Hreljac et al., 2000; James et al., 1978; Milner et al., 2006; Paul et al., 1978; Radin et al., 1973; Voloshin and Wosk, 1982; Williams et al., 2000; Zifchock et al., 2006). However, active forces, which are greater in FF running (Dickinson et al., 1985; Laughton et al., 2003; McClay and Manal, 1995b; Oakley and Pratt, 1988; Williams et al., 2000), can result in 3 – 5 times greater joint forces than the impact peak (Burdett, 1982; Harrison et al., 1986; Scott and Winter, 1990). Therefore the high forces produced with FF running may also contribute to injury mechanisms (Dickinson et al., 1985; Messier et al., 1991; Nigg, 2011; Radin, 1972; Winter, 1983). Therefore, both footfall patterns may have different mechanisms contributing to injury risk.

The differences in vertical GRF profile between footfall patterns may affect the frequency content of the impact shock wave that is attenuated by the body tissues. For example, the initial impact peak is believed to have a frequency content of 10 – 20 Hz

(Derrick et al., 1998; Hamill et al., 1995; Nigg, 2001). Frequencies in this range may have lower power during FF running due to the absence of this peak. Frequency components below 8 Hz are associated to the active force (Potthast et al., 2010; Shorten and Mientjes, 2003) and thus may have greater power during FF running.

Since the initial impact peak occurs too quickly for muscles to directly respond to it as a stimulus (Nigg et al., 1981), passive mechanisms may be primarily responsible for attenuating impact shock during RF running (Williams and Cavanagh, 1987). Passive shock attenuation mechanisms include deformation of the running shoe, heel fat pad, ligaments, bone and articular cartilage (Chu et al., 1986; Paul et al., 1978). Passive mechanisms are responsible for damping the high frequency components of impact forces and the impact shock wave (Lafortune et al., 1996; Nigg et al., 1981; Paul et al., 1978; Voloshin et al., 1985). For example, the heel fat pad has been shown to attenuate all frequencies and bone attenuates frequencies greater than 18 Hz (Paul et al., 1978). FF running does not take advantage of the heel fat pad to attenuate impacts therefore these frequency need to be absorbed by other mechanisms.

Active shock attenuation mechanisms include eccentric muscle contractions, increased muscle activation, changes in segment geometry and adjustments in joint stiffness (Bobbert et al., 1992; Cole et al., 1996a; Denoth, 1986; Derrick et al., 1998; Gerritsen et al., 1995; McMahon et al., 1987). Active mechanisms are responsible for attenuating lower frequency components because muscle latency is too slow to elicit muscular reactions during the short impact phase (Nigg, 1986; Nigg et al., 1981). Differences in impact characteristics between footfall patterns may affect which mechanisms are responsible for attenuating impacts, how much attenuation occurs and

the stress placed on different tissues. Therefore, it may not be that one footfall pattern prevents more injuries than another, but the tissues affected by injury may differ between patterns. Examining the frequency content of the vertical GRFs and tibial impact shock may identify the mechanisms responsible for shock attenuation between footfall patterns. Identifying which tissues may be more affected by shock attenuation with each pattern may be a better indicator of injury risk than traditional loading characteristics.

Differences in the frequency content of vertical GRFs suggest each footfall pattern may have a greater reliance on different attenuation mechanisms. RF running may rely more on passive mechanisms such as footwear and bone deformation whereas FF running may rely more on active mechanisms such as eccentric contractions of the plantar flexors (Pratt, 1989; Williams and Cavanagh, 1987). The difference in how the body attenuates impacts during RF and FF running may subject different tissues to injury as well as the total amount of attenuation that occurs. Attenuation is important to maintain the visual field and vestibular function (Pozzo et al., 1991). Additionally, differences in attenuation mechanisms may explain why more biomechanical factors associated with greater economy were seen in RF running (Williams and Cavanagh, 1987). However, runners tend to optimize for shock attenuation rather than running economy which may result in an increased risk for injury at the expense of improved performance (Hamill et al., 1995). Therefore, the footfall pattern that elicits the greatest attenuation and economy will prevent the need for this trade-off.

The occurrence of overuse injuries in running have been blamed on the vertical GRF loading rate and magnitude of the impact transient (Davis et al., 2010; Grimston et al., 1991; Hreljac et al., 2000; Milner et al., 2006; Voloshin and Wosk, 1982; Zifchock et

al., 2006). However, these findings are not consistent between all studies (Azevedo et al., 2009; Bredeweg, 2011; McCrory et al., 1999; Nigg, 1997; Pohl et al., 2008; Scott and Winter, 1990). Many have speculated that the FF pattern may reduce the risk of impact related injuries because of the absence of the initial impact peak (Cavanagh and Lafortune, 1980; Daoud et al., 2012; Davis et al., 2010; Lieberman et al., 2010; Oakley and Pratt, 1988). Potential differences in how the body attenuates impact shock between footfall patterns, and not just the difference in GRF characteristics, may reveal a misconception of the potential for FF running to prevent injury.

Problem Statement

Several claims and recommendations regarding the performance and injury prevention benefits of FF running have been made without appropriate empirical evidence. Previous studies examining the performance benefits of altering footfall patterns have not found sufficient evidence to support one footfall pattern being more economical than another. The lack of significant differences in the rate of oxygen consumption between footfall patterns suggests each pattern may exhibit characteristics that do not lead to a net improvement in running economy. Therefore, a combination of factors affecting running economy should be investigated to determine the benefits of a specific footfall pattern. Additionally, previous studies investigating biomechanical or performance differences between footfall patterns only used natural RF runners. Not including a natural FF runners group may have limited the ability to identify significant differences in running economy between footfall patterns.

Although FF running has been suggested to improve running economy by increasing the amount of elastic energy contribution, this has not been previously investigated. The only study to examine the possible differences in elastic energy between footfall patterns did so with an inverse dynamics approach (Ardigo et al., 1995). An inverse dynamics approach may not be sensitive enough to determine the differences in muscular mechanics and how they relate to energy consumption because it cannot identify the function of individual muscle components. Other methods, such as muscle models and identifying differences in anthropometrics, may be needed to reveal the functional differences between footfall patterns and their relation to running economy.

FF running has been suggested to reduce the risk of running overuse injuries due to the absence of the initial vertical ground reaction force component. Differences in ground reaction force characteristics may change the frequency content of the impact shock wave which may affect how they are attenuated. Changing the reliance of the body's tissues to attenuate impact may place certain tissues at a greater risk of injury. Therefore, other parameters besides discrete impact characteristics may reveal more information regarding injury risk.

Purpose

FF running has been suggested to improve performance and decrease the risk of injury. Therefore, recommendations have been made for natural RF runners to switch to the FF pattern; however, many of these recommendations are not based on empirical evidence. The purpose of this dissertation was to ascertain the potential advantages

between footfall patterns and of altering running footfall pattern with respect to running economy and injury risk.

Significance

Previous investigations have only enlisted natural RF runners when comparing biomechanical or metabolic differences between running footfall patterns. This dissertation incorporated both natural FF runners as well as natural RF runners to investigate the advantages of each pattern and the efficacy of switching to the alternative pattern. Examining the mechanical and functional differences between those who naturally perform the RF or FF running patterns will allow for a legitimate comparison between patterns and remove any confounding effects from the novelty of performing either footfall pattern. Additionally, incorporating each group may symbolize the effect of training with the opposite pattern. Together, these comparisons may lead to more conclusive evidence for benefit of altering footfall pattern for improving performance or injury prevention.

Identifying the differences in the underlying mechanisms dictating running economy, such as Achilles tendon moment arm length, elastic energy storage and utilization, and the contribution of active and passive muscle-tendon components, may reveal important information about how running economy is affected by running footfall pattern. The elastic energy contribution between footfall patterns has previously been investigated with an inverse dynamics approach (Ardigo et al., 1995). However, differences in muscular mechanics between footfall patterns are not detectable with an inverse dynamics approach (Sasaki et al., 2009). Therefore, this dissertation used a

modeling approach to examine muscular mechanics and resulting energy consumption between patterns.

Although a specific footfall pattern may be more economical due to one or more factors, the different mechanics of each footfall pattern may result in an increased risk of injury. This dissertation assessed the risk of developing running injuries by examining the stress incurred by the Achilles tendon, the amount of shock attenuation, and the frequency content of ground reaction force characteristics. Examining the differences in the frequency content of ground reaction forces between footfall patterns may identify the tissues responsible for attenuation and the risk of damage to these tissues.

Hypotheses

This dissertation proposal consisted of four studies to investigate the metabolic and mechanical differences between the RF and FF running patterns. These studies aimed to determine the efficacy of altering running footfall patterns for enhancing running performance or preventing running injuries. Comparisons were made between two groups: 1) natural RF runners and 2) natural FF runners.

Study 1

The purpose of Study 1 was to determine the difference in running economy (i.e. lowest sub-maximal rate of oxygen consumption) between footfall patterns and if there was an improvement in running economy in either group when performing the alternate footfall pattern. The following hypotheses were created based on the findings of Williams and Cavanagh (1987) who found that those who exhibited running

characteristics indicative of the RF pattern where more economical than those who did not.

Research Aim 1.1;

To investigate the difference in running economy between natural RF runners and natural FF runners when performing their habitual footfall pattern.

Hypothesis 1.1.1	Running economy would be greater in natural RF runners performing the RF pattern compared to natural FF runners performing the FF pattern.

Research Aim 1.2;

To investigate if running economy improves when performing the alternate footfall pattern.

Hypothesis 1.2.1	If the RF pattern was more economical, then running economy would worsen when natural RF runners perform the FF running pattern.
Hypothesis 1.2.2	If the RF pattern was more economical, then running economy would improve when natural FF runners perform the RF running pattern.

Study 2

The purpose of Study 2 was to determine the AT moment arm length during the stance phase of RF and FF running and to investigate the relationship between moment arm length and running economy. Additionally, this study aimed to determine the difference in Achilles tendon force between RF and FF running patterns. The following hypotheses were based on the findings of Scholz et al. (2008) and Maganaris et al. (2000). Together, these studies showed that a dorsiflexed ankle position results in a shorter Achilles tendon moment arm and those with shorter Achilles tendon moment

arms tend to be more economical runners. Additionally, FF running results in greater plantar flexion moments (Williams et al., 2000). Therefore, the reduction in muscle force that would be expected with a longer Achilles tendon moment arm may be diminished by the muscle force required to maintain a plantar flexed ankle position during the stance phase of FF running.

Research Aim 2.1;

To investigate the difference in Achilles tendon moment arm length between footfall patterns during the stance phase of running.

Hypothesis 2.1.1 Achilles tendon moment arm length would be greater during the first third of the stance phase with the FF running compared to RF running (Maganaris et al., 2000).

Research Aim 2.2;

To investigate the relationship between Achilles tendon moment arm and running economy.

Hypothesis 2.2.1 A shorter Achilles tendon moment arm would correlate with running economy during RF running but a longer Achilles tendon moment arm would correlate with running economy during FF running.

Research Aim 2.3;

To determine the difference in Achilles tendon force between RF and FF running patterns calculated by inverse dynamics analysis.

Hypothesis 2.3.1 Achilles tendon force would be similar between footfall patterns during the stance phase of running.

Study 3

The purpose of Study 3 was to compare the mechanical muscle work and muscle metabolic cost of the triceps surae muscle group between footfall patterns using a musculoskeletal modeling approach. The force and work produced by each muscle of the triceps surae was assessed with a muscle model. The following hypotheses were based on the findings of Hof et al. (2002). This study incidentally found that MF runners produced mechanical work in the triceps surae muscle by the muscle fibers acting more isometrically where as a RF runner produced mechanical work concentrically. In addition, producing mechanical work by acting isometrically resulted in greater storage of elastic energy (Hof et al., 2002; Ishikawa et al., 2007; Lichtwark and Wilson, 2007a). Producing mechanical work isometrically and greater storage of elastic energy have been shown to be energy saving mechanisms in running (Cavagna, 1977a; Cavagna et al., 1977b; Lichtwark and Wilson, 2005b; Roberts, 2002; Williams and Cavanagh, 1987).

Research Aim 3.1;

To determine the mechanical work contribution from active and passive elements of the triceps surae muscle between footfall patterns during the stance phase of running.

Hypothesis 3.1.1 RF running would result in the triceps surae producing more mechanical work from the CE whereas FF running would result in the triceps surae producing more mechanical work from the SEE (i.e. greater elastic energy utilization).

Research Aim 3.2;

To determine the energetic consequences of the different muscle mechanics between footfall patterns by modeling the metabolic work of the muscle contractile element.

Hypothesis 3.2.1 FF running would result in lower muscle energy expenditure than RF running due to increased elastic energy utilization.

Study 4

The purpose of Study 4 was to determine the difference in shock attenuation between footfall patterns and to infer the primary mechanisms responsible for attenuating impact shock between footfall patterns. These hypotheses were based on several studies identifying the differences in impact peak magnitude and initial vertical loading rate between RF and FF running (McClay and Manal, 1995b; Nilsson and Thorstensson, 1989; Oakley and Pratt, 1988). Since the impact characteristics between patterns differ, the characteristics of the impact shock wave may also differ and result in altered shock attenuation between patterns.

Research Aim 4.1;

To determine the difference in impact shock wave attenuation between footfall patterns.

Hypothesis 4.1.1 RF running would result in greater shock attenuation between the tibia and the head than FF running as indicated by reduced power of the frequencies contained in the head acceleration signal.

Research Aim 4.2;

To determine if there is an advantage of altering footfall pattern to improve impact shock attenuation.

Hypothesis 4.2.1 Natural RF runners would not increase the amount of impact shock attenuation when switching to a FF pattern.

Hypothesis 4.2.2 Natural FF runners would increase the amount of impact shock attenuated when switching to a RF pattern.

Research Aim 4.3;

To determine if there may be a difference in impact shock attenuation mechanisms between footfall patterns.

Hypothesis 4.3.1 The RF pattern would rely more on passive shock attenuation mechanisms (as indicated by frequencies greater than 10 Hz) whereas the FF pattern would rely more on active shock attenuation mechanisms (as indicated by frequencies below 10 Hz) (Derrick et al., 1998; Shorten and Winslow, 1992).

Assumptions

1. Metabolic cost of running is independent of body mass after scaling for body mass (Martin and Morgan, 1992).
2. The freely chosen stride length and stride frequency for each gait pattern is the most economical combination to maintain speed at a given speed.

Operational Definitions

1. Rearfoot (RF) running pattern consists of initially landing on the posterior portion of the foot, or heel.
2. Forefoot (FF) running pattern consists of initially landing on the forward portion of the foot or toes without the heel making contact with the ground.

Summary

The forefoot running pattern has been speculated to improve performance and reduce the risk of overuse injuries in running (Davis et al., 2010; Hasegawa et al., 2007; Laughton et al., 2003; Lieberman et al., 2010; Oakley and Pratt, 1988; Pratt, 1989; Williams et al., 2000). To date, there is no evidence to support these claims. Previous

investigations on running economy have identified more kinematic and kinetic parameters associated with greater economy that are inherent to the RF running pattern compared to the FF pattern. However, direct comparisons of oxygen consumption have not shown significant differences between the two patterns. Despite potential performance benefits, the mechanics of each footfall pattern may change or increase the risk of running associated injuries. Landing on the toe rather than the heel changes the impact characteristics which may affect how the body attenuates those forces. Each footfall pattern may rely on different shock attenuation mechanisms, putting different tissues at risk for injury.

References

1. Albracht K and Arampatzis A. Influence of the Mechanical Properties of the Muscle-Tendon Unit on Force Generation in Runners with Different Running Economy. *Biol Cybern*. 2006; 95(1):87-96.

2. Ardigo LP, Lafortuna C, Minetti AE, Mognoni P, Saibene F. Metabolic and Mechanical Aspects of Foot Landing Type, Forefoot and Rearfoot Strike, in Human Running. *Acta Physiol Scand*. 1995; 155(1):17-22.

3. Azevedo LB, Lambert MI, Vaughan CL, O'Connor CM, Schwellnus MP. Biomechanical Variables Associated with Achilles Tendinopathy in Runners. *Br J Sports Med*. 2009; 43(4):288-292.

4. Biewener AA. Biomechanical Consequences of Scaling. *J Exp Biol*. 2005; 208(Pt 9):1665-1676.

5. Biewener AA and Roberts TJ. Muscle and Tendon Contributions to Force, Work, and Elastic Energy Savings: A Comparative Perspective. *Exerc Sport Sci Rev*. 2000; 28(3):99-107.

6. Bobbert MF, Yeadon MR, Nigg BM. Mechanical Analysis of the Landing Phase in Heel-Toe Running. *J Biomech*. 1992; 25(3):223-234.

7. Bonacci J, Green D, Saunders PU, Blanch P, Franettovich M, Chapman AR, Vicenzino B. Change in Footstrike Position Is Related to Alterations in Running Economy in Triathletes. International Symposium on Biomechanics in Sports: Conference Proceedings Archive. 2010. 1-2.

8. Boyer KA and Nigg BM. Muscle Activity in the Leg Is Tuned in Response to Impact Force Characteristics. *J Biomech*. 2004; 37(10):1583-1588.

9. Bredeweg S. No Relationship between Running Related Injuries and Kinetic Variables. *Br J Sports Med*. 2011; 45(4):328.

10. Burdett RG. Forces Predicted at the Ankle During Running. *Med Sci Sports Exerc*. 1982; 14(4):308-316.

11. Cavagna GA. Storage and Utilization of Elastic Energy in Skeletal Muscle. *Exerc Sport Sci Rev*. 1977a; 5:89-129.

12. Cavagna GA, Heglund NC, Taylor CR. Mechanical Work in Terrestrial Locomotion: Two Basic Mechanisms for Minimizing Energy Expenditure. *Am J Physiol*. 1977b; 233(5):R243-261.

13. Cavanagh PR and Lafortune MA. Ground Reaction Forces in Distance Running. *J Biomech*. 1980; 13(5):397-406.

14. Chu ML, Yazdani-Ardakani S, Gradisar IA, Askew MJ. An in Vitro Simulation Study of Impulsive Force Transmission Along the Lower Skeletal Extremity. *J Biomech*. 1986; 19(12):979-987.

15. Cole GK, Nigg BM, van Den Bogert AJ, Gerritsen KG. The Clinical Biomechanics Award Paper 1995 Lower Extremity Joint Loading During Impact in Running. *Clin Biomech (Bristol, Avon)*. 1996a; 11(4):181-193.

16. Daniels JT. A Physiologist's View of Running Economy. *Med Sci Sports Exerc*. 1985; 17(3):332-338.

17. Daoud AI, Geissler GJ, Wang F, Saretsky J, Daoud YA, Lieberman DE. Foot Strike and Injury Rates in Endurance Runners: A Retrospective Study. *Med Sci Sports Exerc*. 2012; 44(7):1325-1334.

18. Davis IS, Bowser B, Mullineaux DR. Do Impacts Cause Running Injuries? A Prospective Investigation. Proceedings of the Annual Meeting of the American Society of Biomechanics. 2010.

19. Denoth J. Load on the Locomotor System and Modelling. In: *Biomechanics of Running Shoes*. Nigg BM (Ed.). Human Kinetics, Champaign, Illinois, 1986. 63-116.

20. Derrick TR, Hamill J, Caldwell GE. Energy Absorption of Impacts During Running at Various Stride Lengths. *Med Sci Sports Exerc*. 1998; 30(1):128-135.

21. Dickinson JA, Cook SD, Leinhardt TM. The Measurement of Shock Waves Following Heel Strike While Running. *J Biomech*. 1985; 18(6):415-422.

22. Fenn WO. The Relation between the Work Performed and the Energy Liberated in Muscular Contraction. *J Physiol*. 1924; 58(6):373-395.

23. Gerritsen KG, van den Bogert AJ, Nigg BM. Direct Dynamics Simulation of the Impact Phase in Heel-Toe Running. *J Biomech*. 1995; 28(6):661-668.

24. Grimston SK, Engsberg JR, Kloiber R, Hanley DA. Bone Mass, External Loads, and Stress Fracture in Female Runners. *International Journal of Sport Biomechanics*. 1991; 7(3):293-302.

25. Hamill J, Derrick TR, Holt KG. Shock Attenuation and Stride Frequency During Running. *Human Movement Science*. 1995; 14:45-60.

26. Harrison RN, Lees A, McCullagh PJ, Rowe WB. A Bioengineering Analysis of Human Muscle and Joint Forces in the Lower Limbs During Running. *J Sports Sci*. 1986; 4(3):201-218.

27. Hasegawa H, Yamauchi T, Kraemer WJ. Foot Strike Patterns of Runners at the 15-Km Point During an Elite-Level Half Marathon. *J Strength Cond Res*. 2007; 21(3):888-893.

28. Hof AL, Van Zandwijk JP, Bobbert MF. Mechanics of Human Triceps Surae Muscle in Walking, Running and Jumping. *Acta Physiol Scand*. 2002; 174(1):17-30.

29. Hreljac A, Marshall RN, Hume PA. Evaluation of Lower Extremity Overuse Injury Potential in Runners. *Med Sci Sports Exerc*. 2000; 32(9):1635-1641.

30. Huxley AF. Muscular Contraction. *J Physiol*. 1974; 243(1):1-43.

31. Ishikawa M, Pakaslahti J, Komi PV. Medial Gastrocnemius Muscle Behavior During Human Running and Walking. *Gait Posture*. 2007; 25(3):380-384.

32. James SL, Bates BT, Osternig LR. Injuries to Runners. *Am J Sports Med*. 1978; 6(2):40-50.

33. Kerr BA, Beauchamp L, Fisher V, Neil R. Footstrike Patterns in Distance Running. In: *Biomechanical Aspects of Sport Shoes and Playing Surfaces*. Nigg BMand Kerr B (Eds.). University of Calgary Press, Calgary, 1983.

34. Lafortune MA, Lake MJ, Hennig EM. Differential Shock Transmission Response of the Human Body to Impact Severity and Lower Limb Posture. *J Biomech*. 1996; 29(12):1531-1537.

35. Laughton CA, Davis IS, Hamill J. Effect of Strike Pattern and Orthotic Intervention on Tibial Shock During Running. *J App Biomech*. 2003; 19:153-168.

36. Lichtwark GA and Wilson AM. Effects of Series Elasticity and Activation Conditions on Muscle Power Output and Effeciency. *J Exp Biol*. 2005b; 208(Pt 15):2845-2853.

37. Lichtwark GA and Wilson AM. Muscle Fascicle and Series Elastic Element Length Changes Along the Length of the Human Gastrocnemius During Walking and Running. *J Biomech*. 2007a; 40(1):157-164.

38. Lieberman DE, Venkadesan M, Werbel WA, Daoud AI, D'Andrea S, Davis IS, Mang'eni RO, Pitsiladis Y. Foot Strike Patterns and Collision Forces in Habitually Barefoot Versus Shod Runners. *Nature*. 2010; 463(7280):531-535.

39. Maganaris CN, Baltzopoulos V, Sargeant AJ. Changes in Achilles Tendon Moment Arm from Rest to Maximum Isometric Plantarflexion: In Vivo Observations in Man. *J Physiol*. 1998; 510 (Pt 3):977-985.

40. Maganaris CN, Baltzopoulos V, Sargeant AJ. In Vivo Measurement-Based Estimations of the Human Achilles Tendon Moment Arm. *Eur J Appl Physiol*. 2000; 83(4 -5):363-369.

41. Martin PE and Morgan DW. Biomechanical Considerations for Economical Walking and Running. *Med Sci Sports Exerc*. 1992; 24(4):467-474.

42. McClay I and Manal K. Lower Extremity Kinetic Comparisons between Forefoot and Rearfoot Strikers. 19th Annual Meeting of the American Society of Biomechanics. 1995b. 213-214.

43. McCrory JL, Martin DF, Lowery RB, Cannon DW, Curl WW, Read HM, Jr., Hunter DM, Craven T, Messier SP. Etiologic Factors Associated with Achilles Tendinitis in Runners. *Med Sci Sports Exerc*. 1999; 31(10):1374-1381.

44. McMahon TA, Valiant G, Frederick EC. Groucho Running. *J Appl Physiol*. 1987; 62(6):2326-2337.

45. Messier SP, Davis SE, Curl WW, Lowery RB, Pack RJ. Etiologic Factors Associated with Patellofemoral Pain in Runners. *Med Sci Sports Exerc*. 1991; 23(9):1008-1015.

46. Miller RH and Hamill J. Footfall Pattern Selection for the Performance of Various Running Tasks. *J App Biomech*. 2012; In Review XX(X):XX-XX.

47. Milner CE, Ferber R, Pollard CD, Hamill J, Davis IS. Biomechanical Factors Associated with Tibial Stress Fracture in Female Runners. *Med Sci Sports Exerc*. 2006; 38(2):323-328.

48. Morgan DW, Craib MW, Krahenbuhl GS, Woodall K, Jordan S, Filarski K, Burleson C, Williams T. Daily Variability in Running Economy among Well-Trained Male and Female Distance Runners. *Res Q Exerc Sport*. 1994a; 65(1):72-77.

49. Nigg BM. Biomechanical Aspects of Running. In: *Biomechanics of Running Shoes*. Nigg BM (Ed.). Human Kinetics, Champaign, IL, 1986. 15-19.

50. Nigg BM. Impact Forces in Running. *Current Opinion in Orthopedics*. 1997; 8(6):43-47.

51. Nigg BM. The Role of Impact Forces and Foot Pronation: A New Paradigm. *Clin J Sport Med*. 2001; 11(1):2-9.

52. Nigg BM. Impact Forces. In: *Biomechanics of Sport Shoes*. Nigg BM (Ed.). Univeristy of Calgary Press, Calgary, 2011. 1-35.

53. Nigg BM, Denoth J, Neukomm PA. Quantifying the Load on the Human Body: Problems and Some Possible Solutions. In: *Biomechanics Vii*. Morecki A et al. (Eds.). University Park Press, Baltimore, MD, 1981. 88-89.

54. Nilsson J and Thorstensson A. Ground Reaction Forces at Different Speeds of Human Walking and Running. *Acta Physiol Scand*. 1989; 136(2):217-227.

55. Oakley T and Pratt DJ. Skeletal Transients During Heel and Toe Strike Running and the Effectiveness of Some Materials in Their Attenuation. *Clin Biomech (Bristol, Avon)*. 1988; 3(3):159-165.

56. Paul IL, Munro MB, Abernethy PJ, Simon SR, Radin EL, Rose RM. Musculo-Skeletal Shock Absorption: Relative Contribution of Bone and Soft Tissues at Various Frequencies. *J Biomech*. 1978; 11(5):237-239.

57. Payne AH. Foot to Ground Contact Forces of Elite Runners. In: *Biomechanics Viii-B*. Matsui Hand Kobayashi K (Eds.). Human Kinetics, Champaign, IL, 1983. 748-753.

58. Perl DP, Daoud AI, Lieberman DE. Effects of Footwear and Strike Type on Running Economy. *Med Sci Sports Exerc*. 2012; 44(7):1335-1343.

59. Pohl MB, Mullineaux DR, Milner CE, Hamill J, Davis IS. Biomechanical Predictors of Retrospective Tibial Stress Fractures in Runners. *J Biomech*. 2008; 41(6):1160-1165.

60. Potthast W, Bruggemann GP, Lundberg A, Arndt A. The Influences of Impact Interface, Muscle Activity, and Knee Angle on Impact Forces and Tibial and Femoral Accelerations Occurring after External Impacts. *J Appl Biomech*. 2010; 26(1):1-9.

61. Pozzo T, Berthoz A, Lefort L, Vitte E. Head Stabilization During Various Locomotor Tasks in Humans. Ii. Patients with Bilateral Peripheral Vestibular Deficits. *Exp Brain Res*. 1991; 85(1):208-217.

62. Pratt DJ. Mechanisms of Shock Attenuation Via the Lower Extremity During Running. *Clin Biomech (Bristol, Avon)*. 1989; 4(1):51-57.

63. Radin EL. The Physiology and Degeneration of Joints. *Semin Arthritis Rheum*. 1972; 2(3):245-257.

64. Radin EL, Parker HG, Pugh JW, Steinberg RS, Paul IL, Rose RM. Response of Joints to Impact Loading. 3. Relationship between Trabecular Microfractures and Cartilage Degeneration. *J Biomech*. 1973; 6(1):51-57.

65. Rall JA. Energetic Aspects of Skeletal Muscle Contraction: Implications of Fiber Types. *Exerc Sport Sci Rev*. 1985; 13:33-74.

66. Roberts TJ. The Integrated Function of Muscles and Tendons During Locomotion. *Comp Biochem Physiol A Mol Integr Physiol*. 2002; 133(4):1087-1099.

67. Roberts TJ, Kram R, Weyand PG, Taylor CR. Energetics of Bipedal Running. I. Metabolic Cost of Generating Force. *J Exp Biol*. 1998; 201(Pt 19):2745-2751.

68. Roberts TJ, Marsh RL, Weyand PG, Taylor CR. Muscular Force in Running Turkeys: The Economy of Minimizing Work. *Science*. 1997; 275(5303):1113-1115.

69. Sasaki K, Neptune RR, Kautz SA. The Relationships between Muscle, External, Internal and Joint Mechanical Work During Normal Walking. *J Exp Biol*. 2009; 212(Pt 5):738-744.

70. Scholz MN, Bobbert MF, van Soest AJ, Clark JR, van Heerden J. Running Biomechanics: Shorter Heels, Better Economy. *J Exp Biol*. 2008; 211(Pt 20):3266-3271.

71. Scott SH and Winter DA. Internal Forces of Chronic Running Injury Sites. *Med Sci Sports Exerc*. 1990; 22(3):357-369.

72. Shorten M and Mientjes M. The Effects of Shoe Cushioning on Impact Force During Running. 6th symposium on footwear biomechanics. 2003.

73. Shorten MR and Winslow DS. Spectral Analysis of Impact Shock During Running. *Int J Sports Biomech*. 1992; 8:288-304.

74. Slavin MM. The Effects of Foot Strike Pattern Alteration on Efficiency in Skilled Runners. M.S. thesis, University of Massachusetts, Amherst, MA, 1992.

75. Voloshin A and Wosk J. An in Vivo Study of Low Back Pain and Shock Absorption in the Human Locomotor System. *J Biomech*. 1982; 15(1):21-27.

76. Voloshin AS, Burger CP, Wosk J, Arcan M. An in Vivo Evaluation of the Leg's Shock Absorbing Capacity. In: *Biomechanics Ix-B* Winter D et al. (Eds.). Human Kinetics, Champaign, IL:, 1985. 112-116.

77. Wakeling JM, Von Tscharner V, Nigg BM, Stergiou P. Muscle Activity in the Leg Is Tuned in Response to Ground Reaction Forces. *J Appl Physiol*. 2001b; 91(3):1307-1317.

78. Williams DS, McClay IS, Manal KT. Lower Extremity Mechanics in Runners with a Converted Forefoot Strike Pattern. *J App Biomech*. 2000; 16(2):210-218.

79. Williams KR. Relationship between Distance Running Biomechanics and Running Economy. In: *Biomechanics of Distance Running*. Cavanagh PR (Ed.). Human Kinetics, Champaign, IL, 1990. 271-306.

80. Williams KR and Cavanagh PR. Relationship between Distance Running Mechanics, Running Economy, and Performance. *J Appl Physiol*. 1987; 63(3):1236-1245.

81. Winter DA. Moments of Force and Mechanical Power in Jogging. *Journal of Biomechanics*. 1983; 16(1):91-97.

82. Zifchock RA, Davis IS, Hamill J. Kinetic Asymmetry in Female Runners with and without Retrospective Tibial Stress Fractures. *J Biomech*. 2006; 39(15):2792-2797.

CHAPTER 2

REVIEW OF THE LITERATURE

General Introduction

The overall aim of this dissertation is to determine the advantage of altering running footfall patterns to improve running economy and injury risk. This chapter will review the literature of previous, pertinent research examining: 1) the differences between the footfall patterns used in running; 2) variations in running economy; 3) Achilles tendon moment arm; 4) muscle function and elastic energy utilization in running; and 4) impact force, impact shock and attenuation.

Footfall Patterns used in Running

Humans exhibit three distinct footfall patterns while running: rearfoot (RF), forefoot (FF), or midfoot (MF) (Figure 2.1). When using the RF pattern, the runner initially contacts the ground on the lateral aspect of the heel whereas the FF pattern involves landing on or near the toes without the heel touching the ground. The MF pattern involves the whole foot making ground contact at nearly the same time but with initial contact in the forefoot region. Nearly 75% of runners land with the RF pattern and only 23.7% and 1.4% use the MF and FF patterns respectively (Hasegawa et al., 2007). Distance runners tend to be predominately RF runners whereas middle distance and sprinters tend to land near the toes (Payne, 1983). Since a greater proportion of elite distance runners and sprinters use a FF pattern (Hasegawa et al., 2007; Kerr et al., 1983; Payne, 1983), some believe there is a performance benefit of using this footfall pattern

(Hasegawa et al., 2007; Martin and Cole, 1991; Romanov, 2002; Shorter, 2005; Yessis, 2000).

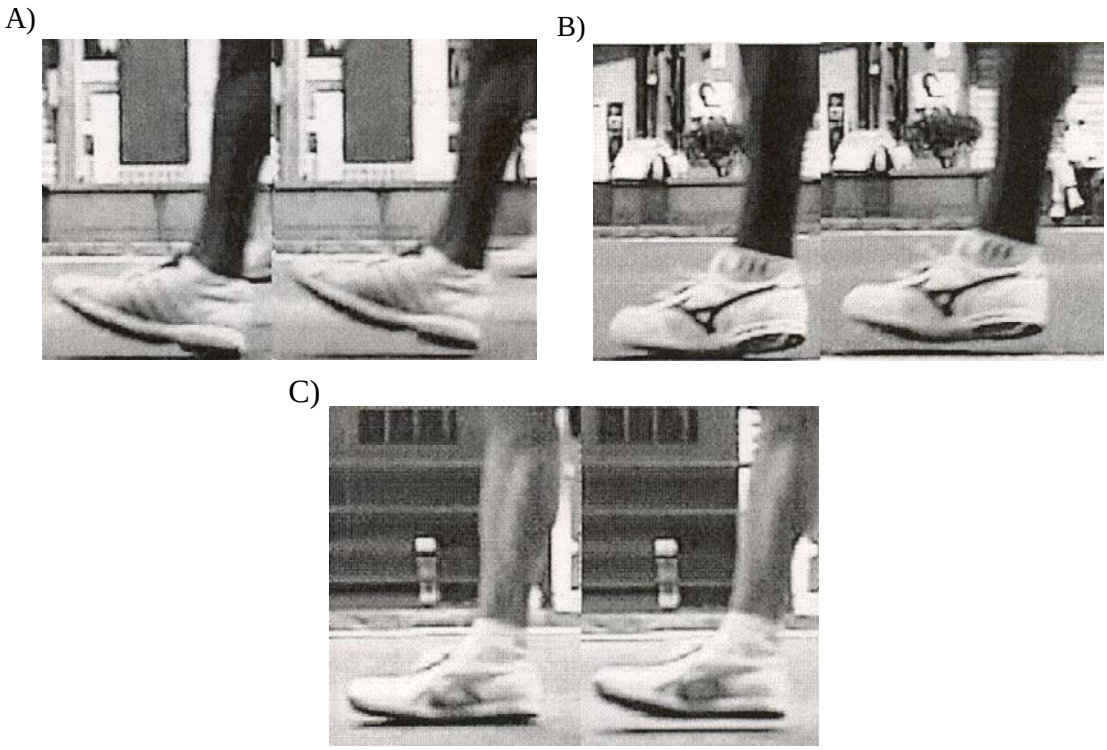

Figure 2.1: Footfall patterns used in running. A) Rearfoot pattern; B) Forefoot pattern; C) Midfoot pattern.

Expert running coaches and several new running programs have suggested RF runners should switch to a FF running pattern to improve performance and reduce the risk of running injuries (Martin and Cole, 1991; Romanov, 2002; Shorter, 2005; Yessis, 2000). It has been suggested that the FF running pattern utilizes the storage and release of elastic energy in the plantar flexors muscles and therefore results in lower metabolic cost (Ardigo et al., 1995; Hasegawa et al., 2007; Perl et al., 2012). Additionally, it has been suggested that the FF running pattern may to reduce the risk of overuse injuries because of the absence of the initial impact ground reaction force (GRF) that is present in

RF running (Cavanagh and Lafortune, 1980; Davis et al., 2010; Dickinson et al., 1985; Lieberman et al., 2010; Pratt, 1989) (Figure 2.2). The FF running pattern and its relationship performance and injury prevention benefits have not been validated in the literature. In order for these claims to be supported, the factors that dictate running economy and injury mechanisms within each pattern must be investigated.

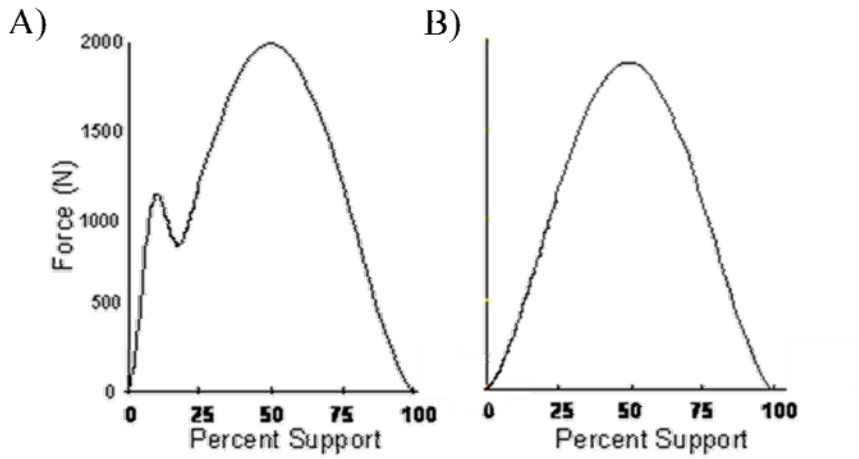

Figure 2.2: Vertical ground reaction force profile for A) the rearfoot running pattern and B) the forefoot running pattern.

Characteristics of the Rearfoot Running Pattern

RF running is characterized by a dorsiflexed and slightly supinated foot position at touchdown (Bates et al., 1978). This position causes initial contact to be made on the lateral boarder of the heel and the center of pressure (COP) positioned within 33% of the foot length relative to the heel (Williams and Cavanagh, 1987) (Figure 2.3). The forefoot is lowered to the ground by eccentric contraction of the tibialis anterior, which is activated during the swing phase (Novacheck, 1998). The calcaneus pronates (i.e. calcaneal eversion) during weight acceptance and reaches maximum eversion at approximately 35-45% of stance (Bates et al., 1978). Maximum eversion is typically coupled with maximum knee flexion. These actions of the foot during running serve to

attenuate impact forces and reduce the center of mass (COM) velocity after ground contact (Bates et al., 1978; Winter, 1983).

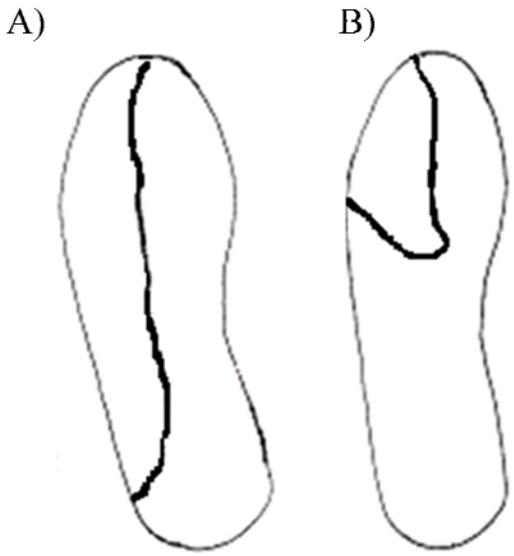

Figure 2.3: The center of pressure trajectory for A) the rearfoot running pattern and B) the forefoot running pattern.

The internal ankle joint moment during rearfoot running is initially dorsiflexor but switches to plantar flexor between 5 – 10% of the running gait cycle (Novacheck, 1998). Ankle power absorption occurs during the first half of stance to attenuate impact forces and reduce the COM velocity after ground contact (Bates et al., 1978; Winter, 1983). Power generation for the remainder of stance serves to generate forward propulsion (Novacheck, 1998). The internal knee flexor moment in late swing is produced by the hamstrings in preparation for impact. During stance, the quadriceps produce a knee extensor moment eccentrically to control the lowering of the body's center of mass and absorb energy (Bates et al., 1978; Winter, 1983). The knee extensors generate power in the second half of stance as they contract concentrically and extend the knee.

The vertical GRF curve during RF running contains an initial impact peak which represents the foot-ground collision (Nigg, 1983). The initial impact peak, or passive peak, is thought to be passive because it occurs too quickly for muscles to respond to it directly (Nigg et al., 1981). However, several muscles, such as the hamstrings and tibialis anterior, are active before the foot makes contact with the ground in order to move the leg through the swing phase and to prepare for touchdown (Novacheck, 1998). Since these muscles are activated before touchdown and early stance, they may serve to attenuate some of the impact shock wave resulting from the initial impact peak. Several researchers speculate this impact peak is responsible for the high rate of overuse injuries in runners (Davis et al., 2010; Grimston et al., 1991; Hreljac et al., 2000; Milner et al., 2006; Paul et al., 1978; Radin et al., 1973; Voloshin and Wosk, 1982; Zifchock et al., 2006); however, these results are not consistent across all studies (Azevedo et al., 2009; Bennell et al., 2004; Bredeweg, 2011; Crossley et al., 1999; Marti et al., 1988; McCrory et al., 1999; Nigg, 1997; Pohl et al., 2008; Scott and Winter, 1990). Therefore, the current approach for investigating the development of running injuries may need to be reexamined or expanded beyond time domain variables.

Characteristics of the Forefoot Running Pattern

During FF running, the foot lands in a plantar flexed and supinated position and then dorsiflexes and everts as the heel is lowered to the ground (McClay and Manal, 1995a; Pratt, 1989). Eccentric contractions of the gastrocnemius, soleus and tibialis posterior will control this foot movement and decrease the vertical velocity of the center of mass (Pratt, 1989). Dorsiflexion, eversion and eccentric contractions of the plantar

flexors may attenuate some of the impact shock during the loading phase (Laughton et al., 2003; Pratt, 1989).

The FF pattern results in greater ankle plantar flexor moment during all of stance and greater ankle power absorption during the first 40% of stance (Williams et al., 2000). The stance phase internal knee extensor moment is similar between footfall patterns but FF running produces a lower peak moment than RF funning. FF running also results in reduced knee power absorption in the first half of stance (Williams et al., 2000). These differences in ankle and knee joint moment between patterns result in greater leg and knee joint stiffness during FF running whereas RF running causes greater ankle joint stiffness. This shift in joint stiffness suggests there is also a shift in the mechanisms of impact shock absorption between patterns (Hamill et al., 2000b; Laughton et al., 2003).

The FF pattern lacks the initial impact peak and has reduced vertical GRF loading rates compared to the RF pattern (McClay and Manal, 1995b; Nilsson and Thorstensson, 1989; Oakley and Pratt, 1988). Therefore, it has been suggested that natural RF runners may benefit from switching to a FF pattern (Daoud et al., 2012b; Davis et al., 2010; Hasegawa et al., 2007; Lieberman et al., 2010; Oakley and Pratt, 1988). However, conflicting results between footfall patterns have been reported for vertical GRF loading rate and peak to peak tibial acceleration but all have found greater peak active forces with FF running compared to RF running (Dickinson et al., 1985; Laughton et al., 2003; McClay and Manal, 1995b; Nilsson and Thorstensson, 1989; Oakley and Pratt, 1988; Williams et al., 2000). Additionally, FF running has been shown to result in greater peak horizontal GRF and greater horizontal GRF loading rate. However, other studies have not found differences in horizontal forces between footfall patterns (Cavanagh and

Lafortune, 1980; Nilsson and Thorstensson, 1989). Most of the published studies comparing impact characteristics have only included natural RF runners as participants. In studies finding greater tibial shock with the FF pattern, the authors warn that the increased tibial shock may be a result of the natural RF runners artificially increasing leg stiffness to prevent heel contact (Laughton et al., 2003). Differences in GRF profiles, loading rates and tibial acceleration between RF and FF running patterns may affect how forces are primarily attenuated.

Some have suggested that the FF running pattern leads to better performance for two reasons. First, many of the top runners for all competitive distances are either a MF or FF runner (Hasegawa et al., 2007). It has been suggested that FF runners are able to run faster with a reduced metabolic cost because of an increase in elastic energy production (Ardigo et al., 1995; Hasegawa et al., 2007; Lieberman et al., 2010; Perl et al., 2012) but these claims have not been supported in the literature (Ardigo et al., 1995; Cunningham et al., 2010; Perl et al., 2012). Second, many RF runners tend to shift to a MF or FF pattern with increasing running speeds (Cavanagh and Lafortune, 1980; Mason, 1980; Slavin and Hamill, 1992). It has been suggested that switching footfall patterns at high running speeds may be an energy saving mechanism to continue increasing running speed when oxygen consumption cannot be increased further (Nigg et al., 1984). However, Cavanagh and Lafortune (1980) found that individual differences in initial contact point and pressure distribution under the foot are large enough to suggest there may not be a relationship between initial contact point and absolute speed.

Most of the previous studies investigating the differences between footfall patterns used natural RF runners performing the FF pattern. Natural RF runners have

been shown to successfully replicate rearfoot kinematics and many kinetic variables compared to natural FF runners with a habituation period of several minutes (Stackhouse et al., 2004; Williams et al., 2000). Despite this confirmation, some subtle differences between those who briefly converted to FF running and natural FF runners may exist. For example, natural RF runners who performed the FF pattern had significantly greater peak vertical GRF, ankle plantar flexion moment and ankle power absorption compared to natural FF runners (Williams et al., 2000). Since no differences in kinematics were observed between the natural RF and FF groups performing the FF pattern, slight differences in segment velocities and contact time may be responsible for the differences in some kinetic variables (Williams et al., 2000). Additionally, Laughton et al. (2003) suggested that greater tibial acceleration and greater leg stiffness during FF running found in their study may be a result of the participants being natural RF runners who do not have extensive experience with the FF pattern. Because these participants were instructed to prevent their heel from touching the ground during the FF running condition, they may have artificially and unnecessarily stiffened the support leg. Laughton et al. (2003) further suggested that runners who initially land on the ball of the foot but allow the heel to touch the ground may have lower tibial shock compared to a FF pattern that does not allow heel contact.

Variations in Running Economy

Running economy, or sub-maximal metabolic energy consumption ($\dot{V}O_2$), is assessed to determine the relationship between running mechanics and running economy (Williams and Cavanagh, 1987). Several biomechanical characteristics have been

identified as significant contributors to greater running economy (Table 2.1). An improvement in running economy, and thereby performance, will be accomplished if a change in movement characteristics, cardiovascular training, footwear, etc. results in a reduction of $\dot{V}O_2$ over a range of running speeds (Williams, 1990).

Table 2.1: Biomechanical characteristics found to be related to greater running economy. These parameters have not been specifically investigated with respect to running footfall patterns.

Reduced peak anteroposterior GRF	Chang & Kram (1999); Williams & Cavanagh (1987)
Greater leg stiffness during ground contact	Heise & Martin (1998)
Lower total vertical impulse Lower net vertical impulse	Heise & Martin (2001)
Reduced plantar flexion moments	Heise et al. (2011)
Longer ground contact time	Kram (2000); Williams & Cavanagh (1987)
Smaller Achilles tendon moment arm length	Scholz et al. (2008)
More extended leg angle at impact Reduced maximum plantar flexion angle at toe-off Greater knee flexion during support Greater elastic energy storage Reduced net positive power and Reduced total mechanical power Reduced peak vertical GRF Less vertical oscillation of the center of mass	Williams & Cavanagh (1987)

Running economy depends on a number of psychological, physiological and mechanical factors; therefore it is highly variable between runners and within an individual (Daniels, 1985; Morgan et al., 1994a). Many of physiological and mechanical factors can be improved with training; however, factors such as genetics, age, gender, anatomical mechanical advantage, cannot be altered with training (Davies et al., 1997; Nevill et al., 1992). Manipulation of certain characteristics that improve economy in one individual may not change or reduce economy in another individual. It has been

suggested that runners self-optimize movement patterns to reduce the metabolic cost of the task (Cavanagh and Williams, 1982). For example, runners will self-select a running speed, stride length and stride frequency, and possibly a footfall pattern, that will result in lower metabolic cost at a given speed (Cavanagh and Williams, 1982; Gutmann et al., 2006; Miller and Hamill, 2012; Morgan et al., 1994b; Morgan et al., 1989). Therefore, deviating from a self-select movement pattern may result in an increase in $\dot{V}O_2$. Nonetheless, studying the movement patterns that are characteristic of more economical runners may provide support for recommendations to improve economy.

A study by Williams and Cavanagh (1987) identified the differences in movement patterns between runners with different economy. In addition to the findings listed in Table 2.1, it was discovered that those with greater economy tended to run with kinematics associated with the RF pattern. Parameters that were characteristic of the RF pattern and seen in the most economical group included longer ground contact time, lower vertical GRF peak, and a more extended leg at touchdown. The authors suggested that RF running may reduce the metabolic cost of running because the RF pattern results in the shoe attenuating some of the impact shock. This finding supports the observation that well-cushioned shoes resulted in a 2.8% reduction of metabolic cost compared to poorly cushioned shoes of the same weight (Frederick et al., 1983). By not utilizing shoe cushioning in FF running, additional muscular contractions may be needed to attenuate impacts thus increasing metabolic energy consumption. Currently, kinematic and kinetic features of the FF running pattern that specifically relate to running economy have yet to be investigated.

Some have speculated that the FF running pattern will improve running economy due to increased elastic energy storage and release in the plantar flexor muscles (Ardigo et al., 1995; Hasegawa et al., 2007; Perl et al., 2012). However, the results from previous studies have shown mixed results. Some studies did not find a difference in running economy between RF and FF running but only examined runners habituated to one footfall pattern (Ardigo et al., 1995; Cunningham et al., 2010; Perl et al., 2012). However, Slavin (1992) observed an increase in $\dot{V}O_2$ when natural RF runners performed the FF pattern whereas natural FF runners had no difference in $\dot{V}O_2$ between patterns. Although the findings from Slavin (1992) suggest the RF pattern may be more economical, differences between footfall patterns were not observed across all three of the speed conditions tested or all metabolic variables. Each of the previous studies investigating the difference in running economy between footfall patterns have methodological limitations. Some included small sample sizes, only one running speed examined, or not assessing running economy in both natural RF runners and natural FF runners.

Future studies investigating the difference in economy between running patterns should incorporate both natural RF and natural FF runners. Comparing both groups performing their natural pattern will eliminate the influence of experience or training as a possible confounding limitation. Additionally, including both groups can substitute the need to investigate how training with the opposite pattern may improve economy. Future studies should also include a larger sample size. With an adequate number of participants, it may be expected that those who naturally perform the more economical footfall pattern will experience a decrease in economy (i.e. increase $\dot{V}O_2$) when switching to the

alternate, less economical pattern. Moreover, those that perform the less economical pattern habitually would improve economy (i.e. decrease $\dot{V}O_2$) or not see an improvement when switching to the more economical pattern. However, if there is no metabolic benefit of altering footfall pattern, then no change in economy may be observed.

Many studies have found conflicting support for biomechanical variables that may relate to running economy. For example, findings from Heise & Martin (2001) suggest less vertical oscillation is not an indicator of economy which conflicts with findings from Williams and Cavanagh (1987). Additionally, ground contact time was not associated with economy in Heise & Martin (2001) which also conflicts with previous reports (Kram, 2000). Individual differences in muscle-tendon properties relating to force generation has been suggested as a more appropriate explanation for individual variation in running economy compared to external mechanical factors (Albracht and Arampatzis, 2006; Martin and Morgan, 1992). However, it is unlikely that a single factor will dominate as the primary influence on running economy or explain the individual variation between suggested mechanical factors that improve economy (Williams, 1990; Williams and Cavanagh, 1987). Identifying the underlying mechanisms that affect running economy between footfall patterns may help determine the benefits and disadvantages of each pattern.

Achilles Tendon Moment Arm

Although many kinematic and kinetic factors of running can be manipulated, an improvement in running economy may be limited by an individual's physiological,

morphological, and anthropometric factors (Albracht and Arampatzis, 2006; Arampatzis et al., 2006; Biewener et al., 2004; Biewener and Roberts, 2000; Lichtwark and Wilson, 2007b; Lichtwark and Wilson, 2008). For example, Scholz et al. (2008) reported that those with shorter Achilles tendon moment arms tend to have greater economy than those with longer Achilles tendon moment arms. However, the study only investigated RF runners. The authors suggest that a smaller Achilles tendon moment arm leads to higher economy because of an increase in tendon stretch and elastic energy storage. The increased elastic energy storage will be accomplished by generating higher forces necessary to produce a given joint moment. Although greater muscle force production is associated with an increase in metabolic cost (Biewener and Roberts, 2000; Roberts et al., 1998), the authors found a smaller Achilles tendon moment arm was associated with a lower metabolic cost, indicating variations in economy were dominated by the cost to produce muscle fiber work and not force (Scholz et al., 2008).

The study by Scholz et al. (2008) did not measure how the length of the Achilles tendon moment arm changes as the foot dorsiflexes and plantar flexes during running. However, static measurements by magnetic resonance imaging (MRI) have shown that the length of the Achilles tendon moment arm increases as ankle plantar flexion angle increases (Maganaris et al., 2000). Given these findings, it may be expected that the FF running pattern will result in a longer Achilles tendon moment arm throughout early stance due to the plantar flexion position at touchdown and, consequently, negatively affect running economy. Additionally, RF running may result in a shorter Achilles tendon moment arm, suggesting it may be more economical than FF running.

Although there is currently no indication of how Achilles tendon moment arm length may be affected by sub-maximal muscle force generation, it's length has been shown to increase when performing an isometric maximum voluntary contraction (MVC) (Maganaris et al., 2000). Since FF running has been speculated to require greater muscle force in the plantar flexors compared to RF running (Pratt, 1989), the difference in plantar flexor force production between patterns may add to the effect of the different foot positions at touchdown. If RF running involves a shorter Achilles tendon moment arm, greater plantar flexor muscle forces would be required to maintain a given joint moment. It may be these greater forces that result in an increase in elastic energy storage and utilization and lead to greater economy (Biewener and Roberts, 2000; Cavagna and Margaria, 1964; Roberts et al., 1998; Scholz et al., 2008). However, previous studies have indicated FF running generates greater plantar flexion joint moments and eccentric work than RF running (Williams et al., 2000). This finding may suggest FF running requires greater plantar flexion muscle force generation in order to maintain a plantar flexed foot position during stance. Therefore, the differences in Achilles tendon moment arm length may not only affect running economy but the stress placed on the Achilles tendon due to increased muscle force production.

Many chronic overuse injuries in running may be a result of repetitive stretch and recoil of tendon (Leadbetter, 1992). Therefore the benefits of a shorter Achilles tendon moment arm of providing increased elastic energy storage and return may potentially increase the risk of tendon injury. Scholz et al. (2008) suggested a small Achilles tendon moment arm combined with greater peak joint moments may compromise the safety factor of the tendon and therefore increase the risk of tendon overuse injuries or tendon

rupture (Biewener, 2005; Scholz et al., 2008). Although RF running may result in a shorter Achilles tendon moment arm during the stance phase, the risk of tendon injury may not be as great as with FF running. Greater ankle joint moments and eccentric work production during FF running has led some authors to suggest that FF running may place increased stress on the Achilles tendon and increase the risk of Achilles tendon injury (Nilsson and Thorstensson, 1989; Oakley and Pratt, 1988; Williams et al., 2000). Therefore, both patterns may result in mechanisms that subject the Achilles tendon to injury.

Muscle Function and Elastic Energy Utilization in Running

Increased storage and release of elastic energy by the muscle's elastic structures may reduce the metabolic cost associated with muscular work during gait (Cavagna, 1977a; Cavagna et al., 1977b; Lichtwark and Wilson, 2005b; Roberts, 2002; Williams and Cavanagh, 1987). Previous investigations on running humans demonstrated that the muscle fibers of the triceps surae act isometrically or concentrically while the whole muscle-tendon complex (MT) lengthens during mid-stance (Hof et al., 2002; Ishikawa et al., 2007; Lichtwark and Wilson, 2007a). As the muscle fibers produce force either isometrically or concentrically, the tendon will stretch resulting in MT lengthening and elastic energy storage. At the end of the stance phase, the MT shortens rapidly causing elastic energy to be released and contributes to positive mechanical work (Biewener and Roberts, 2000; Cavagna and Kaneko, 1977c; Lichtwark and Wilson, 2007a). The positive mechanical work produced by the tendon stretch and recoil will not need to be produced by the muscle fibers, thereby reducing the metabolic cost and heat production

without sacrificing force generation (Biewener, 1998; Ettema, 2001; Fukunaga et al., 2002; Fukunaga et al., 2001). Therefore, the action of the elastic components allows the muscle fibers to produce force isometrically or concentrically at low shortening velocities. Isometric and near isometric contractions will result in greater force production at a lower metabolic cost compared to conditions with substantial changes in fiber length at high velocities (Biewener and Roberts, 2000; Hof et al., 2002; Lichtwark and Wilson, 2007a). These mechanisms have been observed in human running muscle model simulations (Hof et al., 2002) and directly observed by ultrasound (Ishikawa et al., 2005; Ishikawa et al., 2007; Lichtwark and Wilson, 2006; Lichtwark and Wilson, 2007a).

Increased storage and release of elastic energy has been proposed as the reason FF running may be more economical than RF running (Ardigo et al., 1995; Hasegawa et al., 2007; Perl et al., 2012). Although muscle function between different footfall patterns has not been explicitly investigated, a study by Hof et al. (2002) included three subjects that ran with the MF pattern, an intermediate pattern between the RF and FF patterns. By using a muscle model, it was found that the RF runner produced a greater ankle plantar flexor moment than the MF runner. The MT and muscle fibers of the soleus and gastrocnemius muscles in both runners performed nearly zero negative mechanical work but the RF runner produced substantially more positive work by the muscle fibers in both muscles than the MF runner. Less positive mechanical work by the MF runner was accomplished by generating muscle force with the muscle fibers remaining isometric at near optimum length of the force-length relationship. Allowing the muscle fibers to operate isometrically may cause the shortening and lengthening of the MTU to be

accomplished by passive elements; a potentially energy saving mechanism (Biewener and Roberts, 2000).

If the MF running pattern is a true intermediate, FF running may also result in isometric muscle force development and utilization of elastic energy which may result in a decrease of metabolic energy consumption. Despite this potential energy saving mechanism of FF running, a forward dynamics running simulation by Miller and Hamill (2012) exhibited a distinct RF running pattern when optimizing for minimal muscle energy expenditure. This suggests other mechanisms may be involved which counteract the energy savings of FF running or isometric muscle force development and utilization of elastic strain energy.

Each pattern may exhibit a combination of mechanical factors that singularly improve or are detrimental to running economy. Therefore, the net effect of these factors results in neither footfall pattern being more economical than the other. For example, Ardigo et al. (1995) found greater external mechanical work and greater estimated elastic energy production during FF running but no difference in rate of oxygen consumption compared to RF running. The authors suggested the larger elastic energy contribution negated the effects of increased external work production that would have otherwise required a metabolic cost to overcome. Therefore, there was no net increase in metabolic cost with FF running and oxygen consumption between FF and RF running was the same.

The increased stretch of the Achilles tendon in FF running has been assumed to be accompanied by eccentric muscle contractions to prevent the heel from contacting the ground (Ardigo et al., 1995; Perl et al., 2012; Pratt, 1989; Williams et al., 2000). FF running typically results in increased ankle plantar flexor moments which may be

accomplished by increased eccentric contractions and force production by the plantar flexors compared to RF running (Williams et al., 2000). Increased muscle force production in FF running suggests the ankle joint moments would be produced with an increase in metabolic cost (Biewener and Roberts, 2000; Roberts et al., 1998; Scholz et al., 2008). In theory, metabolic cost would not increase if the larger ankle joint moments in FF running were accomplished by the muscle fibers acting with a more optimal contraction velocity (Biewener and Roberts, 2000; Fenn, 1924; Huxley, 1974; Rall, 1985; Roberts et al., 1997).

Differences in mechanical work production between running patterns have only been investigated through inverse dynamics analysis and external mechanical work ratios (Ardigo et al., 1995). These techniques may be inadequate to accurately determine the differences in muscle function between the two patterns and how it relates to metabolic energy consumption and running economy (Sasaki et al., 2009). The differences in muscle function between RF and FF patterns may be too subtle to determine through motion analysis and inverse dynamics. Therefore, a muscle model may be more appropriate to evaluate these differences and determine the individual contributions of passive and active elements.

The use of Musculoskeletal Models for Running Investigations

Musculoskeletal models are frequently used to describe how muscle behaves to produce force during many types of activities, including running. Other methods, such as isokinetic tests and inverse dynamics calculations, can determine the net joint moments produced during movement. However, these methods cannot determine the force

contribution by individual muscles or distinguish between muscle fiber shortening velocity compared to that of the whole muscle-tendon complex. Conversely, musculoskeletal models can be used to simulate the behavior of each element of a muscle that contributes to force production, as well as estimate the force produced by individual muscles without invasive procedures. Musculoskeletal models can also estimate how the muscle and tendon interact to produce force during complex movements and the exact behavior of muscles and tendons will depend on the movement being simulated. However, musculoskeletal models can be difficult to create because of the substantial amount of information needed to create a model. For example, some of the information that is needed for a musculoskeletal model includes muscle force, length and moment arm, time course of the gait data being simulated (e.g. joint angles, ground reaction forces, etc.), muscle architecture and the model parameters of maximum isometric force, optimal fiber length, maximum shortening velocity, tendon slack length and pennation angle (Zajac, 1989). Additionally, the number of unknowns to be estimated by a musculoskeletal model must be equal to the number of equations used to describe the musculoskeletal system (Crowninshield and Brand, 1981).

Typical musculoskeletal models representing the ankle joint complex are composed of rigid segments representing the foot, leg, and thigh as well as two muscles representing the gastrocnemius and soleus. The muscles are generally modeled as a two- or three-component Hill model (Cole et al., 1996b). Hill models are phenomenological models in that they represent the behavior and relationships between muscle, tendon, and other elastic structures, but do not represent the mechanisms by which force is produced (i.e. cross-bridge cycle). With the two-component Hill model, each muscle is represented

by a contractile element (CE) and a series elastic element (SEE). The CE represents the active characteristics of the muscle fibers and the SEE represents the elastic behavior of the tendon, aponeurosis and other passive structures in series with the CE (Cole et al., 1996b). Being located in series, the sum of the lengths of the CE and the SEE equals the length of the whole muscle-tendon complex (MT). A three-component Hill model can be used which includes a parallel elastic element (PEE) in addition to the CE and the SEE. The PEE represents the elastic properties of the passive muscle fibers and muscle fascia, which are in parallel with the CE (Hof et al., 2002). Additionally, other passive structures can be represented by a passive moment (M_{pas}) which acts about the simulated joint. M_{pas} represents the moment produced by passive forces and structures that are not in series with the CE including ligaments, stretch of biarticular muscles, joint capsule and joint contact forces (Hatze, 1997). When using a two-component Hill model, M_{pas} will also include the passive structures that are represented by the PEE in the three-component model.

Muscle properties and how the muscles produce force are dictated by the Hill relationships: CE excitation-activation, CE force-length, CE force-velocity and SEE force-extension (Gordon et al., 1966; Hill, 1938; Wilkie, 1950). All of the Hill model relationships are interrelated. The amount of activation will affect the peak of the force-length curve and thus the peak isometric force potential of the CE. The original Hill relationships assume 100% activation; therefore, appropriate adjustments to the Hill relations must be made when simulating sub-maximal activities (van den Bogert et al., 1998). The magnitude of the maximum isometric force potential will also affect the amount of force that can be produced as a factor of the CE shortening or lengthening

velocity. Because the CE and SEE are in series, the amount of force produced by the CE is transmitted to the SEE and will be equal in both structures. Forces produced by the CE will also cause the SEE to change length. As the SEE increases length, it also becomes stiffer thereby increasing the rate of force production. Additionally, the sum of the CE and SEE velocity and length will be equal to that of the MT.

The Hill model relationships make it possible to calculate the forces produced, as well as the changes in length and velocity of each component included in the model. Although isokinetic and gait studies have also been used to calculate the MT velocity, the results from these studies equate the findings to the CE velocity only, because the SEE cannot be taken into account and muscle-tendon interactions cannot be examined (Fukunaga et al., 2001). Therefore, muscle velocities found by isokinetic dynamometry or gait studies may lead to inaccurate conclusions regarding CE length changes and velocities (Bobbert and van Ingen Schenau, 1990; Fukunaga et al., 2001). Bobbert et al. (1986a) investigated this discrepancy using a musculoskeletal model to examine how the human triceps surae muscle functions during a vertical jumping task. The results from the model demonstrated that the high ankle joint moments and angular velocities required during push-off of a vertical jump would not be possible without the high shortening velocity of the tendon which exceeded that of the CE. The model also revealed that at take-off, the muscle force and the ankle joint moment decline causing the tendon length to decrease. It is the action of the tendon with changing force levels that is responsible for the discrepancy between the torque-angular velocity plots for isokinetic studies compared to the plots from complex movements. Therefore, the muscle model revealed

important information about tendon and muscle function that could not be obtained by isokinetic tests.

Similar models have been used to examine muscle function during running, including the study by Hof et al. (2002) which was previously described in this chapter. The model developed by Hof et al. (2002) used sub-maximal experimental data of walking and running as input. As a result, it differed from the original Hill models that assume 100% activation. The results from Hof et al. (2002) and other studies on running (Ishikawa et al., 2007; Lichtwark and Wilson, 2007a), walking (Fukunaga et al., 2001; Hof et al., 1983; Ishikawa et al., 2005) and hopping (Belli and Bosco, 1992; Fukashiro et al., 2005; Fukunaga et al., 2002; Kurokawa et al., 2001) have indicated that the CE performs very little work during running and functions at shortening velocities that optimize force production. Therefore, the SEE was the structure primarily responsible for the changes in MT length during these complex movements. Additionally, the recoil of the SEE explains why the MT shortens at velocities higher than the CE maximum shortening velocity. These results suggest the stretch and recoil of the SEE acts like a spring, storing elastic strain energy that can contribute to the work produced by the CE that propels the body during push-off (Cavagna et al., 1977b; Cavagna et al., 1964; Fukunaga et al., 2001). Therefore, the SEE affects CE function during walking, running and jumping by allowing the CE to remain near isometric and generate elastic strain energy. Allowing the CE to function near isometrically and increased elastic strain energy generated by the SEE may be significant contributors to muscle function and the metabolic cost of running (Biewener and Roberts, 2000; Fukashiro et al., 2005; Fukunaga et al., 2001).

Several studies have investigated the contribution of elastic energy during complex movements by modeling the amount of CE and SEE length changes or the amount of CE and SEE work (Anderson and Pandy, 1993; Belli and Bosco, 1992; Bohm et al., 2006; Cavagna and Kaneko, 1977c; Fukashiro et al., 1995; Fukunaga et al., 2001; Hof et al., 1983; Ishikawa et al., 2005; Roberts, 2002). These studies found that if the CE does less work or performs work at slower shortening velocities, changes in MT length will be due to changes in primarily SEE length. Therefore, less metabolic energy will be consumed by the CE compared to conditions that cause substantial changes in CE length. Additionally, the reduced CE shortening velocity results in greater force production than if the CE was required to undergo substantial length changes at higher velocities. These findings suggest that maximizing the amount of elastic work performed will depend on the force-velocity characteristics of the muscle (Belli and Bosco, 1992). Therefore, the amount of elastic energy storage and release that occurs during a given movement pattern will depend on the interrelationships of the force generating properties of the CE and SEE.

It has been suggested that humans typically select kinematic and kinetic patterns that minimize metabolic cost (Cavanagh and Williams, 1982; Gutmann et al., 2006). Therefore, the metabolic cost of force generation and the conditions that optimize metabolic efficiency have been a particular interest to many researchers (di Prampero et al., 2005; Donelan et al., 2001; Griffin et al., 2003; Kram, 2000; McNeill Alexander, 2002; Minetti et al., 2002; Roberts et al., 1998; Sih and Stuhmiller, 2003; Wickler et al., 2000). Models that estimate muscle energy liberation have been developed to address this interest. Muscle energetics models calculate the total rate of energy expenditure as

the sum of the activation heat rate, the maintenance heat rate, the shortening/lengthening heat rate and the mechanical work heat rate (Lichtwark and Wilson, 2005a; Umberger et al., 2003). Other, more simplified models have determined the metabolic expenditure of the muscle as a function of relative CE velocity (i.e. instantaneous/maximum), relative force production, and instantaneous activation level (Minetti and Alexander, 1997; Sellers et al., 2003). When combined with a musculoskeletal model, the energetics of a specific task or set of conditions can be determined.

Some previous studies have combined musculoskeletal and muscle energetics models to investigate the variables that affect force production, such as muscle-tendon material properties (Lichtwark and Wilson, 2006; Lichtwark and Wilson, 2007a; Lichtwark and Wilson, 2007b; Lichtwark and Wilson, 2008; Minetti and Alexander, 1997; Sellers et al., 2003). Research by Lichtwark and Wilson (2007b) found that there was an optimal tendon stiffness for improving metabolic efficiency in running. The optimal tendon stiffness allows for the change in MT length to occur primarily by changes in SEE length. The authors proposed that increasing tendon stiffness resulted in changes in MT length occurred primarily from changes in CE length. Therefore, greater tendon stiffness required high CE shortening velocities and greater CE work. The greater shortening velocities of the CE resulted in lower force production as dictated by the force-velocity relationship. Therefore, increasing tendon stiffness results in greater muscle fiber recruitment to produce a given force level thereby activation level and energetic cost increased. Additional studies have found that efficient running also requires longer fiber lengths compared to the fiber lengths needed for efficient walking (Albracht et al., 2008; Lichtwark and Wilson, 2008). This work suggests that material

properties of muscle and muscle architecture maybe tuned to maximize efficiency for a given task or condition.

Despite the potential benefits, musculoskeletal models also have several limitations and drawbacks. For example, models do not account for effects from prior history, fatigue or neural feedback which can decrease the applicability and accuracy of the results. Additionally, the results from a model will depend on the force-generating properties of the muscle including the underlying neural control system, skeletal anatomical features (e.g. anthropometric properties, muscle paths) and muscle architecture parameters (Erdemir et al., 2007). Muscle architecture properties include: the muscle fiber length for optimal force generation, tendon slack length, physiological cross-sectional area and pennation angle. The importance of any one muscle property on the force production calculated by a model can be assessed with a sensitivity analysis. Typically, muscle parameters are based on cadaveric data but can also be taken from imaging or calculations.

The muscle properties used to estimate force generation in muscle models have previously been based on cadaver data with a relatively low number of subjects (Friederich and Brand, 1990; Klein Horsman et al., 2007; Wickiewicz et al., 1983). Arnold et al. (2010) developed a new generic model based on a recent muscle architecture study performed on 21 cadavers (Ward et al., 2009). This model improves on previous models because it uses muscle architecture properties from a single, large group of cadavers, rather than accumulating various properties from several studies. By using more representative data on muscle properties, the Arnold et al. (2010) model improved calculations of fiber length-joint angle relationships and muscle moment arms

which matched experimental data. Improving the estimation of muscle properties will improve the accuracy and applicability of models simulating complex movements.

Impact Force, Impact Shock and Attenuation

Different segment orientations at touchdown between footfall patterns will not only affect muscle function and force generation but also impact characteristics and how those impacts are attenuated (Bobbert et al., 1992; Boyer and Nigg, 2007; Gerritsen et al., 1995; Wakeling et al., 2001b). With RF running, the vertical ground reaction force (GRF) has two distinct phases: a passive or impact phase followed by an active phase. The passive and active phases represent the time of energy absorption and generation, respectively (Derrick et al., 1998; Winter, 1983). Derrick et al. (1998) defined the passive phase as the time between heel contact to the time the support leg center of mass (COM) stops decelerating. The peak force within the passive phase is known as the impact peak. The impact peak results from the collision of the heel with the ground (Nigg, 1986) and has a magnitude of 1.5 to 5 body weights which will increase with running speed (Cavanagh and Lafortune, 1980; Hamill et al., 1983). The impact peak occurs approximately at the same time as peak deceleration of the leg COM (Bobbert et al., 1991). This time-point corresponds to approximately 5 – 50 ms after foot contact or within the first 10% of stance (Bobbert et al., 1991; Nigg et al., 1981). Several studies examining running at a long distance pace have observed the impact peak occurring at approximately 25 ms (Bobbert et al., 1992; Cavanagh and Lafortune, 1980; Dickinson et al., 1985). The impact peak is absent in FF running but the active peak is typically higher with this pattern (Dickinson et al., 1985; Laughton et al., 2003; McClay and Manal,

1995b; Nilsson and Thorstensson, 1989; Oakley and Pratt, 1988; Williams et al., 2000). These differences in time domain features of the vertical GRF profile between footfall patterns may result in differences in frequency domain characteristics as well.

The frequency content of the vertical GRF contains a 10 – 20 Hz component which is associated with the impact peak (Nigg, 2001; Shorten and Winslow, 1992). The frequency characteristics of the impact peak are primarily determined by the acceleration of the leg segments; however, the magnitude of the peak depends on the acceleration of whole body COM (Bobbert et al., 1991). GRF frequencies below 8 Hz are attributed to the active force (Potthast et al., 2010; Shorten and Mientjes, 2003) and therefore may have greater power with FF running. However, the frequency content of GRFs during FF running has not previously been investigated. The differences in the frequency content of the vertical GRF between footfall patterns may also affect how these frequencies are attenuated.

Impact forces generate a shock wave that is transmitted into the foot and through the rest of the body (Nigg et al., 1981; Shorten and Winslow, 1992). The impact peak of the vertical GRF is the main source of this shock wave (Voloshin et al., 1985). Impact shock will increase with running speed and stride length due to the increased acceleration of the tibia (Clarke et al., 1985; Derrick et al., 1998; Hamill et al., 1995). Between footfall patterns difference in segment velocity and stride length, in addition to vertical GRF characteristics, may affect the amount of shock transmitted through the body.

Impact shock can be determined by measuring tibial acceleration with an accelerometer. Accelerometers measure bone vibrations resulting from initial ground contact and acceleration of the segment (Shorten and Winslow, 1992; Wosk and

Voloshin, 1981). Tibial acceleration in running is between 5 – 15 g (Shorten and Winslow, 1992). Peak positive acceleration of the leg occurs approximately 5 ms before the initial impact peak and has a strong relationship with vertical GRF loading rate but only a moderate relationship with impact peak magnitude (Hennig and Lafortune, 1991). The tibial acceleration profile contains a low frequency range (4 – 8 Hz) representing the active movement of the leg during ground contact and a mid-frequency range (12 – 20 Hz) representing foot impact (Derrick et al., 1998; Shorten and Winslow, 1992). The low- and mid-frequency ranges were shown to represent the active and passive phases of the vertical ground reaction force during a vertical jump landing, respectively (Nigg et al., 1981). A higher frequency range (60 – 90 Hz) also exists and represents the resonant frequency of the accelerometer mass and mounting technique (Shorten and Winslow, 1992).

Differences in tibial acceleration may result in differences in peak forces and loading rates between footfall patterns (Laughton et al., 2003). However, artificial stiffening of the leg may be a potential contributor to greater tibial acceleration characteristics some authors have observed with FF running performed by natural RF runners (Laughton et al., 2003). Therefore, recommending a RF runner to switch to the FF pattern may increase impact shock and the amount of shock to be attenuated. Previous studies that have included both natural RF and FF runners only examined basic GRF characteristics such as impact peak magnitude and vertical loading rate (Cavanagh and Lafortune, 1980; Nilsson and Thorstensson, 1989; Payne, 1983). Additionally, other studies have investigated tibial acceleration between footfall patterns in only natural RF runners (Laughton et al., 2003; Oakley and Pratt, 1988). Investigating tibial acceleration

and other impact variables in natural FF should occur in order to accurately assess the differences between footfall patterns.

In order to determine the amount of shock attenuation occurring in the body, several studies have used spectral analysis to transform tibial and head acceleration data from the time domain into the frequency domain (Derrick et al., 1998; Hamill et al., 1995; Lafortune et al., 1995; Lafortune et al., 1996; Shorten and Winslow, 1992; Wosk and Voloshin, 1981). A transfer function is calculated by determining the ratio between the power spectral density of the head acceleration and the power spectral density of the tibial acceleration. The transfer function can identify the frequency ranges that increase or decrease in signal strength as the impact shock wave travels from the tibia to the head (Derrick et al., 1998). Most of the frequency content measured at the head is within the 3 – 8 Hz range (Derrick et al., 1998). Therefore, the body may be more capable of attenuating frequency components greater than 8 Hz than lower frequencies.

Shock attenuation occurs in order to stabilize the head to maintain a runner's visual field and stabilize the vestibular system (Pozzo et al., 1991). Attenuation occurs by a combination of passive and active mechanisms which can reduce the damaging effects of loading (Radin, 1972), such as osteoarthritis (Simon et al., 1972). Examples of shock attenuation mechanisms previously observed in the literature are listed in Table 2.2. Bone deformation (a passive mechanism) and eccentric muscle contractions (an active mechanism) may be the primary mechanisms that attenuate forces transmitted through the body (Radin and Paul, 1970).

Attenuation appears to increase with greater impact magnitudes to maintain head stabilization (Derrick et al., 1998; Hamill et al., 1995; Shorten and Winslow, 1992).

Some suggest attenuation increases by increasing energy absorption from active muscles (Derrick et al., 1998) or by overloading passive tissues responsible for attenuation (Voloshin and Wosk, 1982; Voloshin et al., 1981). If there is a reduced capacity for attenuation by one tissue, changes in gait patterns or increased attenuation by the other tissues may occur (Voloshin and Wosk, 1982). However increasing attenuation subjects the body's tissues to greater deformation which may contribute to tissue injury. If the frequency content of the vertical GRF and impact shock wave is different between footfall patterns, than each pattern may have a different reliance on various attenuation mechanisms.

Table 2.2: Shock attenuation mechanisms found in previous investigations.

Energy absorption through eccentric muscle contractions	Derrick et al., (1998); Novacheck, (1998); Winter, (1983)
Hip adduction during early stance	Novacheck, (1998).
Changes in sagittal plane lower extremity joint angles, especially knee and ankle	Bobbert et al., (1992); Clarke et al., (1983b); Derrick et al., (1998); Lafortune et al., (1996a); Lafortune et al., (1996); McMahon et al., (1987); Potthast et al., (2010); Ratcliffe and Holt, (1997)
Greater rearfoot pronation	Bates et al., (1978); Denoth, (1986); Nigg et al., (1987); Perry & Lafortune, (1995); Winter, (1983)
Decrease stride length and increase stride frequency	Derrick et al., (1998); Hamill et al., (1995); Mercer et al., (2003)
Changes in muscle force	Bobbert et al., (1992); Denoth, (1986); Gerritsen et al., (1995)

Studies identifying the frequency content of GRFs and tibial acceleration during running have found frequency components above 6 Hz are attenuated but the body is most effective at attenuating frequency components within the 15 – 50 Hz range (Hamill et al., 1995; Lafortune et al., 1996; Shorten and Winslow, 1992). More specifically, GRF

frequencies above 60 Hz were shown to be damped by the foot and leg, likely by a combination of passive and active mechanisms. Frequencies between 30 – 60 Hz were transmitted into the knee and the rest of the body and attenuated by kinematic adjustments, muscular contractions and deformation of the spine (Lafortune et al., 1995; Lafortune et al., 1996; Nigg et al., 1981; Voloshin et al., 1985). Additionally, frequencies between 8 – 10 Hz have the greatest power compared to all others at both the head and tibia (Lafortune et al., 1996), suggesting that these frequencies are not attenuated as much as higher frequency components. During walking, frequencies outside of the 15 – 25 Hz range were attenuated below the knee (Voloshin et al., 1985).

Passive Mechanisms of Shock Attenuation in Running

Since muscle latency is 30 ms or more, muscular contractions are unable to directly respond to impacts occurring during the period of initial ground contact (Nigg et al., 1981). Therefore, passive forces are attenuated by deformation of the shoe and the body tissues such as the heel fat pad, ligaments, bone and articular cartilage (Chu et al., 1986; Paul et al., 1978). When subjected to repeated impacts, the heel fat pad has been shown to be responsible for absorbing approximately 85% of the impact energy, therefore it is a significant contributor to impact attenuation in RF running (Cavanagh et al., 1984). In a study performed on rabbits, Paul et al. (1978) showed that the heel fat pad was able to attenuate all frequencies and reduces frequency power by 20 – 28% whereas bone was responsible for attenuating frequencies greater than 18 Hz. Other animal model studies have found increased new bone formation when subjected to a 15 Hz signal, but not a 1 Hz signal, suggesting bone is stressed when exposed to higher frequencies (McLeod and

Rubin, 1990). Passive structures of the knee, including ligaments, capsular and intracapsular tissues, have also been shown to significantly reduce peak accelerations (Chu et al., 1986).

Without the assistance of other attenuation mechanisms, bone may be overloaded and at risk for fracture (Nigg et al., 1981; Voloshin and Wosk, 1982). Therefore, passive forces are believed to be the cause of microtrauma to bone as well as muscle tissue (Nigg et al., 1981). Since the initial impact peak is not visible in the time domain during FF running, it has been speculated that this footfall pattern protects against injury resulting from impact forces (Davis et al., 2010; Hasegawa et al., 2007; Laughton et al., 2003; Lieberman et al., 2010; Oakley and Pratt, 1988; Pratt, 1989; Williams et al., 2000). Although FF running does not cause an initial impact peak, differences in frequency content of the vertical GRF characteristics may reveal that the FF pattern may not prevent injuries sustained with RF running. Therefore, there may be a misconception of the benefits of FF running with respect to injury prevention.

Active Mechanisms of Shock Attenuation in Running

Active shock attenuation mechanisms include eccentric muscle contractions, increased muscle activation, changes in segment geometry and adjustments in joint stiffness (Bobbert et al., 1992; Cole et al., 1996a; Denoth, 1986; Derrick et al., 1998; Gerritsen et al., 1995; McMahon et al., 1987; Wright et al., 1998). The ability for muscle actions to attenuate impacts may be limited by the reaction time to an impact stimulus (McMahon and Green, 1984). Because muscle latency is 30 – 75 ms (Nigg et al., 1981; Simon et al., 1981), active muscle contractions that are specifically responding to an

impact stimulus may only be effective at attenuating frequencies below 10 Hz (Paul et al., 1978). Muscle is capable of large deformations and can adapt in order to attenuate a large range of frequencies. Therefore, muscle has a large shock attenuation capacity. However, if the muscles of the lower extremity are unable to sufficiently absorb impact energy, passive structures may be overloaded to attenuate shock (Derrick et al., 1998).

Although muscles may not be able to respond to passive forces in the time that they are occurring, pre-activation of muscles before ground contact may occur in preparation for impact and may be scaled to different loading conditions (Boyer and Nigg, 2007; Gerritsen et al., 1995; Nigg et al., 1987; Wakeling et al., 2001b). The intensity, timing and frequency of muscle activation will vary before and after impact to change the material properties and increase damping of impact shock wave frequencies (Boyer and Nigg, 2007). Changes in muscle activity may be responsible for absorbing frequencies greater than 40 or 50 Hz. The muscles of the triceps surae may not be as effective as the quadriceps at changing muscle activity to increase frequency damping due to the smaller mass of the triceps surae (Boyer and Nigg, 2007).

Eccentric contractions attenuate shock by controlling the slow deceleration of the body thereby dissipating impacts over a longer period of time (Derrick et al., 1998; Pratt, 1989). During RF running, eccentric contractions of the tibialis anterior, tibialis posterior and flexor hallucis longus muscles assist the foot to control pronation and lower the forefoot to the ground (Novacheck, 1998; Winter, 1983) whereas FF running may result in eccentric contractions of the plantar flexors to prevent the heel from making contact with the ground (Pratt, 1989). The combination of dorsiflexion, eversion and eccentric contractions of the plantar flexors during running may also be partially responsible for

the differences in loading characteristics between footfall patterns (Laughton et al., 2003).

Runners have been shown to alter their gait pattern and segment geometry in order to reduce impact shock wave transmission when subjected to greater impact shock (Clarke et al., 1984; Derrick et al., 1998). In particular, increased knee and ankle joint flexion in the initial portion of the stance phase have been associated with significant impact attenuation and may be responsible for attenuating frequencies above 10 Hz (Derrick et al., 1998; Lafortune et al., 1996a; Lafortune et al., 1996). Increased attenuation from changes in knee joint angle, for example, may be accomplished by increased knee extensor moment and quadriceps eccentric contractions (Derrick et al., 1998). In a study by Derrick et al. (1998), increases in stride length resulted in greater knee flexion and impact forces but also greater shock attenuation between 10 – 20 Hz. However, it is unknown if the changes in knee joint moments and power were due to the muscle increasing attenuation or increased leg control with greater stride lengths.

Adjustments in segment geometry may result in altered leg and joint stiffness and affect impact shock attenuation. Leg and joint stiffness represents the combined passive and dynamic properties of muscles, tendons, and ligaments that contribute to the compliance of the lower extremity (Hamill et al., 2000a). Therefore, leg or joint stiffness implies a greater capacity to perform negative work and attenuate impact shock. FF running results in greater leg and knee stiffness but lower ankle stiffness compared to RF running (Hamill et al., 2000a; Laughton et al., 2003). These results suggest that a compliant ankle is responsible for active shock attenuation during FF running and a compliant knee is responsible for active shock attenuation during RF running (Hamill et

al., 2000a). However, greater muscular contractions and a more extended knee will increase impact forces due to increased leg stiffness, thereby increasing the amount of shock that must be attenuated (Potthast et al., 2010).

Is Forefoot Running Protective Against Running Injuries?

Vertical loading rate and magnitude of the initial impact peak have been suggested as significant factors relating to overuse injuries from running (Daoud et al., 2012a; Davis et al., 2010; Grimston et al., 1991; Hreljac et al., 2000; Milner et al., 2006; Paul et al., 1978; Radin et al., 1973; Voloshin and Wosk, 1982; Zifchock et al., 2006). However, several other investigations have found minimal or no relationship with impact force magnitude or loading rate to the risk of developing running related injuries (Azevedo et al., 2009; Bennell et al., 2004; Bredeweg, 2011; Crossley et al., 1999; Marti et al., 1988; McCrory et al., 1999; Nigg, 1997; Nigg, 2001; Nigg et al., 1995; Pohl et al., 2008; Scott and Winter, 1990).

Many have speculated that the FF pattern may reduce the risk of impact related injury due to the absence of the initial impact peak (Cavanagh and Lafortune, 1980; Daoud et al., 2012b; Davis et al., 2010; Lieberman et al., 2010; Oakley and Pratt, 1988). However, previous studies have found FF running to result in greater active peak vertical GRFs compared to RF running (Dickinson et al., 1985; Laughton et al., 2003; McClay and Manal, 1995b; Nilsson and Thorstensson, 1989; Oakley and Pratt, 1988; Williams et al., 2000). Loads from the active portion of the vertical GRF result in 3 – 5 times greater joint forces than the impact peak (Burdett, 1982; Harrison et al., 1986; Scott and Winter, 1990). Active loads may play an important role to injury mechanisms (Dickinson et al.,

1985; Messier et al., 1991; Nigg, 2011; Radin, 1972; Winter, 1983), which may be exacerbated with FF running. Although RF running causes larger impact forces, some studies have shown that RF running also results in longer strides and a lower stride frequency than FF running (Hamill et al., 2010). Therefore, FF running may result in greater exposure to loading because a greater number of impacts will occur over the same distance.

Kinematic differences such as foot segment orientation at impact, knee flexion angle throughout stance, stride length, and segment velocities are likely the source for differences in impact force characteristics between footfall patterns. Consequently, differences in GRF profiles, loading rates and tibial acceleration between RF and FF running patterns may result in a different reliance on attenuation mechanisms. For example, FF running does not take advantage of the heel fat pad or shoe cushioning in the heel to attenuate impacts; therefore, greater proportions of shock may be applied to other tissues that do not have the same capacity for shock attenuation. As a result, those who run with a FF pattern may need to make adjustments in kinematics and muscle activation to sufficiently attenuate impacts. The difference in impact attenuation mechanisms between footfall patterns may have implications on not only the risk of injury, but the tissues that may be susceptible to injury.

The segment geometries employed by the FF pattern and result in reduced GRF parameters may also affect internal loading conditions. Kinematic changes to prevent amplified impact forces may result in increased muscle forces and, consequently, increased tendon and joint loads (Cole et al., 1996a). Since repetitive loading of joints and tendons can lead to overuse injuries (Bobbert et al., 1992; Luethi et al., 1987; Nigg et

al., 1987; Wright et al., 1998), mechanisms other than impact forces and loading rates may be responsible for the development of an injury. Therefore, FF running may not be protective against overuse injuries from running simply because of the absence of the initial impact peak and reduced vertical loading rates.

Summary

FF running has been suggested to improve running economy and prevent overuse injuries from running. However, the benefits of FF running have yet to be substantiated. Mechanical differences between RF and FF running, such as the length of the Achilles tendon moment arm during the stance phase, muscle fiber contribution to mechanical work, and the storage and release of elastic energy may be significant determinants of the metabolic energy requirements between footfall patterns. Additionally, the differences in segment orientation between footfall patterns may affect GRF loading characteristics and how impact shock is attenuated by the body tissues. Understanding the mechanisms contributing to metabolic energy consumption and mechanical loading between footfall patterns will lead to more appropriate recommendations for runners to improve economy and prevent injury.

References

1. Albracht K and Arampatzis A. Influence of the Mechanical Properties of the Muscle-Tendon Unit on Force Generation in Runners with Different Running Economy. *Biol Cybern*. 2006; 95(1):87-96.

2. Albracht K, Arampatzis A, Baltzopoulos V. Assessment of Muscle Volume and Physiological Cross-Sectional Area of the Human Triceps Surae Muscle in Vivo. *J Biomech*. 2008; 41(10):2211-2218.

3. Anderson FC and Pandy MG. Storage and Utilization of Elastic Strain Energy During Jumping. *J Biomech*. 1993; 26(12):1413-1427.

4. Arampatzis A, De Monte G, Karamanidis K, Morey-Klapsing G, Stafilidis S, Bruggemann GP. Influence of the Muscle-Tendon Unit's Mechanical and Morphological Properties on Running Economy. *J Exp Biol*. 2006; 209(Pt 17):3345-3357.

5. Ardigo LP, Lafortuna C, Minetti AE, Mognoni P, Saibene F. Metabolic and Mechanical Aspects of Foot Landing Type, Forefoot and Rearfoot Strike, in Human Running. *Acta Physiol Scand*. 1995; 155(1):17-22.

6. Arnold EM, Ward SR, Lieber RL, Delp SL. A Model of the Lower Limb for Analysis of Human Movement. *Ann Biomed Eng*. 2010; 38(2):269-279.

7. Azevedo LB, Lambert MI, Vaughan CL, O'Connor CM, Schwellnus MP. Biomechanical Variables Associated with Achilles Tendinopathy in Runners. *Br J Sports Med*. 2009; 43(4):288-292.

8. Bates BT, James SL, Osternig LR. Foot Function During the Support Phase of Running. *Running*. 1978; Fall:24-31.

9. Belli A and Bosco C. Influence of Stretch-Shortening Cycle on Mechanical Behaviour of Triceps Surae During Hopping. *Acta Physiol Scand*. 1992; 144(4):401-408.

10. Bennell K, Crossley K, Jayarajan J, Walton E, Warden S, Kiss ZS, Wrigley T. Ground Reaction Forces and Bone Parameters in Females with Tibial Stress Fracture. *Med Sci Sports Exerc*. 2004; 36(3):397-404.

11. Biewener AA. Muscle-Tendon Stresses and Elastic Energy Storage During Locomotion in the Horse. *Comp Biochem Physiol B Biochem Mol Biol*. 1998; 120(1):73-87.

12. Biewener AA. Biomechanical Consequences of Scaling. *J Exp Biol*. 2005; 208(Pt 9):1665-1676.

13. Biewener AA, Farley CT, Roberts TJ, Temaner M. Muscle Mechanical Advantage of Human Walking and Running: Implications for Energy Cost. *J Appl Physiol*. 2004; 97(6):2266-2274.

14. Biewener AA and Roberts TJ. Muscle and Tendon Contributions to Force, Work, and Elastic Energy Savings: A Comparative Perspective. *Exerc Sport Sci Rev*. 2000; 28(3):99-107.

15. Bobbert MF, Huijing PA, van Ingen Schenau GJ. A Model of the Human Triceps Surae Muscle-Tendon Complex Applied to Jumping. *J Biomech*. 1986a; 19(11):887-898.

16. Bobbert MF, Schamhardt HC, Nigg BM. Calculation of Vertical Ground Reaction Force Estimates During Running from Positional Data. *J Biomech*. 1991; 24(12):1095-1105.

17. Bobbert MF and van Ingen Schenau GJ. Isokinetic Plantar Flexion: Experimental Results and Model Calculations. *J Biomech*. 1990; 23(2):105-119.

18. Bobbert MF, Yeadon MR, Nigg BM. Mechanical Analysis of the Landing Phase in Heel-Toe Running. *J Biomech*. 1992; 25(3):223-234.

19. Bohm H, Cole GK, Bruggemann GP, Ruder H. Contribution of Muscle Series Elasticity to Maximum Performance in Drop Jumping. *J Appl Biomech*. 2006; 22(1):3-13.

20. Boyer KA and Nigg BM. Changes in Muscle Activity in Response to Different Impact Forces Affect Soft Tissue Compartment Mechanical Properties. *J Biomech Eng*. 2007; 129(4):594-602.

21. Bredeweg S. No Relationship between Running Related Injuries and Kinetic Variables. *Br J Sports Med*. 2011; 45(4):328.

22. Burdett RG. Forces Predicted at the Ankle During Running. *Med Sci Sports Exerc*. 1982; 14(4):308-316.

23. Cavagna GA. Storage and Utilization of Elastic Energy in Skeletal Muscle. *Exerc Sport Sci Rev*. 1977a; 5:89-129.

24. Cavagna GA, Heglund NC, Taylor CR. Mechanical Work in Terrestrial Locomotion: Two Basic Mechanisms for Minimizing Energy Expenditure. *Am J Physiol*. 1977b; 233(5):R243-261.

25. Cavagna GA and Kaneko M. Mechanical Work and Efficiency in Level Walking and Running. *J Physiol*. 1977c; 268(2):467--481.

26. Cavagna GA and Margaria R. [Mechanics of the Contraction of Muscle Previously Exposed to Stretching]. *Boll Soc Ital Biol Sper*. 1964; 40(24):Suppl:2051-2054.

27. Cavagna GA, Saibene FP, Margaria R. Mechanical Work in Running. *J Appl Physiol*. 1964; 19:249-256.

28. Cavanagh PR and Lafortune MA. Ground Reaction Forces in Distance Running. *J Biomech*. 1980; 13(5):397-406.

29. Cavanagh PR, Valiant GA, Miserich KW. Biological Aspects of Modelling Shoe/Foot Interactions During Running. In: *Sports Shoes and Playing Surfaces*. Frederick EC (Ed.). Human Kinetics, Champaign, Illinois, 1984. 24-46.

30. Cavanagh PR and Williams KR. The Effect of Stride Length Variation on Oxygen Uptake During Distance Running. *Med Sci Sports Exerc*. 1982; 14(1):30-35.

31. Chang YH and Kram R. Metabolic Cost of Generating Horizontal Forces During Human Running. *J Appl Physiol*. 1999; 86(5):1657-1662.

32. Chu ML, Yazdani-Ardakani S, Gradisar IA, Askew MJ. An in Vitro Simulation Study of Impulsive Force Transmission Along the Lower Skeletal Extremity. *J Biomech*. 1986; 19(12):979-987.

33. Clarke TE, Cooper LB, Hamill CL, Clark DE. The Effect of Varied Stride Rate Upon Shank Deceleration in Running. *J Sports Sci*. 1985; 3(1):41-49.

34. Clarke TE, Frederick EC, Cooper LB. Biomechanical Measurement of Running Shoe Cushioning Properties. In: *Biomechanical Aspects of Sport Shoes and Playing Surfaces*. Nigg BMand Kerr B (Eds.). Univeristy of Calgary Press, Calgary, 1983b. 25-33.

35. Clarke TE, Frederick EC, Hamill CL. The Study of Rearfoot Movement in Running. In: *Sports Shoes and Playing Surfaces*. Frederick EC (Ed.). Human Kinetics, Champaign, IL, 1984. 166-189.

36. Cole GK, Nigg BM, van Den Bogert AJ, Gerritsen KG. The Clinical Biomechanics Award Paper 1995 Lower Extremity Joint Loading During Impact in Running. *Clin Biomech (Bristol, Avon)*. 1996a; 11(4):181-193.

37. Cole GK, van den Bogert AJ, Herzog W, Gerritsen KG. Modelling of Force Production in Skeletal Muscle Undergoing Stretch. *J Biomech*. 1996b; 29(8):1091-1104.

38. Crossley K, Bennell KL, Wrigley T, Oakes BW. Ground Reaction Forces, Bone Characteristics, and Tibial Stress Fracture in Male Runners. *Med Sci Sports Exerc*. 1999; 31(8):1088-1093.

39. Crowninshield RD and Brand RA. The Prediction of Forces in Joint Structures; Distribution of Intersegmental Resultants. *Exerc Sport Sci Rev*. 1981; 9:159-181.

40. Cunningham CB, Schilling N, Anders C, Carrier DR. The Influence of Foot Posture on the Cost of Transport in Humans. *J Exp Biol*. 2010; 213(5):790-797.

41. Daniels JT. A Physiologist's View of Running Economy. *Med Sci Sports Exerc*. 1985; 17(3):332-338.

42. Daoud AI, Geissler GJ, Wang F, Saretsky J, Daoud YA, Lieberman DE. Foot Strike and Injury Rates in Endurance Runners: A Retrospective Study. *Med Sci Sports Exerc*. 2012a.

43. Daoud AI, Geissler GJ, Wang F, Saretsky J, Daoud YA, Lieberman DE. Foot Strike and Injury Rates in Endurance Runners: A Retrospective Study. *Med Sci Sports Exerc*. 2012b; 44(7):1325-1334.

44. Davies MJ, Mahar MT, Cunningham LN. Running Economy: Comparison of Body Mass Adjustment Methods. *Res Q Exerc Sport*. 1997; 68(2):177-181.

45. Davis IS, Bowser B, Mullineaux DR. Do Impacts Cause Running Injuries? A Prospective Investigation. Proceedings of the Annual Meeting of the American Society of Biomechanics. 2010.

46. Denoth J. Load on the Locomotor System and Modelling. In: *Biomechanics of Running Shoes*. Nigg BM (Ed.). Human Kinetics, Champaign, Illinois, 1986. 63-116.

47. Derrick TR, Hamill J, Caldwell GE. Energy Absorption of Impacts During Running at Various Stride Lengths. *Med Sci Sports Exerc*. 1998; 30(1):128-135.

48. di Prampero PE, Fusi S, Sepulcri L, Morin JB, Belli A, Antonutto G. Sprint Running: A New Energetic Approach. *J Exp Biol*. 2005; 208(Pt 14):2809-2816.

49. Dickinson JA, Cook SD, Leinhardt TM. The Measurement of Shock Waves Following Heel Strike While Running. *J Biomech*. 1985; 18(6):415-422.

50. Donelan JM, Kram R, Kuo AD. Mechanical and Metabolic Determinants of the Preferred Step Width in Human Walking. *Proc Biol Sci*. 2001; 268(1480):1985-1992.

51. Erdemir A, McLean S, Herzog W, van den Bogert AJ. Model-Based Estimation of Muscle Forces Exerted During Movements. *Clin Biomech (Bristol, Avon)*. 2007; 22(2):131-154.

52. Ettema GJ. Muscle Efficiency: The Controversial Role of Elasticity and Mechanical Energy Conversion in Stretch-Shortening Cycles. *Eur J Appl Physiol*. 2001; 85(5):457-465.

53. Fenn WO. The Relation between the Work Performed and the Energy Liberated in Muscular Contraction. *J Physiol*. 1924; 58(6):373-395.

54. Frederick EC, Clarke TE, Larsen JL, Cooper LB. The Effects of Shoe Cushioning on the Oxygen Demands of Running. In: *Biomechanical Aspects of Sports Shoes and Playing Surfaces*. Nigg Band Kerr B (Eds.). University of Calgary Printing Services, Calgary, 1983. 107-114.

55. Friederich JA and Brand RA. Muscle Fiber Architecture in the Human Lower Limb. *J Biomech*. 1990; 23(1):91-95.

56. Fukashiro S, Komi PV, Jarvinen M, Miyashita M. In Vivo Achilles Tendon Loading During Jumping in Humans. *Eur J Appl Physiol Occup Physiol*. 1995; 71(5):453-458.

57. Fukashiro S, Kurokawa S, Hay D, Nagano A. Comparison of Muscle-Tendon Ineraction of Human M. Gastrocnemius between Ankle- and Drop-Jumping. *International Journal of Sport and Health Science*. 2005; 3:253-263.

58. Fukunaga T, Kawakami Y, Kubo K, Kanehisa H. Muscle and Tendon Interaction During Human Movements. *Exerc Sport Sci Rev*. 2002; 30(3):106-110.

59. Fukunaga T, Kubo K, Kawakami Y, Fukashiro S, Kanehisa H, Maganaris CN. In Vivo Behaviour of Human Muscle Tendon During Walking. *Proc Biol Sci*. 2001; 268(1464):229-233.

60. Gerritsen KG, van den Bogert AJ, Nigg BM. Direct Dynamics Simulation of the Impact Phase in Heel-Toe Running. *J Biomech*. 1995; 28(6):661-668.

61. Gordon AM, Huxley AF, Julian FJ. The Variation in Isometric Tension with Sarcomere Length in Vertebrate Muscle Fibres. *J Physiol*. 1966; 184(1):170-192.

62. Griffin TM, Roberts TJ, Kram R. Metabolic Cost of Generating Muscular Force in Human Walking: Insights from Load-Carrying and Speed Experiments. *J Appl Physiol*. 2003; 95(1):172-183.

63. Grimston SK, Engsberg JR, Kloiber R, Hanley DA. Bone Mass, External Loads, and Stress Fracture in Female Runners. *International Journal of Sport Biomechanics*. 1991; 7(3):293-302.

64. Gutmann AK, Jacobi B, Butcher MT, Bertram JE. Constrained Optimization in Human Running. *J Exp Biol*. 2006; 209(Pt 4):622-632.

65. Hamill J, Bates BT, Knutzen KM, Sawhill JA. Variations in Ground Reaction Force Parameters at Different Running Speeds. *Human Movement Science*. 1983; 2(1-2):47-56.

66. Hamill J, Derrick TR, Holt KG. Shock Attenuation and Stride Frequency During Running. *Human Movement Science*. 1995; 14:45-60.

67. Hamill J, Derrick TR, McClay I. Joint Stiffness During Running with Different Footfall Patterns. XIth Congress of the Canadian Society of Biomechanics. 2000a.

68. Hamill J, Gruber AH, Russell EM, Miller RH, Van Emmerik REA. Does Changing Footfall Pattern Alter Running Performance? Proceedings of the 6th World Congress of Biomechanics. 2010. 238.

69. Hamill J, Haddad JM, McDermott WJ. Issues in Quantifying Variability from a Dynamical Systems Perspective. *J App Biomech*. 2000b; 16(4):407-418.

70. Harrison RN, Lees A, McCullagh PJ, Rowe WB. A Bioengineering Analysis of Human Muscle and Joint Forces in the Lower Limbs During Running. *J Sports Sci*. 1986; 4(3):201-218.

71. Hasegawa H, Yamauchi T, Kraemer WJ. Foot Strike Patterns of Runners at the 15-Km Point During an Elite-Level Half Marathon. *J Strength Cond Res*. 2007; 21(3):888-893.

72. Hatze H. A Three-Dimensional Multivariate Model of Passive Human Joint Torques and Articular Boundaries. *Clin Biomech (Bristol, Avon)*. 1997; 12(2):128-135.

73. Heise GD and Martin PE. "Leg Spring" Characteristics and the Aerobic Demand of Running. *Med Sci Sports Exerc*. 1998; 30(5):750-754.

74. Heise GD and Martin PE. Are Variations in Running Economy in Humans Associated with Ground Reaction Force Characteristics? *Eur J Appl Physiol*. 2001; 84(5):438-442.

75. Heise GD, Smith JD, Martin PE. Lower Extremity Mechanical Work During Stance Phase of Running Partially Explains Interindividual Variability of Metabolic Power. *Eur J Appl Physiol*. 2011; 111(8):1777-1785.

76. Hennig EM and Lafortune MA. Relationships between Ground Reaction Force and Tibial Bone Acceleration Parameters. *Int J Sports Biomech*. 1991; 7:303-309.

77. Hill AV. The Heat of Shortening and the Dynamic Constants of Muscle. *Proc Royal Soc*. 1938; 126B:136-195.

78. Hof AL, Geelen BA, Van den Berg J. Calf Muscle Moment, Work and Efficiency in Level Walking; Role of Series Elasticity. *J Biomech*. 1983; 16(7):523-537.

79. Hof AL, Van Zandwijk JP, Bobbert MF. Mechanics of Human Triceps Surae Muscle in Walking, Running and Jumping. *Acta Physiol Scand*. 2002; 174(1):17-30.

80. Hreljac A, Marshall RN, Hume PA. Evaluation of Lower Extremity Overuse Injury Potential in Runners. *Med Sci Sports Exerc*. 2000; 32(9):1635-1641.

81. Huxley AF. Muscular Contraction. *J Physiol*. 1974; 243(1):1-43.

82. Ishikawa M, Komi PV, Grey MJ, Lepola V, Bruggemann GP. Muscle-Tendon Interaction and Elastic Energy Usage in Human Walking. *J Appl Physiol*. 2005; 99(2):603-608.

83. Ishikawa M, Pakaslahti J, Komi PV. Medial Gastrocnemius Muscle Behavior During Human Running and Walking. *Gait Posture*. 2007; 25(3):380-384.

84. Kerr BA, Beauchamp L, Fisher V, Neil R. Footstrike Patterns in Distance Running. In: *Biomechanical Aspects of Sport Shoes and Playing Surfaces*. Nigg BMand Kerr B (Eds.). University of Calgary Press, Calgary, 1983.

85. Klein Horsman MD, Koopman HF, van der Helm FC, Prose LP, Veeger HE. Morphological Muscle and Joint Parameters for Musculoskeletal Modelling of the Lower Extremity. *Clin Biomech (Bristol, Avon)*. 2007; 22(2):239-247.

86. Kram R. Muscular Force or Work: What Determines the Metabolic Energy Cost of Running? *Exerc Sport Sci Rev*. 2000; 28(3):138-143.

87. Kurokawa S, Fukunaga T, Fukashiro S. Behavior of Fascicles and Tendinous Structures of Human Gastrocnemius During Vertical Jumping. *J Appl Physiol*. 2001; 90(4):1349-1358.

88. Lafortune MA, Hennig EM, Lake MJ. Dominant Role of Interface over Knee Angle for Cushioning Impact Loading and Regulating Initial Leg Stiffness. *J Biomech*. 1996a; 29(12):1523-1529.

89. Lafortune MA, Lake MJ, Hennig E. Transfer Function between Tibial Acceleration and Ground Reaction Force. *J Biomech*. 1995; 28(1):113-117.

90. Lafortune MA, Lake MJ, Hennig EM. Differential Shock Transmission Response of the Human Body to Impact Severity and Lower Limb Posture. *J Biomech*. 1996; 29(12):1531-1537.

91. Laughton CA, Davis IS, Hamill J. Effect of Strike Pattern and Orthotic Intervention on Tibial Shock During Running. *J App Biomech*. 2003; 19:153-168.

92. Leadbetter WB. Cell-Matrix Response in Tendon Injury. *Clin Sports Med*. 1992; 11(3):533-578.

93. Lichtwark GA and Wilson AM. A Modified Hill Muscle Model That Predicts Muscle Power Output and Effeciency During Sinusoidal Length Changes. *J Exp Biol*. 2005a; 208(Pt 15):2831-2843.

94. Lichtwark GA and Wilson AM. Effects of Series Elasticity and Activation Conditions on Muscle Power Output and Effeciency. *J Exp Biol*. 2005b; 208(Pt 15):2845-2853.

95. Lichtwark GA and Wilson AM. Interactions between the Human Gastrocnemius Muscle and the Achilles Tendon During Incline, Level and Decline Locomotion. *J Exp Biol*. 2006; 209(Pt 21):4379-4388.

96. Lichtwark GA and Wilson AM. Muscle Fascicle and Series Elastic Element Length Changes Along the Length of the Human Gastrocnemius During Walking and Running. *J Biomech*. 2007a; 40(1):157-164.

97. Lichtwark GA and Wilson AM. Is Achilles Tendon Compliance Optimised for Maximum Muscle Efficiency During Locomotion? *J Biomech*. 2007b; 40(8):1768-1775.

98. Lichtwark GA and Wilson AM. Optimal Muscle Fascicle Length and Tendon Stiffness for Maximising Gastrocnemius Efficiency During Human Walking and Running. *J Theor Biol*. 2008; 252(4):662-673.

99. Lieberman DE, Venkadesan M, Werbel WA, Daoud AI, D'Andrea S, Davis IS, Mang'eni RO, Pitsiladis Y. Foot Strike Patterns and Collision Forces in Habitually Barefoot Versus Shod Runners. *Nature*. 2010; 463(7280):531-535.

100. Luethi SM, Denoth J, Kaelin X, Stacoff A. The Influence of Shoe and Foot Movement and Shock Attenuation in Running. In: *Biomechanics X-B*. Jonsson B (Ed.). Human Kinetics, Champaign, IL:, 1987. 921-935.

101. Maganaris CN, Baltzopoulos V, Sargeant AJ. In Vivo Measurement-Based Estimations of the Human Achilles Tendon Moment Arm. *Eur J Appl Physiol*. 2000; 83(4 -5):363-369.

102. Marti B, Vader JP, Minder CE, Abelin T. On the Epidemiology of Running Injuries. The 1984 Bern Grand-Prix Study. *Am J Sports Med*. 1988; 16(3):285-294.

103. Martin DE and Cole PN. Better Training for Distance Runners. Human Kinetics, Champaign, IL, 1991.

104. Martin PE and Morgan DW. Biomechanical Considerations for Economical Walking and Running. *Med Sci Sports Exerc*. 1992; 24(4):467-474.

105. Mason B. Unpublished doctoral dissertation, University of Oregon, Eugene, Oregon, 1980.

106. McClay I and Manal K. Lower Extremity Kinematic Comparisons between Forefoot and Rearfoot Strikers. 19th Annual Meeting of the American Society of Biomechanics. 1995a. 211-212.

107. McClay I and Manal K. Lower Extremity Kinetic Comparisons between Forefoot and Rearfoot Strikers. 19th Annual Meeting of the American Society of Biomechanics. 1995b. 213-214.

108. McCrory JL, Martin DF, Lowery RB, Cannon DW, Curl WW, Read HM, Jr., Hunter DM, Craven T, Messier SP. Etiologic Factors Associated with Achilles Tendinitis in Runners. *Med Sci Sports Exerc*. 1999; 31(10):1374-1381.

109. McLeod KJ and Rubin CT. Frequency Specific Modulation of Bone Adaptation by Induced Electric Fields. *J Theor Biol*. 1990; 145(3):385-396.

110. McMahon TA and Green PR. The Influence of Track Compliance of Running. In: *Sports Shoes and Playing Surfaces*. Frederick EC (Ed.). Human Kinetics, Champaign, IL, 1984. 138-162.

111. McMahon TA, Valiant G, Frederick EC. Groucho Running. *J Appl Physiol*. 1987; 62(6):2326-2337.

112. McNeill Alexander R. Energetics and Optimization of Human Walking and Running: The 2000 Raymond Pearl Memorial Lecture. *Am J Hum Biol*. 2002; 14(5):641-648.

113. Mercer JA, Devita P, Derrick TR, Bates BT. Individual Effects of Stride Length and Frequency on Shock Attenuation During Running. *Med Sci Sports Exerc*. 2003; 35(2):307-313.

114. Messier SP, Davis SE, Curl WW, Lowery RB, Pack RJ. Etiologic Factors Associated with Patellofemoral Pain in Runners. *Med Sci Sports Exerc*. 1991; 23(9):1008-1015.

115. Miller RH and Hamill J. Footfall Pattern Selection for the Performance of Various Running Tasks. *J App Biomech*. 2012; In Review XX(X):XX-XX.

116. Milner CE, Ferber R, Pollard CD, Hamill J, Davis IS. Biomechanical Factors Associated with Tibial Stress Fracture in Female Runners. *Med Sci Sports Exerc*. 2006; 38(2):323-328.

117. Minetti AE and Alexander RM. A Theory of Metabolic Costs for Bipedal Gaits. *J Theor Biol*. 1997; 186(4):467-476.

118. Minetti AE, Moia C, Roi GS, Susta D, Ferretti G. Energy Cost of Walking and Running at Extreme Uphill and Downhill Slopes. *J Appl Physiol*. 2002; 93(3):1039-1046.

119. Morgan DW, Craib MW, Krahenbuhl GS, Woodall K, Jordan S, Filarski K, Burleson C, Williams T. Daily Variability in Running Economy among Well-Trained Male and Female Distance Runners. *Res Q Exerc Sport*. 1994a; 65(1):72-77.

120. Morgan DW, Martin P, Craib M, Caruso C, Clifton R, Hopewell R. Effect of Step Length Optimization on the Aerobic Demand of Running. *J Appl Physiol*. 1994b; 77(1):245-251.

121. Morgan DW, Martin PE, Krahenbuhl GS. Factors Affecting Running Economy. *Sports Med*. 1989; 7(5):310-330.

122. Nevill AM, Ramsbottom R, Williams C. Scaling Physiological Measurements for Individuals of Different Body Size. *Eur J Appl Physiol Occup Physiol*. 1992; 65(2):110-117.

123. Nigg BM. External Force Measurements with Sport Shoes and Playing Surfaces. In: *Biomechanical Aspects of Sport Shoes and Playing Surfaces*. Nigg BMand Kerr B (Eds.). Univeristy of Calgary Press, Calgary, 1983. 11-23.

124. Nigg BM. Biomechanical Aspects of Running. In: *Biomechanics of Running Shoes*. Nigg BM (Ed.). Human Kinetics, Champaign, IL, 1986. 15-19.

125. Nigg BM. Impact Forces in Running. *Current Opinion in Orthopedics*. 1997; 8(6):43-47.

126. Nigg BM. The Role of Impact Forces and Foot Pronation: A New Paradigm. *Clin J Sport Med*. 2001; 11(1):2-9.

127. Nigg BM. Impact Forces. In: *Biomechanics of Sport Shoes*. Nigg BM (Ed.). Univeristy of Calgary Press, Calgary, 2011. 1-35.

128. Nigg BM, Bahlsen HA, Luethi SM, Stokes S. The Influence of Running Velocity and Midsole Hardness on External Impact Forces in Heel-Toe Running. *J Biomech*. 1987; 20(10):951-959.

129. Nigg BM, Cole GK, Bruggemann GP. Impact Forces During Heel Toe Running. *J Appl Biomech*. 1995; 11:407-432.

130. Nigg BM, Denoth J, Kerr B, Luethi S, Smith D, Stacoff A. Load Sport Shoes and Playing Surfaces. In: *Sports Shoes and Playing Surfaces*. Frederick EC (Ed.). Human Kinetics, Champaign, IL, 1984. 1-23.

131. Nigg BM, Denoth J, Neukomm PA. Quantifying the Load on the Human Body: Problems and Some Possible Solutions. In: *Biomechanics Vii*. Morecki A et al. (Eds.). University Park Press, Baltimore, MD, 1981. 88-89.

132. Nilsson J and Thorstensson A. Ground Reaction Forces at Different Speeds of Human Walking and Running. *Acta Physiol Scand*. 1989; 136(2):217-227.

133. Novacheck TF. The Biomechanics of Running. *Gait Posture*. 1998; 7(1):77-95.

134. Oakley T and Pratt DJ. Skeletal Transients During Heel and Toe Strike Running and the Effectiveness of Some Materials in Their Attenuation. *Clin Biomech (Bristol, Avon)*. 1988; 3(3):159-165.

135. Paul IL, Munro MB, Abernethy PJ, Simon SR, Radin EL, Rose RM. Musculo-Skeletal Shock Absorption: Relative Contribution of Bone and Soft Tissues at Various Frequencies. *J Biomech*. 1978; 11(5):237-239.

136. Payne AH. Foot to Ground Contact Forces of Elite Runners. In: *Biomechanics Viii-B*. Matsui Hand Kobayashi K (Eds.). Human Kinetics, Champaign, IL, 1983. 748-753.

137. Perl DP, Daoud AI, Lieberman DE. Effects of Footwear and Strike Type on Running Economy. *Med Sci Sports Exerc*. 2012; 44(7):1335-1343.

138. Perry SD and Lafortune MA. Influences of Inversion/Eversion of the Foot Upon Impact Loading During Locomotion. *Clin Biomech (Bristol, Avon)*. 1995; 10(5):253-257.

139. Pohl MB, Mullineaux DR, Milner CE, Hamill J, Davis IS. Biomechanical Predictors of Retrospective Tibial Stress Fractures in Runners. *J Biomech*. 2008; 41(6):1160-1165.

140. Potthast W, Bruggemann GP, Lundberg A, Arndt A. The Influences of Impact Interface, Muscle Activity, and Knee Angle on Impact Forces and Tibial and Femoral Accelerations Occurring after External Impacts. *J Appl Biomech*. 2010; 26(1):1-9.

141. Pozzo T, Berthoz A, Lefort L, Vitte E. Head Stabilization During Various Locomotor Tasks in Humans. Ii. Patients with Bilateral Peripheral Vestibular Deficits. *Exp Brain Res*. 1991; 85(1):208-217.

142. Pratt DJ. Mechanisms of Shock Attenuation Via the Lower Extremity During Running. *Clin Biomech (Bristol, Avon)*. 1989; 4(1):51-57.

143. Radin EL. The Physiology and Degeneration of Joints. *Semin Arthritis Rheum*. 1972; 2(3):245-257.

144. Radin EL, Parker HG, Pugh JW, Steinberg RS, Paul IL, Rose RM. Response of Joints to Impact Loading. 3. Relationship between Trabecular Microfractures and Cartilage Degeneration. *J Biomech*. 1973; 6(1):51-57.

145. Radin EL and Paul IL. Does Cartilage Compliance Reduce Skeletal Impact Loads? The Relative Force-Attenuating Properties of Articular Cartilage, Synovial Fluid, Periarticular Soft Tissues and Bone. *Arthritis Rheum*. 1970; 13(2):139-144.

146. Rall JA. Energetic Aspects of Skeletal Muscle Contraction: Implications of Fiber Types. *Exerc Sport Sci Rev*. 1985; 13:33-74.

147. Ratcliffe RJ and Holt KG. Low Frequency Shock Absorption in Human Walking. *Gait & Posture*. 1997; 5(2):93-100.

148. Roberts TJ. The Integrated Function of Muscles and Tendons During Locomotion. *Comp Biochem Physiol A Mol Integr Physiol*. 2002; 133(4):1087-1099.

149. Roberts TJ, Kram R, Weyand PG, Taylor CR. Energetics of Bipedal Running. I. Metabolic Cost of Generating Force. *J Exp Biol*. 1998; 201(Pt 19):2745-2751.

150. Roberts TJ, Marsh RL, Weyand PG, Taylor CR. Muscular Force in Running Turkeys: The Economy of Minimizing Work. *Science*. 1997; 275(5303):1113-1115.

151. Romanov N. Pose Method of Running. Pose Tech Corporation, Coral Gables, FL, 2002.

152. Sasaki K, Neptune RR, Kautz SA. The Relationships between Muscle, External, Internal and Joint Mechanical Work During Normal Walking. *J Exp Biol*. 2009; 212(Pt 5):738-744.

153. Scholz MN, Bobbert MF, van Soest AJ, Clark JR, van Heerden J. Running Biomechanics: Shorter Heels, Better Economy. *J Exp Biol*. 2008; 211(Pt 20):3266-3271.

154. Scott SH and Winter DA. Internal Forces of Chronic Running Injury Sites. *Med Sci Sports Exerc*. 1990; 22(3):357-369.

155. Sellers WI, Dennis LA, Crompton RH. Predicting the Metabolic Energy Costs of Bipedalism Using Evolutionary Robotics. *J Exp Biol*. 2003; 206(Pt 7):1127-1136.

156. Shorten M and Mientjes M. The Effects of Shoe Cushioning on Impact Force During Running. 6th symposium on footwear biomechanics. 2003.

157. Shorten MR and Winslow DS. Spectral Analysis of Impact Shock During Running. *Int J Sports Biomech*. 1992; 8:288-304.

158. Shorter F. Running for Peak Performance. Dorling Kindersley Publishing, New York, NY, 2005.

159. Sih BL and Stuhmiller JH. The Metabolic Cost of Force Generation. *Med Sci Sports Exerc*. 2003; 35(4):623-629.

160. Simon SR, Paul IL, Mansour J, Munro M, Abernethy PJ, Radin EL. Peak Dynamic Force in Human Gait. *J Biomech*. 1981; 14(12):817-822.

161. Simon SR, Radin EL, Paul IL, Rose RM. The Response of Joints to Impact Loading. Ii. In Vivo Behavior of Subchondral Bone. *J Biomech*. 1972; 5(3):267-272.

162. Slavin M and Hamill J. Alterations in Footstrike Pattern in Distance Running. The Xth Symposium of the International Society of Biomechanics In Sports. 1992. 53-57.

163. Slavin MM. The Effects of Foot Strike Pattern Alteration on Efficiency in Skilled Runners. M.S. thesis, University of Massachusetts, Amherst, MA, 1992.

164. Stackhouse CL, Davis IM, Hamill J. Orthotic Intervention in Forefoot and Rearfoot Strike Running Patterns. *Clin Biomech (Bristol, Avon)*. 2004; 19(1):64-70.

165. Umberger BR, Gerritsen KG, Martin PE. A Model of Human Muscle Energy Expenditure. *Comput Methods Biomech Biomed Engin*. 2003; 6(2):99-111.

166. van den Bogert AJ, Gerritsen KG, Cole GK. Human Muscle Modelling from a User's Perspective. *J Electromyogr Kinesiol*. 1998; 8(2):119-124.

167. Voloshin A and Wosk J. An in Vivo Study of Low Back Pain and Shock Absorption in the Human Locomotor System. *J Biomech*. 1982; 15(1):21-27.

168. Voloshin A, Wosk J, Brull M. Force Wave Transmission through the Human Locomotor System. *J Biomech Eng*. 1981; 103(1):48-50.

169. Voloshin AS, Burger CP, Wosk J, Arcan M. An in Vivo Evaluation of the Leg's Shock Absorbing Capacity. In: *Biomechanics Ix-B* Winter D et al. (Eds.). Human Kinetics, Champaign, IL:, 1985. 112-116.

170. Wakeling JM, Von Tscharner V, Nigg BM, Stergiou P. Muscle Activity in the Leg Is Tuned in Response to Ground Reaction Forces. *J Appl Physiol*. 2001b; 91(3):1307-1317.

171. Ward SR, Eng CM, Smallwood LH, Lieber RL. Are Current Measurements of Lower Extremity Muscle Architecture Accurate? *Clin Orthop Relat Res*. 2009; 467(4):1074-1082.

172. Wickiewicz TL, Roy RR, Powell PL, Edgerton VR. Muscle Architecture of the Human Lower Limb. *Clin Orthop Relat Res*. 1983; (179):275-283.

173. Wickler SJ, Hoyt DF, Cogger EA, Hirschbein MH. Preferred Speed and Cost of Transport: The Effect of Incline. *J Exp Biol*. 2000; 203(Pt 14):2195-2200.

174. Wilkie DR. The Relation between Force and Velocity in Human Muscle. *J Physiol*. 1950; 110:249-280.

175. Williams DS, McClay IS, Manal KT. Lower Extremity Mechanics in Runners with a Converted Forefoot Strike Pattern. *J App Biomech*. 2000; 16(2):210-218.

176. Williams KR. Relationship between Distance Running Biomechanics and Running Economy. In: *Biomechanics of Distance Running*. Cavanagh PR (Ed.). Human Kinetics, Champaign, IL, 1990. 271-306.

177. Williams KR and Cavanagh PR. Relationship between Distance Running Mechanics, Running Economy, and Performance. *J Appl Physiol*. 1987; 63(3):1236-1245.

178. Winter DA. Moments of Force and Mechanical Power in Jogging. *Journal of Biomechanics*. 1983; 16(1):91-97.

179. Wosk J and Voloshin A. Wave Attenuation in Skeletons of Young Healthy Persons. *J Biomech*. 1981; 14(4):261-267.

180. Wright IC, Neptune RR, van Den Bogert AJ, Nigg BM. Passive Regulation of Impact Forces in Heel-Toe Running. *Clin Biomech (Bristol, Avon)*. 1998; 13(7):521-531.

181. Yessis M. Explosive Running. McGraw-Hill, Columbus, OH, 2000.

182. Zajac FE. Muscle and Tendon: Properties, Models, Scaling, and Application to Biomechanics and Motor Control. *Crit Rev Biomed Eng*. 1989; 17(4):359-411.

183. Zifchock RA, Davis IS, Hamill J. Kinetic Asymmetry in Female Runners with and without Retrospective Tibial Stress Fractures. *J Biomech*. 2006; 39(15):2792-2797.

CHAPTER 3

METHODOLOGY

General Introduction

The purpose of this dissertation was to investigate the potential advantages of altering running footfall patterns to improve running economy and reduce the risk of injury. The aims were to examine the musculoskeletal and mechanical as determinants for running economy and risk of developing running related injuries. Additionally, this dissertation aimed to determine the potential advantages of altering from a preferred footfall pattern. Two groups of participants were recruited to participate in this dissertation: 1) natural rearfoot (RF) runners and 2) natural forefoot (FF) runners. Four studies were developed to satisfy the aims of the study.

Study 1 determined the difference in metabolic cost between footfall patterns and determined if there was an economical advantage of adopting the alternate footfall pattern. Previous studies have not found a difference in rate of oxygen consumption between RF and FF patterns or had methodological limitations (Ardigo et al., 1995; Cunningham et al., 2010). Study 1 addressed the differences in rate of oxygen consumption and cost of transport between footfall patterns by comparing runners who habitually perform RF or FF footfall patterns. Additionally, Study 1 determined if there was an advantage for each group to switch to the alternate footfall pattern to improve running economy.

Anthropometric and mechanical differences may influence the metabolic cost of performing each footfall pattern. It has previously been observed that individuals with

shorter Achilles tendon moment arms have greater running economy than those with longer moment arms (Scholz et al., 2008). Since the Achilles tendon moment arm is longest when the ankle is plantar flexed (Maganaris et al., 2000), the FF pattern may be less economical because of its characteristic plantar flexed ankle position at initial contact and throughout stance. Study 2 investigated the length of the Achilles tendon moment arm during standing and during the stance phase of running between the RF and FF running patterns. Additionally, due to increased ankle joint moments and suspected eccentric work during FF running, some have speculated FF running may place increased stress on the Achilles tendon (Nilsson and Thorstensson, 1989). Therefore, Study 2 also determined the force transmitted through the Achilles tendon.

FF running pattern has been suggested to result in greater utilization of elastic energy which may result in an improvement in running economy (Ardigo et al., 1995; Hasegawa et al., 2007; Nilsson and Thorstensson, 1989; Perl et al., 2012; Pratt, 1989). RF running results in concentric force production at low shortening velocities and small changes in fascicle length during the stance phase (Hof et al., 2002; Lichtwark and Wilson, 2005d,2007). Low contraction velocities allow for more efficient force production at a reduced metabolic cost than higher shortening velocities; however, a greater metabolic advantage would occur if the muscle fascicles remained isometric (Biewener and Roberts, 2000; Fenn, 1924; Huxley, 1974; Rall, 1985; Roberts et al., 1997). Since a mid-foot (MF) pattern has been shown to produce force isometrically (Hof et al., 2002), the FF pattern may also result in more optimal work production than RF running. Therefore, Study 3 investigated the function of the triceps surae muscle to uncover the mechanical and energetic differences between footfall patterns.

Previous studies have indicated that runners optimize for metabolic cost rather than impact shock attenuation which may lead to an increased risk of impact related injuries at the expense of improved performance (Hamill et al., 1995). Study 4 determined the difference in impact shock attenuation and the frequency content of the vertical ground reaction force (GRF) between footfall patterns. Differences in these parameters between footfall patterns may alter how the impact shock wave is attenuated through the body.

Study 1: Is there a difference in running economy between rearfoot and forefoot running patterns?

Introduction

The purpose of Study 1 was to determine the difference in running economy (i.e. lowest sub-maximal rate of oxygen consumption) between footfall patterns and if there was an improvement in running economy for either natural RF or natural FF runners when performing the alternate footfall pattern. Comparisons were made between two groups: 1) natural RF runners and 2) natural FF runners.

Participant Selection

A priori sample size estimation was performed using the cost of transport data during running from Cunningham et al. (2010). A sample size of 20 for each group was selected to provide a minimum statistical power of 0.8 with the alpha value of 0.05.

For inclusion into the study, participants had to be experienced runners completing a minimum of 16 km per week with an average speed of approximately 3.5 $m \cdot s^{-1}$ for long running bouts. Participants were included if they were a healthy male or female, ages 18 – 45 yrs, and had not experienced an injury to the lower extremity or lumbar region within the past year. Exclusion criteria included: 1) currently smoking cigarettes; 2) neurological disease or injury and lightheadedness or dizziness with exercise; 3) cardiovascular problems including heart attack, high cholesterol, uncontrolled high blood pressure, pace maker, coronary artery disease, peripheral artery disease, chest pain with exercise; 4) musculoskeletal injury or surgery to the lower extremity or back within the past 1 year; and 5) other health problems including cancer, diabetes, vision problems, etc. Each participant gave written approval to participate in accordance with the University of Massachusetts Institutional Review Board policies.

Participants were classified into the natural RF group or the natural FF group by the footfall pattern they habitually perform during runs longer than one mile. The natural footfall pattern was determined by the investigator recording vertical ground reaction forces (GRF) and high speed video of each participant while running over-ground at their preferred running speed. RF running was defined as making initial contact with the heel. FF running was defined as making initial contact on the metatarsal heads and preventing the heel from contacting the ground. Participants who exhibited a MF pattern were placed in the RF or FF groups based on their ankle kinematics and GRF. Natural MF runners were classified into the RF group if they made contact with a flat foot position (approximately zero degrees of dorsiflexion) and generated an initial impact peak within the vertical GRF component (n = 5). MF participants were classified into the FF group if

they landed on the metatarsal heads but allowed the heel to touch the ground (foot position approximately below zero degrees, i.e. plantar flexion) and did not generate an initial impact peak (n = 6).

Participants data were excluded from the analysis if they were unable to run comfortably until sufficient steady state oxygen consumption was collected for a given footfall pattern or speed or if some anomaly in the data was detected. Data from other speed conditions were not excluded if the participant performed both footfall patterns comfortably within that speed and sufficient oxygen consumption data were collected. Twenty RF runners were collected, however, but only 19 were included in the analysis. Specifically, data from 18/20 RF group participants were included in the analysis for the slow speed, 19/20 analyzed for the medium speed, and 17/20 analyzed for the fast speed. In the FF group, 21 participants were collected; however, one participant was excluded because they could not comfortably perform each footfall pattern at the medium or fast speeds, one participant had unusual data, and one participant was excluded for misclassification into the FF group. Therefore, data from 18 FF group participants were used in the analysis for the slow and medium speeds and 17/18 participants were analyzed for the fast speed.

Experimental Setup

The volume and content of gases expired by each participant while running on a motorized treadmill was measured by indirect calorimetry using a metabolic cart (TrueOne, ParvoMedics, Sandy, UT, USA). The volume of gas exchange was used to calculate the gross rate of oxygen consumption. Three-dimensional motion of reflective

markers placed on the right foot and leg (McClay and Manal, 1999) (Appendix B) were recorded by an eight-camera Qualisys Oqus 3-Series optical motion capture system (Qualisys, Inc., Gothenberg, Sweden) sampling at 240 Hz. A treadmill was placed in the center of the motion capture collection volume. Camera calibration was performed to define a right-hand laboratory coordinate system. A wand with two markers separated by a known length was used to scale the perspective of individual camera views to the collection volume in reference to a 90^{o} rigid frame to define the origin. The corner of the frame was placed at the edge of the treadmill to define the X and Y axes as mediolateral and anteroposterior axes respectively. Motion capture data were used to monitor the footfall pattern used by the participants during each condition. Calibration markers included the medial and lateral femoral condyles, medial and lateral malleoli, and the heads of the first and fifth metatarsals. Calibration markers were used to determine segment local coordinate systems, segment origins, segment length and joint center locations. The long axis of the thigh and leg were defined as the distance between the proximal and distal joint centers. The long axis of the foot was defined as the distance between the ankle joint center and the center of the metatarsal calibration markers. Tracking markers included a rigid plate with three non-collinear markers placed on the posterior calcaneus. Tracking markers were used to measure the marker movements in space by determining deviations from the standing calibration. Marker tracking was completed by calculating the transformation of the markers to the position and orientation of each segment. A standing calibration trial was collected with the participant in quiet stance in order to orient the local coordinate system in the laboratory coordinate system. Calibration markers were removed prior to performing the movement trials. Each

participant wore a neutral racing flat running shoe provided by the laboratory to standardize any effects of cushioning and other footwear properties (RC 550, New Balance, Brighton, MA, USA).

Protocol

Each participant refrained from caffeine consumption and was fasted for at least three hours prior to arrival for the test session. Upon arrival at the laboratory, participants completed: 1) an informed consent form; 2) a Physical Activity Readiness Questionnaire (PAR-Q); and 3) a demographic information form. If a participant answered "Yes" to any question on the PAR-Q, they were immediately excluded from the study. The test session began with measurements of body mass and height. Each participant was allowed to warm-up on the treadmill for several minutes as needed and also practiced each footfall pattern at a slow, medium, and fast speed which were 3.0, 3.5 and 4.0 $m \cdot s^{-1}$, respectively. Running speed was adjusted by ±5% if necessary to allow the participant to run more comfortably. The participant was then prepared for data collection by securing the reflective markers onto the right leg and foot and then the standing calibration was recorded. Each participant began the data collection by standing quietly for 10 minutes on the treadmill to record baseline oxygen consumption. Next, the participant performed each footfall pattern within one speed condition before continuing to the next speed condition. The order of the footfall patterns and running speeds was randomized. Each participant ran for a minimum of five minutes during each speed and footfall pattern condition or until two minutes of steady state oxygen consumption was recorded. Steady state was attained when there was less than a 10% change in oxygen

consumption over a two minute period (Stephens et al., 2006). Each participant rested until the volume of expired air returned within 0.02 $L \bullet min^{-1}$ of the baseline value.

The most appropriate speed to assess running economy is currently unknown. However, Williams (1990) suggests that any change resulting in a reduction of sub-maximal oxygen consumption over a range of speeds would be sufficient to detect in an improvement in running economy.

Data Reduction

The absolute ($L \bullet min^{-1}$) and relative ($ml \bullet kg^{-1} \bullet min^{-1}$) rates of steady state oxygen consumption ($\dot{V}O_2$) over the last two minutes of each condition was averaged to determine the net and gross $\dot{V}O_2$ and cost of transport (COT). The first five minutes of the baseline oxygen consumption measure was typically highly variable as the participants became accustom to breathing with the mouthpiece. As a result, the average rate of oxygen consumption over the last five minutes of the baseline period was used to calculate net $\dot{V}O_2$ and COT by subtracting the baseline value from the average rate of oxygen consumption during the last two minutes of each running condition. Absolute ($J \bullet m^{-1}$) and relative ($J \bullet m^{-1} \bullet kg^{-1}$) COT were first calculated by converting the relative rate of oxygen consumption ($ml \bullet kg^{-1} \bullet min^{-1}$) to metabolic rate ($W \bullet kg^{-1}$) by (Weir, 1949):

$$\text{Metabolic rate} = \dot{V}O_2 * \frac{(3.876 + \text{RER} * 1.2411)}{1000} * \frac{4184}{60} \quad (3.1)$$

where $\dot{V}O_2$ is the rate of oxygen consumption in $ml \bullet kg^{-1} \bullet min^{-1}$, RER was the respiratory exchange ratio calculated by volume of carbon dioxide expired divided by the volume of

oxygen consumed averaged over the last two minutes of steady state, 3.876 was the number of kcals expended per liter of oxygen consumed, 1.2411 kcals expended per liter of carbon dioxide expired, and 4184 was the number of Joules (J) per kcal, 1000 ml•L^{-1}, and 60 s•min^{-1}. COT was then determined by dividing metabolic rate by the velocity of the treadmill belt.

Absolute rate of carbohydrate oxidation (gCHO) in g•hr^{-1} was determined from the volume of carbon dioxide expired and the volume of oxygen consumed by (McArdle et al., 2001):

$$gCHO = (4.58\ \dot{V}CO_2 - 3.23\ \dot{V}O_2) * 60 \quad (3.2).$$

Relative carbohydrate oxidation (%CHO) was expressed as the percentage of energy expenditure resulting from carbohydrate oxidation was calculated from $\dot{V}O_2$ in L•min^{-1} and gCHO:

$$\%CHO = \frac{g\ CHO * 4\ kcal \bullet g^{-1}}{5\ kcal \bullet L^{-1} \bullet VO_2^{-1} * L\ VO_2 \bullet min^{-1}} * 100 \quad (3.3)$$

where 4 kcal•g^{-1} is the number of kcals liberated from oxidizing 1 g of CHO and 5 kcal•L^{-1} is the number of kcals expended per liter of oxygen consumed.

The 3D positions of the markers placed on the foot and leg were tracked using Qualisys Track Manager software (Qualisys, Inc., Gothenberg, Sweden). The data were exported in .C3D format to calculate sagittal plane ankle joint angles at touchdown (AATD) using Visual 3D software (C-Motion, Inc, Rockville, MD, USA). Raw

kinematic data were filtered with a 4th order, zero-lag Butterworth digital low-pass filter with a cutoff frequency of 12 Hz (Winter et al., 1974). Ankle joint angle was calculated by a rotation matrix of the distal segment with respect to the coordinate system of the proximal segment using a Cardan rotation sequence of x (dorsiflexion/plantar flexion) – y (eversion/inversion) – z (axial rotation) (Cole et al., 1993). Stride frequency (SF) was calculated as the number of strides occurring during the 15 s motion capture period and multiplied by four to result in units of strides per minute. Stride length (SL) was calculated by dividing the treadmill belt speed by SF. Contact time (CT) was calculated for each stance phase as the time between initial impact and toe-off of the right foot.

Statistical Analysis

The kinematic variables that were assessed included the AATD, SL, SF and CT. The running economy variables assessed included net absolute and relative steady state $\dot{V}O_2$, gross absolute and relative $\dot{V}O_2$, net absolute and relative COT, and gross absolute and relative COT, gCHO, and %CHO. Each variable was subjected to a mixed model analysis of variance (ANOVA) with footfall pattern and group as fixed variables and participant nested within group as a random variable. The differences between footfall patterns (2 levels) and between groups (2 levels) and the interaction of footfall pattern and group were assessed with a significance level of $\alpha = 0.05$. When a significant group by pattern interaction was observed, a post-hoc assessment was performed by partitioning the interaction by group and by pattern. Partitioning by group determined the significance between each footfall pattern within each group. Partitioning by pattern determined the significance between groups within each footfall pattern. A one-way

ANOVA was used to determine the differences in running economy variables between groups at baseline and each speed when performing their preferred pattern ($\alpha = 0.05$). Effect sizes were also calculated to determine if the differences between footfall pattern and groups were biologically meaningful. An effect size (d) lower than 0.4 indicated a small effect, an effect size between 0.5 and 0.7 indicated a moderate effect and an effect size greater than 0.8 indicated a large effect (Cohen, 1992).

Study 2: Achilles tendon forces and moment arm length in rearfoot and forefoot running

Introduction

The purpose of Study 2 was to determine the AT moment arm length during the stance phase of running and to investigate the relationship between moment arm length and running economy. Additionally, this study aimed to determine the difference in AT force between RF and FF running patterns. Results from this study were combined with the results of Study 1 to determine the relationship of Achilles tendon moment arm length to running economy.

Participant Selection

Study 2 used the participants from Study 1 that were included in the oxygen consumption analysis for the medium speed. Therefore, 19 participants were included in the RF group and 18 participants were included in the FF group. These participants performed over-ground running trials with each footfall pattern at a single speed, as

described below. Rate of oxygen consumption data from these participants was correlated with measurements of the Achilles tendon moment arm. All participants read and completed an informed consent document and questionnaires approved by the University of Massachusetts Amherst Institutional Review Board.

Experimental Setup

An eight-camera Qualisys Oqus 3-Series optical motion capture system (Qualisys, Inc., Gothenberg, Sweden), sampling at 240 Hz, surrounded the center of a 25 m runway and was used to collect unilateral three-dimensional kinematic data. Camera calibration was performed to define a right-hand laboratory coordinate system. A wand with two markers separated by a known length was used to scale the perspective of individual camera views to the collection volume in reference to a 90^{o} rigid frame to define the origin. The corner of the frame was placed at the edge of a force platform to define the X and Y axes as mediolateral and anteroposterior axes respectively. A floor mounted strain gauge force platform (OR6-5, AMTI, Inc. Watertown, MA, USA) was located in the center of the collection volume. Ground reaction forces (GRF) and center of pressure were recorded with the force platform with a sampling frequency of 1200 Hz. Photoelectric sensors (Lafayette Instrument Company, Lafayette, IN) were placed 3m before and after the force platform to record movement speed.

Retro-reflective markers were placed on the right lower extremity and pelvis of the participant according to McClay and Manal (1999) (Appendix B). Calibration markers included the iliac crests, greater trochanters, medial and lateral femoral condyles, medial and lateral malleoli, and the heads of the first and fifth metatarsals. Calibration

markers were used to determine segment local coordinate systems, segment origins, segment length and joint center locations. The long axis of the thigh and leg were defined as the distance between the proximal and distal joint centers. The long axis of the foot was defined as the distance between the ankle joint center and the center of the metatarsal calibration markers. Tracking markers included four non-collinear markers secured onto a rigid plate, positioned on the lateral thigh and leg, as well as a rigid plate with three non-collinear markers placed on the posterior calcaneus. Additional tracking markers, secured onto the skin or form fitting clothing, included the right and left anterior superior iliac spine and between the 5th lumbar-1st sacral vertebrae. Tracking markers were used to measure the marker movements in space by determining deviations from the standing calibration. Marker tracking was completed by calculating the transformation of the markers to the position and orientation of each segment. A standing calibration trial was collected with the participant in quiet stance in order to orient the local coordinate system in the laboratory coordinate system. Calibration markers were removed prior to performing the movement trials. Participants wore form-fitting clothing and a neutral racing flat running shoe provided by the laboratory.

The static AT moment arm length was measured using methods similar to those of Scholz et al. (2008). The static AT moment arm was defined as the shortest distance from the line of action of the AT to the center of rotation of the ankle. The center of rotation of the ankle was approximately the midpoint between the medial and lateral malleoli (Lundberg et al., 1989). The location of the lateral malleolus and its center were marked with a pen while the participant was standing (Figure 3.1). A high speed video camera (Exilim EX-F1, Casio Computer Co., LTD, Shibuya-ku, Tokyo, Japan) sampling

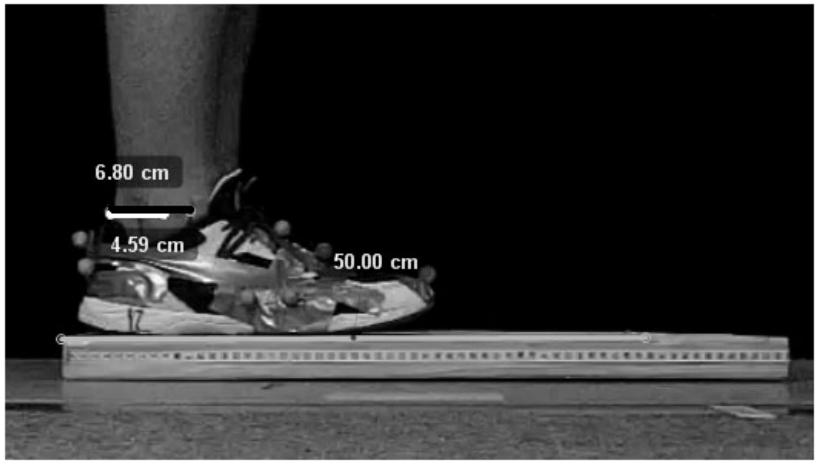

Figure 3.1: Measurement of Achilles tendon (AT) moment arm length during standing. The visual field was calibrated by determining the pixels in 50 cm reference distance. The distance between the ankle joint center and the posterior aspect of the AT was determined by averaging the distance between the medial (black line) and lateral malleoli (white line).

at 300 Hz was used to record video of the foot and leg during a standing. The length of the static AT moment arm was recorded with each participant standing on a wooden block of known length. The lateral boarder of the foot was aligned with the edge of the block. The posterior aspect of the AT was identified on the video. The length of the static AT moment arm was determined by taking the average of the horizontal distance between the mark on the center of the lateral malleolus and the posterior aspect of the AT and the horizontal distance between the mark on the anterior aspect of the lateral malleolus and the posterior aspect of the AT. This procedure was used to better estimate the ankle joint center which lies on an axis connecting the medial and lateral malleoli. If the shoe upper covered the point on the AT necessary for indicating the posterior aspect, the thickness of the shoe upper was included in the measurement of the perpendicular distance then subtracted from the total length. This method was previously used by both Scholz et al. (2008) and Fath et al. (2010) who reported values that were well correlated with more precise magnetic resonance imaging data. The motion capture data were used

to derive a second order polynomial to estimate the dynamic AT moment arm across the stance phase as a function of ankle joint angle (Arnold et al., 2010).

Oxygen consumption data were recorded during the data collection for Study 1. The volume and content of gases expired by each participant while running on a motorized treadmill was measured by indirect calorimetry using a metabolic cart (TrueOne, ParvoMedics, Sandy, UT, USA). The volume of gas exchange was used to calculate the gross rate of oxygen consumption.

Protocol

After signing the informed consent documents, the participants were prepared for data collection and the standing calibration and static AT moment arm length measurement were performed. Each participant was instructed on how to run across the force platform at the desired speed and without targeting or adjusting speed or stride. The data collection for the over-ground running conditions began with the participants performing five trials without any instruction on speed or footfall. This condition was used to identify the natural running pattern of each participant in accordance with the footfall pattern definitions described in the methods for Study 1. Each participant then performed 10 successful trials of each footfall pattern while running at 3.5 $m \cdot s^{-1}$ ±5%. The order of the footfall conditions was randomized between participants. Most biomechanical studies on running incorporate a single fixed running speed. A single fixed running speed was chosen for this study to limit the number of conditions performed in order to minimize the occurrence and severity of delayed onset muscle

soreness. The speed 3.5 $m \cdot s^{-1}$ was chosen because it is similar to speeds selected in the literature and was similar to the preferred speed of the participants (Queen et al., 2006).

Data collection for the treadmill conditions were described in the methods for Study 1. However, for Study 2 only the baseline oxygen consumption recording and the steady state oxygen consumption when running at 3.5 $m \cdot s^{-1}$ were included in Study 2. Participants arrived at the laboratory having fasted for at least three hours and had refrained from exercise before the data collection. Participants were allowed to warm-up on the treadmill for a several minutes as needed and also practiced each footfall pattern at 3.5 $m \cdot s^{-1}$. Running speed was adjusted by ±5% if necessary to allow for the participant to run comfortably with each footfall pattern. Participants began the data collection protocol by standing quietly for 10 minutes on the treadmill to record baseline oxygen consumption. Participants ran for a minimum of five minutes during each footfall pattern condition or until two minutes of steady state oxygen consumption was recorded. Steady state was reached when there was less than a 10% change in oxygen consumption over a two minute period (Stephens et al., 2006). Participants rested for a minimum of five minutes between conditions or until the volume of expired air returned within 0.02 $L \cdot min^{-1}$ of the baseline value.

Data Reduction

Kinematic data were tracked using Qualisys Track Manager software (Qualisys, Inc., Gothenberg, Sweden) and exported in .C3D format for processing with Visual 3D software (C-Motion, Inc, Rockville, MD, USA). Raw kinematic and kinetic data were filtered with a 4^{th} order, zero-lag Butterworth digital low-pass filter with a cutoff

frequency of 12 Hz and 50 Hz respectfully (Winter et al., 1974). Three dimensional joint angles were calculated by a rotation matrix of the distal segment with respect to the coordinate system of the proximal segment using a Cardan rotation sequence of x (flexion/extension) – y (abduction/adduction) – z (axial rotation) (Cole et al., 1993). For the knee, positive angles indicated extension, adduction and internal rotation. For the ankle, positive angles indicated dorsiflexion, inversion and adduction. Ankle joint angles were averaged over early ($AAave_1$), mid- ($AAave_2$), and late stance ($AAave_3$). Early stance was defined as 0-33% of the stance phase, mid-stance as 34-66%, and late stance as 67-100%.

A Newton-Euler inverse dynamics approach was used to calculate three dimensional joint moments. Segment geometries were modeled as a frustra of a right cone for the foot, leg and thigh, and as a cylinder for the pelvis. Segment mass, location of segmental center of mass, and moment of inertia were estimated by techniques described by Hanavan (1964). Internal joint moments were calculated with respect to the local coordinate system of the proximal segment. For the knee, positive values indicated extensor, adduction and internal rotation moments. For the ankle, positive values indicated dorsiflexor, inversion and adductor moments. Ankle joint angle and joint moments from the stance phase of each condition were interpolated to 101 data points from initial contact to toe-off, with each point representing 1% of the stance phase.

Kinovea Motion Tuner software v. 0.8.15 (www.kinovea.org/en/) was used to calculate the static AT moment arm length (dmt_0). A scaling factor was determined from the reference distance by the number of pixels that equaled the length of two points, 50 cm apart. The Euclidean distance between the center of the lateral malleolus and the

posterior aspect of the Achilles tendon was determined. The distance in pixels was divided by the scaling factor to determine the length of the AT moment arm in cm.

A custom MATLAB program was developed to determine the AT force and the dynamic AT moment arm length during the stance phase. A separate plots for the moment arm of the plot soleus and the medial and lateral heads of the gastrocnemius moment arm at the ankle were created as a function of ankle joint angle (θ) based on generic model by Arnold et al. (2010). The data from each muscle were combined by scaling each by its physiological cross sectional area. The data were fit to a second-order polynomial by a custom MATLAB program (Mathworks, Inc., Natick, MA) and used to determine the polynomial coefficients. A second-order polynomial was the lowest order that adequately fit the moment arm data, based on an assessment of the root mean square error between the polynomial prediction and the data. The zeroth-order polynomial coefficient was scaled for each subject individually by the static Achilles tendon moment arm measurement. The experimental ankle joint angle data were entered into the polynomial to determine the dynamic AT moment arm for each instant of the stance phase. The dynamic AT moment arm length was averaged over early (dmt_1), mid- (dmt_2), and late stance (dmt_3) and compared between footfall patterns.

To calculate AT force, the ankle and knee joint angles were used to estimate the passive joint moment (Riener and Edrich, 1999). The passive joint moment was subtracted from the net joint moment calculated by the inverse dynamics procedure to determine the active muscle moment. The maximum active ankle joint moment (AMmax) and the active ankle joint moment averaged over early ($AMave_1$), mid- ($AMave_2$), and late stance ($AMave_3$) were calculated and compared between patterns.

The active ankle moment was divided by the dynamic AT moment arm at each instant of stance to determine the AT force. It was assumed that the force in the AT was zero whenever the active ankle moment was dorsiflexor. The maximum AT force (ATmax) and the AT force averaged over early ($ATave_1$), mid- ($ATave_2$), and late stance ($ATave_3$) were calculated. The active ankle joint moment (AM_{10}), AT force (AT_{10}), and the dynamic AT moment arm (dmt_{10}) were averaged over the period of stance at which ±10% of the maximum AT force was generated. The relationship of these variables in addition to dmt_0 and of the rate of oxygen consumption was determined and compared between footfall patterns. However, the results of the correlation between each oxygen consumption variable and AM_{10} and AT_{10} are presented in Appendix D. Only the correlation results between net and gross rate of oxygen consumption and dmt_0 and dmt_{10} will be presented in the results, as they are the only relationships that pertain to the hypotheses.

The absolute ($L \bullet min^{-1}$) and relative ($ml \bullet kg^{-1} \bullet min^{-1}$) rates of steady state oxygen consumption ($\dot{V}O_2$) over the last two minutes of each condition was averaged to determine the net and gross $\dot{V}O_2$. The first five minutes of the baseline oxygen consumption measure was typically highly variable as the participants became accustom to breathing with the mouthpiece. As a result, the average rate of oxygen consumption over the last five minutes of the baseline period was used to calculate net $\dot{V}O_2$ by subtracting the baseline value from the average rate of oxygen consumption during the last two minutes of each running condition.

Statistical Analysis

Each ankle joint angle, ankle joint moment, AT force, AT moment arm, and $\dot{V}O_2$ variable was compared between the RF and FF patterns. A one-way analysis of variance (ANOVA) was used to assess the differences in dmt_0 between groups with a significance level of $\alpha = 0.05$. Additionally, each variable was subjected to a mixed model analysis of variance with footfall pattern and group as fixed variables and subject nested within group as a random variable. The differences between footfall patterns (2 levels) and between groups (2 levels) and the interaction of footfall pattern and group were assessed with a significance level of $\alpha = 0.05$. When a significant group by pattern interaction was observed, a post-hoc assessment was performed by partitioning the interaction by group and by pattern. Partitioning by group determined the significance between each footfall pattern within each group. Partitioning by pattern determined the significance between groups within each footfall pattern. A Pearson product moment correlation coefficient was calculated to determine the relationship between absolute and relative $\dot{V}O_2$ and dmt_0 and dmt_{10}. Effect sizes were also calculated to determine if the differences between footfall pattern and groups were biologically meaningful. An effect size (*d*) greater than 0.3 indicated a small effect, an effect size greater than 0.5 indicated a moderate effect and an effect size greater than 0.8 indicated a large effect (Cohen, 1992).

Study 3: Muscle mechanics and energy expenditure of the triceps surae during rearfoot and forefoot running

Introduction

The purpose of Study 3 was to compare the mechanical muscle work and muscle metabolic cost of the triceps surae muscle group between footfall patterns using a musculoskeletal modeling approach. The force and work produced by each muscle of the triceps surae was assessed with a muscle model. The resulting effects on metabolic cost were determined by comparing the muscle energy expenditure between footfall patterns.

Participant Selection

Study 3 used the over-ground kinematic and kinetic data as well as the static Achilles tendon moment arm length of 10 participants from each group collected from Study 2. Included participants were selected by matching for body mass, body height, and steady state oxygen consumption when running with their preferred footfall pattern at 3.5 $m \cdot s^{-1}$. This data was used to develop a muscle model. Individual participant data for 10 trials of each footfall pattern condition were averaged across conditions. Therefore, the mean data from each condition of each participant were used as input into the muscle model. Each variable was compared by the following group-condition combinations: 1) natural RF runners performing the RF pattern; 2) natural RF runners performing the FF pattern; 3) natural FF runners performing the RF pattern; and 4) natural FF runners performing the FF pattern. All participants read and completed an informed consent

document and questionnaires approved by the University of Massachusetts Amherst Institutional Review Board before participating.

Musculoskeletal Model

A two-dimensional musculoskeletal model was developed similar to the methods of previous studies (Bobbert et al., 1986a; Hof et al., 2002; van Soest and Bobbert, 1993). Properties of the muscle-tendon complex (MT) reflected the action of the gastrocnemius (GA) and soleus (SO), which together comprise the muscles of the triceps surae. The model consisted of three rigid segments representing the foot, leg and thigh (Appendix E, Figure E.1). Segments were connected by two frictionless hinge joints to represent the ankle and knee joints. A Hill-type muscle model was employed to simulate the action of the GA and the soleus SO individually. Each muscle contained a contractile element (CE) and a series elastic element (SEE) in series with the CE. Although Hill-type muscle models are phenomenological models, the CE is primarily associated with the muscle fascicles and the SEE is primarily associated with the Achilles tendon, aponeurosis and other elastic structures in series with the CE. Passive elements which act in parallel with the muscle fibers, such as muscle fascia, ligaments and joint capsule were represented by a passive moment (M_{pas}). The equation developed by Riener and Edrich (1999) was used to estimate M_{pas} as a function of ankle and knee joint angles:

$$M_{pas} = -\exp(2.1016 + 0.0843\varphi_A - 0.0176\varphi_K) - \exp(-7.9763 - 0.1949\varphi_A + 0.0008\varphi_K) - 1.792 \quad (3.4).$$

The mean ankle angle, knee angle, and ankle joint moment was compiled across trials for each participant served as inputs into the muscle model (Figure 6.1). The model was run on each participant individually for the following group-condition combinations: 1) natural RF runners performing the RF pattern; 2) natural RF runners performing the FF pattern; 3) natural FF runners performing the RF pattern; and 4) natural FF runners performing the FF pattern.

A generic model by Arnold et al. (2010) was used to determine the moment arm length (d_{MT}) for the GA and SO. A plot of d_{MT} as a function of joint angle (θ) for each muscle was created based on generic model by Arnold et al. (2010). d_{MT} for the SO was plotted against ankle joint angle. Plots for the d_{MT} of the GA as a function of knee and ankle joint angles were created separately. Additionally, the plots for d_{MT} of the medial and lateral heads of the GA were created separately for each joint angle. The data from the medial and lateral heads of the GA were combined by scaling each muscle by its physiological cross sectional area (PCSA). The modal data were fit to a second-order polynomial by a custom MATLAB program (Mathworks, Inc., Natick, MA) and used to determine the polynomial coefficients. A second-order polynomial was the lowest order that adequately fit the moment arm data, based on an assessment of the root mean square error between the polynomial prediction and the data. The zeroth-order polynomial coefficient was scaled for each subject individually by the static Achilles tendon moment arm measurement. Each d_{MT} polynomial was integrated with respect to the knee and ankle joint angle, thus creating third-order polynomials for GA and SO muscle-tendon complex length (L_{MT}) as a function of θ. The zeroth-order coefficients for the L_{MT} polynomials were scaled based on the participant's static leg length. The experimental

joint angle data were entered into these polynomials to determine L_{MT} and d_{MT} for each instant of the stance phase. L_{MT} of the GA and SO was used as a constraint for the model by requiring the sum of the CE and SEE lengths equal that of the L_{MT}.

Active moment (M_{act}) produced by the GA and SO was determined by subtracting M_{pas} from the ankle joint moment (M_A) found by the inverse dynamics procedure. M_{act} was used to calculate the force generated by the triceps surae as a sum of the forces produced by the GA and SO multiplied by their respective moment arms. Force produced by each muscle was partitioned by the ratio of each muscle's PCSA to the total triceps surae PCSA. A ratio of 1.88:1 SO to GA was used (Arnold et al., 2010).

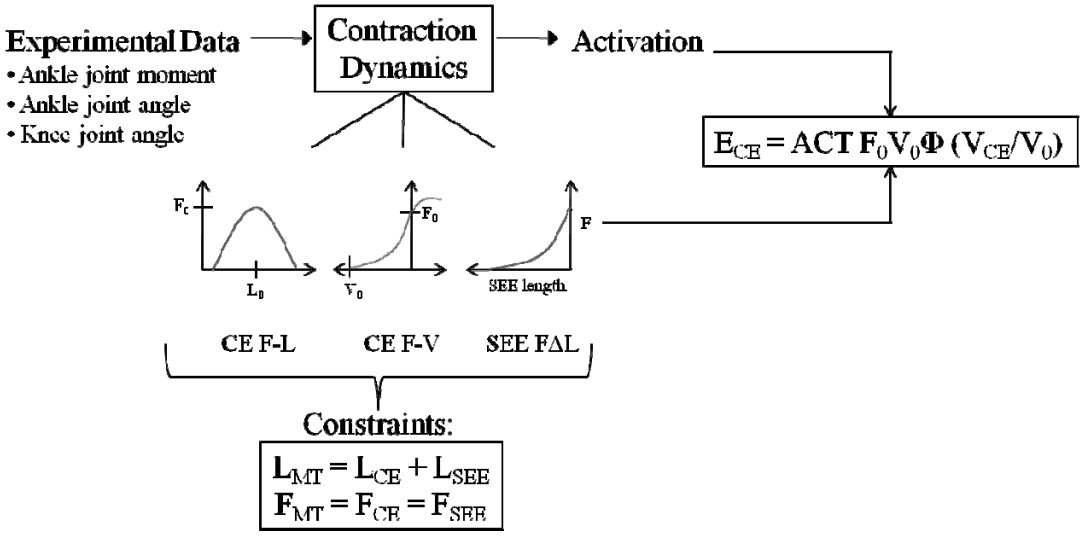

Figure 3.2: Schematic representing the steps of the muscle and muscle energetic model. The model begins by entering experimental data into the model. Based on the contraction dynamics (force-length CE F-L, force-velocity CE F-V and SEE force-extension SEE FΔL relationships), activation level of the muscle was determined, followed by the excitation level. The model was then constrained to the equilibrium condition ($L_{MT} = L_{CE} + L_{SEE}$) then the rate of muscle energy expenditure was determined.

The amount of force that could be generated by the muscle fibers was dependent on the contraction dynamics dictated by three relationships. The force-length relationship (F-L) represents the isometric force potential at any CE length (Gordon et al., 1966).

Peak isometric force production (F_0) occurs when the CE is at optimal length (L_o). The F-L relationship is modeled as a parabola and is scaled down depending on the sub-maximal activation level. The F-L relationship also determines the magnitude of F_0 used in the force-velocity relationship. The force velocity relationship (F-V) represents the CE force that is produced, based on the CE velocity (i.e. shortening, lengthening or isometric) (Hill, 1938). The F-V relationship is modeled by a rectangular hyperbola and is scaled up or down by the amount of activation and the F-L parameters. The force-extension relationship (FΔL) of the SEE represents the change in SEE elasticity, or stiffness, as SEE length is increased or decreased (Bahler, 1967). The FΔL relationship is modeled as a quadratic function. Determining the properties in the MT, CE and SEE based on the Hill relationships allowed for the activation level to be calculated. The internal states of the muscle model were based on the experimental data and constrained by the muscle geometry of the equilibrium condition ($L_{MT} = L_{CE} + L_{SEE}$ and $F_{MT} = F_{CE} = F_{SEE}$). After determining the MT, CC and SEE dynamics, the metabolic power produced by each muscle was calculated as a function of the CE velocity and activation (Minetti and Alexander, 1997; Sellers et al., 2003). Appendix E describes the equations and relationships used for the muscle and muscle energy expenditure models. Appendix F lists of all abbreviations that were used in the model.

Data Analysis

The power output of the MT, CE, and SEE was calculated by multiplying their respective force by velocity for each instant in time. Mechanical work was calculated by integrating the power output of the MT, CE, and SEE with respect to time. The amount

of elastic energy stored and released during the stance phase was determined by the amount of positive and negative mechanical work, respectively, performed by the SEE. Metabolic energy expenditure by the CE was calculated by integrating CE metabolic power with respect to time. Mechanical work of the MT, CE, and SEE as well as the metabolic energy expended by the CE of the GA and SO was calculated for each participant under the RF and FF pattern conditions.

Statistical Analysis

Mechanical work and metabolic energy expenditure were compared between the RF and FF running footfall patterns. Each variable was subjected to a mixed model analysis of variance with footfall pattern and group as fixed variables and subject nested within group as a random variable. The differences between footfall patterns (2 levels) and between groups (2 levels) and the interaction of footfall pattern and group were assessed with a significance level of $\alpha = 0.05$. When a significant group by pattern interaction was observed, a post-hoc assessment was performed by partitioning the interaction by group and by pattern. Partitioning by group determined the significance between each footfall pattern within each group. Effect sizes were also calculated to determine if the differences between footfall pattern and groups were biologically meaningful. An effect size (d) greater than 0.3 indicated a small effect, an effect size greater than 0.5 indicated a moderate effect and an effect size greater than 0.8 indicated a large effect (Cohen, 1992).

Study 4: Impact characteristics and shock attenuation between footfall patterns in running

Introduction

The purpose of Study 4 was to determine the difference in shock attenuation between footfall patterns and to infer the primary mechanisms responsible for attenuating impact shock between footfall patterns.

Participant Selection

Data for 20 participants in each group were used in Study 4. Ground reaction force data collected during Study 2 were used to determine impact force characteristics of these participants. Head and tibia accelerometer data were collected while running on a treadmill of all participants. However, the accelerometer data from one FF group participant was excluded from the analysis because of an anomaly in the data. All participants read and completed an informed consent document and questionnaires approved by the University of Massachusetts Amherst Institutional Review Board.

Experimental Setup

Three-dimensional kinematics of the right leg and foot were recorded with an eight-camera Qualisys Oqus 3-Series optical motion capture system (Qualisys, Inc., Gothenberg, Sweden) sampling at 240 Hz. Motion of retro-reflective markers placed on the foot and leg were used to monitor the footfall pattern performed by each participant (Appendix B). Calibration markers included the medial and lateral femoral condyles,

medial and lateral malleoli, and the heads of the first and fifth metatarsals. Tracking markers included a rigid plate with three non-collinear markers placed on the lower leg and the posterior calcaneus.

The cameras surrounded an AMTI force platform (OR6-5, AMTI Inc., Watertown, MA, USA) mounted flush with the floor surface. The force platform was located in the center of a 25 m runway. GRFs and center of pressure were recorded at a sampling frequency of 1200 Hz and were synchronized with the motion capture data. Running speed was monitored with photoelectric sensors (Lafayette Instrument Company, Lafayette, IN) placed 3 m before and after the force platform.

For collecting the accelerometer data, a treadmill was placed in the center of the motion capture space in order for continuous accelerometer data to be captured synchronously with kinematics. A low-mass (<4 grams), uniaxial, piezoelectric accelerometers (ICP®, PCB Piezotronics, Depew, NY, USA) were placed in accordance with the methods of Valiant et al. (1987). The head accelerometer was attached to the center of the frontal bone and the tibial accelerometer was attached to the anteromedial aspect of the distal tibia (Hamill et al., 1995). Each attachment site was chosen to reduce the effects of soft tissue vibration (Valiant et al., 1987; Wosk and Voloshin, 1981). The axis of each accelerometer was aligned with the vertical axis of the lab coordinate system. The accelerometers were sampled at 1200 Hz and voltage was amplified by a factor of 10.

Protocol

GRFs and kinematics were recorded while the participants ran over the force platform at 3.5 $m \cdot s^{-1}$ ± 5%. Ten trials of each condition were performed. Conditions included RF and FF running. The order of the conditions was randomized. For the FF running condition, the participants were instructed to land on the ball of the foot and prevent the heel from making contact with the ground.

After the over-ground conditions were performed, accelerometers were secured to the head and anteromedial distal tibia by rubber straps tightened to participant tolerance. Participants were then asked to run on a treadmill at 3.5 $m \cdot s^{-1}$ ± 5% with each footfall pattern condition. The order of conditions performed on the treadmill was also randomized. Participants practiced running on the treadmill with each footfall pattern for several minutes before data was collected. After sufficient practice was performed, participants ran for two minutes on the treadmill before data was collected for each condition. Accelerometer data was collected for 15 seconds during the last minute of each condition.

Data Reduction

Motion capture, GRF and accelerometer data were exported in .C3D format for processing with Visual 3D software (C-Motion, Inc, Rockville, MD, USA). Raw kinematic data was filtered with a 4^{th} order, zero-lag Butterworth digital low-pass filter with a cutoff frequency of 12 Hz (Winter et al., 1974). Joint angles were calculated using a rotation matrix of the distal segment with respect to proximal segment with a Cardan rotation sequence of x (flexion/extension; dorsiflexion/plantar flexion) – y

(abduction/adduction; inversion/eversion) – z (axial rotation) (Cole et al., 1993). The sagittal plane ankle angles during the stance phase of each condition were analyzed in order to confirm the footfall pattern performed during each condition. Kinematic data were interpolated from heel-strike to toe-off to 101 data points, with each point representing 1% of the stance phase. Ground contact time was calculated as the time from initial ground contact to toe-off of each stance phase.

Sagittal plane ankle joint and leg segment angles were also determined from the motion capture data collected during the treadmill conditions using the same procedures as with the over ground data. Stride frequency (SF; strides per minute) was determined from the treadmill conditions by multiplying the number of strides occurring during the 15 second recording of each treadmill condition by four. Stride length (SL; m) was calculated by dividing the running speed set on the treadmill by the SF. Contact time (CT) was calculated for both the over ground and treadmill conditions as the time between initial ground contact and toe-off.

Time domain and frequency parameters from the vertical GRF and tibia and head accelerometers were calculated using a custom MATLAB program (Mathworks, Inc., Natick, MA). In the time domain, impact peak (IMP) and active peak (ActP) of the vertical GRF (in units of body weights, BW) was determined during the stance phase over-ground running. Since the FF pattern does not result in an impact peak, IMP during the FF pattern was calculated by determining the magnitude of the vertical GRF at 25 ms of the stance phase (Bobbert et al., 1992; Cavanagh and Lafortune, 1980; Munro et al., 1987). The active peak was calculated by determining the maximum of the vertical GRF across the stance phase. Vertical GRF loading rate (VLR) was calculated from the slope

of line between 20-80% of the time before the first peak of the GRF was reached during the RF pattern. VLR during the FF pattern was calculated between 20 – 80% of the first 25 ms of the stance phase (Bobbert et al., 1992; Cavanagh and Lafortune, 1980; Munro et al., 1987).

Time domain parameters from the tibia and head accelerometers were determined from 15 stance phases in each condition during treadmill running. A least-squares best fit line was subtracted from the raw data of each signal to remove any linear trend (Shorten and Winslow, 1992). Data were then filtered with a second order Butterworth low-pass filter with a cut-off frequency of 60 Hz (Hennig and Lafortune, 1991). The first (HP1) and second (HP2) peak of the head acceleration signal were identified as the peak between 1 – 30% of stance and 31 – 101% of stance, respectively. Impact shock characteristics were determined by calculating peak positive tibial acceleration (PPA) and rate of positive tibial acceleration (RPA). RPA was calculated from the slope of line between 10-90% of the time before peak acceleration is reached (Lafortune, 1991).

The frequency content of the vertical GRF, tibia acceleration and head acceleration was determined by expressing the signal in the frequency domain (Shorten and Winslow, 1992). Unfiltered, detrended and zero padded data were transformed into the frequency domain by a discrete Fourier Transform (DFT). A DFT was performed on each trial or stance phase then normalized to 1 Hz bins. The amplitude at each frequency 1 – 50 Hz was averaged across all stance phases and participants. GRF frequencies above 10 Hz indicated impact was attenuated by passive mechanisms and frequencies below 10 Hz indicated impact was attenuated by active mechanisms (Derrick et al., 1998).

The degree of shock attenuation occurring during the stance phase with each footfall pattern was calculated by first using the frequency data of the tibia and head acceleration to determine the power spectral density (PSD) at frequencies 0 to the Nyquist frequency (Nyquist, F_N = one half of sampling rate, therefore $F_N = 600$). Powers from each stance phase were normalized into 1 Hz bins. After binning, the PSD was normalized in order for the sum of the powers from 0 to F_N to be equal to the mean squared amplitude of the data in the time domain. Normalizing allowed for a group average to be calculated for each frequency bin (Derrick et al., 1998; Hamill et al., 1995). A transfer function was then calculated to determine the degree of shock attenuation occurring between the tibia to the head by:

$$\text{Shock Attenuation} = 10 \cdot \log_{10}(PSD_{head}/PSD_{tibia}) \quad (3.5).$$

For each frequency, the transfer function calculated the gain or attenuation, in decibels, between the tibia and head signals. Positive values indicated a gain, or increase in signal strength between signals, and negative values indicated attenuation, or decrease in signal strength (Derrick et al., 1998; Hamill et al., 1995; Shorten and Winslow, 1992).

Statistical Analysis

Differences in each of the following variables were assessed between footfall from the over-ground running conditions: sagittal plane ankle and knee joint angle at initial contact, CT, IMP, ActP, VLR and the amplitude of the vertical GRF in the frequency domain from frequencies 1-50 Hz. Additionally, the differences between

footfall patterns in the following variables were assessed from the treadmill conditions: sagittal plane ankle joint and leg segment angles at initial contact, SF, SL, CT, HP1, HP2, PPA, RPA, tibia and head acceleration in the frequency domain from frequencies 1-50 Hz and the transfer function between the tibia and head. Each variable was subjected to a mixed model analysis of variance with footfall pattern and group as fixed variables and subject nested within group as a random variable. The differences between footfall patterns (2 levels) and between groups (2 levels) and the interaction of footfall pattern and group were assessed with a significance level of $\alpha = 0.05$. When a significant group by pattern interaction was observed, a post-hoc assessment was performed by partitioning the interaction by group and by pattern. Partitioning by group determined the significance between each footfall pattern within each group. Partitioning by pattern determined the significance between groups within each footfall pattern. Effect sizes were also calculated to determine if the differences between footfall pattern and groups were biologically meaningful. An effect size (d) greater than 0.3 indicated a small effect, an effect size greater than 0.5 indicated a moderate effect and an effect size greater than 0.8 indicated a large effect (Cohen, 1992).

References

1. Ardigo LP, Lafortuna C, Minetti AE, Mognoni P, Saibene F. Metabolic and Mechanical Aspects of Foot Landing Type, Forefoot and Rearfoot Strike, in Human Running. *Acta Physiol Scand*. 1995; 155(1):17-22.

2. Arnold EM, Ward SR, Lieber RL, Delp SL. A Model of the Lower Limb for Analysis of Human Movement. *Ann Biomed Eng*. 2010; 38(2):269-279.

3. Bahler AS. Series Elastic Component of Mammalian Skeletal Muscle. *Am J Physiol*. 1967; 213(6):1560-1564.

4. Biewener AA and Roberts TJ. Muscle and Tendon Contributions to Force, Work, and Elastic Energy Savings: A Comparative Perspective. *Exerc Sport Sci Rev*. 2000; 28(3):99-107.

5. Bobbert MF, Huijing PA, van Ingen Schenau GJ. A Model of the Human Triceps Surae Muscle-Tendon Complex Applied to Jumping. *J Biomech*. 1986a; 19(11):887-898.

6. Bobbert MF, Yeadon MR, Nigg BM. Mechanical Analysis of the Landing Phase in Heel-Toe Running. *J Biomech*. 1992; 25(3):223-234.

7. Cavanagh PR and Lafortune MA. Ground Reaction Forces in Distance Running. *J Biomech*. 1980; 13(5):397-406.

8. Cohen J. A Power Primer. *Psychol Bull*. 1992; 112(1):155-159.

9. Cole GK, Nigg BM, Ronsky JL, Yeadon MR. Application of the Joint Coordinate System to Three-Dimensional Joint Attitude and Movement Representation: A Standardization Proposal. *J Biomech Eng*. 1993; 115(4A):344-349.

10. Cunningham CB, Schilling N, Anders C, Carrier DR. The Influence of Foot Posture on the Cost of Transport in Humans. *J Exp Biol*. 2010; 213(5):790-797.

11. Derrick TR, Hamill J, Caldwell GE. Energy Absorption of Impacts During Running at Various Stride Lengths. *Med Sci Sports Exerc*. 1998; 30(1):128-135.

12. Fath F, Blazevich AJ, Waugh CM, Miller SC, Korff T. Direct Comparison of in Vivo Achilles Tendon Moment Arms Obtained from Ultrasound and Mr Scans. *J Appl Physiol*. 2010; 109(6):1644-1652.

13. Fenn WO. The Relation between the Work Performed and the Energy Liberated in Muscular Contraction. *J Physiol*. 1924; 58(6):373-395.

14. Gordon AM, Huxley AF, Julian FJ. The Variation in Isometric Tension with Sarcomere Length in Vertebrate Muscle Fibres. *J Physiol*. 1966; 184(1):170-192.

15. Hamill J, Derrick TR, Holt KG. Shock Attenuation and Stride Frequency During Running. *Human Movement Science*. 1995; 14:45-60.

16. Hanavan EP, Jr. A Mathematical Model of the Human Body. Amrl-Tr-64-102. *AMRL TR*. 1964:1-149.

17. Hasegawa H, Yamauchi T, Kraemer WJ. Foot Strike Patterns of Runners at the 15-Km Point During an Elite-Level Half Marathon. *J Strength Cond Res*. 2007; 21(3):888-893.

18. Hennig EM and Lafortune MA. Relationships between Ground Reaction Force and Tibial Bone Acceleration Parameters. *Int J Sports Biomech*. 1991; 7:303-309.

19. Hill AV. The Heat of Shortening and the Dynamic Constants of Muscle. *Proc Royal Soc*. 1938; 126B:136-195.

20. Hof AL, Van Zandwijk JP, Bobbert MF. Mechanics of Human Triceps Surae Muscle in Walking, Running and Jumping. *Acta Physiol Scand*. 2002; 174(1):17-30.

21. Huxley AF. Muscular Contraction. *J Physiol*. 1974; 243(1):1-43.

22. Lafortune MA. Three-Dimensional Acceleration of the Tibia During Walking and Running. *J Biomech*. 1991; 24(10):877-886.

23. Lichtwark GA and Wilson AM. Muscle Fascicle and Series Elastic Element Length Changes Along the Length of the Human Gastrocnemius During Walking and Running. *J Biomech*. 2005d,2007; 40:157-164.

24. Lundberg A, Svensson OK, Nemeth G, Selvik G. The Axis of Rotation of the Ankle Joint. *J Bone Joint Surg Br*. 1989; 71(1):94-99.

25. Maganaris CN, Baltzopoulos V, Sargeant AJ. In Vivo Measurement-Based Estimations of the Human Achilles Tendon Moment Arm. *Eur J Appl Physiol*. 2000; 83(4 -5):363-369.

26. McArdle WD, Katch FI, Katch VL. Exercise Physiology. Lippincott, Williams & Wilkins, Philadelphia, PA, 2001.

27. McClay I and Manal K. Three-Dimensional Kinetic Analysis of Running: Significance of Secondary Planes of Motion. *Med Sci Sports Exerc*. 1999; 31(11):1692-1737.

28. Minetti AE and Alexander RM. A Theory of Metabolic Costs for Bipedal Gaits. *J Theor Biol*. 1997; 186(4):467-476.

29. Munro CF, Miller DI, Fuglevand AJ. Ground Reaction Forces in Running: A Reexamination. *J Biomech*. 1987; 20(2):147-155.

30. Nilsson J and Thorstensson A. Ground Reaction Forces at Different Speeds of Human Walking and Running. *Acta Physiol Scand*. 1989; 136(2):217-227.

31. Perl DP, Daoud AI, Lieberman DE. Effects of Footwear and Strike Type on Running Economy. *Med Sci Sports Exerc*. 2012; 44(7):1335-1343.

32. Pratt DJ. Mechanisms of Shock Attenuation Via the Lower Extremity During Running. *Clin Biomech (Bristol, Avon)*. 1989; 4(1):51-57.

33. Queen RM, Gross MT, Liu HY. Repeatability of Lower Extremity Kinetics and Kinematics for Standardized and Self-Selected Running Speeds. *Gait Posture*. 2006; 23(3):282-287.

34. Rall JA. Energetic Aspects of Skeletal Muscle Contraction: Implications of Fiber Types. *Exerc Sport Sci Rev*. 1985; 13:33-74.

35. Riener R and Edrich T. Identification of Passive Elastic Joint Moments in the Lower Extremities. *J Biomech*. 1999; 32(5):539-544.

36. Roberts TJ, Marsh RL, Weyand PG, Taylor CR. Muscular Force in Running Turkeys: The Economy of Minimizing Work. *Science*. 1997; 275(5303):1113-1115.

37. Scholz MN, Bobbert MF, van Soest AJ, Clark JR, van Heerden J. Running Biomechanics: Shorter Heels, Better Economy. *J Exp Biol*. 2008; 211(Pt 20):3266-3271.

38. Sellers WI, Dennis LA, Crompton RH. Predicting the Metabolic Energy Costs of Bipedalism Using Evolutionary Robotics. *J Exp Biol*. 2003; 206(Pt 7):1127-1136.

39. Shorten MR and Winslow DS. Spectral Analysis of Impact Shock During Running. *Int J Sports Biomech*. 1992; 8:288-304.

40. Stephens BR, Cole AS, Mahon AD. The Influence of Biological Maturation on Fat and Carbohydrate Metabolism During Exercise in Males. *Int J Sport Nutr Exerc Metab*. 2006; 16(2):166-179.

41. Valiant GA, McMahon TA, Frederick EC. A New Test to Evaluate the Cushioning Properties of Athletic Shoes. In: *Biomechanics X-B*. Jonsson BE (Ed.). Human Kinetics, Champaign, IL, 1987. 937-941.

42. van Soest AJ and Bobbert MF. The Contribution of Muscle Properties in the Control of Explosive Movements. *Biol Cybern*. 1993; 69(3):195-204.

43. Weir JB. New Methods for Calculating Metabolic Rate with Special Reference to Protein Metabolism. *J Physiol*. 1949; 109(1-2):1-9.

44. Williams KR. Relationship between Distance Running Biomechanics and Running Economy. In: *Biomechanics of Distance Running*. Cavanagh PR (Ed.). Human Kinetics, Champaign, IL, 1990. 271-306.

45. Winter DA, Sidwall HG, Hobson DA. Measurement and Reduction of Noise in Kinematics of Locomotion. *Journal of Biomechanics*. 1974; 7(2):157-159.

46. Wosk J and Voloshin A. Wave Attenuation in Skeletons of Young Healthy Persons. *J Biomech*. 1981; 14(4):261-267.

CHAPTER 4

IS THERE A DIFFERENCE IN RUNNING ECONOMY BETWEEN REARFOOT AND FOREFOOT RUNNING PATTERNS?

Abstract

The forefoot (FF) running pattern has been advocated to improve running economy compared to the rearfoot (RF) pattern although no empirical evidence currently exists to support these claims. Therefore, the purposes of this study were to determine if there were differences in running economy between footfall patterns in habitual RF and FF runners and if running economy was improved when habitual RF and FF runners ran with the alternate footfall pattern. Nineteen habitual RF and 18 habitual FF runners ran with the RF and FF patterns on a treadmill at 3.0, 3.5 and 4.0 $m \bullet s^{-1}$. Oxygen consumption was measured until two minutes of steady state were recorded for which rate of oxygen consumption ($\dot{V}O_2$), cost of transport (COT), and absolute (gCHO) and relative (%CHO) carbohydrate oxidation were calculated. Mixed model ANOVA with participant nested within group was used to assess the differences in each variable between footfall patterns (α=0.05). Significant group by pattern interactions revealed the RF pattern resulted in decreased $\dot{V}O_2$, gCHO, and %CHO compared to the FF pattern at the slow and medium speeds in the RF group (p<0.05) but not in the FF group (p>0.05). At the fast speed, a significant pattern main effect revealed the FF pattern resulted in greater $\dot{V}O_2$ and gCHO, but not %CHO compared to the RF pattern (p<0.05) but the difference in %CHO was not significant (p>0.05). The results suggest that the FF pattern does not result in an improvement in running economy.

Introduction

Humans are capable of running with different footfall patterns which are defined by the location of the center or pressure at initial contact with the ground. These patterns include: 1) rearfoot (RF) in which initial contact is made on the lateral heel; 2) midfoot (MF) in which initial contact is made on the lateral side of the midfoot or on the metatarsal heads with subsequent heel contact; and 3) forefoot in which initial contact is made with the lateral portion of the metatarsal heads. It has been shown that the top finishers in short, middle, and long distance events tend to run with the FF or MF footfall pattern (Kerr et al., 1983; Pratt, 1989). Additional studies have also reported that the greatest proportion of FF and MF runners was among the top finishers of a half marathon (Hasegawa et al., 2007). These observations have led to claims that the MF and FF patterns enhance running economy compared to the RF pattern (Bonacci et al., 2010; Hasegawa et al., 2007; Lieberman et al., 2010) and thus RF runners should change to a MF or FF pattern (Martin and Cole, 1991; Romanov, 2002; Shorter, 2005; Yessis, 2000).

Although results from competitive events provide some intriguing suggestions, there is currently a lack of empirical evidence supporting a single pattern as being optimal for running economy. Greater running economy is generally quantified by the lowest sub-maximal rate of oxygen consumption. Running economy is dependent on numerous biomechanical, physiological and anthropometric factors (Daniels, 1985; Morgan et al., 1994a). Williams and Cavanagh (1987) identified several biomechanical features in more economical runners, such as longer ground contact time, lower vertical GRF active and impact peaks, decreased vertical oscillation of the center of mass, greater

trunk angle, greater maximum knee flexion during the stance phase and a more extended leg at touchdown.

Interestingly, many of the features found in more economical runners were characteristic of those who ran with the RF pattern (Williams and Cavanagh, 1987). In a computer simulation study, it was found that the RF pattern required a lower metabolic energy expenditure compared to the FF pattern; however the FF pattern was superior to the RF pattern for optimizing running velocity (Miller and Hamill, 2012). These results suggest RF running may be more economical; however, human studies investigating the difference in economy between patterns have failed to observe any differences (Ardigo et al., 1995; Cunningham et al., 2010; Perl et al., 2012). The primary limitation of most previous studies was that they included only one group of runners; a natural RF runners group or a natural FF runners group. Only one previous study incorporated both natural RF and natural FF runners and found the RF pattern resulted in a lower rate of oxygen consumption compared to the FF pattern (Slavin, 1992). However, significant differences between footfall patterns were not observed over all running speeds or for additional metabolic variables (e.g. respiratory exchange ratio, ventilation volume). Other studies used a sample size of less than eight participants, which may result in difficulty detecting significant differences across all speeds and respiratory variables. Examining alternative metabolic variables, such as carbohydrate oxidation, may be more a more meaningful measure of running performance as it is the limiting factor in endurance exercise (Coyle et al., 1986).

Comparing both groups of runners performing their natural footfall pattern could eliminate the potential for artificially high oxygen consumption the due to the novelty of

performing an alternate footfall pattern. Including both groups of runners also has a number of advantages over performing a training study. Training studies can be long and arduous and may require extensive hours from research technicians to ensure training protocol adherence. Additionally, incorporating both groups could be a surrogate for the effect of training with the opposite pattern.

Although previous studies suggest that the gait mechanics associated with running using the RF pattern are more economical than FF running (Heise et al., 2011; Miller and Hamill, 2012; Williams and Cavanagh, 1987), this relationship has not been shown in human studies directly comparing economy between footfall patterns. Previous studies examining the difference in running economy between the RF and FF running have had methodological limitations which may have affected the results. Therefore, the first purpose of this study was to determine the difference in running economy between footfall patterns in both natural RF and FF runners. A secondary purpose was to determine if there was an improvement in running economy for either natural RF or natural FF runners when performing the alternate footfall pattern. The hypotheses investigated in this study were: 1) running economy would be greater (e.g. lower sub-maximal rate of oxygen consumption and cost of transport) in natural RF runners performing the RF pattern compared to natural FF runners performing the FF pattern as suggested by Williams and Cavanagh (1987); 2) running economy would worsen when natural RF runners perform the FF running pattern; and finally 3) running economy would improve when natural FF runners perform the RF running pattern.

Methodology

Participant Selection

The abbreviations and acronyms used in this study are listed in Table 4.1. Nineteen natural RF and 18 natural FF runners participated in this study (Table 4.2) after reading and completing the informed consent document and questionnaires approved by the University of Massachusetts Amherst Institutional Review Board. All participants were experienced runners completing a minimum of 16 km per week with an average speed of approximately 3.5 $m \cdot s^{-1}$ for long running bouts. Both groups consisted of healthy individuals, with no history of cardiovascular or neurological problems and had not sustained an injury to the lower extremity or back within the past year. The natural footfall pattern was determined by the investigator recording vertical ground reaction forces (GRF) and high speed video of each participant while running over-ground at their preferred running speed. RF running was defined as making initial contact with the heel. FF running was defined as making initial contact on the metatarsal heads and preventing the heel from contacting the ground. Participants who exhibited a MF pattern were placed in the RF or FF groups based on their ankle kinematics and GRF. Natural MF runners were classified into the RF group if they made contact with a flat foot position (approximately zero degrees of dorsiflexion) and generated an initial impact peak within the vertical GRF component (n = 5). MF participants were classified into the FF group if they landed on the metatarsal heads but allowed the heel to touch the ground (foot position approximately below zero degrees, i.e. plantar flexion) and did not generate an initial impact peak (n = 6).

Table 4.1: Acronyms and abbreviations for each variable.

AATD	ankle joint angle at touchdown	%CHO	relative rate of carbohydrate oxidation
CHO	carbohydrate oxidation	RER	respiratory exchange ratio
COT	cost of transport	RF	rearfoot running footfall pattern
CT	contact time	SL	stride length
FF	forefoot running footfall pattern	SF	stride frequency
gCHO	absolute rate of carbohydrate oxidation	$\dot{V}CO_2$	volume of expired carbon dioxide
GRF	ground reaction force	$\dot{V}O_2$	steady state rate of oxygen consumption
MF	midfoot running footfall pattern		

Table 4.2: Mean ± SD participant characteristics of the rearfoot group (RF) and the forefoot group (FF) for the participants included in Study 1. Differences between groups were assessed by a student's t-test (α = 0.05).

	Males/Females (#)	Age (yrs)	Height (m)	Mass (kg)	Pref. Speed ($m \cdot s^{-1}$)	Distance/week (km)
RF group	12/7	26.7 ± 6.1	1.75 ± 0.09	70.10 ± 10.00	3.47 ± 0.90	42.85 ± 29.04
FF group	13/5	25.6 ± 6.4	1.76 ± 0.10	68.69 ± 9.77	3.70 ± 0.27	49.79 ± 25.90
p-value	-	0.585	0.918	0.668	0.288	0.449

Experimental Setup

The volume and content of gases expired by each participant while running on a motorized treadmill was measured by indirect calorimetry using a metabolic cart (TrueOne, ParvoMedics, Sandy, UT, USA). The volume of gas exchange was used to calculate the gross rate of oxygen consumption. Three-dimensional motion of reflective markers placed on the right foot and leg (McClay and Manal, 1999) (Appendix B) were recorded by an eight-camera Qualisys Oqus 3-Series optical motion capture system (Qualisys, Inc., Gothenberg, Sweden) sampling at 240 Hz. Motion capture data were used to monitor the footfall pattern used by the participants during each condition. Calibration markers included the medial and lateral femoral condyles, medial and lateral malleoli, and the heads of the first and fifth metatarsals. Tracking markers included a rigid plate with three non-collinear markers placed on the posterior calcaneus. A

treadmill was placed in the center of the motion capture collection volume. Each participant wore a neutral racing flat running shoe provided by the laboratory to standardize any effects of cushioning and other footwear properties (RC 550, New Balance, Brighton, MA, USA).

Protocol

Each participant arrived at the laboratory having fasted for at least three hours and had refrained from exercise before the data collection. Each participant was allowed to warm-up on the treadmill for several minutes as needed and also practiced each footfall pattern at a slow, medium, and fast speed which were 3.0, 3.5 and 4.0 $m \cdot s^{-1}$, respectively. Running speed was adjusted by ±5% if necessary to allow the participant to run more comfortably. The participant was then prepared for data collection by securing the reflective markers onto the right leg and foot and a standing calibration of the marker placement was recorded. Each participant began the data collection by standing quietly for 10 minutes on the treadmill to record baseline oxygen consumption. Next, the participant performed each footfall pattern within one speed condition before continuing to the next speed condition. The order of the footfall patterns and running speeds was randomized. Each participant ran for a minimum of five minutes during each speed and footfall pattern condition or until two minutes of steady state oxygen consumption was recorded. Steady state was attained when there was less than a 10% change in oxygen consumption over a two minute period (Stephens et al., 2006). Each participant rested until the volume of expired air returned within 0.02 $L \cdot min^{-1}$ of the baseline value.

Data Reduction

The absolute ($L \cdot min^{-1}$) and relative ($ml \cdot kg^{-1} \cdot min^{-1}$) rates of steady state oxygen consumption ($\dot{V}O_2$) over the last two minutes of each condition was averaged to determine the net and gross $\dot{V}O_2$ and cost of transport (COT). The first five minutes of the baseline oxygen consumption measure was typically highly variable as the participants became accustomed to breathing with the mouthpiece. As a result, the average rate of oxygen consumption over the last five minutes of the baseline period was used to calculate net $\dot{V}O_2$ and COT by subtracting the baseline value from the average rate of oxygen consumption during the last two minutes of each running condition. Absolute ($J \cdot m^{-1}$) and relative ($J \cdot m^{-1} \cdot kg^{-1}$) COT were first calculated by converting the relative rate of oxygen consumption ($ml \cdot kg^{-1} \cdot min^{-1}$) to metabolic rate ($W \cdot kg^{-1}$) by (Weir, 1949):

$$\text{Metabolic rate} = \dot{V}O_2 * \frac{(3.876 + \text{RER} * 1.2411)}{1000} * \frac{4184}{60} \quad (4.1)$$

where $\dot{V}O_2$ was the rate of oxygen consumption in $ml \cdot kg^{-1} \cdot min^{-1}$, RER was the respiratory exchange ratio calculated by volume of carbon dioxide expired divided by the volume of oxygen consumed averaged over the last two minutes of steady state, 3.876 was the number of kcals expended per liter of oxygen consumed, 1.2411 kcals expended per liter of carbon dioxide expired, 4184 was the number of Joules (J) per kcal, 1000 $ml \cdot L^{-1}$, and 60 $s \cdot min^{-1}$. COT was then determined by dividing metabolic rate by the velocity of the treadmill belt.

Absolute rate of carbohydrate oxidation (gCHO) in $g \bullet hr^{-1}$ was determined from the volume of carbon dioxide expired ($\dot{V}CO_2$) and the volume of oxygen consumed by (McArdle et al., 2001):

$$gCHO = (4.58\ \dot{V}CO_2 - 3.23\ \dot{V}O_2) * 60 \quad (4.2).$$

Relative carbohydrate oxidation (%CHO) was expressed as the percentage of energy expenditure resulting from carbohydrate oxidation was calculated from $\dot{V}O_2$ in $L \bullet min^{-1}$ and gCHO:

$$\%CHO = \frac{g\ CHO * 4\ kcal \bullet g^{-1}}{5\ kcal \bullet L^{-1} \bullet VO_2^{-1} * L\ VO_2 \bullet min^{-1}} * 100 \quad (4.3)$$

where 4 $kcal \bullet g^{-1}$ was the number of kcals liberated from oxidizing 1 g of CHO and 5 $kcal \bullet L^{-1}$ was the number of kcals expended per liter of oxygen consumed.

The 3D positions of the markers placed on the foot and leg were tracked using Qualisys Track Manager software (Qualisys, Inc., Gothenberg, Sweden). The data were exported in .C3D format to calculate sagittal plane ankle joint angles at touchdown (AATD) using Visual 3D software (C-Motion, Inc, Rockville, MD, USA). Raw kinematic data were filtered with a 4^{th} order, zero-lag Butterworth digital low-pass filter with a cutoff frequency of 12 Hz (Winter et al., 1974). Ankle joint angle was calculated by a rotation matrix of the distal segment with respect to the coordinate system of the proximal segment using a Cardan rotation sequence of x (dorsiflexion/plantar flexion) – y (eversion/inversion) – z (axial rotation) (Cole et al., 1993). Stride frequency (SF) was calculated as the number of strides occurring during the 15 s motion capture period and

multiplied by four to result in units of strides per minute. Stride length (SL) was calculated by dividing the treadmill belt speed by SF. Contact time (CT) was calculated for each stance phase as the time between initial impact and toe-off of the right foot.

Statistical Analysis

The kinematic variables that were assessed included the AATD, SL, SF and CT. The running economy variables assessed included net absolute and relative steady state $\dot{V}O_2$, gross absolute and relative $\dot{V}O_2$, net absolute and relative COT, and gross absolute and relative COT, gCHO, and %CHO. Each variable was subjected to a mixed model analysis of variance (ANOVA) with footfall pattern and group as fixed variables and participant nested within group as a random variable. The differences between footfall patterns (2 levels) and between groups (2 levels) and the interaction of footfall pattern and group were assessed with a significance level of $\alpha = 0.05$. When a significant group by pattern interaction was observed, a post-hoc assessment was performed by partitioning the interaction by group and by pattern. Partitioning by group determined the significance between each footfall pattern within each group. Partitioning by pattern determined the significance between groups within each footfall pattern. A one-way ANOVA was used to determine the differences in running economy variables between groups at baseline and each speed when performing their preferred pattern ($\alpha = 0.05$). Effect sizes were also calculated to determine if the differences between footfall patterns and groups were biologically meaningful. An effect size (d) lower than 0.4 indicated a small effect, an effect size between 0.5 and 0.7 indicated a moderate effect and an effect size greater than 0.8 indicated a large effect (Cohen, 1992).

Results

Kinematics

There was a significant group by pattern interaction for AATD at all three running speeds ($p < 0.05$) (Table 4.3; Figure 4.1). Partitioning the interaction by group revealed RF running resulted in a greater AATD than FF running at each speed in both the RF group ($p < 0.001$, $d = 5.7$; medium $p < 0.001$, $d = 5.4$; fast $p < 0.001$, $d = 5.2$) and FF group (slow: $p < 0.001$, $d = 4.3$; medium $p < 0.001$, $d = 3.9$; fast $p < 0.001$, $d = 3.9$). Partitioning the interaction by pattern revealed no difference in AATD between groups when performing the RF pattern at each speed (slow: $p = 0.455$, $d = 0.3$; medium $p = 0.146$, $d = 0.6$; fast $p = 0.399$, $d = 0.3$). However, when performing the FF pattern, the RF group ran with a significantly greater plantar flexion AATD than the FF group at all three speeds (slow: $p = 0.015$, $d = 0.8$; medium $p = 0.030$, $d = 0.6$; fast $p = 0.047$, $d = 0.6$).

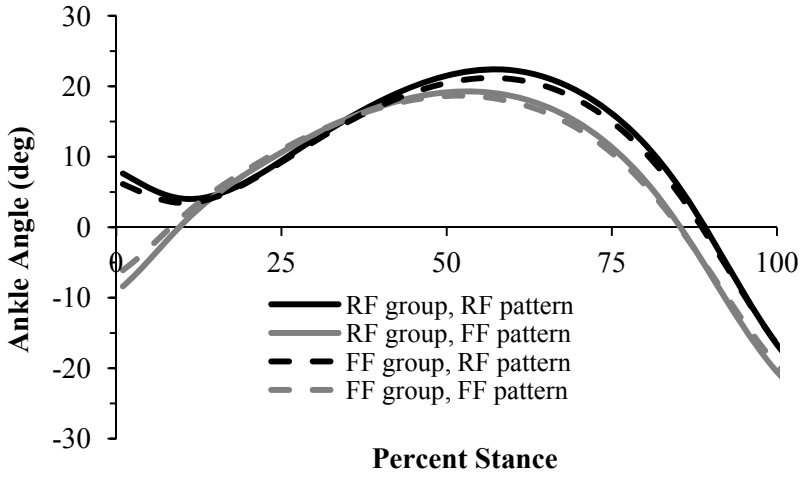

Figure 4.1: Group mean time series of sagittal plane ankle joint motion of all subjects in the rearfoot (RF) and forefoot (FF) groups performing the RF and FF patterns at the medium speed. Only touchdown angle when performing the FF pattern was different between groups (*p*-value > 0.05).

Table 4.3: Mean ± SD for the kinematic variables when performing the rearfoot (RF) and forefoot (FF) patterns. Variables include ankle angle at touch-down (AATD), stride length (SL), stride frequency (SF) and contact time (CT). Listed statistics include the *p*-value for the group by pattern interaction (GxP), the p-value (effect size) for the group main effect (G) and pattern main effect (P).

	Speed	RF Group		FF Group		GxP	G	P
		RF	FF	RF	FF			
AATD (deg)	Slow	8.27 ± 2.39	-8.37 ± 3.41	7.48 ± 2.65	-5.70 ± 3.55	0.025	-	-
	Medium	7.62 ± 2.45	-8.38 ± 3.52	6.13 ± 2.65	-6.10 ± 3.66	0.012	-	-
	Fast	7.56 ± 3.17	-8.97 ± 3.14	6.62 ± 2.78	-6.69 ± 3.98	0.047	-	-
SL (m)	Slow	2.17 ± 0.14	2.15 ± 0.13	2.21 ± 0.22	2.16 ± 0.18	0.553	0.680 (0.1)	0.137 (0.2)
	Medium	2.49 ± 0.20	2.44 ± 0.19	2.49 ± 0.17	2.43 ± 0.19	0.734	0.956 (0.0)	0.012 (0.3)
	Fast	2.76 ± 0.16	2.78 ± 0.23	2.79 ± 0.27	2.74 ± 0.27	0.425	0.953 (0.0)	0.726 (0.1)
SF ($strides \cdot s^{-1}$)	Slow	83.08 ± 5.18	84.21 ± 5.13	83.45 ± 6.35	84.54 ± 5.47	0.951	0.848 (0.1)	0.010 (0.2)
	Medium	84.25 ± 5.90	85.92 ± 5.83	85.09 ± 5.12	86.66 ± 6.30	0.862	0.725 (0.1)	0.006 (0.3)
	Fast	86.24 ± 4.42	86.75 ± 5.05	86.52 ± 5.77	87.84 ± 6.48	0.449	0.716 (0.1)	0.094 (0.2)
CT (s)	Slow	0.27 ± 0.02	0.24 ± 0.01	0.26 ± 0.02	0.23 ± 0.01	0.410	0.100 (0.5)	<0.001 (1.7)
	Medium	0.25 ± 0.02	0.23 ± 0.01	0.24 ± 0.02	0.21 ± 0.02	0.516	0.045 (0.7)	<0.001 (1.5)
	Fast	0.23 ± 0.01	0.21 ± 0.01	0.22 ± 0.02	0.20 ± 0.01	0.642	0.056 (0.7)	<0.001 (1.6)

Stride Characteristics

No significant group by pattern interactions were observed for SF, SL or CT across all speeds ($p > 0.05$) (Table 4.3). A significant pattern main effect revealed SL was 2.2% greater during RF running compared to the FF pattern at the medium speed ($p < 0.05$, $d = 0.3$) but not different at the slow or fast speeds ($p > 0.05$, $d < 0.2$). SF was 1.3% greater during FF running compared to RF running at the slow speed and was also 1.7% greater at the medium speed as indicated by significant pattern main effects ($p <$

0.05, d = 0.2 – 0.3). Although SF was 1.1% greater during FF running at the fast speed, a significant pattern main effect was not observed (p > 0.05, d = 0.2). A significant pattern main effect was observed for CT at all three speeds (p < 0.05, d = 1.5 – 1.7). CT was over 10% greater during the RF pattern compared to the FF pattern at each speed. Additionally, a significant group main effect was observed at the medium speed (p < 0.05, d = 0.7) but not at the slow or fast speeds (p > 0.05, d = 0.5 – 0.7). The FF group had 1.8% decrease in CT during FF running at the medium speed whereas the RF group had a 1.6% decrease in CT with FF running. Both groups changed CT similarly at the slow and medium speeds.

Running Economy Variables

There was no significant difference in the baseline rate of oxygen consumption, gCHO or %CHO between groups (p > 0.05, d = 0.1) (Table 4.4). No significant differences in any economy variable was found when comparing the RF and FF groups running with their preferred footfall pattern at any speed (p > 0.05, d < 0.4) (Table 4.5 and 4.5). However, a moderately large effect size was found for %CHO between groups when running with their preferred pattern at the slow speed. The RF group had lower %CHO compared to the FF group, but this difference was not significant.

Table 4.4: Mean ± SD and *p*-value (*d*) for the baseline rate of oxygen consumption ($\dot{V}O_2$) and absolute (gCHO) and relative (%CHO) carbohydrate oxidation in the rearfoot (RF) and forefoot (FF) groups.

group	$\dot{V}O_2$ $L \cdot min^{-1}$	$\dot{V}O_2$ $ml \cdot kg^{-1} \cdot min^{-1}$	gCHO $g \cdot hr^{-1}$	%CHO %
RF	0.32 ± 0.05	4.57 ± 0.39	12.61 ± 8.24	50.61 ± 24.19
FF	0.32 ± 0.06	4.58 ± 0.64	13.32 ± 7.58	56.08 ± 24.49
p-value (*d*)	0.819 (0.1)	0.960 (0.1)	0.788 (0.1)	0.499 (0.2)

Table 4.5: Mean ± SD and *p*-value (*d*) for A) rate of oxygen consumption ($\dot{V}O_2$) during the preferred footfall pattern condition and B) cost of transport (COT) during the preferred footfall pattern condition at the slow, medium and fast speeds.

A)

Speed	Group	Net $\dot{V}O_2$ $L \cdot min^{-1}$	Net $\dot{V}O_2$ $ml \cdot kg^{-1} \cdot min^{-1}$	Gross $\dot{V}O_2$ $L \cdot min^{-1}$	Gross $\dot{V}O_2$ $ml \cdot kg^{-1} \cdot min^{-1}$
Slow	RF	2.09 ± 0.36	29.60 ± 1.80	2.42 ± 0.40	34.19 ± 1.93
	FF	2.03 ± 0.34	29.49 ± 2.56	2.35 ± 0.38	34.08 ± 2.71
	p-value (*d*)	0.588 (0.2)	0.886 (0.0)	0.591 (0.2)	0.890 (0.0)
Medium	RF	2.44 ± 0.38	34.79 ± 1.85	2.76 ± 0.42	39.36 ± 2.00
	FF	2.34 ± 0.39	33.93 ± 2.51	2.65 ± 0.43	38.51 ± 2.63
	p-value (*d*)	0.425 (0.3)	0.240 (0.4)	0.457 (0.2)	0.273 (0.4)
Fast	RF	2.88 ± 0.46	40.19 ± 2.13	3.21 ± 0.50	44.77 ± 2.26
	FF	2.76 ± 0.45	39.54 ± 2.67	3.08 ± 0.49	44.15 ± 2.87
	p-value (*d*)	0.668 (0.3)	0.654 (0.3)	0.715 (0.3)	0.756 (0.2)

B)

Speed	Group	Net COT $J \cdot m^{-1}$	Net COT $J \cdot m^{-1} \cdot kg^{-1}$	Gross COT $J \cdot m^{-1}$	Gross COT $J \cdot m^{-1} \cdot kg^{-1}$
Slow	RF	237.3 ± 39.9	3.36 ± 0.20	274.0 ± 45.0	3.88 ± 0.22
	FF	231.2 ± 39.1	3.36 ± 0.29	267.2 ± 44.0	3.89 ± 0.31
	p-value (*d*)	0.645 (0.2)	0.939 (0.0)	0.649 (0.2)	0.918 (0.0)
Medium	RF	241.3 ± 36.1	3.45 ± 0.20	273.1 ± 40.6	3.90 ± 0.22
	FF	231.1 ± 38.3	3.36 ± 0.26	262.4 ± 42.4	3.82 ± 0.27
	p-value (*d*)	0.410 (0.3)	0.284 (0.4)	0.439 (0.3)	0.321 (0.3)
Fast	RF	253.8 ± 38.6	3.54 ± 0.18	282.7 ± 42.3	3.95 ± 0.20
	FF	242.8 ± 39.1	3.49 ± 0.23	271.1 ± 42.6	3.90 ± 0.24
	p-value (*d*)	0.693 (0.3)	0.784 (0.2)	0.659 (0.3)	0.681 (0.2)

Table 4.6: Mean ± SD and *p*-value (*d*) absolute (gCHO) and relative (%CHO) carbohydrate oxidation during the preferred footfall pattern condition at the slow, medium and fast speeds.

Speed	Group	gCHO $g \cdot hr^{-1}$	%CHO %
Slow	RF	88.89 ± 23.41	51.3 ± 12.7
	FF	100.23 ± 21.76	58.5 ± 8.3
	p-value (*d*)	0.141 (0.5)	0.051 (0.7)
Medium	RF	131.17 ± 39.65	64.7 ± 15.5
	FF	140.08 ± 33.00	71.3 ± 11.4
	p-value (*d*)	0.464 (0.2)	0.152 (0.5)
Fast	RF	187.87 ± 58.05	77.93 ± 16.8
	FF	186.12 ± 39.82	80.9 ± 11.8
	p-value (*d*)	0.837 (0.0)	0.556 (0.2)

Significant group by pattern interactions were observed for all $\dot{V}O_2$ and COT variables during the slow and medium speeds ($p < 0.05$) but not at the fast speed ($p > 0.05$) (Figure 4.2). At the slow speed, partitioning the interaction by group revealed that the RF group ran with over 4.7% greater $\dot{V}O_2$ and over 5.0% greater COT when performing the FF pattern compared to when performing the RF pattern ($p < 0.05$, $d = 0.3 – 0.9$) (Appendix C, Table C.1 and C.2). Conversely, the FF group did not experience a significant difference in any $\dot{V}O_2$ or COT variable between footfall patterns at the slow speed ($p > 0.05$, $d < 0.1$). Partitioning the interaction by pattern revealed that when performing the RF pattern at the slow speed, the RF group had over 3% greater absolute net and gross $\dot{V}O_2$ and over 2.5% greater absolute net and gross COT compared to the FF group ($p < 0.05$, $d = 0.2$). Although significant, the differences in relative net and gross $\dot{V}O_2$ and COT were less than 1% between groups when performing the RF pattern at the slow speed ($p < 0.05$, $d < 0.1$). When performing the FF pattern at the slow speed, the RF group had over 7.7% greater absolute net and gross $\dot{V}O_2$ and COT compared to the FF group ($p < 0.05$, $d = 0.5$) and relative $\dot{V}O_2$ and COT variables were over 5% greater in the RF group.

At the medium speeds, partitioning the interaction by group revealed that the RF group ran with over 3% greater $\dot{V}O_2$ and COT when performing the FF pattern compared to when performing the RF pattern ($p < 0.05$, $d = 0.2 – 0.7$) (Figure 4.2) (Appendix C, Table C.1 and C.2). Similar to running at the slow speed, the FF group did not have a significant difference in any economy variable between footfall patterns at the medium speed ($p > 0.05$, $d < 0.1$). Partitioning the interaction by pattern revealed that performing the RF pattern at the medium speed resulted in the RF group having over 4.7% greater

absolute net and gross $\dot{V}O_2$ and COT compared to the FF group ($p < 0.05$, $d = 0.3 – 0.5$). When performing the FF pattern at the medium speed, absolute net and gross $\dot{V}O_2$ and COT were over 7.2% greater in the RF group compared to the FF group ($p < 0.05$, $d = 0.4 – 0.5$) and relative net and gross $\dot{V}O_2$ and COT were over 5.3% greater in the RF group ($p < 0.05$, $d = 0.9 – 1.0$).

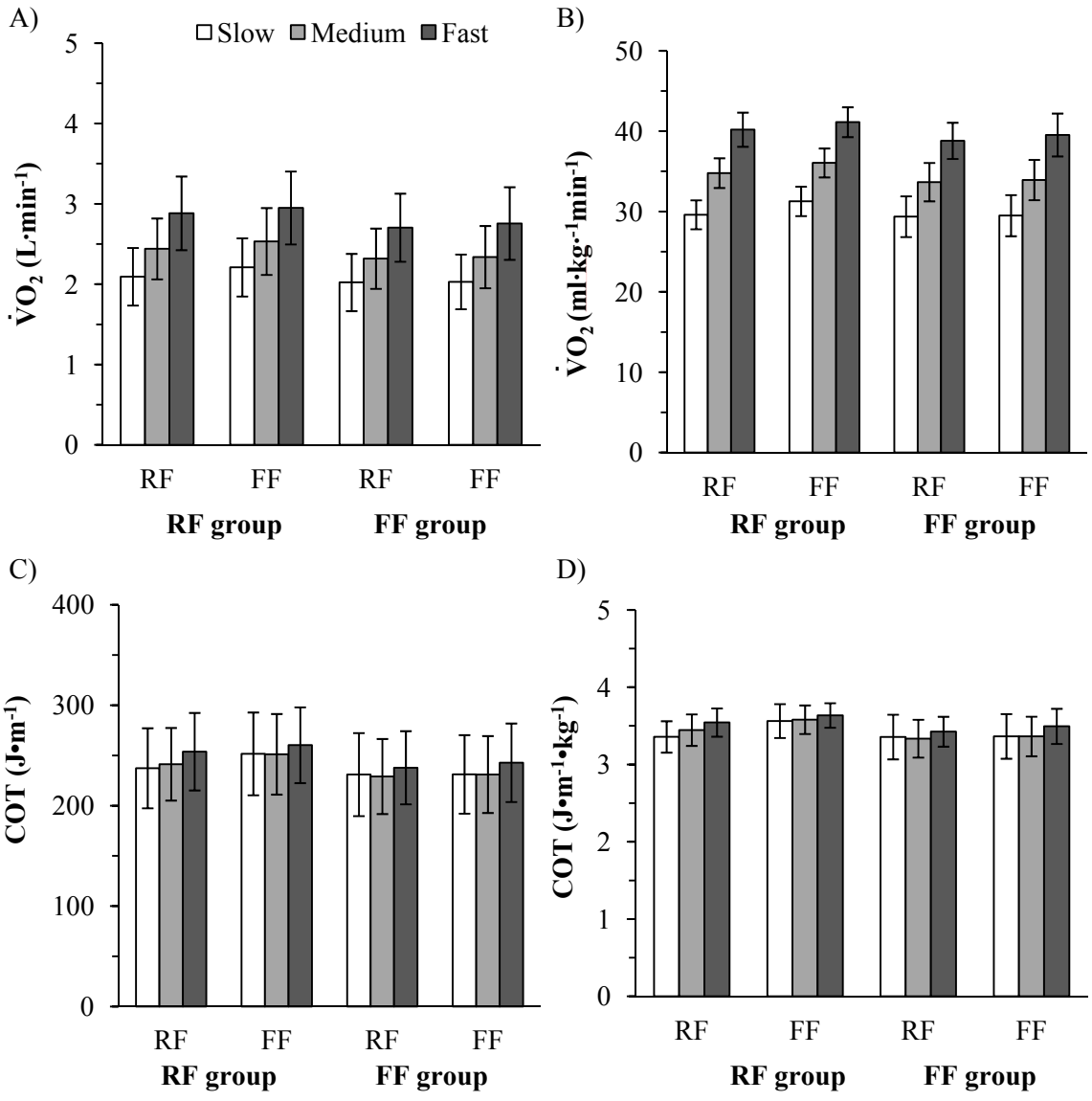

Figure 4.2: Group mean results for net A) absolute and B) relative rate of oxygen consumption ($\dot{V}O_2$) and net C) absolute and D) relative cost of transport when performing the rearfoot (RF) and forefoot (FF) footfall patterns at each speed. Error bars are ±1SD.

Although no significant group by pattern interactions were observed at the fast speed, a significant pattern main effect was observed for all $\dot{V}O_2$ at the fast speed ($p < 0.001$, $d = 0.1 – 0.4$) (Figure 4.2) (Appendix C, Table C.3). When running at the fast speed, the FF pattern resulted in approximately 2% greater $\dot{V}O_2$ and COT compared to the RF pattern. No significant group main effects were observed at the fast speed indicating the RF and FF groups had similar $\dot{V}O_2$ and COT when performing both footfall patterns at the fast speed ($p > 0.05$, $d = 0.4 – 0.7$).

There was a significant group by pattern interaction for gCHO at the slow ($p = 0.002$) and medium speeds ($p = 0.028$) but not the fast speed ($p = 0.552$) (Figure 4.3A) (Appendix C, Table C.4). Partitioning the interaction by group revealed FF running resulted in 16.3% greater gCHO in the RF group at the slow speed ($p = 0.001$, $d = 0.6$) and 9.5% greater gCHO at the medium speed ($p < 0.001$, $d = 0.3$) (Figure 4.3A). Although not statistically significant, the FF group had 4.3% greater gCHO with the RF pattern at the slow speed ($p = 0.313$, $d = 0.2$) but 2.1% greater gCHO with the FF pattern at the medium speed ($p = 0.371$, $d = 0.1$). Partitioning the interaction by pattern revealed the FF group had 16.3% greater gCHO than the RF group when performing the RF pattern at the slow speed ($p = 0.001$, $d = 0.6$) (Figure 4.3A). The FF group had 4.5% greater than the RF group when performing the RF pattern at the medium speed, but this difference was not significant ($p = 0.064$, $d = 0.2$). When performing the FF pattern, the RF group had 4.3% greater gCHO than the FF group the slow speed and 3.0% greater gCHO at the medium speed, but these differences were not significant (slow: $p = 0.312$, $d = 0.2$; medium ($p = 0.191$, $d = 0.1$). At the fast speed, a significant pattern main effect was observed for gCHO ($p = 0.028$, $d = 0.2$) (Figure 4.3A) (Appendix C, Table C.5);

however a significant group main effect was not observed ($p = 0.710$, $d = 0.2$). FF running resulted in 5.2% greater gCHO compared to RF running.

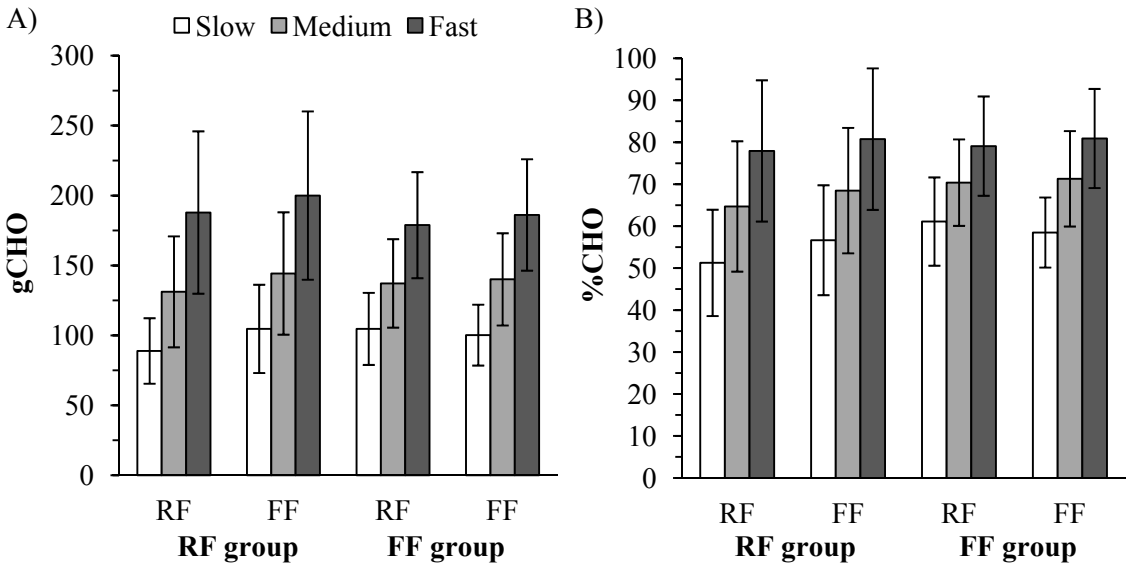

Figure 4.3: Group mean absolute (gCHO) and relative (%CHO) carbohydrate oxidation when performing the rearfoot (RF) and forefoot (FF) patterns at the slow, medium and fast speeds in the RF and FF groups. Error bars are ±1SD.

There was a significant group by pattern interaction for %CHO at the slow speed ($p = 0.007$) (Appendix C, Table C.4). Partitioning the interaction by group revealed %CHO was 10.0% greater with the FF pattern in the RF group ($p = 0.009$, $d = 0.4$) (Figure 4.3B). No significant difference in %CHO was observed between patterns in the FF group although RF running resulted in a 4.4% increase in %CHO in this group ($p = 0.191$, $d = 0.3$). Partitioning the interaction by pattern revealed that during RF running, the RF group had a 17.5% lower %CHO than the FF group ($p < 0.001$, $d = 0.8$). No significant difference in %CHO was observed between groups when performing the FF pattern although %CHO was 3.2% greater in the FF group ($p = 0.359$, $d = 0.2$). No significant interaction ($p = 0.153$) or main effect of group ($p = 0.326$, $d = 0.3$) was found

for %CHO at the medium speed (Appendix C, Table C.5). However, a significant pattern main effect revealed that FF running resulted in 3.4% greater %CHO compared to RF running ($p = 0.022$, $d = 0.2$) (Figure 4.3B). No significant interactions or main effects were observed for %CHO at the fast speed ($p < 0.05$, $d < 0.2$) (Figure 4.3B).

Discussion

The present study was the first to incorporate a natural RF and natural FF group in order to compare running economy between footfall patterns. Previous studies have failed to find a relationship between footfall patterns and running economy but have only used runners habituated to one footfall pattern (Ardigo et al., 1995; Cunningham et al., 2010; Perl et al., 2012). The first purpose of this study was to determine if there were differences in economy between natural RF and natural FF runners performing their preferred footfall pattern. The first hypothesis, that running economy would be lower in natural RF runners performing the RF pattern compared to natural FF runners performing the FF pattern, was rejected. There were no statistically significant differences in the rate of oxygen consumption, cost of transport, or carbohydrate oxidation between groups when performing their natural pattern at a slow, medium, or fast speed. These results suggest that neither footfall pattern was more economical than the other when comparing natural RF and natural FF runners performing their habitual footfall pattern. However, at the slow speed, a moderately large effect size ($d = 0.7$) was found for %CHO between groups indicating that the RF group had decreased %CHO and the difference may be biologically meaningful. This result suggests that the RF group running with the RF

pattern may be able to sustain an endurance run longer than the FF group running with the FF pattern.

Since the fastest runners in short, middle, and long distance events land on the anterior portion of the foot (Hasegawa et al., 2007; Kerr et al., 1983; Payne, 1983), it has been suggested that natural RF runners should switch to a FF pattern to improve running economy (Hasegawa et al., 2007). However, previous studies have identified that features associated with more economical runners were characteristic of a RF pattern (Heise et al., 2011; Williams and Cavanagh, 1987). Therefore, the second purpose of this study was to determine if running economy would change when natural RF and natural FF runners performed the alternate footfall pattern. The second hypothesis, that running economy would worsen when the natural RF group performed the FF pattern, was supported (Table 4.5). It was found that RF group increased the rate of oxygen consumption and cost of transport by 2 – 6% and carbohydrate oxidation by approximately 3 – 16% when running with a FF pattern compared to a RF pattern. In the FF group, the rate of oxygen consumption, cost of transport, and carbohydrate oxidation was not different between footfall patterns. Therefore, the third hypothesis, that running economy would improve when natural FF runners performed the RF running pattern, was not supported at the slow and medium speeds. However, at the fast speed, the FF pattern resulted in approximately 2% greater rate of oxygen consumption and cost of transport and 5% greater absolute carbohydrate oxidation compared to the RF pattern when the data were collapsed across group. Despite statistical significance between patterns at the fast speed, these results may not be biologically meaningful as indicated by low effect sizes and percent differences that were lower than the smallest worthwhile difference

(Brisswalter and Legros, 1994; Morgan et al., 1994a; Pereira and Freedson, 1997; Saunders et al., 2004).

When comparing the groups performing their habitual footfall pattern, the RF group and FF group had similar running economy as indicated by similar rates of oxygen consumption and cost of transport between groups. However, when both groups performed the RF pattern at the slow and medium speeds, the FF group was more economical compared the RF group. A movement pattern that brings about an immediate reduction in rate of oxygen consumption is considered more economical than the previous movement pattern (Williams, 1990). However, performing novel tasks typically causes an increase in the rate of oxygen consumption and requires habituation to see any improvement in economy (Cavanagh and Williams, 1982; Sparrow and Newell, 1998). Therefore, these finding suggests that RF running was more economical without a habituation period than FF running because the FF group had a lower rate of oxygen consumption when performing the RF pattern compared to the RF group performing the RF pattern.

A limitation of this study was that running with an alternate running pattern was a novel task for most participants. However, the RF and FF groups were able to successfully replicate the kinematics of the alternate footfall pattern (Figure 4.1; Table 4.3). This result supports previous studies that have found habituation periods of only a few minutes are adequate at replicating the gait mechanics of a new running pattern (MacLean et al., 2008; Stackhouse et al., 2004; Williams et al., 2000). A study by Williams et al. (2000) also found no differences in joint angles between natural RF and FF groups performing the FF pattern but slight differences in segment velocities and

contact time resulted in differences in joint moment variables between groups performing the same footfall pattern. Although not measured in the present study, differences in joint moments and muscle forces between groups likely contributed to differences in running economy variables between groups when performing the same footfall pattern. Although the kinematics of a new gait mode may be adapted quickly, muscle activation patterns, co-contraction and muscle forces take much longer to accommodate (Duchateau et al., 2006). Future studies should utilize a training protocol to fully habituate participants to the alternative running footfall pattern.

Training, or habituation to a new gait mode, results in a reduction in oxygen consumption from the initial performance of the task (Cavanagh and Williams, 1982; Sparrow and Newell, 1998). A benefit of the present study was that it used both habitual RF and FF runners. Thus, each group represents the outcome of training with the opposite footfall pattern where both mechanical and physiological adaptations have been completed. If the RF group trained with the FF pattern, running economy when performing the FF pattern would improve. However, this improvement may not result in the FF pattern becoming more economical than the RF pattern. The results from the FF group suggest that training with the FF pattern does not result in this pattern being more economical than the RF pattern. Since running economy was not different between patterns in the FF group, training with the RF pattern would improve running economy in this group and result in it becoming more economical than the FF pattern. Alternatively, additional training of the FF group with the FF pattern could also result in an improvement in running economy, resulting in it becoming more economical than RF running in this group. However, the natural FF group was comprised of trained, highly

skilled FF runners, so it can be assumed that their oxygen consumption while performing their natural pattern was already optimized (Brooks et al., 2004; Sparrow and Newell, 1998). This suggests that more training with the FF pattern may not lead to improved economy above the RF pattern in the FF group.

Deviations from preferred stride length and stride frequency have previously been shown to increase the rate of oxygen consumption and cost of transport (Cavanagh and Williams, 1982; Holt et al., 1991; Morgan et al., 1994b; Morgan et al., 1989). It has been suggested that the FF pattern results in different stride characteristics compared to the RF pattern (Divert et al., 2008; Perl et al., 2012; Squadrone and Gallozzi, 2009). Thus, differences in these variables between footfall patterns may be explained by stride characteristics rather than ankle joint angle at touchdown. At the slow speed, only stride frequency, and not stride length, statistically differed between patterns. However, this is a statistical difference rather than a functional difference because the running speed was constant. Stride length and stride frequency only differed between patterns at the medium speed whereas no differences in either stride length or stride frequency occurred at the fast speed. The present study also found that contact time was decreased during FF running at all speeds. These results are consistent with Ardigo et al. (1995) who suggested that these results were a result of increased vertical oscillation of the center of mass during FF running compared to RF. Previous studies have found lower running economy in those that had large vertical deviations of the center of mass (Williams, 1990; Williams and Cavanagh, 1987). Additionally, decreased CT has been suggested to result in a greater metabolic cost of running (Kram, 2000; Kram and Taylor, 1990). Although vertical oscillation was not measured in the present study, vertical oscillation and

decreased CT may partially explain the increased rates of oxygen consumption observed with the FF pattern.

Although FF running resulted in greater rate of oxygen consumption and cost of transport in the present study, the effect sizes and the differences in magnitude between patterns in economy variables were small. Although the FF pattern performed by the RF group resulted in a statistically significant increase in the rate of oxygen consumption of 2 – 6% at all speeds and an increase of 2% at the fast speed in the FF group, these differences equated to less than 1.0 $L \cdot min^{-1}$ and 14 $J \cdot m^{-1}$ difference for rate of oxygen consumption and cost of transport, respectively. Variation of greater than 2 – 5% in the rate of oxygen consumption may be needed to detect differences in running economy between conditions or individuals (Brisswalter and Legros, 1994; Morgan et al., 1994a; Pereira and Freedson, 1997; Saunders et al., 2004). However, if a 2% difference in economy was real, and not a result of measurement error or day-to-day variation, than a 2% difference in economy would result in a 2% improvement in performance time or approximately 30 s reduction in 10K performance time at a world-record pace (Frederick, 1983; Williams, 1990). Thus, small differences may be relevant to an elite athlete (Cavanagh and Kram, 1985).

Any enhancement of running economy in an elite athlete may improve his or her placement in an elite endurance race. Improvements in additional variables, such as carbohydrate oxidation, may also be beneficial to both elite and recreational runners. The rate of carbohydrate oxidation is especially important during long endurance events that have the potential to deplete muscle glycogen stores and is the limiting factor in performance of endurance events (Coyle et al., 1986). Compared to RF running in the

present study, FF running resulted in greater relative carbohydrate oxidation at each speed in the RF group and greater absolute carbohydrate oxidation at the fast speed in the FF group. Therefore, the RF pattern may be the more appropriate footfall pattern for endurance events because carbohydrate oxidation is reduced. In a recent study on recreational runners, it was found that natural FF runners switched to using a RF pattern between the 10 km and 32 km locations of a marathon (Larson et al., 2011). This change in footfall pattern within a race may be a mechanism to spare glycogen stores when they are reaching depletion.

Conclusion

The present study found no difference in the rate of oxygen consumption, cost of transport, and absolute and relative carbohydrate oxidation between natural RF and FF runners when performing their preferred pattern, indicating no difference in running economy between footfall patterns. Performing the FF pattern did not result in greater running economy in either natural RF or natural FF runners. However, the RF pattern resulted in decreased absolute carbohydrate oxidation at the fast speed and relative carbohydrate oxidation at the medium speed. These data suggest that the FF running footfall pattern is not more economical than the RF pattern but there may be an improvement in running economy with the RF pattern. Due to low-to-moderate biological significance in economy variables, the benefits of altering footfall pattern may only be beneficial for high level, elite athletes.

References

1. Ardigo LP, Lafortuna C, Minetti AE, Mognoni P, Saibene F. Metabolic and Mechanical Aspects of Foot Landing Type, Forefoot and Rearfoot Strike, in Human Running. *Acta Physiol Scand*. 1995; 155(1):17-22.

2. Bonacci J, Green D, Saunders PU, Blanch P, Franettovich M, Chapman AR, Vicenzino B. Change in Footstrike Position Is Related to Alterations in Running Economy in Triathletes. International Symposium on Biomechanics in Sports: Conference Proceedings Archive. 2010. 1-2.

3. Brisswalter J and Legros P. Daily Stability in Energy Cost of Running, Respiratory Parameters and Stride Rate among Well-Trained Middle Distance Runners. *Int J Sports Med*. 1994; 15(5):238-241.

4. Brooks GA, Fahey TD, Baldwin KM. Exercise Physiology: Human Bioenergetics and Its Applications. McGraw-Hill, New York, NY, 2004.

5. Cavanagh PR and Kram R. Mechanical and Muscular Factors Affecting the Efficiency of Human Movement. *Med Sci Sports Exerc*. 1985; 17(3):326-331.

6. Cavanagh PR and Williams KR. The Effect of Stride Length Variation on Oxygen Uptake During Distance Running. *Med Sci Sports Exerc*. 1982; 14(1):30-35.

7. Cohen J. A Power Primer. *Psychol Bull*. 1992; 112(1):155-159.

8. Cole GK, Nigg BM, Ronsky JL, Yeadon MR. Application of the Joint Coordinate System to Three-Dimensional Joint Attitude and Movement Representation: A Standardization Proposal. *J Biomech Eng*. 1993; 115(4A):344-349.

9. Coyle EF, Coggan AR, Hemmert MK, Ivy JL. Muscle Glycogen Utilization During Prolonged Strenuous Exercise When Fed Carbohydrate. *J Appl Physiol*. 1986; 61(1):165-172.

10. Cunningham CB, Schilling N, Anders C, Carrier DR. The Influence of Foot Posture on the Cost of Transport in Humans. *J Exp Biol*. 2010; 213(5):790-797.

11. Daniels JT. A Physiologist's View of Running Economy. *Med Sci Sports Exerc*. 1985; 17(3):332-338.

12. Divert C, Mornieux G, Freychat P, Baly L, Mayer F, Belli A. Barefoot-Shod Running Differences: Shoe or Mass Effect? *Int J Sports Med*. 2008; 29(6):512-518.

13. Duchateau J, Semmler JG, Enoka RM. Training Adaptations in the Behavior of Human Motor Units. *J Appl Physiol*. 2006; 101(6):1766-1775.

14. Frederick EC. Extrinsic Biomechanical Aids In: *Ergogenic Aids in Sport*. Williams M (Ed.). Human Kinetics, Champaign, IL, 1983. 323-339.

15. Hasegawa H, Yamauchi T, Kraemer WJ. Foot Strike Patterns of Runners at the 15-Km Point During an Elite-Level Half Marathon. *J Strength Cond Res*. 2007; 21(3):888-893.

16. Heise GD, Smith JD, Martin PE. Lower Extremity Mechanical Work During Stance Phase of Running Partially Explains Interindividual Variability of Metabolic Power. *Eur J Appl Physiol*. 2011; 111(8):1777-1785.

17. Holt KG, Hamill J, Andres RO. Predicting the Minimal Energy Costs of Human Walking. *Med Sci Sports Exerc*. 1991; 23(4):491-498.

18. Kerr BA, Beauchamp L, Fisher V, Neil R. Footstrike Patterns in Distance Running. In: *Biomechanical Aspects of Sport Shoes and Playing Surfaces*. Nigg BMand Kerr B (Eds.). University of Calgary Press, Calgary, 1983.

19. Kram R. Muscular Force or Work: What Determines the Metabolic Energy Cost of Running? *Exerc Sport Sci Rev*. 2000; 28(3):138-143.

20. Kram R and Taylor CR. Energetics of Running: A New Perspective. *Nature*. 1990; 346(6281):265-267.

21. Larson P, Higgins E, Kaminski J, Decker T, Preble J, Lyons D, McIntyre K, Normile A. Foot Strike Patterns of Recreational and Sub-Elite Runners in a Long-Distance Road Race. *J Sports Sci*. 2011; 29(15):1665-1673.

22. Lieberman DE, Venkadesan M, Werbel WA, Daoud AI, D'Andrea S, Davis IS, Mang'eni RO, Pitsiladis Y. Foot Strike Patterns and Collision Forces in Habitually Barefoot Versus Shod Runners. *Nature*. 2010; 463(7280):531-535.

23. MacLean CL, Davis IS, Hamill J. Short- and Long-Term Influences of a Custom Foot Orthotic Intervention on Lower Extremity Dynamics. *Clin J Sport Med*. 2008; 18(4):338-343.

24. Martin DE and Cole PN. Better Training for Distance Runners. Human Kinetics, Champaign, IL, 1991.

25. McArdle WD, Katch FI, Katch VL. Exercise Physiology. Lippincott, Williams & Wilkins, Philadelphia, PA, 2001.

26. McClay I and Manal K. Three-Dimensional Kinetic Analysis of Running: Significance of Secondary Planes of Motion. *Med Sci Sports Exerc*. 1999; 31(11):1692-1737.

27. Miller RH and Hamill J. Footfall Pattern Selection for the Performance of Various Running Tasks. *J App Biomech*. 2012; In Review XX(X):XX-XX.

28. Morgan DW, Craib MW, Krahenbuhl GS, Woodall K, Jordan S, Filarski K, Burleson C, Williams T. Daily Variability in Running Economy among Well-Trained Male and Female Distance Runners. *Res Q Exerc Sport*. 1994a; 65(1):72-77.

29. Morgan DW, Martin P, Craib M, Caruso C, Clifton R, Hopewell R. Effect of Step Length Optimization on the Aerobic Demand of Running. *J Appl Physiol*. 1994b; 77(1):245-251.

30. Morgan DW, Martin PE, Krahenbuhl GS. Factors Affecting Running Economy. *Sports Med*. 1989; 7(5):310-330.

31. Payne AH. Foot to Ground Contact Forces of Elite Runners. In: *Biomechanics Viii-B*. Matsui Hand Kobayashi K (Eds.). Human Kinetics, Champaign, IL, 1983. 748-753.

32. Pereira MA and Freedson PS. Intraindividual Variation of Running Economy in Highly Trained and Moderately Trained Males. *Int J Sports Med*. 1997; 18(2):118-124.

33. Perl DP, Daoud AI, Lieberman DE. Effects of Footwear and Strike Type on Running Economy. *Med Sci Sports Exerc*. 2012; 44(7):1335-1343.

34. Pratt DJ. Mechanisms of Shock Attenuation Via the Lower Extremity During Running. *Clin Biomech (Bristol, Avon)*. 1989; 4(1):51-57.

35. Romanov N. Pose Method of Running. Pose Tech Corporation, Coral Gables, FL, 2002.

36. Saunders PU, Pyne DB, Telford RD, Hawley JA. Reliability and Variability of Running Economy in Elite Distance Runners. *Med Sci Sports Exerc*. 2004; 36(11):1972-1976.

37. Shorter F. Running for Peak Performance. Dorling Kindersley Publishing, New York, NY, 2005.

38. Slavin MM. The Effects of Foot Strike Pattern Alteration on Efficiency in Skilled Runners. M.S. thesis, University of Massachusetts, Amherst, MA, 1992.

39. Sparrow W and Newell K. Metabolic Energy Expenditure and the Regulation of Movement Economy. *Psychonomic Bulletin & Review*. 1998; 5(2):173-196.

40. Squadrone R and Gallozzi C. Biomechanical and Physiological Comparison of Barefoot and Two Shod Conditions in Experienced Barefoot Runners. *J Sports Med Phys Fitness*. 2009; 49(1):6-13.

41. Stackhouse CL, Davis IM, Hamill J. Orthotic Intervention in Forefoot and Rearfoot Strike Running Patterns. *Clin Biomech (Bristol, Avon)*. 2004; 19(1):64-70.

42. Stephens BR, Cole AS, Mahon AD. The Influence of Biological Maturation on Fat and Carbohydrate Metabolism During Exercise in Males. *Int J Sport Nutr Exerc Metab*. 2006; 16(2):166-179.

43. Weir JB. New Methods for Calculating Metabolic Rate with Special Reference to Protein Metabolism. *J Physiol*. 1949; 109(1-2):1-9.

44. Williams DS, McClay IS, Manal KT. Lower Extremity Mechanics in Runners with a Converted Forefoot Strike Pattern. *J App Biomech*. 2000; 16(2):210-218.

45. Williams KR. Relationship between Distance Running Biomechanics and Running Economy. In: *Biomechanics of Distance Running*. Cavanagh PR (Ed.). Human Kinetics, Champaign, IL, 1990. 271-306.

46. Williams KR and Cavanagh PR. Relationship between Distance Running Mechanics, Running Economy, and Performance. *J Appl Physiol*. 1987; 63(3):1236-1245.

47. Winter DA, Sidwall HG, Hobson DA. Measurement and Reduction of Noise in Kinematics of Locomotion. *Journal of Biomechanics*. 1974; 7(2):157-159.

48. Yessis M. Explosive Running. McGraw-Hill, Columbus, OH, 2000.

CHAPTER 5

ACHILLES TENDON FORCES AND MOMENT ARM LENGTH IN REARFOOT AND FOREFOOT RUNNING

Abstract

A short Achilles tendon (AT) moment arm has been associated with greater running economy; however, this has only been investigated in those that use a rearfoot (RF) footfall pattern. The length of the AT moment arm during running may affect running economy in two ways. First, a short AT moment arm length, as found with a dorsiflexed ankle position, may improve running economy by increasing the force necessary to produce a given joint moment and thereby increase the storage and release of elastic energy. Second, a long AT moment arm, which is found with a plantar flexed ankle position, may improve running economy by reducing the force necessary to produce a given joint moment and thereby reduce the necessary active muscle volume and metabolic cost. The FF pattern may result in either of these potential mechanisms for more economical running because of the plantar flexed position in early stance and the dorsiflexed position in mid and late stance. Therefore, the purpose of this study was to determine the AT moment arm length during the stance phase of RF and FF running and to investigate the relationship between moment arm length and running economy and to determine the difference in AT force between RF and FF running patterns. Nineteen natural RF runners and 18 natural FF runners performed over-ground running with the RF and FF patterns at 3.5 $m \cdot s^{-1}$ ± 5%. Additionally, oxygen consumption was measured while the participants ran on a treadmill at 3.5 $m \cdot s^{-1}$ ± 5% with each footfall pattern.

Static moment arm was recorded by video in order to measure the length of the AT moment arm during quiet stance. Ankle and knee joint kinematics and ankle joint moments were used to determine the length of the AT moment arm and AT force during the stance phase of running with each footfall pattern. The oxygen consumption was correlated with the static and dynamic moment arms to determine the relationship between each footfall pattern and group. A mixed-factor ANOVA ($\alpha = 0.05$) and a Pearson's product moment coefficient were determined to assess the differences in each variable between footfall patterns and the relationship of running economy and AT moment arm length. The RF group had a moderate correlation with the rate of oxygen consumption consumed during both footfall patterns and either the static or dynamic moment arm ($r^2 < 0.25$). No relationship was found in the FF group. AT force was greater in early and mid-stance of running with the FF pattern compared to the RF pattern. Although the trend was weaker than previous studies, this study supports previous findings that a shorter AT moment arm was associated with greater running economy. Metabolic cost associated with the production of large AT forces during FF running may negate any benefit provided by AT moment arm length or elastic energy utilization.

Introduction

Running economy is influenced by several biomechanical and morphological characteristics (Anderson, 1996; Cavanagh and Kram, 1985; Martin and Morgan, 1992; Saunders et al., 2004; Williams and Cavanagh, 1987). For example, a recent study by Scholz et al. (2008) found that runners with a shorter Achilles tendon (AT) moment arm

(Figure 5.1) tended to be more economical than runners with a longer AT moment arm. However, this study was only performed on runners that naturally use the rearfoot (RF) footfall pattern. Nearly 25% of runners use a midfoot (MF) or a forefoot (FF) pattern (Hasegawa et al., 2007; Kerr et al., 1983) and the popularity of performing the FF pattern has increased based on claims that it improves running economy and prevents overuse injuries compared to the RF pattern (Cavanagh and Lafortune, 1980; Daoud et al., 2012; Davis et al., 2010; Hasegawa et al., 2007; Lieberman et al., 2010; Oakley and Pratt, 1988). The relationship between AT moment arm and running economy may be different with FF running because a plantar flexed ankle position results in a longer AT moment arm than a dorsiflexed position (Maganaris et al., 2000). However, previous measurements of the AT moment arm have only been performed statically (Maganaris et al., 2000; Scholz et al., 2008) and thus, it is unknown how the dynamic AT moment arm may be related to running economy or if the relationship is different between footfall patterns.

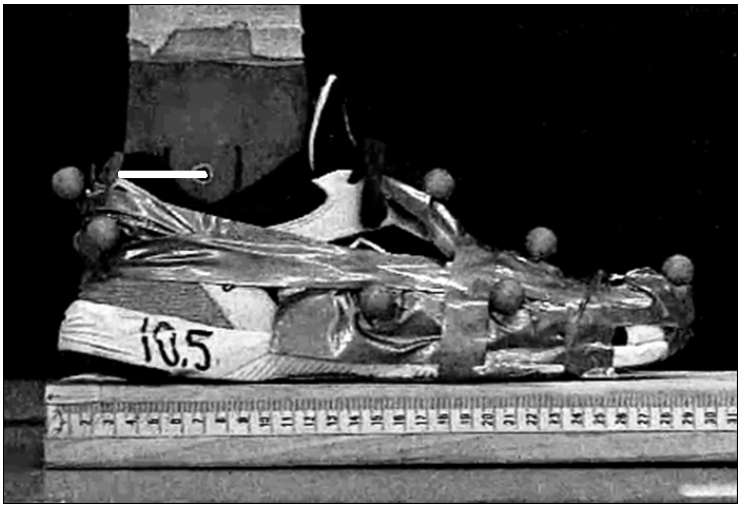

Figure 5.1: The length and location of the Achilles tendon (AT) moment arm (white line).

Scholz et al. (2008) suggested that a shorter AT moment arm improves running economy by increasing elastic energy storage as a result of a higher muscle force requirement to produce a given joint moment compared to if the moment arm was long (Biewener and Roberts, 2000; Roberts et al., 1998; Scholz et al., 2008). The FF pattern has also been suggested to improve running economy by increasing the storage and release of elastic energy compared to the RF pattern (Ardigo et al., 1995; Hasegawa et al., 2007; Lieberman et al., 2010; Perl et al., 2012). The FF pattern may result in greater muscle forces and thus greater stretch and elastic energy as a result of increased plantar flexion moments generated in the first 60% of stance compared to RF running (Arendse et al., 2004; Williams et al., 2000). However, a longer AT moment arm resulting from the plantar flexed position in early stance during FF running suggests that the increased plantar flexion moments may be produced without substantial differences in muscle forces compared to RF running. If the muscle forces between footfall patterns are more similar than the differences in plantar flexion moments may indicate, then the amount of elastic energy storage may also be similar between footfall patterns. Therefore, differences in the dynamic AT moment arm between footfall patterns may explain why previous studies have not found a difference in running economy between footfall patterns (Ardigo et al., 1995; Cunningham et al., 2010; Perl et al., 2012).

In addition to the cause for increased elastic energy utilization during FF running, the greater plantar flexion moments and eccentric work produced during this pattern compared to RF running have also lead some to suggest that FF running places increased stress on the AT and increase the risk of AT injury (Nilsson and Thorstensson, 1989; Oakley and Pratt, 1988; Williams et al., 2000). Greater muscle forces required to

produce a given joint moment may compromise the safety factor of the tendon and increase the risk of a tendon overuse injury or rupture (Biewener, 2005; Scholz et al., 2008). However, if the plantar flexed position at touch-down with the FF pattern results in a longer AT moment arm, greater muscle forces may not be required to produce these moments compared to the muscle forces produced if the moment arm was shorter.

Differences in AT moment arm between footfall patterns during the stance phase of running may play a role in muscle force production and thus running economy between RF and FF running. The FF pattern may be more economical by resulting in a longer AT moment arm in early stance to reduce the required muscle force but also by increasing elastic energy utilization later in stance as a result of greater muscle forces and tendon stretch. Therefore, the purpose of this study was to determine the AT moment arm length during the stance phase of RF and FF running and to investigate the relationship between moment arm length and running economy. Because the dynamic AT moment arm may affect the differences in muscle forces required between footfall patterns, an additional purpose of this study was to determine the difference in AT force between RF and FF running patterns. The following hypotheses were investigated: 1) AT moment arm length would be greater during the first third of the stance phase with the FF running pattern compared to RF running and similar during the rest of the stance; 2) a shorter AT moment arm would correlate with running economy during RF running but a longer AT moment arm would correlate with running economy during FF running; and 3) AT force would be similar between footfall patterns during the stance phase of running.

Methodology

Participant Selection

A list of acronyms and abbreviations used in this study are listed in Table 5.1. Nineteen healthy natural RF runners and 18 natural FF runners participated in this study (Table 5.2). Participants were experienced runners completing a minimum of 16 km per week with an average speed of approximately 3.5 $m \cdot s^{-1}$ for long running bouts. Exclusion criteria included a history of cardiovascular or neurological problems and injury to the lower extremity or back within the past year. Vertical ground reaction forces (GRF) and high speed video recordings were used to determine the natural footfall pattern of each participant while running at their preferred running speed. RF running was defined as making initial contact with the heel. FF running was defined as making initial contact with the metatarsal heads and preventing the heel from touching the ground. If a participant was classified as a midfoot runner (MF), they were placed in the RF group if they made contact with (approximately zero degrees of dorsiflexion or greater) and generated an initial impact peak within the vertical GRF component (n = 4). MF runners were classified into the FF group if they landed with a plantar flexed foot position but allowed the heel to touch the ground and did not generate an initial impact peak (n = 6). All participants read and completed an informed consent document and questionnaires approved by the University of Massachusetts Amherst Institutional Review Board before participating.

Table 5.1: Acronyms and abbreviations for each variable.

$AAave_1$	early stance average ankle angle	ATmax	maximum Achilles tendon force
$AAave_2$	mid-stance average ankle angle	dmt_0	static Achilles tendon moment arm length
$AAave_3$	late stance average ankle angle	dmt_1	early stance average Achilles tendon moment arm length
AM_{10}	average active ankle joint moment when Achilles tendon force was 10% of maximum the maximum value	dmt_2	mid-stance average Achilles tendon moment arm length
$AMave_1$	early stance average active ankle joint moment	dmt_3	late stance average Achilles tendon moment arm length
$AMave_2$	mid-stance average active ankle joint moment	dmt_{10}	average Achilles tendon moment arm length when Achilles tendon force was 10% of maximum the maximum value
$AMave_3$	late stance average active ankle joint moment	FF	forefoot
AMmax	maximum active ankle joint moment	GRF	ground reaction force
AT	Achilles tendon	MF	midfoot
AT_{10}	average Achilles tendon force when Achilles tendon force was 10% of maximum the maximum value	r	Pearson product moment correlation coefficient
$ATave_1$	early stance average Achilles tendon force	r^2	coefficient of determination
$ATave_2$	mid-stance average Achilles tendon force	RF	Rearfoot
$ATave_3$	late stance average Achilles tendon force	$\dot{V}O_2$	steady state rate of oxygen consumption

Table 5.2: Mean ± SD participant characteristics of the rearfoot group (RF) and the forefoot group (FF) for the participants included in Study 2. Differences between groups were assessed with a student's t-test ($\alpha = 0.05$).

	Males/Females (#)	Age (yrs)	Height (m)	Mass (kg)	Pref. Speed ($m \cdot s^{-1}$)	Distance/week (km)
RF group	12/7	26.7 ± 6.1	1.75 ± 0.09	70.10 ± 10.00	3.47 ± 0.90	42.85 ± 29.04
FF group	13/5	25.6 ± 6.4	1.76 ± 0.10	68.69 ± 9.77	3.73 ± 0.25	51.22 ± 24.76
p-value	-	0.585	0.918	0.668	0.242	0.353

Experimental Setup

An eight-camera Qualisys Oqus 3-Series optical motion capture system (Qualisys, Inc., Gothenberg, Sweden), sampling at 240 Hz, surrounded the center of a 25 m runway and was used to collect unilateral three-dimensional kinematic data. A floor mounted

AMTI force platform (OR6-5, AMTI Inc., Watertown, MA, USA) was located in the center of the collection volume and collected GRF and center of pressure data at a sampling frequency of 1200 Hz. Running speed was monitored with photoelectric sensors (Lafayette Instrument Company, Lafayette, IN) placed 3 m before and after the force platform.

Retro-reflective markers were placed on the right lower extremity and pelvis of the participant according to McClay and Manal (1999) (Appendix B). Calibration markers included the iliac crests, greater trochanters, medial and lateral femoral condyles, medial and lateral malleoli, and the heads of the first and fifth metatarsals. Tracking markers included four non-collinear markers secured onto a rigid plate, positioned on the lateral thigh and leg, as well as a rigid plate with three non-collinear markers placed on the posterior calcaneus. Additional tracking markers, secured onto the skin or form fitting clothing, included the right and left anterior superior iliac spine and between the 5^{th} lumbar-1^{st} sacral vertebrae. Participants wore form-fitting clothing and neutral racing flats provided by the laboratory (RC 550, New Balance, Brighton, MA, USA).

The static AT moment arm length was measured using methods similar to those of Scholz et al. (2008). The static AT moment arm was defined as the shortest distance from the line of action of the AT to the center of rotation of the ankle. The center of rotation of the ankle was approximated as the midpoint between the medial and lateral malleoli (Lundberg et al., 1989). The location of the lateral malleolus and its center were marked with a pen while the participant was standing (Figure 5.2). A high speed video camera (Exilim EX-F1, Casio Computer Co., LTD, Shibuya-ku, Tokyo, Japan) sampling at 300 Hz was used to record video of the foot and leg during a static standing trial. The

length of the static AT moment arm was recorded with each participant standing on a wooden block of known length. The lateral edge of the shoe was aligned with the edge of the block. The posterior aspect of the AT was identified on the video. The length of the static AT moment arm was determined by taking the average of the horizontal distance between the mark on the center of the lateral malleolus and the posterior aspect of the AT and the horizontal distance between the mark on the anterior aspect of the lateral malleolus and the posterior aspect of the AT. This procedure was used to better estimate the ankle joint center which lies on an axis connecting the medial and lateral malleoli. If the shoe upper covered the point on the AT necessary for indicating the posterior aspect, the thickness of the shoe upper was included in the measurement of the perpendicular distance then subtracted from the total length. This method was previously used by both Scholz et al. (2008) and Fath et al. (2010) who reported values that were well correlated with more precise magnetic resonance imaging data. The motion capture data were used to derive a second order polynomial to estimate the dynamic AT moment arm across the stance phase as a function of ankle joint angle (Arnold et al., 2010).

The volume and content of gases expired by each participant while running on a motorized treadmill was measured by indirect calorimetry using a metabolic cart (TrueOne, ParvoMedics, Sandy, UT, USA). The volume of gas exchange was used to calculate the gross rate of oxygen consumption.

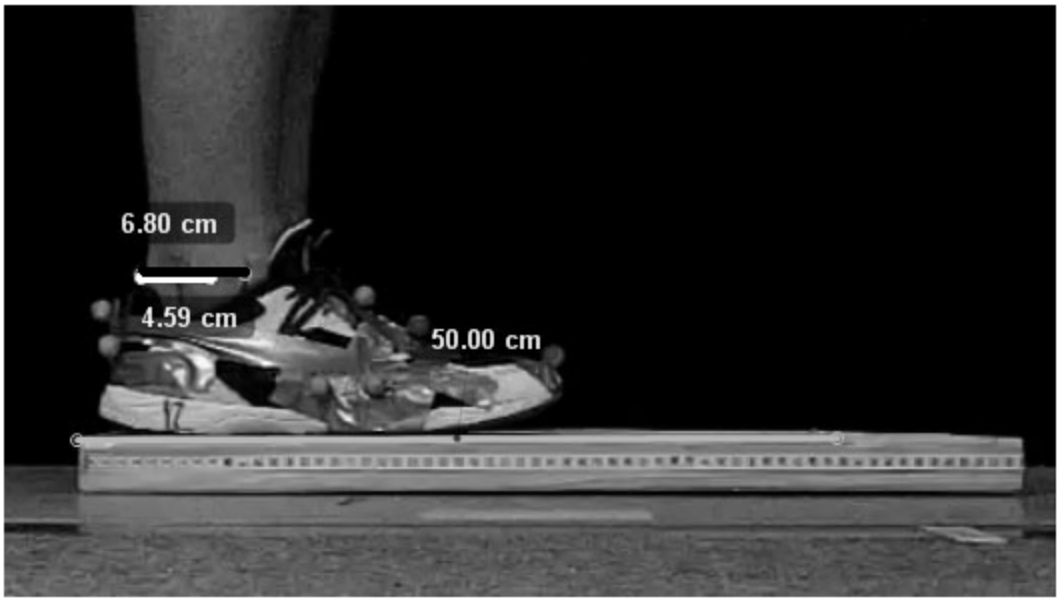

Figure 5.2: Measurement of Achilles tendon (AT) moment arm length during standing. The visual field was calibrated by determining the pixels in 50 cm reference distance. The distance between the ankle joint center and the posterior aspect of the AT was determined by averaging the distance between the medial (black line) and lateral malleoli (white line).

Protocol

After standing calibration of the reflective markers and the measurement of the AT moment arm were completed, each participant performed ten successful trials of each footfall pattern while running at 3.5 $m \cdot s^{-1}$ ±5%. A trial was deemed successful if the participant landed on the force platform with the right foot without targeting or adjusting speed or stride. The order of the footfall pattern conditions was randomized across participants.

Oxygen consumption was recorded during a separate data collection. Participants arrived at the laboratory having fasted for at least three hours and had refrained from exercise before the data collection. Participants were allowed to warm-up on the treadmill for a several minutes as needed and also practiced each footfall pattern at 3.5 $m \cdot s^{-1}$. Running speed was adjusted by ±5% if necessary to allow for the participant to

run comfortably with each footfall pattern. Participants began the data collection protocol by standing quietly for 10 minutes on the treadmill to record baseline oxygen consumption. Participants ran for a minimum of five minutes during each footfall pattern condition or until two minutes of steady state oxygen consumption was recorded. Steady state was reached when there was less than a 10% change in oxygen consumption over a two minute period (Stephens et al., 2006). Participants rested for a minimum of five minutes between conditions or until the volume of expired air returned within 0.02 $L \bullet min^{-1}$ of the baseline value.

Data Reduction

Kinematic data were tracked using Qualisys Track Manager software (Qualisys, Inc., Gothenberg, Sweden) and exported in .C3D format for processing with Visual 3D software (C-Motion, Inc, Rockville, MD, USA). Raw kinematic and kinetic data were filtered with a 4^{th} order, zero-lag Butterworth digital low-pass filter with a cutoff frequency of 12 Hz and 50 Hz respectfully (Winter et al., 1974). Three dimensional knee and ankle joint angles were calculated by a rotation matrix of the distal segment with respect to the coordinate system of the proximal segment using a Cardan rotation sequence of x (flexion/extension) – y (abduction/adduction) – z (axial rotation) (Cole et al., 1993). Ankle joint angles were averaged over early ($AAave_1$), mid- ($AAave_2$), and late stance ($AAave_3$). Early stance was defined as 0-33% of the stance phase, mid-stance as 34-66%, and late stance as 67-100%.

A Newton-Euler inverse dynamics approach was used to calculate three dimensional ankle joint moments. Segment geometries were modeled as a frustra of a

right cone for the foot and leg. Segment mass, location of segmental center of mass, and moment of inertia were estimated by techniques described by Hanavan (1964). Internal joint moments were calculated with respect to the local coordinate system of the proximal segment. Ankle joint angle and joint moments from the stance phase of each condition were interpolated to 101 data points from initial contact to toe-off, with each point representing 1% of the stance phase.

Kinovea Motion Tuner software v. 0.8.15 (www.kinovea.org/en/) was used to calculate the static AT moment arm length (dmt_0). A scaling factor was determined from the reference distance by the number of pixels that equaled the length of two points, 50 cm apart. The Euclidean distance between the center of the lateral malleolus and the posterior aspect of the Achilles tendon was determined. The distance in pixels was divided by the scaling factor to determine the length of the AT moment arm in cm.

A custom MATLAB program was developed to determine the AT force and the dynamic AT moment arm length during the stance phase of running with each footfall pattern. A separate plots for the moment arm of the plot soleus and the medial and lateral heads of the gastrocnemius moment arm at the ankle were created as a function of ankle joint angle (θ) based on generic model by Arnold et al. (2010). The data from each muscle were combined by scaling each by its physiological cross sectional area. The model data were fit to a second-order polynomial by a custom MATLAB program (Mathworks, Inc., Natick, MA) and used to determine the polynomial coefficients. A second-order polynomial was the lowest order that adequately fit the moment arm data, based on an assessment of the root mean square error between the polynomial prediction and the data. The zeroth-order polynomial coefficient was scaled for each subject

individually by the static Achilles tendon moment arm measurement. The experimental ankle joint angle data were entered into the polynomial to determine the dynamic AT moment arm for each instant of the stance phase. The model-predicted dynamic AT moment arm length was averaged over early (dmt_1), mid- (dmt_2), and late stance (dmt_3) and compared between footfall patterns.

To calculate AT force, the ankle and knee joint angles were used to estimate the passive joint moment (Riener and Edrich, 1999). The passive joint moment was subtracted from the net joint moment calculated by the inverse dynamics procedure to determine the active muscle moment. The maximum active ankle joint moment (AMmax) and the active ankle joint moment averaged over early ($AMave_1$), mid- ($AMave_2$), and late stance ($AMave_3$) were calculated and compared between patterns. The active ankle moment was divided by the dynamic AT moment arm at each instant of stance to determine the AT force. It was assumed that the force in the AT was zero whenever the active ankle moment was in the direction of dorsiflexion. The model-predicted maximum AT force (ATmax) and the AT force averaged over early ($ATave_1$), mid- ($ATave_2$), and late stance ($ATave_3$) were calculated. The model-predicted active ankle joint moment (AM_{10}), AT force (AT_{10}), and the dynamic AT moment arm (dmt_{10}) were averaged over the period of stance at which the AT force was within 10% of the maximum value. The relationship of these variables in addition to dmt_0 and of the rate of oxygen consumption was determined and compared between footfall patterns. The results of the correlation between each oxygen consumption variable and AM_{10} and AT_{10} are presented in Appendix D.

The absolute ($L \cdot min^{-1}$) and relative ($ml \cdot kg^{-1} \cdot min^{-1}$) rates of steady state oxygen consumption ($\dot{V}O_2$) over the last two minutes of each condition was averaged to determine the net and gross $\dot{V}O_2$. The first five minutes of the baseline oxygen consumption measure was typically highly variable as the participants became accustom to breathing with the mouthpiece. As a result, the average rate of oxygen consumption over the last five minutes of the baseline period was used to calculate net $\dot{V}O_2$ by subtracting the baseline value from the average rate of oxygen consumption during the last two minutes of each running condition.

Statistical Analysis

Each ankle joint angle, ankle joint moment, AT force, AT moment arm, and $\dot{V}O_2$ variable was compared between the RF and FF patterns. A one-way analysis of variance (ANOVA) was used to assess the differences in dmt_0 between groups with a significance level of $\alpha = 0.05$. Additionally, each variable was subjected to a mixed model analysis of variance with footfall pattern and group as fixed variables and subject nested within group as a random variable. The differences between footfall patterns (2 levels) and between groups (2 levels) and the interaction of footfall pattern and group were assessed with a significance level of $\alpha = 0.05$. When a significant group by pattern interaction was observed, a post-hoc assessment was performed by partitioning the interaction by group and by pattern. Partitioning by group determined the significance between each footfall pattern within each group. Partitioning by pattern determined the significance between groups within each footfall pattern. A Pearson product moment correlation coefficient (r) was calculated to determine the relationship between absolute and relative $\dot{V}O_2$ and the

static (dmt_0) and dynamic (dmt_{10}) AT moment arm lengths. A correlation coefficient of 0.00 – 0.09 indicated no correlation, 0.10 – 0.30 was a weak correlation, 0.30 – 0.50 was a moderate, and 0.50 – 1.00 was a strong correlation (Cohen, 1988). Effect sizes were also calculated to determine if the differences between footfall pattern and groups were biologically meaningful. An effect size (d) greater than 0.3 indicated a small effect, an effect size greater than 0.5 indicated a moderate effect and an effect size greater than 0.8 indicated a large effect (Cohen, 1992).

Results

Ankle Joint Angle

No significant group by pattern interactions or group main effects were observed for $AAave_1$, $AAave_2$, or $AAave_3$ ($p > 0.05$). Significant pattern main effects, however, were found for these variables ($p < 0.05$, $d = 0.8 – 3.4$) (Table 5.3). AA ave_1 from each footfall pattern reflected the characteristic initial dorsiflexed position of RF running as well as the initial plantar flexed position of the FF pattern (Figure 5.3A). $AAave_2$ and $AAave_3$ were 2.21 degrees (11.3%) and 5.43 degrees (101.1%) more dorsiflexed, respectively, during the RF pattern compared to the FF pattern.

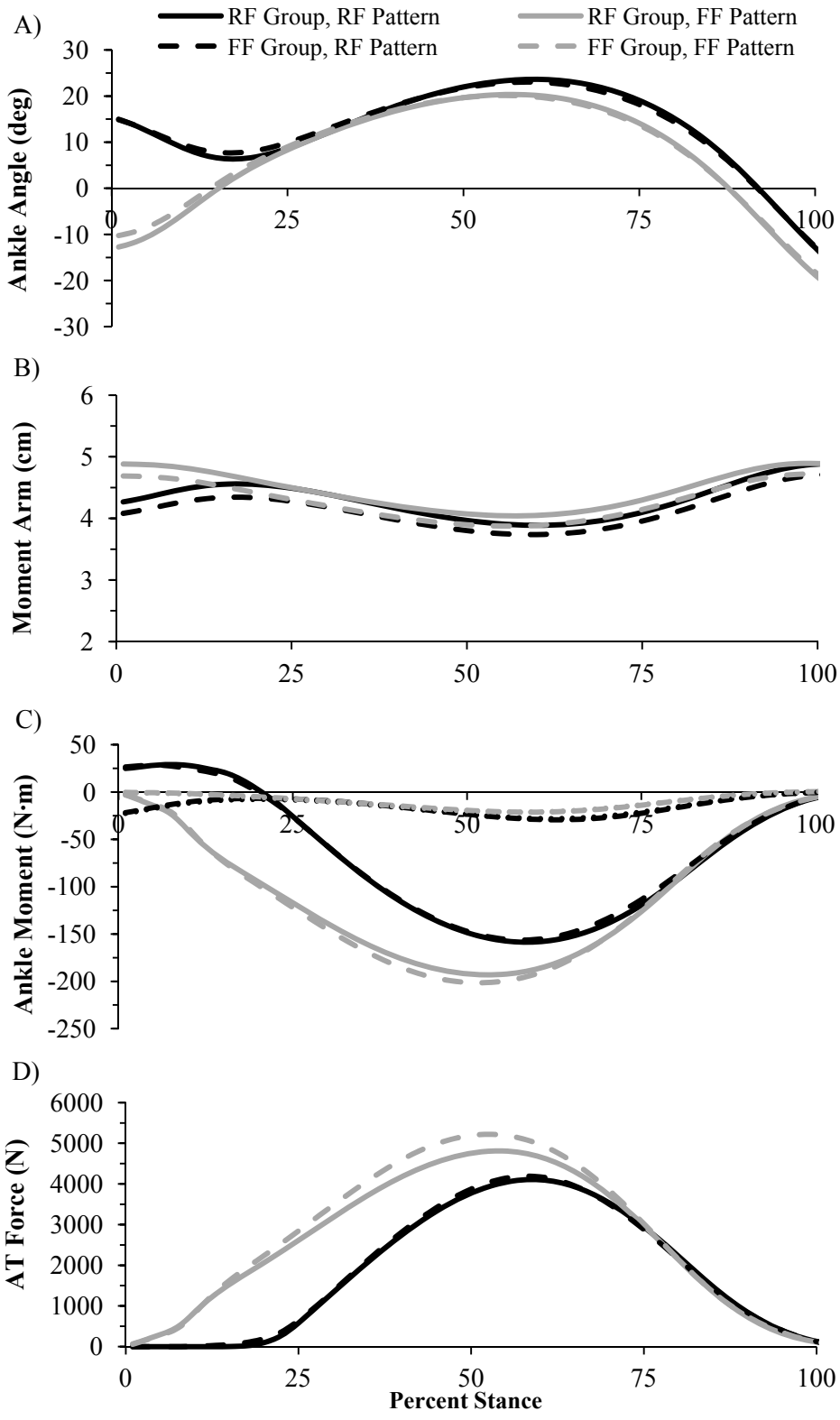

Figure 5.3: Group mean time series of the A) sagittal plane ankle angle, B) Achilles tendon (AT) moment arm, C) active and passive (small dashed line) ankle joint moment, and D) AT force of the rearfoot (RF) and forefoot (FF) groups performing the RF and FF patterns.

Table 5.3: Mean ± SD for the ankle joint angle and Achilles tendon (AT) moment arm variables when performing the rearfoot (RF) and forefoot (FF) patterns. Variables include ankle joint angle averaged over early ($AAave_1$), mid- ($AAave_2$), and late stance ($AAave_3$), and the AT moment arm averaged over early (dmt_1), mid- (dmt_2), and late stance (dmt_3). The AT moment arm length (dmt_{10}) was also averaged over the period of stance at which the AT force was within 10% of the maximum value. Listed statistics include the *p*-value for the group by pattern interaction (GxP), the p-value (*d*) for the group main effect (G) and the pattern main effect (P).

	RF Group		FF Group		GxP	G	P
	RF	FF	RF	FF			
$AAave_1$ deg	9.94 ± 2.23	0.92 ± 2.62	10.52 ± 2.73	2.04 ± 2.85	0.695	0.157 (0.3)	<0.001 (3.4)
$AAave_2$ deg	20.81 ± 2.51	18.48 ± 2.73	20.85 ± 2.59	18.49 ± 2.78	0.612	0.906 (0.0)	<0.001 (0.8)
$AAave_3$ deg	8.35 ± 2.77	2.67 ± 3.18	7.83 ± 2.64	2.65 ± 2.53	0.458	0.755 (0.1)	<0.001 (2.0)
dmt_1 cm	4.45 ± 0.64	4.65 ± 0.66	4.24 ± 0.33	4.44 ± 0.29	0.796	0.215 (0.4)	<0.001 (0.4)
dmt_2 cm	4.02 ± 0.66	4.12 ± 0.68	3.84 ± 0.32	3.94 ± 0.31	0.498	0.303 (0.4)	<0.001 (0.2)
dmt_3 cm	4.42 ± 0.67	4.56 ± 0.68	4.25 ± 0.31	4.38 ± 0.30	0.417	0.331 (0.3)	<0.001 (0.3)
dmt_{10} cm	3.90 ± 0.66	4.05 ± 0.69	3.74 ± 0.33	3.88 ± 0.32	0.393	0.351 (0.3)	<0.001 (0.3)

Achilles Tendon Moment Arm Length

There was no significant difference in dmt_0 between groups ($p = 0.286$, $d = 0.4$). dmt_0 was 4.72 ± 0.67 cm in the RF group and 4.53 ± 0.29 in the FF group. No significant group by pattern interactions or group main effects were found for any dynamic AT moment arm length variable during the stance phase ($p > 0.05$). However, dmt_{10}, dmt_1, dmt_2, and dmt_3 were all greater during the FF pattern compared to the RF pattern as indicated by significant group main effects ($p < 0.05$, $d = 0.2 – 0.4$) (Table 5.3). dmt_{10}, dmt_1, dmt_2, and dmt_3 were 0.15 cm (3.8%), 0.20 cm (4.6%), 0.10 cm (2.5%), and 0.14 cm (3.1%) longer, respectively, during FF running compared to RF running (Figure 5.3B).

Table 5.4: Mean ± SD for the stance phase kinetic variables when performing the rearfoot (RF) and forefoot (FF) patterns. Variables include the maximum active ankle joint moment (AMmax), the active ankle moment averaged over early ($AMave_1$), mid- ($AMave_2$), and late stance ($AMave_3$), the maximum Achilles tendon force (ATmax), the AT force averaged over early ($ATave_1$), mid- ($ATave_2$), and late stance ($ATave_3$). The ankle joint moment (AM_{10}) and AT force (AT_{10}) are the ankle joint moment and AT force were also averaged over the period of stance at which the AT force was within 10% of the maximum value. Listed statistics include the *p*-value for the group by pattern interaction (GxP), the p-value (*d*) for the group main effect (G) and the pattern main effect (P).

	RF Group		FF Group		GxP	G	P
	RF	FF	RF	FF			
AMmax N•m	-159.45 ± 36.47	-193.46 ± 47.10	-156.27 ± 36.99	-200.18 ± 44.72	0.128	0.895 (0.0)	<0.001 (0.9)
$AMave_1$ N•m	-1.42 ± 10.46	-77.05 ± 20.37	-3.59 ± 18.75	-78.53 ± 19.67	0.934	0.659 (0.1)	<0.001 (4.3)
$AMave_2$ N•m	-137.05 ± 29.60	-181.73 ± 44.01	-134.66 ± 34.24	-187.59 ± 41.92	0.288	0.885 (0.0)	<0.001 (1.3)
$AMave_3$ N•m	-73.10 ± 17.48	-75.03 ± 18.08	-68.31 ± 14.50	-72.98 ± 15.64	0.206	0.525 (0.2)	0.004 (0.2)
AM_{10} N•m	-157.89 ± 36.01	-192.14 ± 46.82	-154.73 ± 36.59	-198.75 ± 44.39	0.134	0.897 (0.0)	<0.001 (1.0)
ATmax N	4127.77 ± 810.37	4824.80 ± 1055.78	4200.39 ± 988.39	5204.52 ± 1251.18	0.071	0.498 (0.2)	<0.001 (0.8)
$ATave_1$ N	362.53 ± 144.54	1706.20 ± 399.97	409.57 ± 269.78	1825.29 ± 495.59	0.625	0.362 (0.3)	<0.001 (4.2)
$ATave_2$ N	3459.03 ± 658.27	4454.60 ± 966.52	3529.63 ± 882.10	4804.89 ± 1162.85	0.167	0.473 (0.2)	<0.001 (1.2)
$ATave_3$ N	1757.91 ± 392.91	1740.38 ± 418.93	1698.82 ± 367.32	1775.09 ± 418.53	0.161	0.865 (0.1)	0.459 (0.0)
AT_{10} N	4079.78 ± 799.72	4786.32 ± 1047.09	4149.96 ± 974.73	5160.48 ± 1240.79	0.074	0.501 (0.2)	<0.001 (0.8)

Active Ankle Joint Moment

No significant group by pattern interactions or group main effects were observed for any ankle joint moment variable ($p > 0.05$). A significant pattern main effect was observed for AM_{10}, AMmax, $AMave_1$, $AMave_2$, and $AMave_3$ ($p < 0.05$, $d = 0.2 – 4.2$) (Table 5.4). AM_{10}, AMmax, $AMave_1$, $AMave_2$, and $AMave_3$ were 39.13 N•m (22.2%),

38.96 N•m (21.9%), 75.28 N•m (187.7%), 48.81 N•m (30.4%), and 3.30 N•m (4.2%) greater, respectively, in FF running compared to RF running (Figure 5.3C).

Achilles Tendon Force

No significant group by pattern interactions or group main effects were observed for any AT force variable ($p > 0.05$). A significant pattern main effect was observed for AT_{10}, ATmax, $ATave_1$, and $ATave_2$ ($p < 0.05$, $d = 0.8 – 4.2$) but not $ATave_3$ ($p < 0.05$, $d = 0.0$) (Table 5.4). AT_{10}, ATmax, $ATave_1$, and $ATave_2$ were 858.5 N (18.8%), 850.58 N (18.5%), 1379.70 N (128.2%), and 1135.42 N (27.9%) greater, respectively, in FF running compared to RF running (Figure 5.3D). $ATave_3$ was only 19.37 N (1.1%) different between patterns.

Rate of Oxygen Consumption

Significant group by pattern interactions were observed for net and gross $\dot{V}O_2$ ($p < 0.05$) (Table 5.5). Partitioning the interaction by group revealed that the RF group ran with over 3% greater $\dot{V}O_2$ when performing the FF pattern compared to when performing the RF pattern ($p < 0.05$, $d = 0.2 – 0.7$). The FF group did not have a significant difference in net or gross $\dot{V}O_2$ between footfall patterns ($p > 0.05$, $d < 0.1$). Partitioning the interaction by pattern revealed that performing the RF pattern resulted in the RF group having between 2.9 – 5.1% greater net and gross $\dot{V}O_2$ compared to the FF group ($p < 0.05$, $d = 0.3 – 0.5$) (Table 5.5). When performing the FF pattern, net and gross $\dot{V}O_2$ were between 5.3 – 8.0% greater in the RF group compared to the FF group ($p < 0.05$, $d = 0.5 – 1.0$).

Table 5.5: Mean ± SD net and gross rate of oxygen consumption ($\dot{V}O_2$) during running with a rearfoot (RF) and a forefoot (FF) pattern in the RF and FF groups. Listed statistics include the *p*-value for the group by pattern interaction (GxP), the *p*-value (*d*) for the group main effect (G), and the pattern main effect (P). If the interaction was significant, the *p*-value (*d*) for each partition by group and partition by pattern were given. dmt_0 was evaluated with a one-way analysis of variance, thus only a single *p*-value (*d*) are given for the difference of dmt_0 between groups. Negative percent difference indicates the FF pattern resulted in a larger value.

Group	Pattern	Net $\dot{V}O_2$ $L \cdot min^{-1}$	Gross $\dot{V}O_2$ $L \cdot min^{-1}$	Net $\dot{V}O_2$ $ml \cdot kg^{-1} \cdot min^{-1}$	Gross $\dot{V}O_2$ $ml \cdot kg^{-1} \cdot min^{-1}$
RF	RF	2.44 ± 0.38	2.76 ± 0.42	34.79 ± 1.85	39.36 ± 2.00
RF	FF	2.53 ± 0.42	2.85 ± 0.46	36.05 ± 1.80	40.62 ± 2.02
% difference		-3.7%	-3.3%	-3.6%	-3.2%
FF	RF	2.32 ± 0.38	2.63 ± 0.42	33.66 ± 2.39	38.25 ± 2.61
FF	FF	2.34 ± 0.39	2.65 ± 0.43	33.93 ± 2.51	38.51 ± 2.63
% difference		-0.9%	-0.8%	-0.8%	-0.7%
GxP		0.004	0.004	0.003	0.003
G		-	-	-	-
P		-	-	-	-
G Partition	RF Grp	<0.001(0.2)	<0.001(0.2)	<0.001(0.7)	<0.001(0.6)
G Partition	FF Grp	0.245 (0.1)	0.239(0.0)	0.255(0.1)	0.255(0.1)
P Partition	RF Patt	<0.001(0.3)	<0.001(0.3)	<0.001(0.5)	<0.001(0.5)
P Partition	FF Patt	<0.001(0.5)	<0.001(0.4)	<0.001(1.0)	<0.001(0.9)

Relationship of Rate of Oxygen Consumption and Achilles Tendon Moment Arm

In the RF group performing the RF pattern, moderate correlations were found between net and gross absolute $\dot{V}O_2$ and dmt_0 (net: $r = 0.484$, $r^2 = 0.234$; gross: $r = 0.490$, $r^2 = 0.240$) (Figure 5.4A) and dmt_{10} (net: $r = 0.488$, $r^2 = 0.238$; gross: $r = 0.492$, $r^2 = 0.242$) (Figure 5.5A). When the RF group performed the FF pattern, a moderate was also found between net and gross absolute $\dot{V}O_2$ and dmt_0 (net: $r = 0.466$, $r^2 = 0.217$; gross: $r = 0.472$, $r^2 = 0.223$) (Figure 5.4A) and net and gross absolute $\dot{V}O_2$ and dmt_{10} (net: r =

0.457, $r^2 = 0.209$; gross: r = 0.462, $r^2 = 0.213$) (Figure 5.5A). Both dmt_0 and dmt_{10} explained less than 25% of the variance of net and gross absolute $\dot{V}O_2$ in the RF group when performing the RF or FF patterns. In the FF group performing the RF pattern, weak were only found between gross absolute $\dot{V}O_2$ and dmt_0 (r = 0.137, $r^2 = 0.019$) (Figure 5.4A) and net absolute $\dot{V}O_2$ and dmt_{10} (r = -0.120, $r^2 = 0.014$) (Figure 5.5A). No correlations were between net absolute $\dot{V}O_2$ and dmt_0 and gross absolute $\dot{V}O_2$ and dmt_{10} for the FF group when performing the RF pattern (Figure 5.4A and 5.5A). Additionally, no correlations were found between net or gross absolute $\dot{V}O_2$ and dmt_0 when the FF group performed the FF pattern ($r < 0.09$, $r^2 < 0.007$) (Figure 5.4A). However, weak correlations were found between net and gross absolute and dmt_{10} when the FF group performed the FF pattern (net: r = -0.141, $r^2 = 0.020$; gross: r = -0.093, $r^2 = 0.009$) (Figure 5.5A). Less than 2% of the variance in net and gross absolute $\dot{V}O_2$ was explained by either dmt_0 or dmt_{10} in the FF group when performing the RF or FF footfall patterns.

There was no correlation between net or gross relative $\dot{V}O_2$ between dmt_0 and dmt_{10} in the RF group when performing either footfall pattern ($r < 0.042$, $r^2 < 0.002$) (Figures 5.4B and 5.5B). In the FF group performing the RF pattern, weak to moderate correlations were found between net and gross relative $\dot{V}O_2$ and dmt_0 (net: r = -0.273, $r^2 = 0.075$; gross: r = -0.124, $r^2 = 0.015$) and dmt_{10} (net: r = -0.459, $r^2 = 0.211$; gross: r = -0.352, $r^2 = 0.124$) (Figures 5.4B and 5.5B). When the FF group performed the FF pattern, net and gross relative $\dot{V}O_2$ was weak to moderately correlated with dmt_0 (net: r = -0.381, $r^2 = 0.145$; gross: r = -0.237, $r^2 = 0.056$) (Figure 5.4B) and dmt_{10} (net: r = -0.446, $r^2 = 0.120$; gross: r = -0.358, $r^2 =$, 0.128) (Figure 5.5B). In the FF group performing the RF pattern, dmt_0 explained less than 8% of the variance in net and gross relative $\dot{V}O_2$

whereas dmt_{10} explained approximately 22% of the variance in net and gross relative

. However, when the FF group performed the FF pattern, less than 13% of the variance in net and gross relative was explained by either dmt_0 or dmt_{10}.

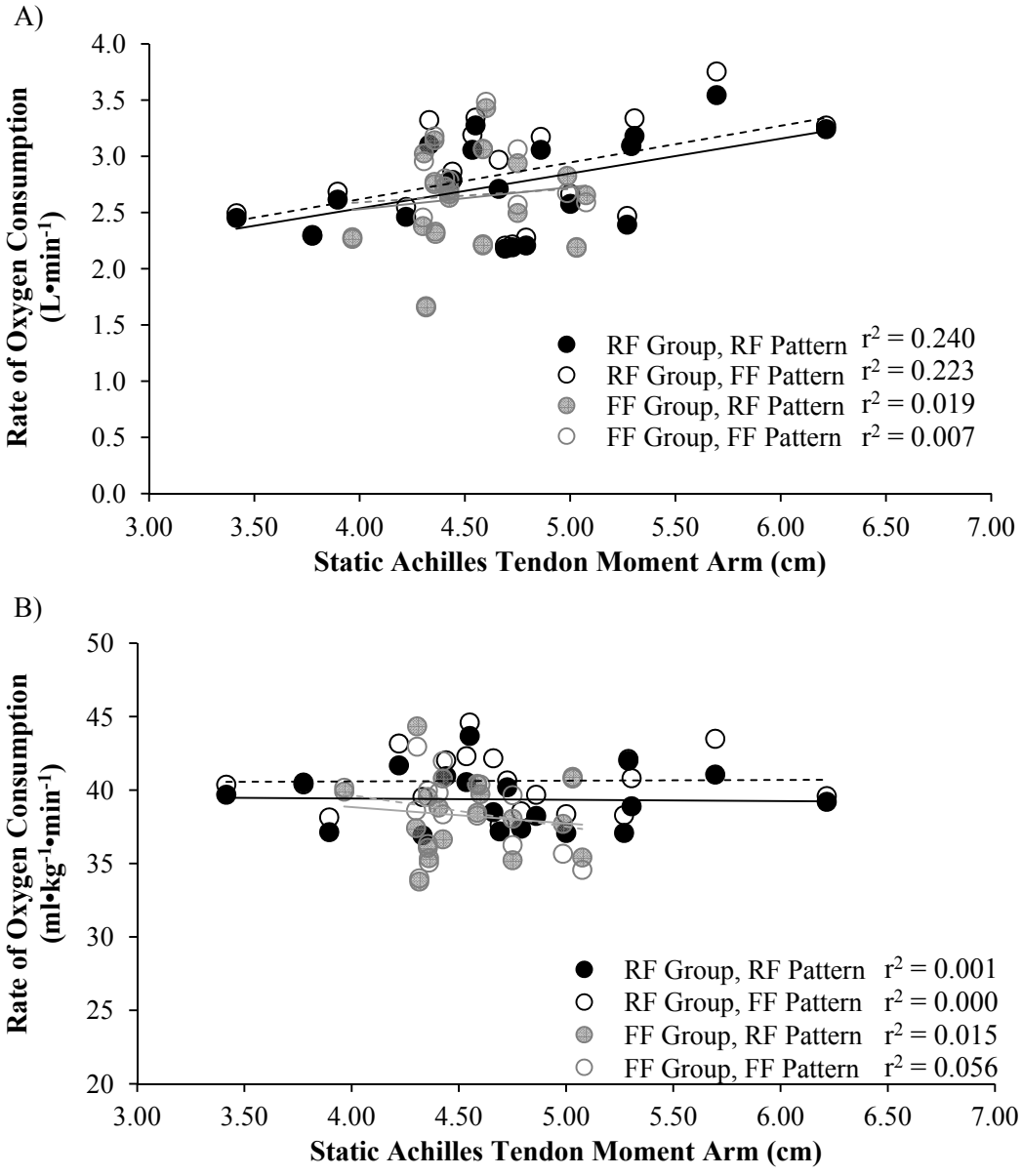

Figure 5.4 The relationship of Achilles tendon moment arm length measured during standing and the gross A) absolute and B) relative rate of oxygen consumption measured during rearfoot (RF) and forefoot (FF) running in the RF and FF groups.

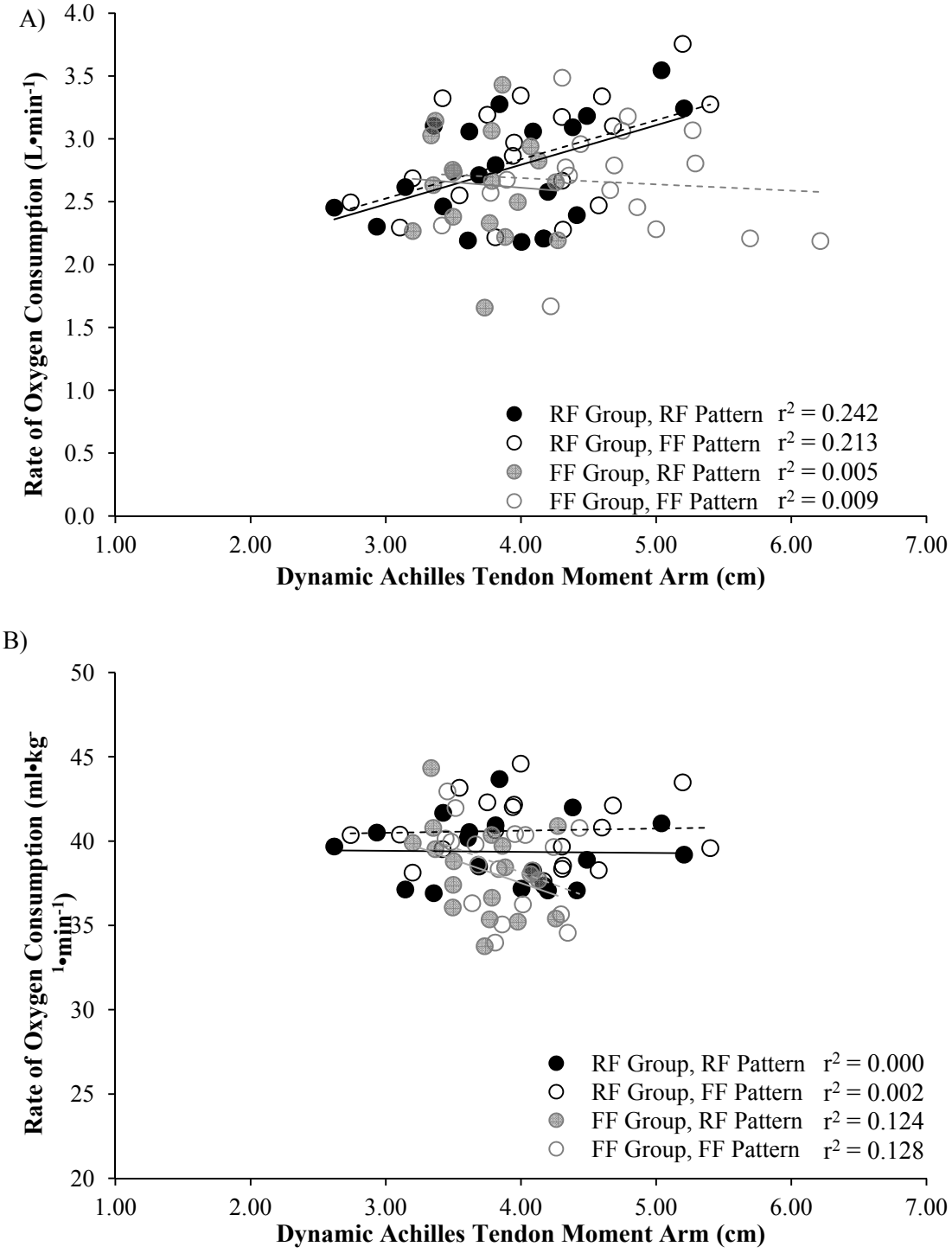

Figure 5.5: The relationship of the dynamic Achilles tendon moment arm length and the gross A) absolute and B) relative rate of oxygen consumption measured during rearfoot (RF) and forefoot (FF) running in the RF and FF groups.

Discussion

The purposes of this study were to investigate the relationship of AT moment arm length and running economy in RF and FF running patterns and to determine the difference in AT force between RF and FF running patterns. This study expands on the results of previous studies by investigating the relationship between static as well as dynamic AT moment arm length and sub-maximal rate of oxygen consumption in both RF and FF runners. Previous studies investigated the relationship of static AT moment arm length and rate of oxygen consumption in a group of RF runners (Scholz et al., 2008). The first hypothesis, that the model-predicted dynamic AT moment arm length would be greater during the early stance phase in the FF running pattern compared to the RF pattern, was supported. The FF pattern resulted in a longer dynamic AT moment arm during the first portion of stance as well as across the rest of the stance phase compared to the RF pattern. A longer AT moment arm during FF running was a result of the decreased dorsiflexion angle throughout the stance phase with this pattern.

A study by Scholz et al. (2008) reported that a shorter static AT moment arm resulted in greater running economy due to increased tendon stretch and elastic energy storage. A shorter static AT moment arm is a morphological measure that will result in increased force production for a given joint moment. Although muscle moment arm length is a morphological measure, it changes with joint position and it may be possible to manipulate joint position to improve economy. If the kinematics of a particular running style result in joint angles that are smaller, then running economy may improve compared to a running style that utilizes a longer AT moment arm. However, with the FF pattern, a longer AT moment arm resulting from the plantar flexed position in early

stance may decrease the force and thus metabolic cost compared if the moment arm was shorter. Although the dynamic AT moment arm was shorter throughout stance with the RF pattern and longer with the FF pattern in the present study, similar correlations between rates of oxygen consumption and dynamic AT moment arm were observed between footfall patterns. Thus, the second hypothesis that a shorter AT moment arm would correlate with running economy during RF running but a longer AT moment arm would correlate with running economy during FF running, was not supported. Weak to moderate correlations between absolute or relative $\dot{V}O_2$ and static and dynamic moment arm were found in the present study. The relationship between absolute $\dot{V}O_2$ and dmt_0 or dmt_{10} in the both groups were less than 0.03 larger in RF running compared to FF running, but this difference is likely irrelevant. Some negative correlations were found which indicated that a longer moment arm was related to a lower rate of oxygen consumption; however, they were found between data from both the RF and FF pattern. This finding may be a reflection of the variability in the moment arm data.

Although the static AT moment arm lengths determined in the present study were in good agreement with those of Scholz et al. (2008), the results of the correlation analysis, however, were not in agreement. Scholz et al. (2008) found that static AT moment arm length explained approximately 56% of the variance in sub-maximal rate of oxygen consumption. The present study, however, found less than 25% of the variance in the rate of oxygen consumption was explained by either static or dynamic moment arm in both RF and FF runners performing either the RF or FF pattern. However, depending on the group, footfall pattern or absolute or relative rate of oxygen consumption, the strength of the correlation decreased, resulting in AT moment arm explaining less than

1% of the variance in oxygen consumption. Since no differences in static AT moment arm were found between groups in the present study and were in good agreement with Scholz et al. (2008), the discrepancy in the findings between studies was not a result of morphological differences between participants or between natural RF and FF runners. Other differences between the present study and that of Scholz et al. (2008) may also contribute to the discrepancy between results. For example, the present study used a running speed 1.0 $m \cdot s^{-1}$ slower than Scholz et al. (2008), which may have affected the rates of oxygen consumption between participants of each study. However, as part of a separate study, the participants in the present study performed each footfall pattern at an additional running speed which was within 0.5 $m \cdot s^{-1}$ of Scholz et al (2008). The methods between the present study and the additional data set were the same except the dynamic moment arm was not measured at the higher running speed. In this additional data set, static AT moment arm explained less than 10% of the variance in gross relative rate of oxygen consumption across both groups and conditions (Figure 5.6). Therefore, the differences between results of the present study and Scholz et al. (2008) may not be due to differences in running speed. The difference in the spread of the data may also account for the differences in correlations found in each study. The present study had a larger range in static AT moment arm values but a smaller range in rate of oxygen consumption values compared to Scholz et al. (2008) (Figure 5.6). A similarity between the studies was that they examined RF runners performing the RF pattern. The largest correlations found in the present study were found in the RF group when performing the RF pattern. Additionally, the RF pattern resulted in both a shorter AT moment arm throughout the stance phase as well as a lower rate of oxygen consumption compared to

the FF pattern. The result that lower rates of oxygen consumption were found with the footfall pattern that utilizes a shorter moment arm was consistent with the relationships found in Scholz et al. (2008). It is possible that AT moment arm and running economy may only be related to those performing and are habituated to the RF pattern. Scholz et al. (2008) acknowledged that inter-individual variation in kinetic factors may account for additional variation in running economy. Thus compared to the RF pattern, the different kinetic features of the FF pattern may alter the relationship between dynamic AT moment arm and the rate of oxygen consumption.

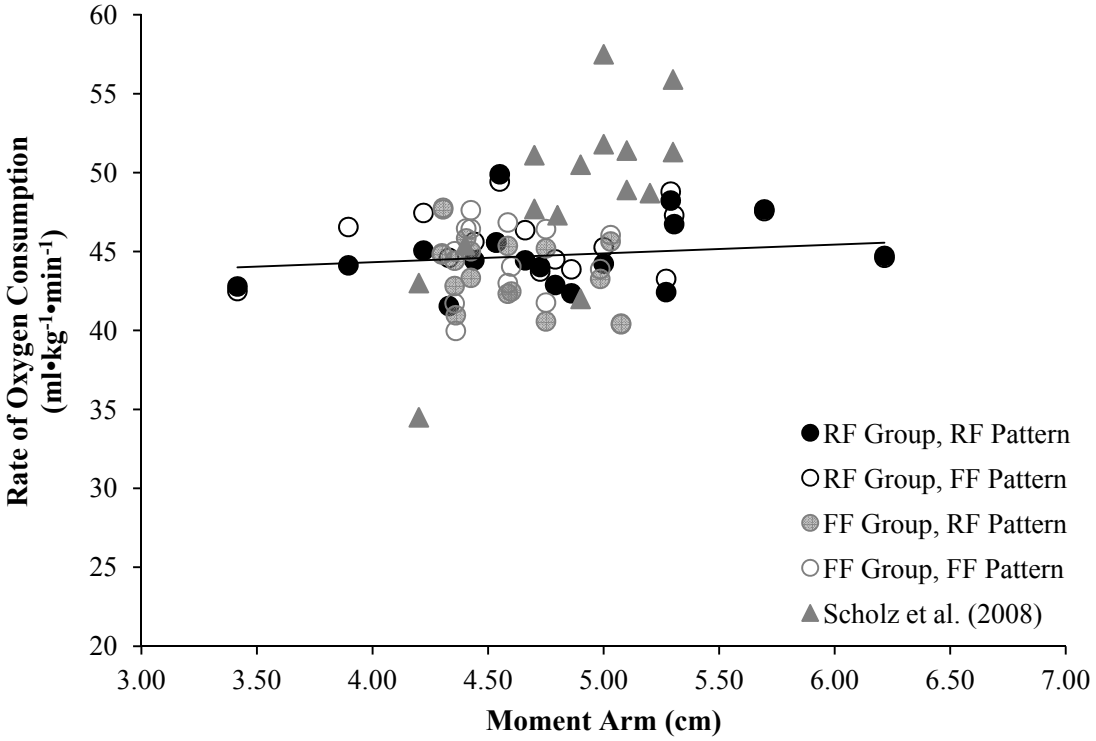

Figure 5.6: Results for the additional data set of the relationship between the Achilles tendon moment arm length measured during standing and the gross rate of oxygen consumption measured during rearfoot (RF) and forefoot (FF) running in the RF and FF groups for running at 4.0 m·s^{-1} (for comparison with the results of Scholz et al. (2008), running speed = 4.4 m·s^{-1}).

For a given joint moment, a shorter dynamic AT moment arm may improve running economy as a result of requiring greater muscle forces compared to if the moment arm was longer. Although greater force generation will increase the metabolic energy consumption of the muscle, increased muscle force will also increase the tendon stretch and thus the potential for greater energy storage and more economical running by allowing the muscle fibers to act more isometrically (Biewener and Roberts, 2000; Roberts et al., 1998). In the present study, FF running resulted in greater plantar flexion moments and AT forces compared to RF running, which supports the third hypothesis and was consistent with other studies (Arendse et al., 2004; Perl et al., 2012; Williams et al., 2000). It has been previously speculated that these larger plantar flexion moments generated with FF running result in greater elastic energy utilization and thus improve running economy compared to RF running. It was not within the scope of the present study to determine the differences in elastic energy utilization between footfall patterns; however, it is likely that the increased AT forces generated during FF running also resulted in greater elastic energy storage. Despite this possibility, the present study also observed that FF running did not result in an improvement in running economy over that of RF running. The metabolic cost associated with greater AT forces during FF running may have negated the energy savings from elastic recoil, if elastic recoil was also greater compared to RF running. Alternatively, a combination of increased elastic energy recoil and utilizing a longer moment arm throughout stance during FF running may have prevented larger differences in rates of oxygen consumption between footfall patterns given the differences in AT force generation. However, the results from the present study suggest that FF running may not be more economical than RF running because of the

greater muscle forces required with the FF pattern. The sources of variation in economy between RF and FF footfall patterns requires further study to examine the differences and relationships of muscle mechanical work and metabolic cost between RF and FF running patterns.

Although greater AT force may result in a beneficial elastic energy contribution to metabolic cost, the disadvantage of greater AT forces is the risk of developing tendon injury. Many chronic overuse injuries in running may be a result of repetitive stretch and recoil of tendon that could be exacerbated by increased tendon forces (Leadbetter, 1992). Compared to RF running, FF running resulted in greater AT force which suggests that it may increase the risk of developing tendon injury. Calculating the safety factor and the stressed imposed on the AT with each footfall pattern may provide some insight for this risk. By using 95 mm^2 as the cross-sectional area for the distal AT found in runners of previous studies (Magnusson and Kjaer, 2003; Rosager et al., 2002), the peak AT forces measured in the present study resulted in an AT stress of 43.5 MPa and 44.2 MPa during RF running in the RF and FF groups, respectively. During the FF pattern, AT force results in 50.8 MPa for the RF group and 54.8 MPa for the FF group. Although the FF pattern resulted in a greater AT stress than the RF pattern, both patterns resulted in an approximate safety factor of 4 – 5.5 and an AT stress far below the rupture stress of the AT (100 MPa) (Ker et al., 2000). However, it is likely that the rupture stress of the AT is greater than 100 MPa, as this value was found *in vitro* (Farris et al., 2011).

Repetitive impact loading from running may also result in adaptations to protect against tendon injury (Magnusson and Kjaer, 2003; Rosager et al., 2002). Previous studies have shown that runners have a greater AT cross-sectional area than non-runners,

which suggests runners may experience lower tendon stress and a greater safety factor for a given load compared to non-runners (Magnusson et al., 2001; Magnusson and Kjaer, 2003; Rosager et al., 2002). These findings suggest that habitual exposure to greater AT forces in FF runners may lead to an adaptation in which the cross-sectional area of the AT is larger than RF runners. Therefore, an AT cross-sectional area of 95 mm^2 may be an underestimate for FF runners and the AT stress calculated above may be an overestimate. However, the distal AT width was measured in a subgroup of participants from the present study (RF group n = 8; FF group n = 7) and was similar between groups (RF group = 17.0 ± 2.0 mm; FF group = 17.7 ± 2.0 mm; *p*-value = 0.895). Assuming a similar AT thickness between groups, these data suggest that FF running may not result in further adaptation the AT cross-sectional area compared to RF running. The calculated stress values above showed that the AT stress values are far below the failure stress; however, they represent the AT stress experienced during a single stance phase. For each stance phase, a natural RF runner performing their habitual pattern will experience approximately 43.5 MPa of AT stress each stance phase whereas a natural FF runner performing their habitual footfall pattern will experience approximately 54.8 MPa of AT stress each stance phase. These results suggest that the cumulative micro-trauma experienced by a FF runner will be greater than a RF runner due to the greater AT stressed experienced each stance phase, which will likely increase the risk of a FF runner developing tendinopathology.

Conclusion

Previous studies have observed a relationship between static AT moment arm length and the rate of oxygen consumption. The present study, however, found that only the RF pattern performed by the RF group resulted in a moderate correlation between these variables. The FF pattern may result in running mechanics that negate any relationship between AT moment arm length and the rate of oxygen consumption. A longer AT moment arm will provide a mechanical advantage in which reduced muscle forces are required to produce a given ankle joint moment; however, the longer AT moment arm resulting from FF running did not reduce the AT forces generated compared to the RF pattern. Additionally, the plantar flexor muscle force required during FF running may negate any metabolic energy savings from increased elastic energy recoil. These increased AT forces with the FF pattern may also increase the risk of developing tendinopathology.

References

1. Anderson T. Biomechanics and Running Economy. *Sports Med*. 1996; 22(2):76-89.

2. Ardigo LP, Lafortuna C, Minetti AE, Mognoni P, Saibene F. Metabolic and Mechanical Aspects of Foot Landing Type, Forefoot and Rearfoot Strike, in Human Running. *Acta Physiol Scand*. 1995; 155(1):17-22.

3. Arendse RE, Noakes TD, Azevedo LB, Romanov N, Schwellnus MP, Fletcher G. Reduced Eccentric Loading of the Knee with the Pose Running Method. *Med Sci Sports Exerc*. 2004; 36(2):272-277.

4. Arnold EM, Ward SR, Lieber RL, Delp SL. A Model of the Lower Limb for Analysis of Human Movement. *Ann Biomed Eng*. 2010; 38(2):269-279.

5. Biewener AA. Biomechanical Consequences of Scaling. *J Exp Biol*. 2005; 208(Pt 9):1665-1676.

6. Biewener AA and Roberts TJ. Muscle and Tendon Contributions to Force, Work, and Elastic Energy Savings: A Comparative Perspective. *Exerc Sport Sci Rev*. 2000; 28(3):99-107.

7. Cavanagh PR and Kram R. Mechanical and Muscular Factors Affecting the Efficiency of Human Movement. *Med Sci Sports Exerc*. 1985; 17(3):326-331.

8. Cavanagh PR and Lafortune MA. Ground Reaction Forces in Distance Running. *J Biomech*. 1980; 13(5):397-406.

9. Cohen J. Statistical Power Analysis for the Behavioral Sciences. Lawrence Erlbaum Associates, Hillsdale (NJ), 1988.

10. Cohen J. A Power Primer. *Psychol Bull*. 1992; 112(1):155-159.

11. Cole GK, Nigg BM, Ronsky JL, Yeadon MR. Application of the Joint Coordinate System to Three-Dimensional Joint Attitude and Movement Representation: A Standardization Proposal. *J Biomech Eng*. 1993; 115(4A):344-349.

12. Cunningham CB, Schilling N, Anders C, Carrier DR. The Influence of Foot Posture on the Cost of Transport in Humans. *J Exp Biol*. 2010; 213(5):790-797.

13. Daoud AI, Geissler GJ, Wang F, Saretsky J, Daoud YA, Lieberman DE. Foot Strike and Injury Rates in Endurance Runners: A Retrospective Study. *Med Sci Sports Exerc*. 2012; 44(7):1325-1334.

14. Davis IS, Bowser B, Mullineaux DR. Do Impacts Cause Running Injuries? A Prospective Investigation. Proceedings of the Annual Meeting of the American Society of Biomechanics. 2010.

15. Farris DJ, Trewartha G, McGuigan MP. Could Intra-Tendinous Hyperthermia During Running Explain Chronic Injury of the Human Achilles Tendon? *J Biomech*. 2011; 44(5):822-826.

16. Fath F, Blazevich AJ, Waugh CM, Miller SC, Korff T. Direct Comparison of in Vivo Achilles Tendon Moment Arms Obtained from Ultrasound and Mr Scans. *J Appl Physiol*. 2010; 109(6):1644-1652.

17. Hanavan EP, Jr. A Mathematical Model of the Human Body. Amrl-Tr-64-102. *AMRL TR*. 1964:1-149.

18. Hasegawa H, Yamauchi T, Kraemer WJ. Foot Strike Patterns of Runners at the 15-Km Point During an Elite-Level Half Marathon. *J Strength Cond Res*. 2007; 21(3):888-893.

19. Ker RF, Wang XT, Pike AV. Fatigue Quality of Mammalian Tendons. *J Exp Biol*. 2000; 203(Pt 8):1317-1327.

20. Kerr BA, Beauchamp L, Fisher V, Neil R. Footstrike Patterns in Distance Running. In: *Biomechanical Aspects of Sport Shoes and Playing Surfaces*. Nigg BMand Kerr B (Eds.). University of Calgary Press, Calgary, 1983.

21. Leadbetter WB. Cell-Matrix Response in Tendon Injury. *Clin Sports Med*. 1992; 11(3):533-578.

22. Lieberman DE, Venkadesan M, Werbel WA, Daoud AI, D'Andrea S, Davis IS, Mang'eni RO, Pitsiladis Y. Foot Strike Patterns and Collision Forces in Habitually Barefoot Versus Shod Runners. *Nature*. 2010; 463(7280):531-535.

23. Lundberg A, Svensson OK, Nemeth G, Selvik G. The Axis of Rotation of the Ankle Joint. *J Bone Joint Surg Br*. 1989; 71(1):94-99.

24. Maganaris CN, Baltzopoulos V, Sargeant AJ. In Vivo Measurement-Based Estimations of the Human Achilles Tendon Moment Arm. *Eur J Appl Physiol*. 2000; 83(4 -5):363-369.

25. Magnusson SP, Aagaard P, Dyhre-Poulsen P, Kjaer M. Load-Displacement Properties of the Human Triceps Surae Aponeurosis in Vivo. *J Physiol*. 2001; 531(Pt 1):277-288.

26. Magnusson SP and Kjaer M. Region-Specific Differences in Achilles Tendon Cross-Sectional Area in Runners and Non-Runners. *Eur J Appl Physiol*. 2003; 90(5-6):549-553.

27. Martin PE and Morgan DW. Biomechanical Considerations for Economical Walking and Running. *Med Sci Sports Exerc*. 1992; 24(4):467-474.

28. McClay I and Manal K. Three-Dimensional Kinetic Analysis of Running: Significance of Secondary Planes of Motion. *Med Sci Sports Exerc*. 1999; 31(11):1692-1737.

29. Nilsson J and Thorstensson A. Ground Reaction Forces at Different Speeds of Human Walking and Running. *Acta Physiol Scand*. 1989; 136(2):217-227.

30. Oakley T and Pratt DJ. Skeletal Transients During Heel and Toe Strike Running and the Effectiveness of Some Materials in Their Attenuation. *Clin Biomech (Bristol, Avon)*. 1988; 3(3):159-165.

31. Perl DP, Daoud AI, Lieberman DE. Effects of Footwear and Strike Type on Running Economy. *Med Sci Sports Exerc*. 2012; 44(7):1335-1343.

32. Riener R and Edrich T. Identification of Passive Elastic Joint Moments in the Lower Extremities. *J Biomech*. 1999; 32(5):539-544.

33. Roberts TJ, Kram R, Weyand PG, Taylor CR. Energetics of Bipedal Running. I. Metabolic Cost of Generating Force. *J Exp Biol*. 1998; 201(Pt 19):2745-2751.

34. Rosager S, Aagaard P, Dyhre-Poulsen P, Neergaard K, Kjaer M, Magnusson SP. Load-Displacement Properties of the Human Triceps Surae Aponeurosis and Tendon in Runners and Non-Runners. *Scand J Med Sci Sports*. 2002; 12(2):90-98.

35. Saunders PU, Pyne DB, Telford RD, Hawley JA. Factors Affecting Running Economy in Trained Distance Runners. *Sports Med*. 2004; 34(7):465-485.

36. Scholz MN, Bobbert MF, van Soest AJ, Clark JR, van Heerden J. Running Biomechanics: Shorter Heels, Better Economy. *J Exp Biol*. 2008; 211(Pt 20):3266-3271.

37. Stephens BR, Cole AS, Mahon AD. The Influence of Biological Maturation on Fat and Carbohydrate Metabolism During Exercise in Males. *Int J Sport Nutr Exerc Metab*. 2006; 16(2):166-179.

38. Williams DS, McClay IS, Manal KT. Lower Extremity Mechanics in Runners with a Converted Forefoot Strike Pattern. *J App Biomech*. 2000; 16(2):210-218.

39. Williams KR and Cavanagh PR. Relationship between Distance Running Mechanics, Running Economy, and Performance. *J Appl Physiol*. 1987; 63(3):1236-1245.

40. Winter DA, Sidwall HG, Hobson DA. Measurement and Reduction of Noise in Kinematics of Locomotion. *Journal of Biomechanics*. 1974; 7(2):157-159.

CHAPTER 6

MUSCLE MECHANICS AND ENERGY EXPENDITURE OF THE TRICEPS SURAE DURING REARFOOT AND FOREFOOT RUNNING

Abstract

The forefoot (FF) running footfall pattern has been advocated to improve running economy compared to the rearfoot (RF) footfall pattern as a result of increased elastic energy storage and release. However, this claim has not been previously investigated nor have previous studies found a difference in running economy between footfall patterns. Therefore, the purpose of this study was to compare the mechanical muscle work and muscle metabolic cost of the triceps surae muscle group between footfall patterns using a musculoskeletal modeling approach. Ten natural RF runners and ten natural FF runners performed over-ground running with each footfall pattern at 3.5 $m \cdot s^{-1}$ ±5%. Ankle and knee joint angles and ankle joint moments were used as inputs into a musculoskeletal model. A generic model was used to determine the muscle-tendon length of the gastrocnemius (GA) and soleus (SO) and each muscle's moment arm as a function of joint angle across the stance phase. A two-component Hill muscle model was used to determine the contraction dynamics of each muscle's contractile element (CE) and series elastic element (SEE). Muscle metabolic energy expenditure was calculated as a function of muscle activation, maximum isometric force, maximum shortening velocity, and the relative velocity of the CE. A mixed-factor ANOVA was used to determine the difference in each variable between footfall patterns and groups ($\alpha = 0.05$). The FF pattern resulted in greater SEE mechanical work in the GA compared to the RF pattern

but no differences were found in CE mechanical work or CE metabolic energy expenditure. The FF pattern resulted in near isometric contractions that allowed for greater force production with a similar metabolic cost compared to the low force production and high contraction velocities occurring with the RF pattern. In the SO, the FF pattern resulted in greater CE and SEE mechanical work and greater CE metabolic energy expenditure compared to the RF pattern. The greater metabolic cost of the SO during FF running was a result of greater CE positive work compared to the RF pattern. These findings indicate that the FF pattern does not result in lower muscle metabolic energy expenditure despite increased elastic energy utilization compared to the RF pattern.

Introduction

Elastic energy utilization reduces muscle work, and thereby metabolic cost, without sacrificing force generation (Alexander, 1984; Biewener and Roberts, 2000; Cavagna, 1977a; Cavagna et al., 1977b; Fukunaga et al., 2002; Fukunaga et al., 2001; Ishikawa et al., 2007; Roberts et al., 1997). Previous researchers have speculated that the forefoot (FF) running footfall pattern will result in greater stretch of the triceps surae muscle-tendon complex (Figure 6.1), resulting in greater elastic energy utilization and reduced metabolic cost compared to the rearfoot (RF) running footfall pattern (Ardigo et al., 1995; Hasegawa et al., 2007; Lieberman et al., 2010; Perl et al., 2012). Although muscle function between different footfall patterns has not been explicitly investigated, Hof et al. (2002) incidentally found that the contractile element of soleus and gastrocnemius muscles in a RF runner produced substantially more positive work than in

a midfoot (MF) runner. Less positive mechanical work of the simulated contractile elements in the MF runner was accomplished by generating force isometrically at near optimum length of the force-length relationship which allowed for whole muscle length changes to occur from length changes of elastic elements. The contractile elements of RF runner behaved more concentrically but length change was still relatively low (Hof et al., 2002). If the MF running pattern is an intermediate between RF and FF running, FF running may also result in near-isometric muscle force development and utilization of elastic energy which may decrease the metabolic cost compared to the muscle contracting concentrically.

Figure 6.1: Triceps surae muscle complex is comprised of the gastrocnemius and the soleus muscles.

The FF pattern is characterized by making initial contact with the ground on the metatarsal heads and preventing the heel from making contact with the ground whereas in the RF pattern, initial ground contact is with the heel. It has been suggested that FF running requires eccentric contraction of the gastrocnemius and soleus in order to control

the lowering of the heel to the ground after impact. This controlled lowering of the heel is believed to result in greater Achilles tendon stretch and more elastic energy storage than in the RF pattern (Perl et al., 2012; Pratt, 1989). Despite this potential energy saving mechanism, recent investigations have failed to observe greater economy (i.e. lower sub-maximal rate of oxygen consumption) with a FF running pattern compared to the RF pattern (Ardigo et al., 1995; Cunningham et al., 2010; Perl et al., 2012). Greater plantar flexion moments, Achilles tendon forces, and external work occurring with the FF pattern have been speculated to negate any energy savings from elastic recoil (Ardigo et al., 1995; Perl et al., 2012). However, muscle function during FF running has yet to be investigated directly. It is possible greater plantar flexion moments in FF running are accomplished by the muscle fibers behaving at optimal velocities and lengths in order to produce force with a lower metabolic cost. The results from studies that did not find the FF pattern to be more economical may be attributed to confounding factors such as the novelty of performing an alternate footfall pattern.

Differences in muscle mechanical work production between running footfall patterns have only been investigated through inverse dynamics analysis, motion analysis, and mechanical work ratios (Ardigo et al., 1995; Perl et al., 2012). These techniques may be inadequate to accurately determine the differences in muscle function between footfall patterns and how it relates to metabolic energy expenditure (Sasaki et al., 2009). Direct measurements of individual muscle behavior and energetics *in vivo* (e.g. blood flow, tendon buckles, magnetic resonance spectroscopy) are ideal methods to investigate muscle function (Umberger and Rubenson, 2011). However, such methods are impractical in humans because they require invasive surgical procedures or specialized

equipment. A muscle model may be more appropriate to evaluate the differences in muscle function between footfall patterns and their relation to running economy in humans. Therefore, the purpose of this study was to compare the mechanical muscle work and muscle metabolic cost of the triceps surae muscle group between footfall patterns using a musculoskeletal modeling approach. It was hypothesized that RF running would result in the triceps surae producing more mechanical work from the muscle contractile element whereas FF running would result in the triceps surae producing more mechanical work from in series elastic structures (i.e. greater elastic energy utilization). Secondly, it was hypothesized that FF running would result in lower muscle energy expenditure than RF running due to increased elastic energy utilization.

Methodology

Participant Selection

Ten healthy natural RF and 10 natural FF runners participated in this study (Table 6.1). Participants were required to run a minimum of 16 km per week with a preferred speed of approximately 3.5 $m \bullet s^{-1}$ for long running bouts. Participants were excluded if they had a history of cardiovascular or neurological problems or injury to the lower extremity or back within the past year. The natural footfall pattern of each participant was determined by vertical ground reaction forces (GRF) and high speed video recordings while running at their preferred running speed. Participants were classified into the RF group if they made initial contact with the heel or if they made contact with a semi-dorsiflexed or flat foot position (approximately zero degrees of dorsiflexion or

greater) and generated an initial vertical GRF impact peak (n = 1). Participants were entered into the FF group if they made initial contact on the metatarsal heads and did not generate an initial vertical GRF impact peak (n = 3). All participants read and completed an informed consent document and questionnaires approved by the University of Massachusetts Amherst Institutional Review Board before participating. A list of acronyms and abbreviations used in this study are listed in Table 6.2. Abbreviations specific to the musculoskeletal model are listed in Appendix F.

Table 6.1: Mean ± SD participant characteristics of the rearfoot group (RF) and the forefoot group (FF) for the participants included in Study 3. $\dot{V}O_2$ is steady state, mass normalized sub-maximal oxygen consumption measured at 3.5 m•s^{-1}. Differences between groups were assessed by a student's t-test (α = 0.05).

	Males/ Females (#)	Age (yrs)	Height (m)	Mass (kg)	Pref. Speed (m•s^{-1})	km/week (km)	$\dot{V}O_2$ (ml•kg^{-1} •min^{-1})
RF group	7/3	27.5 ± 4.8	1.76 ± 0.08	70.55 ± 9.77	3.67 ± 0.40	40.71 ± 35.33	39.86 ± 2.24
FF group	9/1	25.5 ± 7.7	1.79 ± 0.07	70.50 ± 7.10	3.80 ± 0.20	43.52 ± 22.86	39.65 ± 2.26
p-value	-	0.495	0.363	0.991	0.368	0.835	0.837

Table 6.2: Acronyms and abbreviations for each variable. Abbreviations used specifically for the musculoskeletal model are listed in Appendix F.

CE	contractile element	MT	muscle-tendon complex
E	metabolic energy expenditure	P	mechanical power
FF	forefoot	RF	rearfoot
GA	gastrocnemius	SEE	series elastic element
GRF	ground reaction force	SO	soleus
L	muscle component length	W	mechanical work
MF	mid-foot		

The groups were matched by body mass and sub-maximal rate of oxygen consumption. Sub-maximal rate of oxygen consumption was measured by indirect calorimetry using a metabolic cart (TrueOne, ParvoMedics, Sandy, UT, USA) while the participant ran on a motorized treadmill with their preferred footfall pattern at 3.5 $m \cdot s^{-1}$. No difference in sub-maximal oxygen consumption was observed between groups.

Experimental Setup

Unilateral three-dimensional kinematic data were collected with an eight-camera Qualisys Oqus 3-Series optical motion capture system (Qualisys, Inc., Gothenberg, Sweden) sampling at 240 Hz. The cameras surrounded a floor mounted AMTI force platform (OR6-5, AMTI Inc., Watertown, MA, USA) located at the center of a 25m runway. The force platform collected GRF and center of pressure with a sampling frequency of 1200 Hz. Photoelectric sensors (Lafayette Instrument Company, Lafayette, IN) placed 3 m before and after the force platform were used to monitor running speed.

Retro-reflective calibration markers were placed on the iliac crests, greater trochanters, medial and lateral femoral condyles, medial and lateral malleoli, and the heads of the first and fifth metatarsals. Tracking markers included four non-collinear markers secured onto a rigid plate, positioned on the lateral thigh and leg, as well as a rigid plate with three non-collinear markers placed on the posterior calcaneus. Additional tracking markers included the right and left anterior superior iliac spine and between the 5^{th} lumbar-1^{st} sacral vertebrae (McClay and Manal, 1999) (Appendix B). Participants wore form-fitting clothing and neutral racing flat shoes provided by the laboratory (RC 550, New Balance, Brighton, MA, USA).

Protocol

Participants practiced each footfall pattern at the designated speed until they felt comfortable with the protocol. Each participant performed ten successful trials with each footfall pattern while running at 3.5 $m \cdot s^{-1}$ ±5%. A trial was considered successful if the participant correctly performed the footfall pattern, landed on the force platform with the right foot without targeting, and without adjusting speed or stride. The order of the footfall conditions was randomized between participants.

Data Reduction

Qualisys Track Manager software (Qualisys, Inc., Gothenberg, Sweden) was used to track kinematic data and export it in .C3D format for processing with Visual 3D software (C-Motion, Inc, Rockville, MD, USA). Raw kinematic and kinetic data were filtered with a 4^{th} order, zero-lag Butterworth digital low-pass filter with a cutoff frequency of 12 Hz and 50 Hz respectfully (Winter et al., 1974). Three dimensional ankle and knee joint angles were calculated by a rotation matrix of the distal segment with respect to the coordinate system of the proximal segment using a Cardan rotation sequence of x (flexion/extension) – y (abduction/adduction) – z (axial rotation) (Cole et al., 1993).

A Newton-Euler inverse dynamics approach was used to calculate three dimensional ankle joint moments. Internal joint moments were calculated with respect to the local coordinate system of the proximal segment with positive values indicating dorsiflexor, inversion and adductor moments. Kinematic and kinetic data from initial

contact to toe-off of each condition were interpolated to 101 data points, with each point representing 1% of the stance phase.

Kinovea Motion Tuner software v. 0.8.15 (www.kinovea.org/en/) was used to calculate the static Achilles tendon moment arm length determined by previously reported methods (Scholz et al., 2008). The static Achilles tendon moment arm was defined as the shortest distance from the line of action of the AT to the center of rotation of the ankle. The Euclidean distance between the center of the lateral malleolus and the posterior aspect of the Achilles tendon was determined.

Musculoskeletal Model

A two-dimensional musculoskeletal model was developed similar to the methods of previous studies (Bobbert et al., 1986a; Hof et al., 2002; van Soest and Bobbert, 1993). Properties of the muscle-tendon complex (MT) reflected the action of the gastrocnemius (GA) and soleus (SO), which together comprise the muscles of the triceps surae. The model consisted of three rigid segments representing the foot, leg and thigh (Appendix E, Figure E.1). Segments were connected by two frictionless hinge joints to represent the ankle and knee joints. A Hill-type muscle model was employed to simulate the action of the GA and the soleus SO individually. Each muscle contained a contractile element (CE) and a series elastic element (SEE) in series with the CE. Although Hill-type muscle models are phenomenological models, the CE is primarily associated with the muscle fascicles and the SEE is primarily associated with the Achilles tendon, aponeurosis and other elastic structures in series with the CE. Passive elements which act in parallel with the muscle fibers, such as muscle fascia, ligaments and joint capsule were represented by

a passive moment (M_{pas}). The equation developed by Riener and Edrich (1999) was used to estimate M_{pas} as a function of ankle and knee joint angles:

$$M_{pas} = -\exp(2.1016 + 0.0843\varphi_A - 0.0176\varphi_K) - \exp(-7.9763 - 0.1949\varphi_A + 0.0008\varphi_K) - 1.792 \quad (6.1).$$

The mean ankle angle, knee angle, and ankle joint moment was compiled across trials for each participant served as inputs into the muscle model (Figure 6.2). The model was run on each participant individually for the following group-condition combinations: 1) natural RF runners performing the RF pattern; 2) natural RF runners performing the FF pattern; 3) natural FF runners performing the RF pattern; and 4) natural FF runners performing the FF pattern.

A generic model by Arnold et al. (2010) was used to determine the moment arm length (d_{MT}) for the GA and SO. A plot of d_{MT} as a function of joint angle (θ) for each muscle was created based on generic model by Arnold et al. (2010). d_{MT} for the SO was plotted against ankle joint angle. Plots for the d_{MT} of the GA as a function of knee and ankle joint angles were created separately. Additionally, the plots for d_{MT} of the medial and lateral heads of the GA were created separately for each joint angle. The data from the medial and lateral heads of the GA were combined by scaling each muscle by its physiological cross sectional area (PCSA). The modal data were fit to a second-order polynomial by a custom MATLAB program (Mathworks, Inc., Natick, MA) and used to determine the polynomial coefficients. A second-order polynomial was the lowest order that adequately fit the moment arm data, based on an assessment of the root mean square

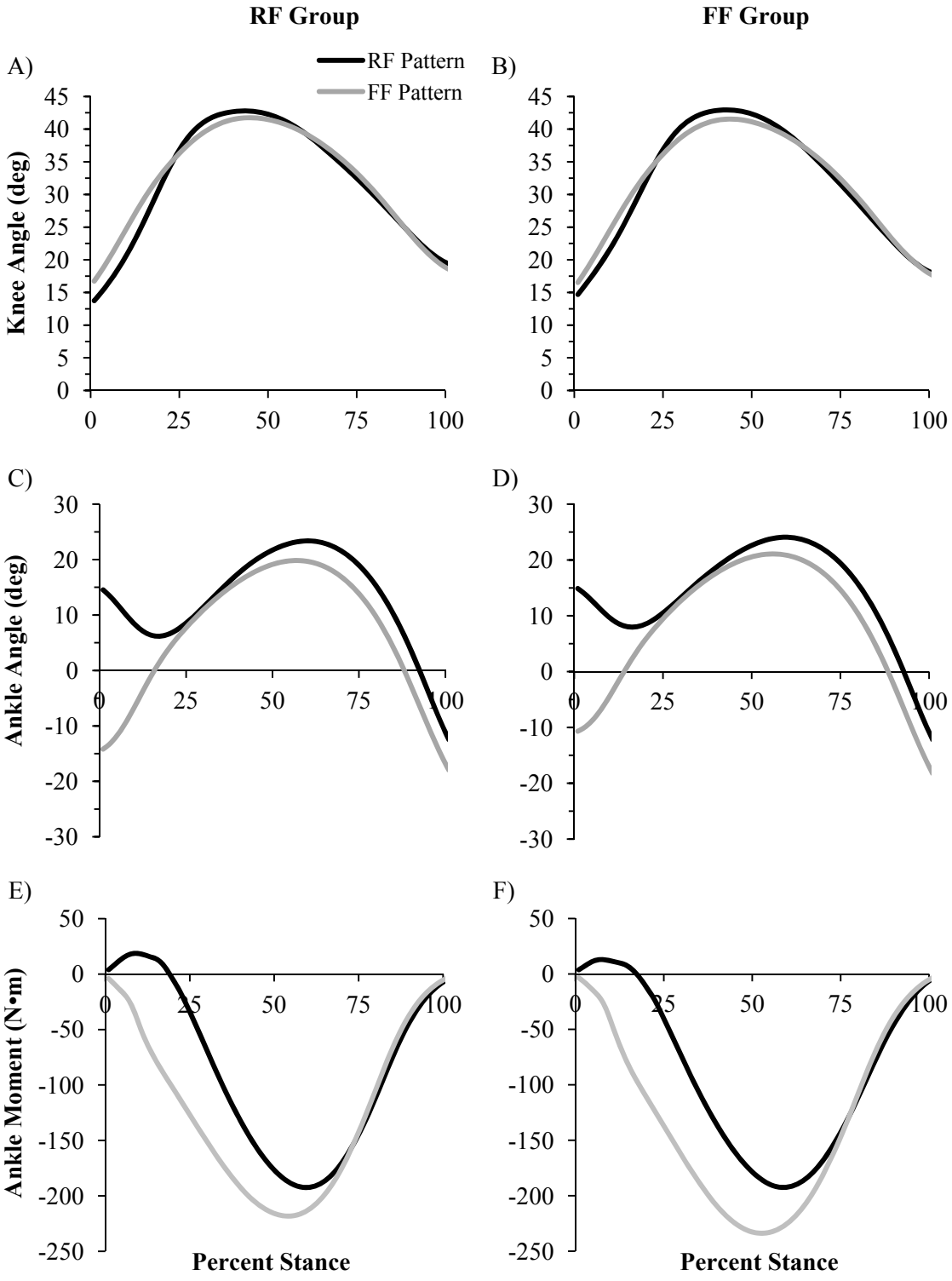

Figure 6.2: Group mean knee and ankle joint angles and ankle joint moment during the stance phase of rearfoot (RF) and forefoot (FF) running in the RF and FF groups.

error between the polynomial prediction and the data. The zeroth-order polynomial coefficient was scaled for each subject individually by the static Achilles tendon moment arm measurement. Each d_{MT} polynomial was integrated with respect to the knee and ankle joint angle, thus creating third-order polynomials for GA and SO muscle-tendon complex length (L_{MT}) as a function of θ. The zeroth-order coefficients for the L_{MT} polynomials were scaled based on the participant's static leg length. The experimental joint angle data were entered into these polynomials to determine L_{MT} and d_{MT} for each instant of the stance phase. L_{MT} of the GA and SO was used as a constraint for the model by requiring the sum of the CE and SEE lengths equal that of the L_{MT}.

Active moment (M_{act}) produced by the GA and SO was determined by subtracting M_{pas} from the ankle joint moment (M_A) found by the inverse dynamics procedure. M_{act} was used to calculate the force generated by the triceps surae as a sum of the forces produced by the GA and SO multiplied by their respective moment arms. Force produced by each muscle was partitioned by the ratio of each muscle's PCSA to the total triceps surae PCSA. A ratio of 1.88:1 SO to GA was used (Arnold et al., 2010). The muscle force in the GA and SO where assumed to be zero when a dorsiflexor moment was being produced.

The amount of force that could be generated by the muscle fibers was dependent on the contraction dynamics dictated by three relationships. The force-length relationship (F-L) represents the isometric force potential at any CE length (Gordon et al., 1966). Peak isometric force production (F_0) occurs when the CE is at optimal length (L_o). The F-L relationship is modeled as a parabola and is scaled down depending on the sub-maximal activation level. The F-L relationship also determines the magnitude of F_0 used

in the force-velocity relationship. The force velocity relationship (F-V) represents the CE force that is produced, based on the CE velocity (i.e. shortening, lengthening or isometric) (Hill, 1938). The F-V relationship is modeled by a rectangular hyperbola and is scaled up or down by the amount of activation and the F-L parameters. The force-extension relationship (FΔL) of the SEE represents the change in SEE elasticity, or stiffness, as SEE length is increased or decreased (Bahler, 1967). The FΔL relationship is modeled as a quadratic function. Determining the properties in the MT, CE and SEE based on the Hill relationships allowed for the activation level to be calculated. The internal states of the muscle model were based on the experimental data and constrained by the muscle geometry of the equilibrium condition ($L_{MT} = L_{CE} + L_{SEE}$ and $F_{MT} = F_{CE} = F_{SEE}$). After determining the MT, CC and SEE dynamics, the metabolic power produced by each muscle was calculated as a function of the CE velocity and activation (Minetti and Alexander, 1997; Sellers et al., 2003). Appendix E describes the equations and relationships used for the muscle and muscle energy expenditure models. Appendix F lists of all abbreviations that were used in the model.

Data Analysis

The power output of the MT, CE, and SEE was calculated by multiplying their respective force by velocity for each instant in time. Mechanical work was calculated by integrating the power output of the MT, CE, and SEE with respect to time. The amount of elastic energy stored and released during the stance phase was determined by the amount of positive and negative mechanical work, respectively, performed by the SEE. Metabolic energy expenditure by the CE was calculated by integrating CE metabolic

power with respect to time. Mechanical work of the MT, CE, and SEE as well as the metabolic energy expenditure by the CE of the GA and SO were calculated during the stance phase and the push-off phase for each participant under the RF and FF pattern conditions. The push-off phase was defined as the first instance the MT was producing positive power in the second half of stance.

Statistical Analysis

Mechanical work and metabolic energy expenditure were compared between the RF and FF running footfall patterns across the stance phase and during the push-off phase. Each variable was subjected to a mixed model analysis of variance with footfall pattern and group as fixed variables and subject nested within group as a random variable. The differences between footfall patterns (2 levels) and between groups (2 levels) and the interaction of footfall pattern and group were assessed with a significance level of $\alpha = 0.05$. When a significant group by pattern interaction was observed, a post-hoc assessment was performed by partitioning the interaction by group and by pattern. Partitioning by group determined the significance between each footfall pattern within each group. Partitioning by pattern determined the significance between groups within each footfall pattern. Effect sizes were also calculated to determine if the differences between footfall pattern and groups were biologically meaningful. An effect size (*d*) greater than 0.3 indicated a small effect, an effect size greater than 0.5 indicated a moderate effect and an effect size greater than 0.8 indicated a large effect (Cohen, 1992).

Results

Muscle Velocity

Data presented over the stance phase included an indicator of the start and end of when the muscle force was above 25% of the maximum value. During the first 30% of the stance phase, RF running resulted in MT_{GA} shortening (Figure 6.3A & C) while FF running resulted in MT_{GA} lengthening (Figures 6.3B & D). The difference in MT_{GA} velocity between footfall patterns in early stance was associated with a higher CE_{GA} shortening velocity and an initial increase in the SEE_{GA} lengthening velocity with RF running compared to FF running. Additionally, the FF pattern resulted in near zero CE_{GA} velocity from approximately 20 – 40% of stance (Figure 6.3B & D). Both footfall patterns resulted in MT_{GA} and CE_{GA} lengthening after approximately 30% of stance but began rapid shortening at approximately 75% and 85% of stance, respectively. The highest shortening velocities occurred after the muscle force had dropped below 25% of the maximum value at the end of the stance phase. The CE_{GA} velocity was close to zero for a short period around 25% of stance during the FF pattern (Figure 6.3B & D). The lengthening velocity of the SEE_{GA} decreased from early stance during both footfall patterns until approximately 50% of stance then increased shortening velocity for the remainder of stance.

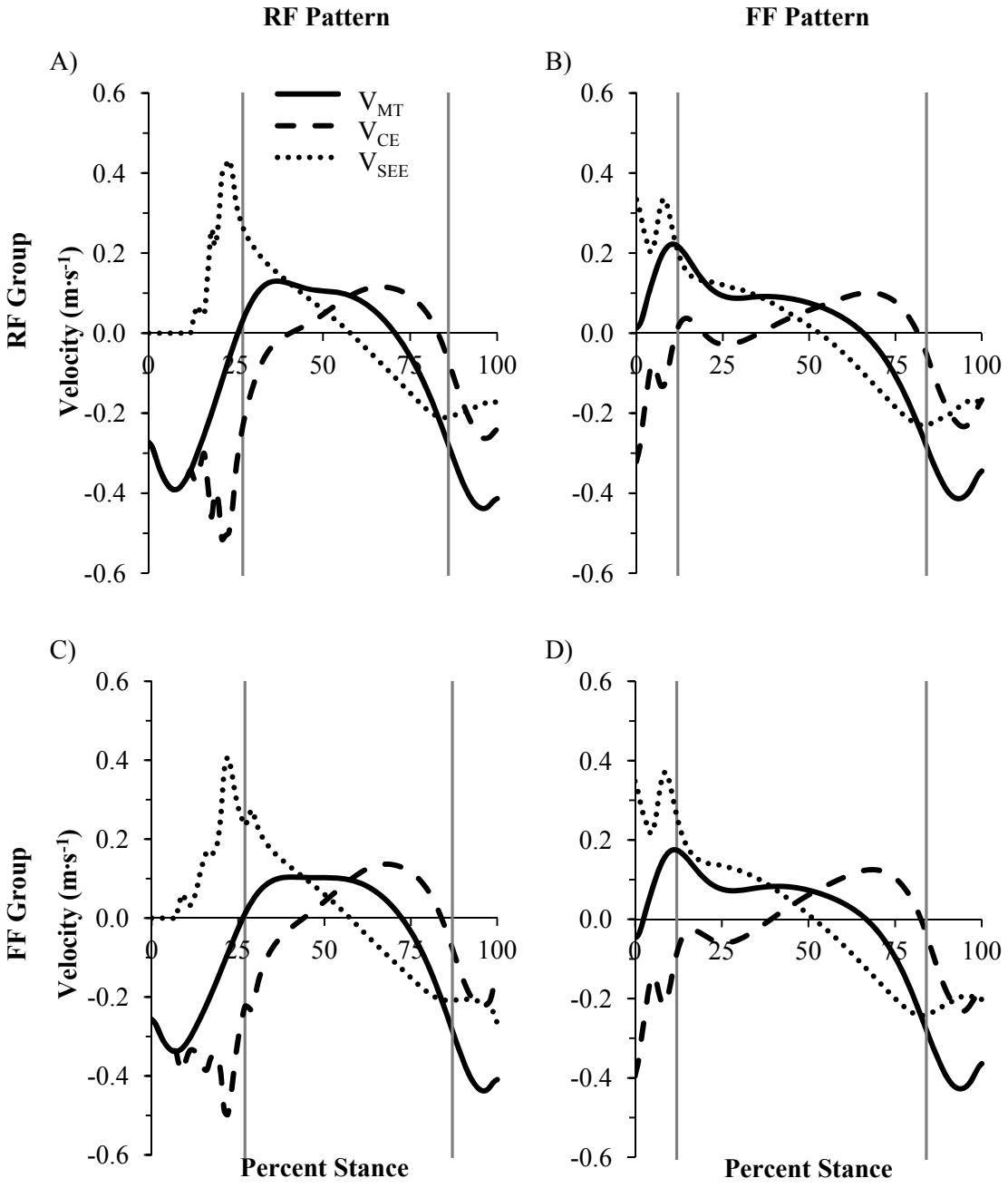

Figure 6.3: Group mean velocity of the muscle-tendon unit (MT), the series elastic element (SEE) and contractile element (CE) of the gastrocnemius during the stance phase of rearfoot (RF) and forefoot (FF) running in the RF and FF groups. The vertical lines in each panel indicate the range of time when the GA was generating greater than 25% of the maximum force produced during the stance phase.

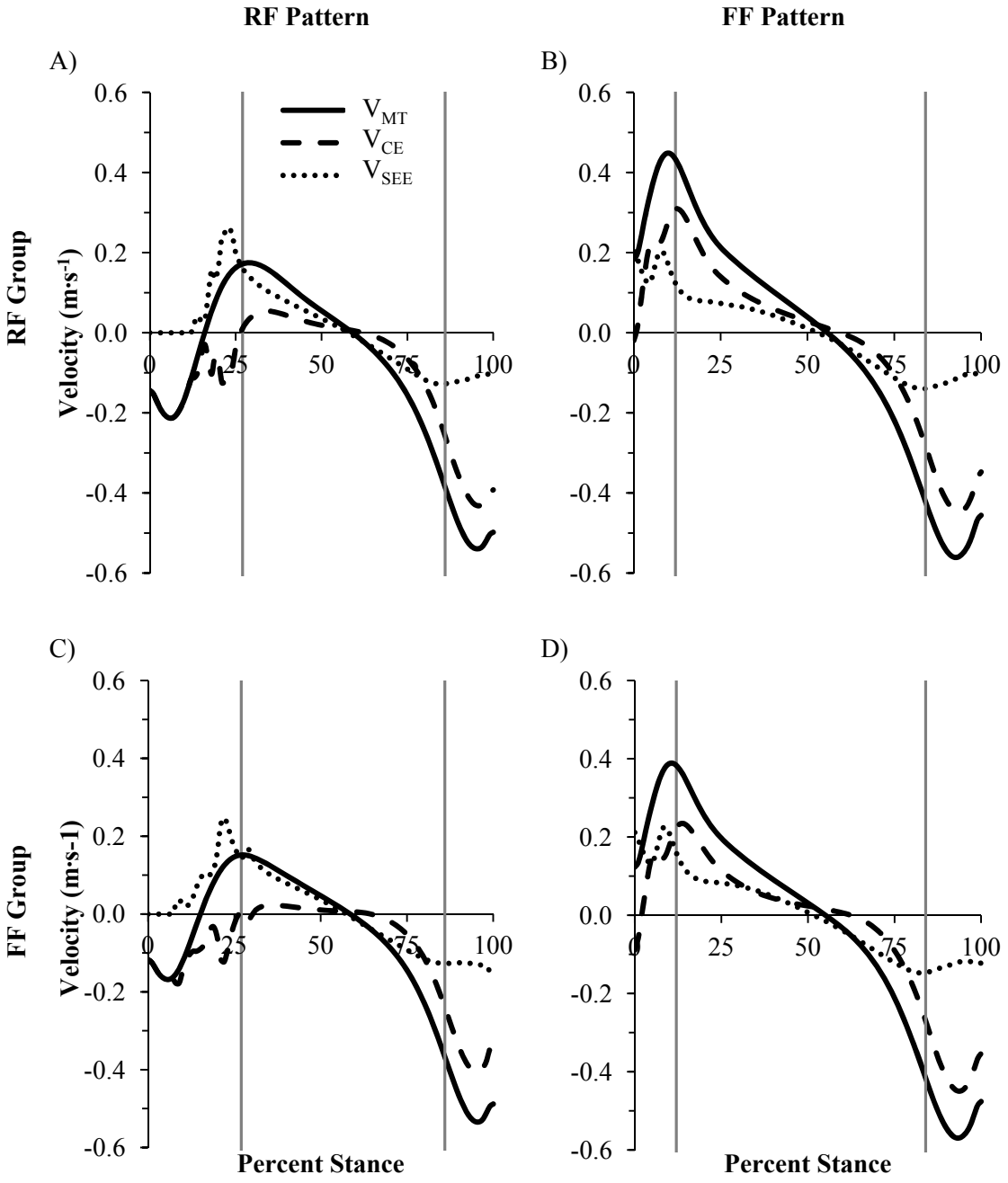

Figure 6.4: Group mean velocity of the muscle-tendon unit (MT), the series elastic element (SEE) and contractile element (CE) of the soleus during the stance phase of rearfoot (RF) and forefoot (FF) running in the RF and FF groups. The vertical lines in each panel indicate the range of time when the SO was generating greater than 25% of the maximum force produced during the stance phase.

RF running resulted in MT_{SO} and CE_{SO} shortening after ground contact, whereas FF running resulted in MT_{SO}, CE_{SO}, and SEE_{SO} lengthening (Figure 6.4). The MT_{SO} and SEE_{SO} began lengthening at approximately 20% of stance during RF running while the CE_{SO} velocity was near zero from approximately 25 – 75% of stance (Figure 6.4A & C). Peak lengthening velocities of the MT_{SO} and the CE_{SO} occurring in early stance were reduced with the RF pattern compared to the FF pattern but the peak SEE_{SO} velocity was similar between footfall patterns. The velocity of the MT_{SO}, CE_{SO}, and SEE_{SO} were similar between footfall patterns when the muscle force was above 25% of the maximum value. Rapid shortening of the MT_{SO} and CE_{SO} occurred in late stance of both footfall patterns after the muscle force dropped below 25% of the maximum value. Peak MT_{SO} and CE_{SO} shortening velocity in late stance were greater with the FF pattern.

Muscle Force

The model predicted GA or SO force during the first ~20% of the stance phase of RF running was zero due to the dorsiflexor moment generated during this time period (Figure 6.2). In FF running, the GA and SO began to produce force at initial ground contact. The SO always produced 61.0% greater force than the GA, consistent with the difference in PCSA between muscles. Peak GA and SO muscle force was 13.8% greater during FF running compared to RF running in the RF group (Figure 6.5A & B); whereas, peak muscle force was 22.2% greater during FF running compared to RF running in the FF group (Figure 6.5C & D). FF running resulted in greater force production from 0 – 75% of the stance phase in both the GA and SO and were nearly identical between patterns over the final 25% of the stance phase.

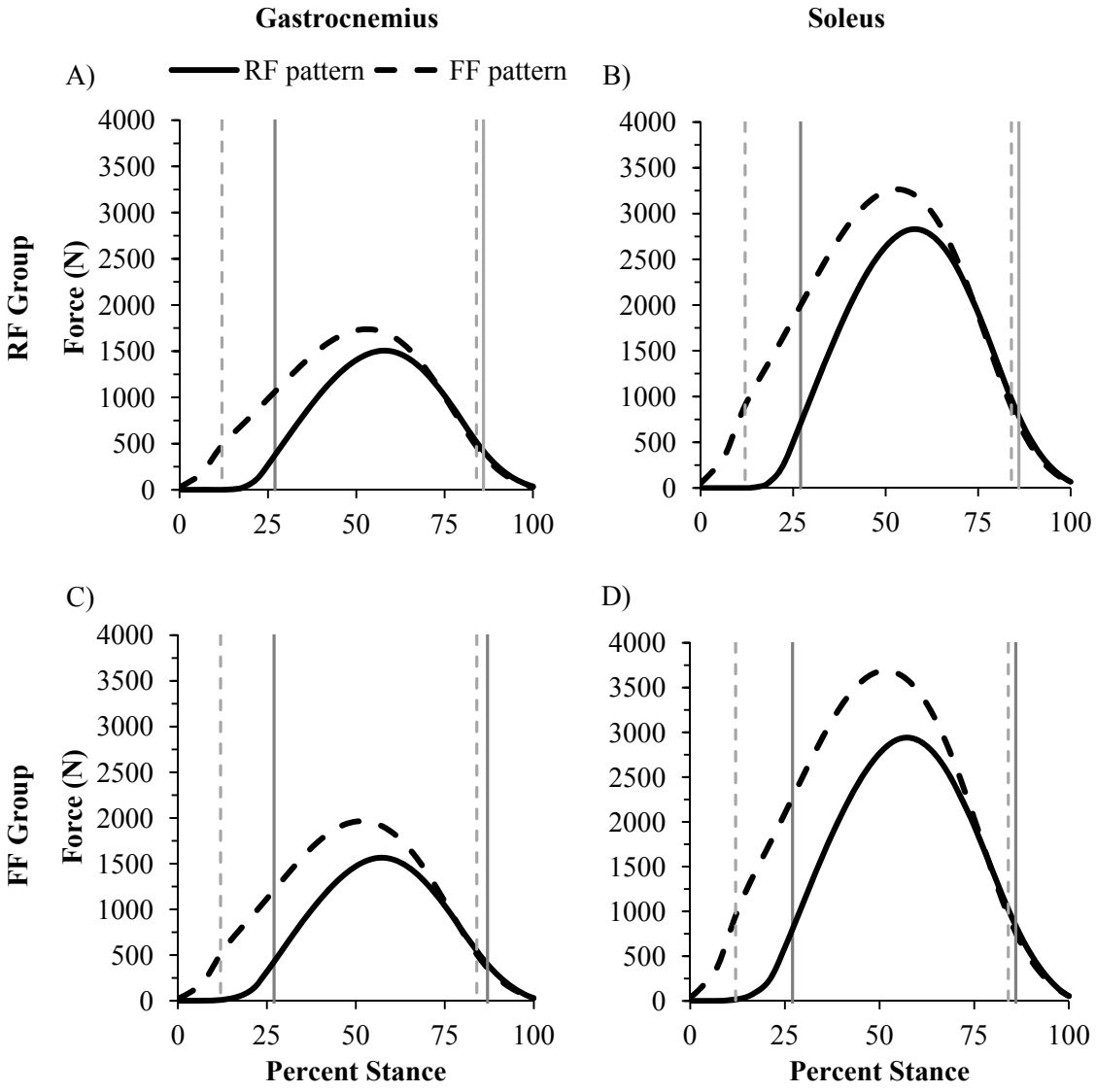

Figure 6.5: Group mean gastrocnemius and soleus muscle forces during the stance phase of rearfoot (RF) and forefoot (FF) running in the RF and FF groups. The vertical lines in each panel indicate the range of time when the muscle was generating greater than 25% of the maximum force produced during the stance phase.

Muscle Power

Both footfall patterns resulted in large negative $P_{MT\text{-}GA}$ and $P_{SEE\text{-}GA}$ whereas $P_{CE\text{-}GA}$ was positive during early stance (Figure 6.6). Peak positive $P_{CE\text{-}GA}$ in early stance was similar between groups and conditions except that it was lower in the RF group during FF running. Peak positive $P_{CE\text{-}GA}$ occurring in late stance was similar between groups and

footfall patterns. Peak negative $P_{CE\text{-}GA}$ was similar between footfall patterns within each group but was greater in the FF group compared to the FF group. Peak negative $P_{SEE\text{-}GA}$ was similar between patterns in the RF group (Figures 6.6A & B). The FF group had greater negative $P_{SEE\text{-}GA}$ compared to the RF group during both footfall patterns; however, negative $P_{SEE\text{-}GA}$ was greater in FF running within the FF group (Figures 6.6A & B). Positive and negative $P_{MT\text{-}GA}$ were similar between groups within each footfall pattern but were greater during FF running. $P_{SEE\text{-}GA}$ was the primary contributor to $P_{MT\text{-}GA}$ throughout the stance phase during both RF and FF running.

Positive and negative $P_{MT\text{-}SO}$, $P_{CE\text{-}SO}$, and $P_{SEE\text{-}SO}$ was considerably less during RF running (Figure 6.7A & C) compared to FF running (Figure 6.7B & D). $P_{SEE\text{-}SO}$ was the primary contributor to negative $P_{MT\text{-}SO}$ during RF running, whereas $P_{CE\text{-}SO}$ was the primary contributor to negative $P_{MT\text{-}SO}$ during FF running. $P_{CE\text{-}SO}$ and $P_{SEE\text{-}SO}$ had a near equal contribution to positive $P_{MT\text{-}SO}$ in the second half of stance of both RF and FF running, although positive $P_{CE\text{-}SO}$ was slightly greater than positive $P_{SEE\text{-}SO}$ in both patterns. Positive and negative $P_{MT\text{-}SO}$ and $P_{CE\text{-}SO}$ were similar between groups within each footfall pattern. Conversely, the FF group produced more negative $P_{SEE\text{-}SO}$ during FF running and more positive $P_{SEE\text{-}SO}$ during both footfall patterns compared to the RF group.

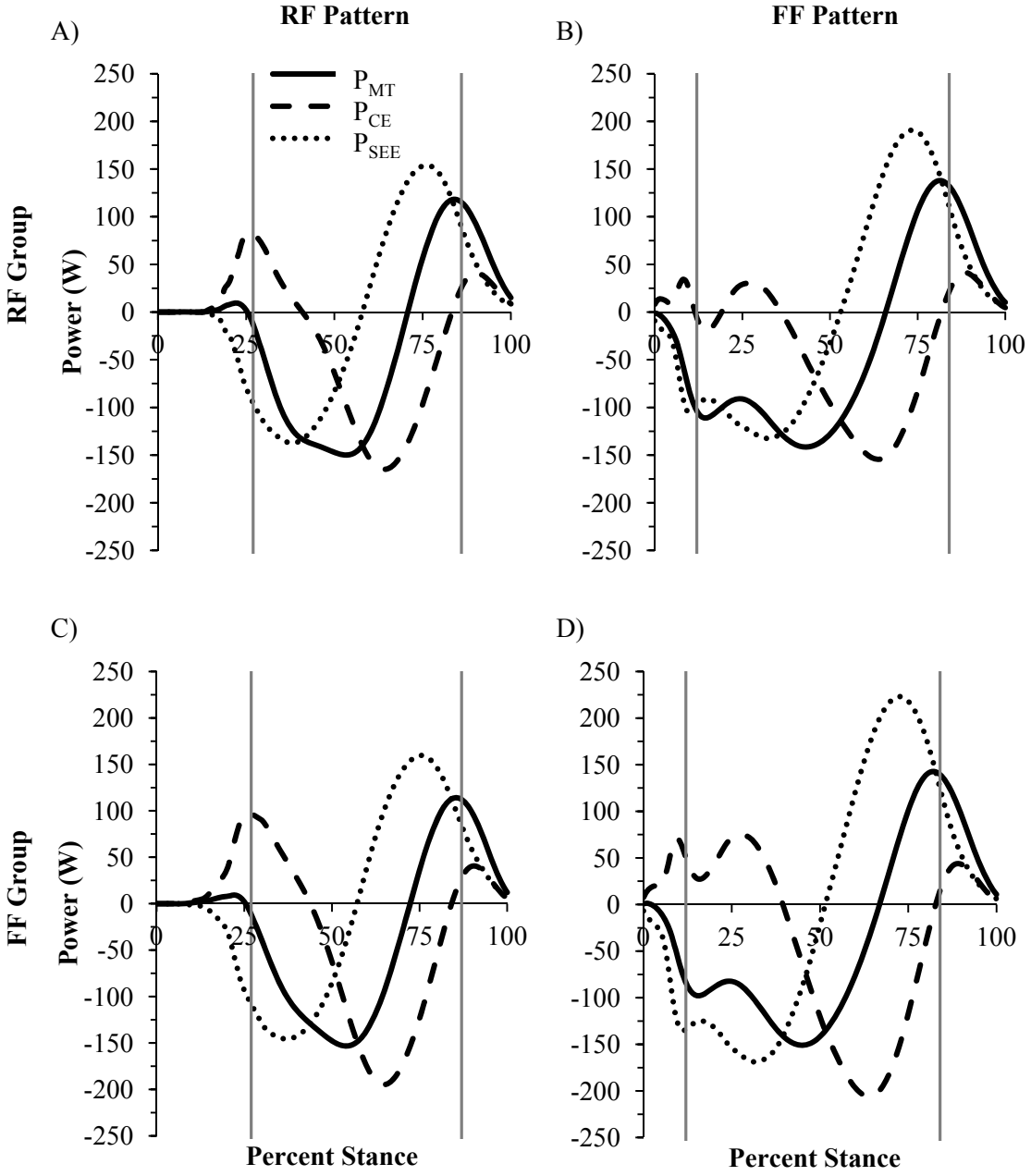

Figure 6.6: Group mean muscle power production of the muscle-tendon unit (MT), the series elastic element (SEE) and contractile element (CE) of the gastrocnemius during the stance phase of rearfoot (RF) and forefoot (FF) running in the RF and FF groups. The vertical lines in each panel indicate the range of time when the GA was generating greater than 25% of the maximum force produced during the stance phase.

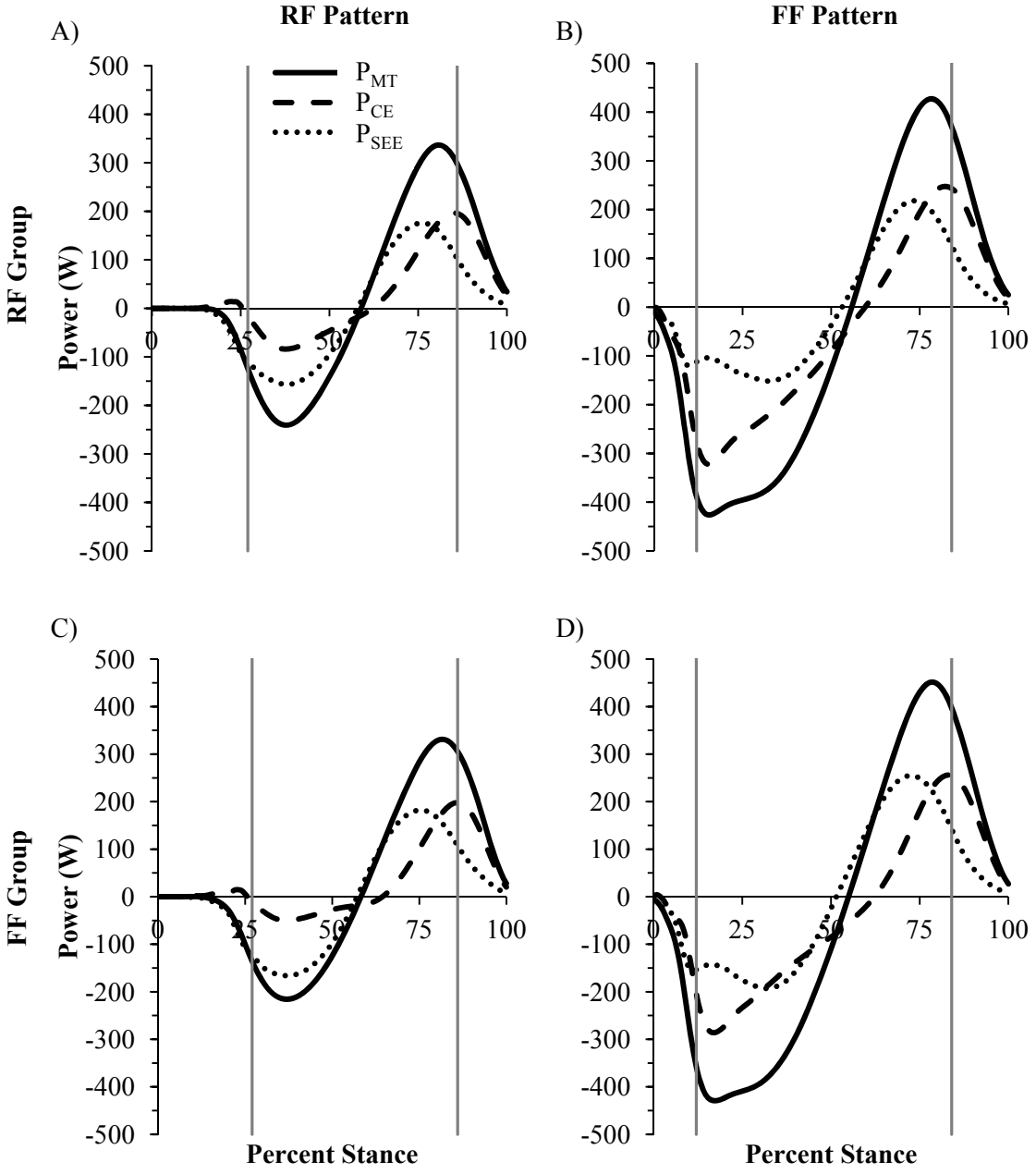

Figure 6.7: Group mean muscle power production of the muscle-tendon unit (MT), the series elastic element (SEE) and contractile element (CE) of the soleus during the stance phase of rearfoot (RF) and forefoot (FF) running in the RF and FF groups. The vertical lines in each panel indicate the range of time when the SO was generating greater than 25% of the maximum force produced during the stance phase.

Several notable differences in muscle power occurred between the GA and SO. The transition between positive and negative $P_{SEE\text{-}GA}$ and $P_{SEE\text{-}SO}$ occurred at approximately 50% of stance during both footfall patterns (Figure 6.6 & 6.7). However, the transition between negative and positive $P_{MT\text{-}GA}$ and $P_{CE\text{-}GA}$ was delayed until approximately 70% and 80% of stance, respectively, during both footfall patterns compared to that of the SO. This delay was a result of the large negative $P_{CE\text{-}GA}$ during mid-late stance (Figure 6.6). The transition between positive and negative $P_{MT\text{-}SO}$, $P_{CE\text{-}SO}$, and $P_{SEE\text{-}SO}$ occurred at approximately 50% of stance during both footfall patterns (Figure 6.7). Additionally, positive $P_{SEE\text{-}GA}$ was the primary contributor to $P_{MT\text{-}GA}$ in the GA, whereas $P_{SEE\text{-}SO}$ and $P_{CE\text{-}SO}$ had a near equal contribution to positive $P_{MT\text{-}SO}$ in the SO.

Mechanical Work Production

Mechanical Work Produced During Stance

Positive and negative $W_{SEE\text{-}GA}$ produced over the stance phase were the only mechanical work variables that had a significant group by pattern interaction for the GA ($p < 0.044$); all others were not significant ($p > 0.05$). Partitioning the interactions by group revealed that FF running resulted in greater positive $W_{SEE\text{-}GA}$ and greater negative $W_{SEE\text{-}GA}$ compared to RF running, with large effect size ($p < 0.002$, $d = 0.7 – 1.0$) (Figure 6.8C–F). Partitioning the interaction by pattern revealed no difference in positive and negative $W_{SEE\text{-}GA}$ between groups when performing the RF pattern ($p > 0.05$, $d = 0.3$). During the FF pattern, positive and negative $W_{SEE\text{-}GA}$ had moderately greater magnitudes in the FF group compared to the RF group ($p < 0.001$, $d = 0.7$). No significant group main effects were observed for any GA mechanical work variable over stance ($p > 0.05$,

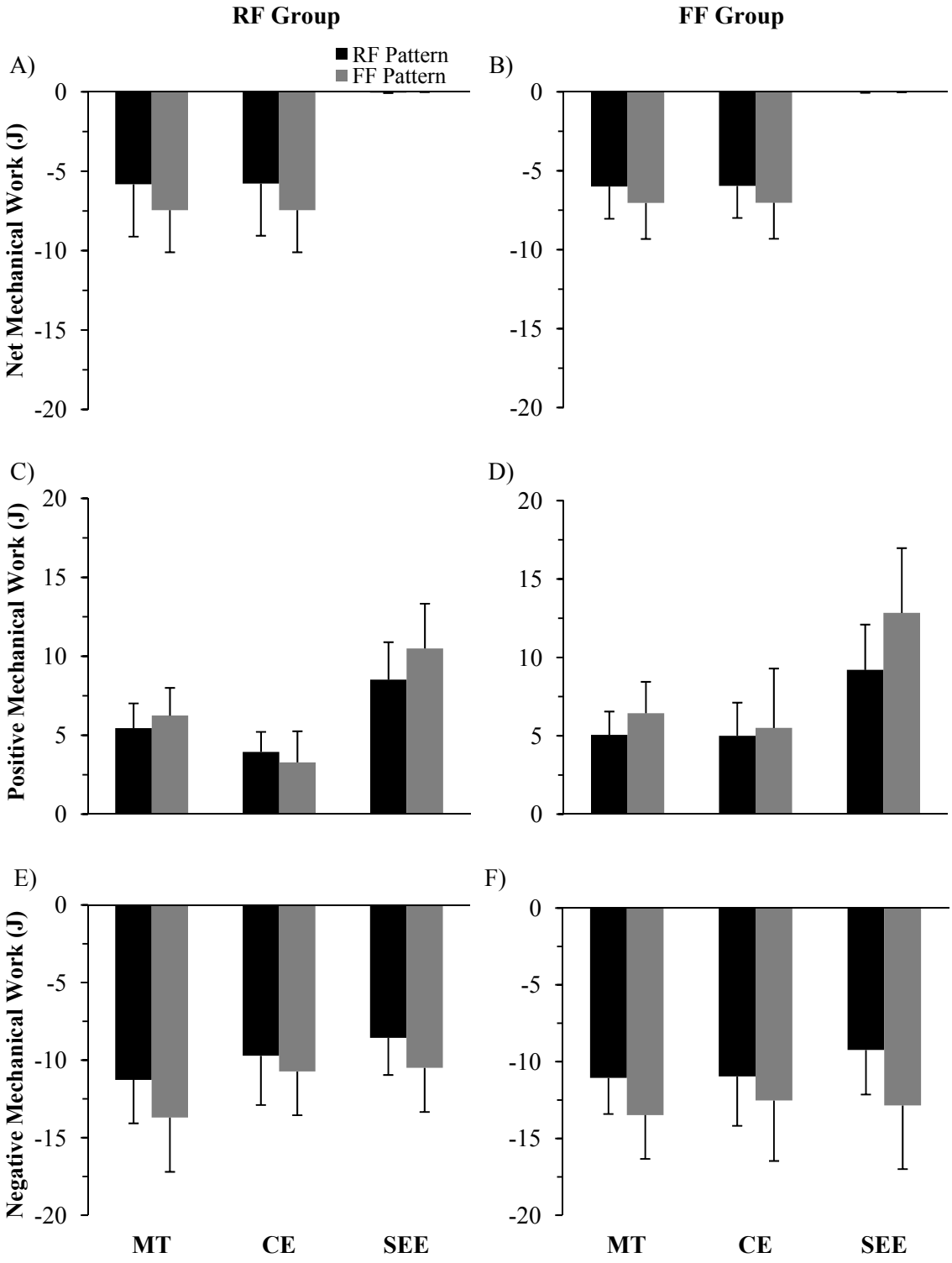

Figure 6.8: Group mean mechanical work produced by the muscle-tendon unit (MT), the series elastic element (SEE) and the contractile element (CE) of the gastrocnemius during the stance phase of rearfoot (RF) and forefoot (FF) running in the RF and FF groups. Error bars are ±1SD.

d: 0.0 – 0.7); however, a moderate effect size was observed for the difference in positive $W_{CE\text{-}GA}$ between groups ($d = 0.7$). Significant pattern main effects were observed for positive and negative $W_{MT\text{-}GA}$ and net $W_{SEE\text{-}GA}$ ($p < 0.000$, *d*: 0.6 – 1.8) (Figure 6.8). Large effect sizes were observed between footfall patterns for net $W_{SEE\text{-}GA}$ ($d = 1.8$) and negative $W_{MT\text{-}GA}$ ($d = 0.8$), but positive $W_{SEE\text{-}GA}$ only had moderate effect size ($d = 0.6$). No significant differences between footfall patterns were observed for or net, positive or negative $W_{CE\text{-}GA}$ or net $W_{MT\text{-}GA}$ produced over the stance phase ($p > 0.05$, *d*: 0.0 – 0.5). Net $W_{MT\text{-}GA}$ was similar between footfall patterns as a result of similar net $W_{CE\text{-}GA}$ and near zero net $W_{SEE\text{-}GA}$ being done during stance (Figure 6.8A & B). Although the amount of net, positive and negative $W_{CE\text{-}GA}$ was similar between patterns, positive and negative $W_{MT\text{-}GA}$ and $W_{SEE\text{-}GA}$ were greater with FF running.

A significant group by pattern interaction was observed for positive and negative $W_{SEE\text{-}SO}$ ($p < 0.044$) (Figure 6.9). Partitioning the interactions by group revealed that FF running resulted in greater positive $W_{SEE\text{-}SO}$ and greater negative $W_{SEE\text{-}SO}$ compared to RF running with large effect size ($p < 0.002$, $d = 0.7 – 1.0$) (Figure 6.9C – F). Partitioning the interaction by pattern revealed no difference in positive and negative $W_{SEE\text{-}SO}$ between groups when performing the RF pattern ($p > 0.05$, $d = 0.3$). However, positive and negative $W_{SEE\text{-}SO}$ had moderately greater magnitudes in the FF group compared to the RF group when performing the FF pattern ($p < 0.000$, $d = 0.7$). No significant group main effects were observed for any SO mechanical work variable over stance ($p > 0.05$, *d*: 0.1 – 0.7). Significant pattern main effects were observed for all SO mechanical work variables over the stance phase ($p < 0.000$, *d*: 0.6 – 4.6). Very large effect sizes were observed for all variables ($d > 1.0$) except positive $W_{CE\text{-}SO}$ ($d = 0.6$). Net $W_{CE\text{-}SO}$ was the

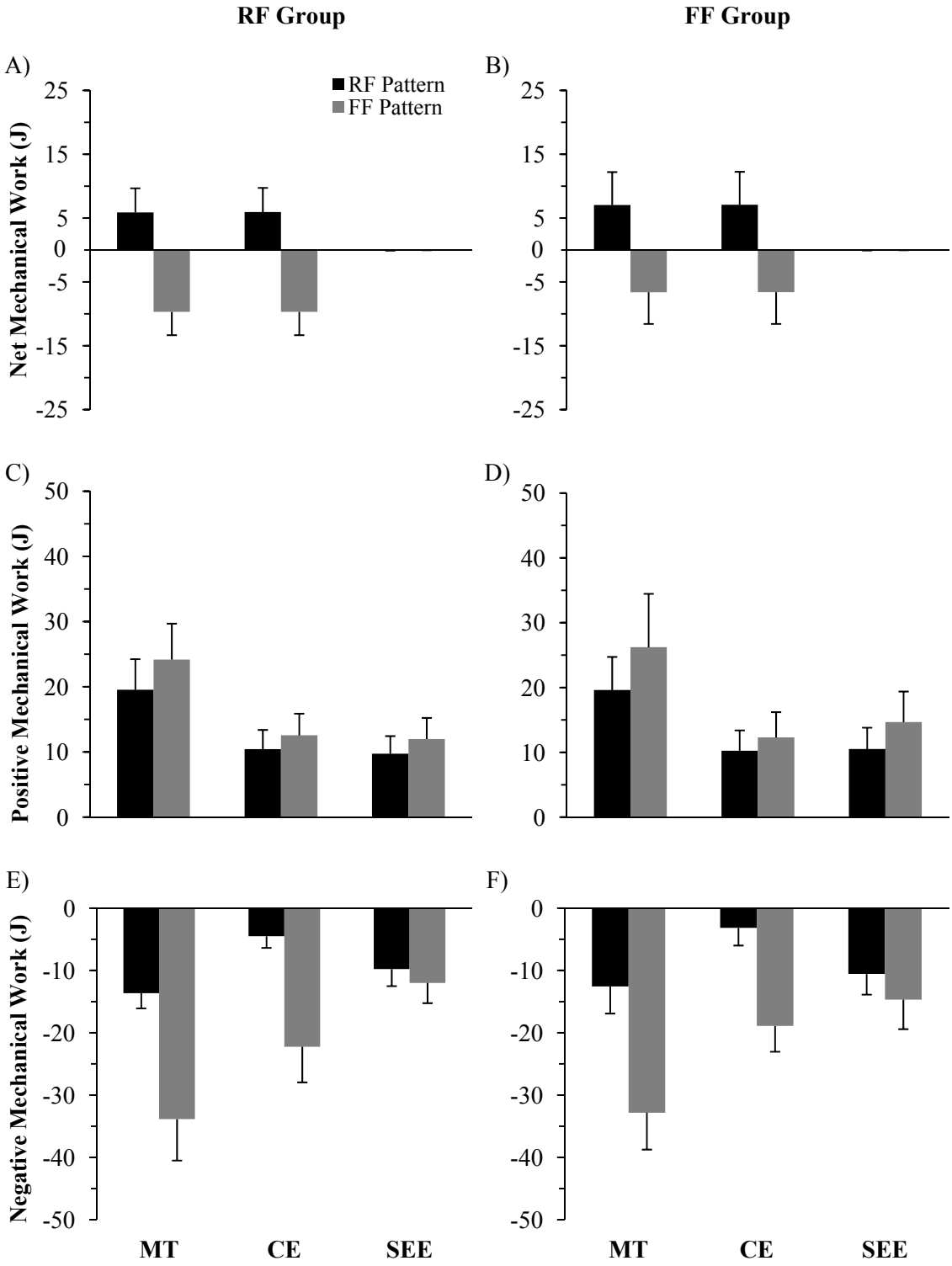

Figure 6.9: Group mean mechanical work produced by the muscle-tendon unit (MT), the series elastic element (SEE) and the contractile element (CE) of the soleus during the stance phase of rearfoot (RF) and forefoot (FF) running in the RF and FF groups. Error bars are ±1SD.

primary contributor to net $W_{MT\text{-}SO}$ during both patterns because net $W_{SEE\text{-}SO}$ was near zero (Figure 6.9A & B). RF running resulted in net $W_{MT\text{-}SO}$ and $W_{CE\text{-}SO}$ being positive, whereas both were negative with FF running. Positive and negative $W_{MT\text{-}SO}$, $W_{CE\text{-}SO}$, and $W_{SEE\text{-}SO}$ were all greater during FF running compared to RF running (Figure 6.9C–F).

Mechanical Work Produced During Push-off

Significant group by pattern interactions were found for positive $W_{SEE\text{-}GA}$ and negative $W_{CE\text{-}GA}$ produced during push-off ($p < 0.030$) (Figure 6.10). Partitioning the interaction by group revealed positive $W_{SEE\text{-}GA}$ and negative $W_{CE\text{-}GA}$ produced during push-off were greater in FF running compared to RF running, with large effect sizes ($p < 0.000$, d: 0.9 – 1.6). Partitioning the interaction by pattern revealed no difference in either variable between groups when performing the RF pattern ($p > 0.05$, $d = 0.1$). However, when performing the FF pattern, both variables had moderately greater magnitudes in the FF group compared to the RF group ($p < 0.020$, $d = 0.4 – 0.7$). No significant group main effects were observed for mechanical work produced during push-off ($p > 0.05$, d: 0.1 – 0.4). A significant pattern main effect was observed for positive $W_{MT\text{-}GA}$ produced during push-off, with a moderately large effect size ($p < 0.000$, $d = 0.7$). No significant differences were observed for positive $W_{CE\text{-}GA}$ produced during push-off ($p > 0.05$, $d = 0.1$). $W_{SEE\text{-}GA}$ was the primary contributor to $W_{MT\text{-}GA}$ during push-off. However, more mechanical work overall was produced during the push-off phase in the FF pattern (Figure 6.10). The amount of positive $W_{MT\text{-}GA}$ and $W_{SEE\text{-}GA}$, and negative $W_{CE\text{-}GA}$ during the push-off phase were all greater in FF running compared to RF running.

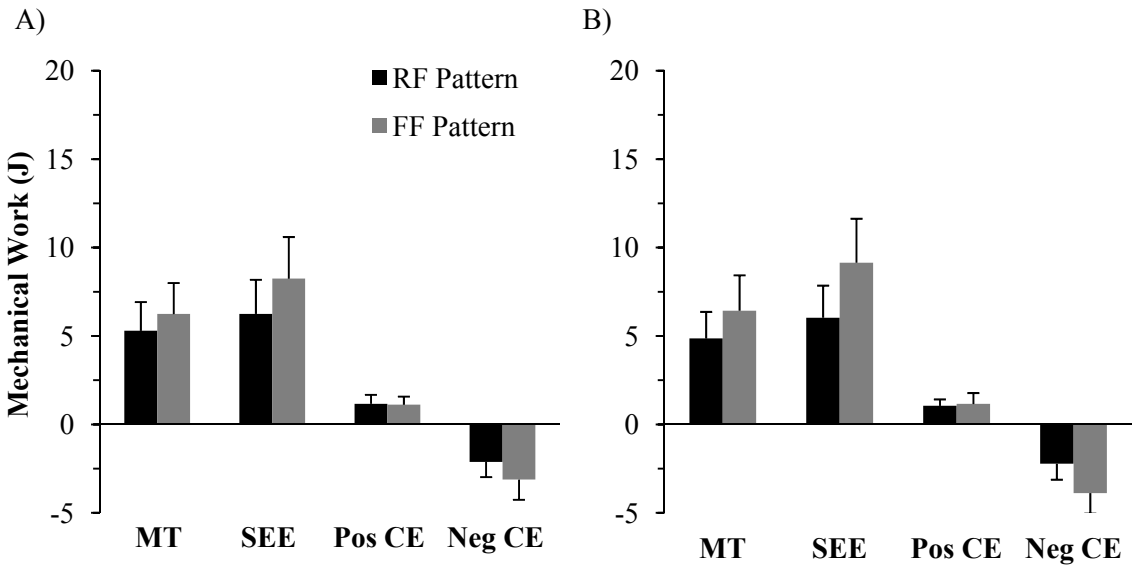

Figure 6.10: Group mean mechanical work produced by the muscle-tendon unit (MT), the series elastic element (SEE) and the contractile element (CE) of the gastrocnemius during the push-off phase of rearfoot (RF) and forefoot (FF) running in the A) RF and B) FF groups. Error bars are ±1SD.

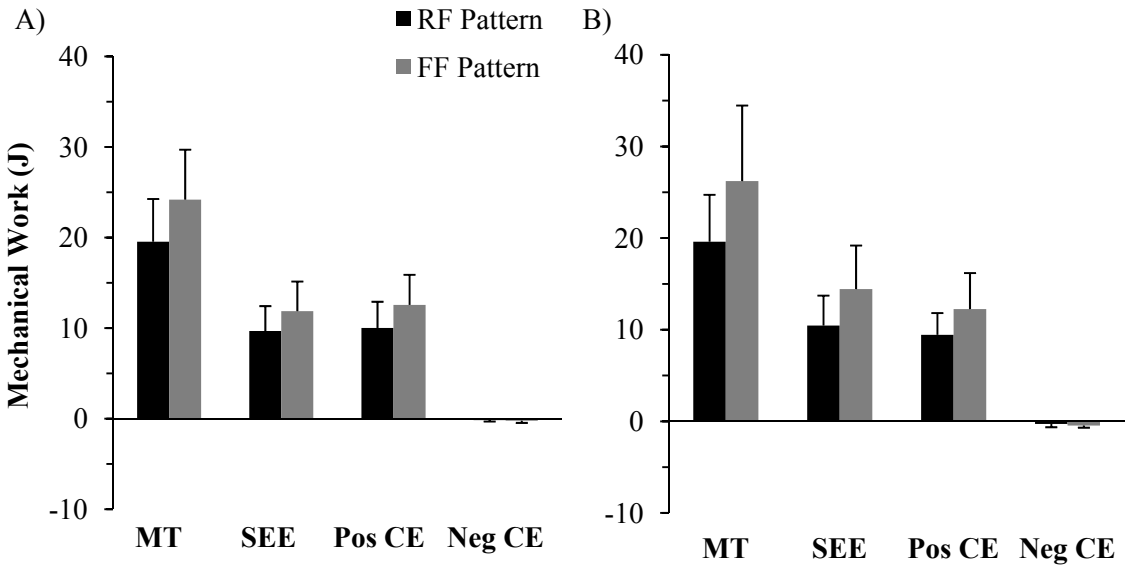

Figure 6.11: Group mean mechanical work produced by the muscle-tendon unit (MT), the series elastic element (SEE) and the contractile element (CE) of the soleus during the push-off phase in rearfoot (RF) and forefoot (FF) running in the A) RF and B) FF groups. Error bars are ±1SD.

More mechanical work was done during push-off in the SO compared to the GA (Figures 6.10 and 6.11). In the GA, W_{SEE-GA} was the largest contributor to W_{MT-GA} during push-off (Figure 6.10). Conversely, the W_{SEE-SO} and W_{CE-SO} were near equal contributors to W_{MT-SO} in the SO during push-off (Figure 6.11).

No significant group by pattern interactions or group main effects were observed for any SO mechanical work variable calculated during the push-off phase ($p > 0.05$) (Figure 6.11). Significant pattern main effects indicated that positive W_{MT-SO}, positive W_{SEE-SO}, positive W_{CE-SO}, and negative W_{CE-SO} produced during push-off were greater in FF running compared to RF running ($p < 0.000$, d: 0.5 – 1.0). All variables had a large effect size between footfall patterns ($d > 0.9$) except for negative W_{CE-SO} ($d = 0.5$). W_{SEE-SO} and W_{CE-SO} had a similar contribution to W_{MT-SO} during push-off in both footfall patterns. Positive W_{CE-SO} was larger than W_{SEE-SO} during push-off in both patterns in the RF group while the opposite was true for the FF group (Figure 6.11A vs. B). Negative W_{CE-SO} contributed less than 1.0 J of mechanical work during push-off in both footfall patterns.

Metabolic Energy Expenditure

Metabolic Energy Expenditure During Stance

No significant interactions or main effects were observed for E_{CE-GA} across the stance phase ($p > 0.05$) (Figure 6.12A, C, E). However, a large effect size was observed in E_{CE-GA} between groups ($d = 0.8$), which indicated higher E_{CE-GA} in the FF group compared to the RF group (Figure 6.12C). Although FF running resulted in 14% greater E_{CE} by the GA compared to RF running, no significant pattern main effect was observed

($p > 0.05$, $d = 0.3$) (Figure 6.12C). The differences between groups and footfall patterns in $E_{CE\text{-}GA}$ occurred during the first half of the stance phase (Figure 6.12A). The FF group had larger metabolic power during FF running whereas the $E_{CE\text{-}GA}$ between groups was similar during RF running (Figure 6.12A & C).

No significant interactions or group main effects were observed for $E_{CE\text{-}SO}$ across the stance phase ($p > 0.05$) (Figure 6.12B, D, F). However, a significant pattern main effect was observed for $E_{CE\text{-}SO}$ across stance ($p < 0.000$, $d = 1.0$). $E_{CE\text{-}SO}$ was 28% greater during FF running compared to RF running (Figure 6.12D).

Metabolic Energy Expenditure During Push-off

No significant interactions or group main effects were observed for E_{CE} of the GA or SO during the push-off phase ($p > 0.05$, d: 0.1 – 0.2) (Figure 6.12E & F). No significant pattern main effect was observed for $E_{CE\text{-}GA}$ during push-off as FF running resulted in less than 2% greater $E_{CE\text{-}GA}$ compared to RF running ($p > 0.05$, $d = 0.0$) (Figure 6.12E). However, a significant pattern main effect was observed for $E_{CE\text{-}SO}$ during push-off with large effect size ($p < 0.001$, $d = 1.1$). The FF pattern resulted in 33% greater $E_{CE\text{-}SO}$ during push-off than the RF pattern (Figure 6.12F). Similarly to mechanical work, E_{CE} was greater during early stance in the GA and during late stance in the SO (Figures 6.12A & B). Additionally, the contribution to the amount of E_{CE} during push-off was considerably greater in the SO compared to the GA (Figures 6.12E & F).

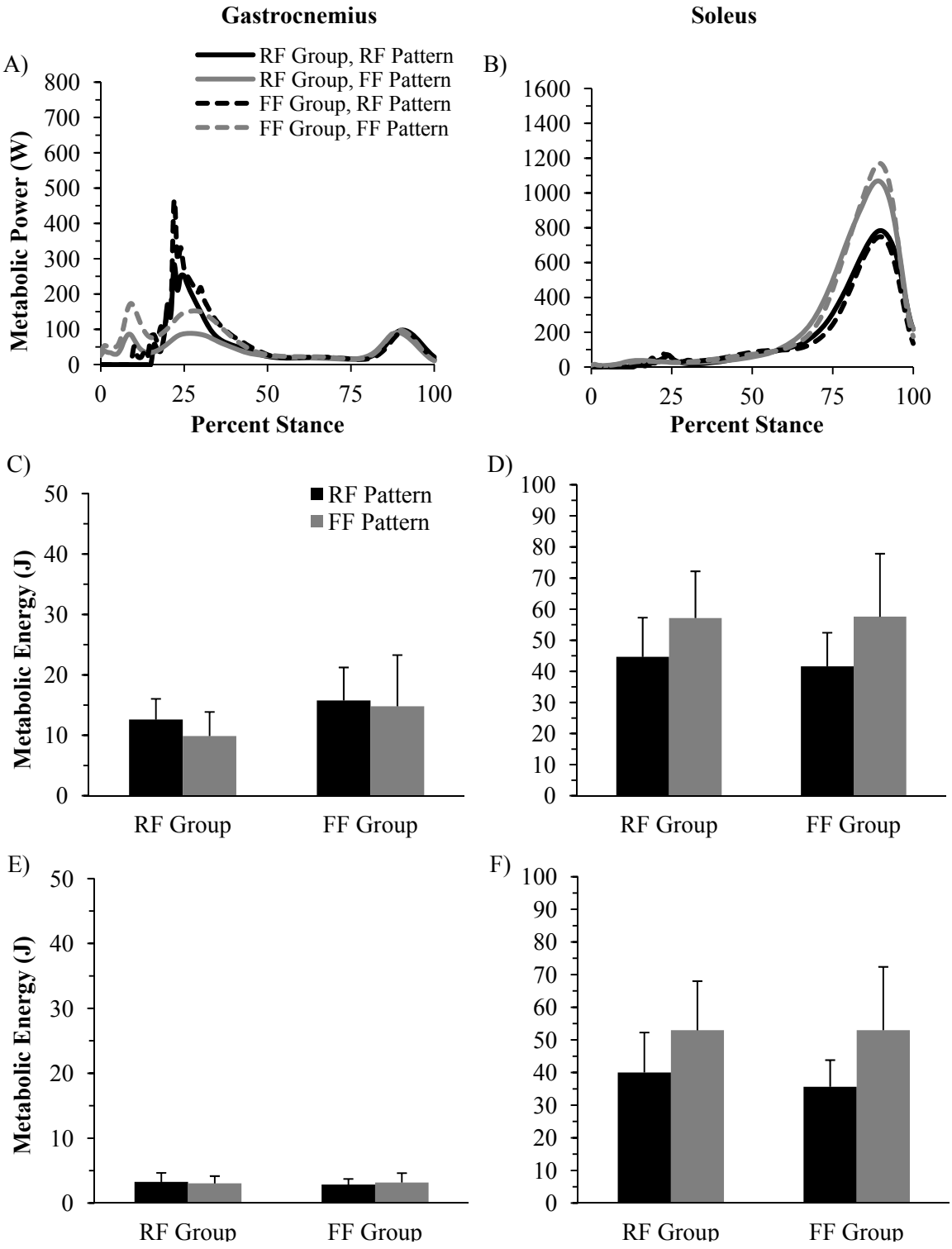

Figure 6.12: Group mean gastrocnemius (GA) and soleus (SO) metabolic energy expenditure during rearfoot (RF) and forefoot (FF) running in the RF and FF groups. A) GA and B) SO metabolic power generated across the stance phase, C) GA and D) SO total metabolic energy produced during the stance phase and E) GA and F) metabolic energy produced during the push-off phase. Error bars are ±1SD.

Discussion

Effective storage and release of elastic strain energy that results in less muscle fiber work will reduce muscle metabolic energy consumption (Alexander, 1984; Biewener and Roberts, 2000; Cavagna, 1977a; Cavagna et al., 1977b). A reduction in muscle fiber work is accomplished by the CE operating at low contraction velocities and results in the SEE being primarily responsible for changes in MTU length. Decreased CE velocities result in more optimal force production and a lower rate of ATP consumption (Biewener and Roberts, 2000; Fenn, 1924; Huxley, 1974; Rall, 1985; Roberts et al., 1997). It has been suggested that the FF running pattern is more economical than the RF pattern because of greater elastic energy utilization (Ardigo et al., 1995; Hasegawa et al., 2007; Lieberman et al., 2010). However, this has not been directly assessed previously. The purpose of the present study was to compare the mechanical muscle work and muscle metabolic cost of the GA and SO between RF and FF running patterns. The first hypothesis was that RF running would result in the GA and SO producing more mechanical work from the CE whereas FF running would result in more mechanical work produced from the SEE. This hypothesis was partially supported with respect to the GA because FF running resulted in more positive and negative $W_{SEE\text{-}GA}$; however, no differences in $W_{CE\text{-}GA}$ were observed between footfall patterns (Figure 6.8). In FF running, more mechanical work was done in the GA as a result of greater $W_{SEE\text{-}GA}$ and thus an increase in elastic energy utilization compared to RF running. The first hypothesis was also partially supported with respect to the SO because FF running resulted in greater overall $W_{SEE\text{-}SO}$ but also greater overall $W_{CE\text{-}SO}$ compared to RF running (Figure 6.9). The substantial difference in negative $W_{CE\text{-}SO}$ between footfall

patterns resulted in greater overall $W_{CE\text{-}SO}$ production verses the overall $W_{SEE\text{-}SO}$ production during FF running compared to RF running. Both the GA and SO produced more force during the FF pattern which resulted in greater stretch and recoil of the SEE compared to the RF pattern. However, the increased stretch and recoil of the SEE with the FF pattern was not accompanied by less overall W_{CE}.

The current study supports previous suggestions that the controlled lowering of the heel after ground impact in FF running will result in greater storage of elastic energy (Ardigo et al., 1995; Hasegawa et al., 2007; Lieberman et al., 2010; Perl et al., 2012). The present study investigated this claim and hypothesized that FF running would result in lower muscle energy expenditure than RF running due to increased elastic energy utilization. Although FF running resulted in greater elastic energy utilization compared to RF running, FF running did not result in lower muscle energy expenditure than RF running. Thus the second hypothesis was not supported. In the GA, greater elastic energy recoil found during FF running did not result in reduced $W_{CE\text{-}GA}$. Consequently, more overall work was done in the GA during FF running but at the same metabolic cost as RF running. In the SO, FF running resulted in greater metabolic energy expenditure than RF running. FF running substantially increased overall $W_{CE\text{-}SO}$ without a comparable increase in $W_{SEE\text{-}SO}$, which may explain the increased metabolic cost.

The differences in mechanical work production between footfall patterns can be explained by the CE velocity and the differences in muscle force production. RF running resulted in high shortening CE_{GA} velocity in early stance compared to FF running (Figure 6.3A & C). Although FF running also resulted in lower shortening CE_{GA} velocity in early stance compared to RF running, it was followed by a period of near zero CE_{GA}

velocity from approximately 20 – 40% of stance (Figure 6.3B & D). In the RF group, the near isometric period of the CE_{GA} contributed to decreased positive $P_{CE\text{-}GA}$ in early stance during FF running compared to RF running (Figure 6.6A & B). As a result, reduced metabolic energy was expended during FF running in the RF group in the first 30% of stance (Figure 6.12A & C). However, statistical significance in GA metabolic cost between footfall patterns was not found when collapsed across both groups. This result may be partially explained by the FF group having smaller differences in GA metabolic cost between patterns as well as greater GA metabolic cost during both footfall patterns compared to the RF group. In the FF group, FF running also resulted in the GA having a near isometric period in early stance. However, the positive $W_{CE\text{-}GA}$ in early stance was similar between footfall patterns and thus resulted in similar metabolic cost between patterns in this group (Figure 6.8 and 6.12A & C).

Typically, greater muscle force production results in a greater muscle metabolic energy expenditure because of an increase in the active muscle volume required to meet the demands of the task (Biewener and Roberts, 2000; Roberts et al., 1998). However, in the GA, less force was produced during the RF pattern without a comparable decrease in the amount of metabolic energy expenditure compared to the FF pattern. RF running also resulted in greater CE_{GA} shortening velocity and no isometric period. This high CE_{GA} shortening velocity occurring with RF running resulted in a lower force generation capability, and thus active GA muscle volume and GA metabolic cost, than if CE_{GA} velocity was slower or isometric. Conversely, in FF running, force was produced at slower CE_{GA} velocities allowing more force generation with a smaller active muscle volume than if the CE_{GA} shortening velocity was increased. Although the differences in

GA metabolic cost was not significantly different between footfall patterns, the velocity at which force was produced may explain the trend toward less GA metabolic cost with the FF pattern compared to the RF pattern.

In the SO, CE_{SO} velocity was near isometric for the majority of stance during RF running whereas FF running resulted in CE_{SO} lengthening for the first half of stance followed by a brief isometric phase before push-off. These differences in CE_{SO} velocity between footfall patterns contributed to more negative $W_{CE\text{-}SO}$ in FF running compared to RF running (Figure 6.9E & F). However, the differences in negative $W_{CE\text{-}SO}$ cannot explain the differences in SO metabolic cost between footfall patterns because metabolic cost was similar when negative $W_{CE\text{-}SO}$ was being produced (Figure 6.7B & D and Figure 6.12B). Metabolic energy of the SO did not differ between footfall patterns until approximately 65% of stance but CE_{SO} velocity and force production were the same between patterns after 70% and 75% of stance, respectively (Figure 6.4B & D and 6.12B). The force economy of the different contraction types may explain the similarity in SO metabolic cost despite substantial differences in SO force between footfall patterns.

RF running resulted in isometric force production of the SO, which has been identified as the mechanism in which elastic energy recoil reduces metabolic cost. However, isometric force production requires a greater metabolic cost and results in a lower force production than eccentric contractions (Biewener and Roberts, 2000; Fenn, 1924). FF running resulted in greater force production that was produced by less costly eccentric contractions. Therefore, the similarity in SO metabolic cost between footfall patterns in the first 65% of stance was a result of a lower force requirement at a higher

metabolic cost in RF running whereas FF running resulted in less costly force production but more force was required.

During the push-off phase, however, SO metabolic cost was different between footfall patterns when SO force was similar between footfall patterns. However, peak CE_{SO} and MT_{SO} shortening velocity was slightly greater during FF running compared to RF running (Figure 6.4). The increased shortening velocities observed with FF running resulted in more positive $W_{MT\text{-}SO}$, $W_{CE\text{-}SO}$, and $W_{SEE\text{-}SO}$ in the second half of stance compared to RF running (Figure 6.9C & D). Because SO force during the push-off phase was similar between footfall patterns, the difference in shortening velocity and thus muscle work during push-off explains the difference in SO metabolic cost between RF and FF running. Thus, muscle work, not force, distinguishes the difference in SO metabolic cost between footfall patterns, which supports some previous conclusions on the metabolic cost of running (Roberts et al., 1997; Scholz et al., 2008).

SO metabolic cost was greatest during the push-off phase compared to the rest of stance and was greater in FF running compared to RF running (Figure 6.12D & E). Positive $W_{MT\text{-}SO}$ during push-off was accomplished by both elastic recoil as well as positive $W_{CE\text{-}SO}$. As a result, efficiency (the ratio of MT_{SO} to the SO metabolic cost) of the SO during push-off during the RF pattern was 0.49 and 0.55 in the RF and FF groups, respectively, and 0.46 and 0.49 during the FF pattern in the RF and FF groups, respectively. The efficiency of the push-off phase was similar to the efficiency of the stance phase because nearly all of the metabolic work and all of the positive $W_{MT\text{-}SO}$ occurred during push-off. The SO stance phase efficiency was 0.44 and 0.47 during RF running for the RF and FF groups, respectively, and was 0.42 and 0.46 during FF running

for the RF and FF groups, respectively. Both stance phase and push-off efficiency were greater during RF running because overall $W_{CE\text{-}SO}$ contributed less to overall $W_{MT\text{-}SO}$ production compared to FF running.

GA metabolic energy expenditure during the push-off phase of either footfall pattern was substantially decreased compared to that of the whole stance phase (Figure 6.12C & E). The push-off efficiency of the GA (the ratio of MT_{GA} push-off work to the push-off metabolic cost) was 1.62 and 1.70 during the RF pattern for the RF and FF groups, respectively, and 2.05 and 2.03 during the FF pattern the RF and FF groups, respectively. Efficient GA muscle work production was accomplished during push-off as a result of elastic recoil, which was greater during FF running compared to RF running. Increased elastic recoil occurring with the FF pattern allowed for more positive $W_{CE\text{-}GA}$ to be done without an increase in metabolic cost. Compared to the push-off phase, GA stance phase efficiency was 0.43 and 0.32 during RF running in the RF and FF groups, respectively, and was 0.63 and 0.44 during FF running for the RF and FF groups, respectively. Stance phase efficiency was less than the push-off efficiency because nearly all of the positive $W_{MT\text{-}GA}$ and very little metabolic work occurred during push-off. The stance phase efficiency was greater in FF running compared to RF running because of increased elastic recoil that occurred during push-off during FF running.

Previous studies have speculated that the FF pattern results in greater force transmission through the Achilles tendon and will result in greater elastic energy storage (Ardigo et al., 1995; Hasegawa et al., 2007; Nilsson and Thorstensson, 1989; Perl et al., 2012). Ardigo et al. (1995) indirectly estimated elastic energy utilization between footfall patterns by calculating the ratio between external work and deceleration time to

external work and acceleration time ($W_{ext}\ t_{dec}^{-1}/W_{ext}\ t_{acc}^{-1}$). Similar to the present study, the authors found that FF running resulted in greater elastic energy utilization compared to the RF pattern although no difference in sub-maximal oxygen consumption was observed between footfall patterns. The authors suggested that greater elastic energy recoil during FF running compensated for the additional external work observed with this pattern. The present study expands on these results by demonstrating that the greater force generation requirement of FF running diminishes any metabolic savings resulting from greater elastic energy utilization compared to RF running.

The present study was consistent with previous studies identifying elastic energy utilization as an energy saving mechanism as a result of optimal contraction velocities (Cavagna and Kaneko, 1977c; Hof et al., 2002; Ishikawa et al., 2007; Lichtwark and Wilson, 2006; Lichtwark and Wilson, 2007a). Hof et al. (2002) found that a MF runner produced force isometrically with less CE work than a RF runner. However, the present study found that FF running resulted in greater W_{CE} in the SO and both footfall patterns resulted in some isometric force production. Between participant variation likely explains the differences in results between Hof et al. (2002) and the present study in addition to the possible differences in muscle mechanics between MF verses FF running.

A study by Heise et al. (2011) found that more economical runners tended to perform less negative work at the ankle. The present study found similar results in that RF running resulted in lower negative work of the triceps surae muscle-tendon complex and also resulted in a lower metabolic cost of the SO. Although the ankle plantar flexors produce more positive joint work in running compared to the hip and the ankle in running (Devita et al., 2008; Heise et al., 2011; Stefanyshyn and Nigg, 1998; Winter, 1983), the

triceps surae muscle tendon complex has a relatively small active muscle volume in running compared to other muscles of the lower extremity. Therefore, the muscle-tendon interactions of other larger, muscles of the lower extremity may have a greater affect on running economy than the triceps surae. For example, one previous study found the quadriceps had greater SEE elongation and elastic energy release in more economical runners (Albracht and Arampatzis, 2006). FF running results in less knee flexion at ground contact than RF running but knee flexion is similar through the rest of stance (Figure 6.2A & B). However, it is currently unknown how elastic energy contribution or metabolic energy cost of the quadriceps differ between footfall patterns.

An additional source of elastic strain energy is the longitudinal arch of the foot. The longitudinal are can store approximately 17 J of elastic strain energy, which is about half of the strain energy stored in the Achilles tendon under the same load (Ker et al., 1987). It was recently found that barefoot FF running resulted in greater longitudinal arch strain during the stance phase compared to barefoot RF running (Perl et al., 2012). The authors concluded that more arch strain during FF running contributes to reduced whole body metabolic cost compared to RF running, despite finding no difference in whole body metabolic cost between footfall patterns. The present study demonstrated that greater elastic energy utilization does not necessarily result in reduced metabolic cost as a result of high muscle forces. The authors of this previous study failed to question whether the increased strain was a result of ground reaction forces with the FF pattern and may have resulted in no difference in whole body metabolic cost between patterns despite differences in arch strain.

Conclusion

FF running was speculated to improve running economy over that of the RF pattern as a result of greater elastic energy utilization by the triceps surae muscle complex. Although FF running did result in greater elastic energy utilization of in both the gastrocnemius and the soleus, FF running did not result in lower muscle metabolic cost of either muscle because this pattern required greater muscle force production, negating any benefit of elastic recoil. In the soleus, FF running resulted in greater muscle metabolic cost as a result of greater contractile element mechanical work. These results suggest that there is no muscle metabolic expenditure benefit of FF running over RF running.

References

1. Albracht K and Arampatzis A. Influence of the Mechanical Properties of the Muscle-Tendon Unit on Force Generation in Runners with Different Running Economy. *Biol Cybern*. 2006; 95(1):87-96.

2. Alexander RM. Elastic Energy Stores in Running Vertebrates. *American Zoologist*. 1984; 24(1):85-94.

3. Ardigo LP, Lafortuna C, Minetti AE, Mognoni P, Saibene F. Metabolic and Mechanical Aspects of Foot Landing Type, Forefoot and Rearfoot Strike, in Human Running. *Acta Physiol Scand*. 1995; 155(1):17-22.

4. Arnold EM, Ward SR, Lieber RL, Delp SL. A Model of the Lower Limb for Analysis of Human Movement. *Ann Biomed Eng*. 2010; 38(2):269-279.

5. Bahler AS. Series Elastic Component of Mammalian Skeletal Muscle. *Am J Physiol*. 1967; 213(6):1560-1564.

6. Biewener AA and Roberts TJ. Muscle and Tendon Contributions to Force, Work, and Elastic Energy Savings: A Comparative Perspective. *Exerc Sport Sci Rev*. 2000; 28(3):99-107.

7. Bobbert MF, Huijing PA, van Ingen Schenau GJ. A Model of the Human Triceps Surae Muscle-Tendon Complex Applied to Jumping. *J Biomech*. 1986a; 19(11):887-898.

8. Cavagna GA. Storage and Utilization of Elastic Energy in Skeletal Muscle. *Exerc Sport Sci Rev*. 1977a; 5:89-129.

9. Cavagna GA, Heglund NC, Taylor CR. Mechanical Work in Terrestrial Locomotion: Two Basic Mechanisms for Minimizing Energy Expenditure. *Am J Physiol*. 1977b; 233(5):R243-261.

10. Cavagna GA and Kaneko M. Mechanical Work and Efficiency in Level Walking and Running. *J Physiol*. 1977c; 268(2):467--481.

11. Cohen J. A Power Primer. *Psychol Bull*. 1992; 112(1):155-159.

12. Cole GK, Nigg BM, Ronsky JL, Yeadon MR. Application of the Joint Coordinate System to Three-Dimensional Joint Attitude and Movement Representation: A Standardization Proposal. *J Biomech Eng*. 1993; 115(4A):344-349.

13. Cunningham CB, Schilling N, Anders C, Carrier DR. The Influence of Foot Posture on the Cost of Transport in Humans. *J Exp Biol*. 2010; 213(5):790-797.

14. Devita P, Janshen L, Rider P, Solnik S, Hortobagyi T. Muscle Work Is Biased toward Energy Generation over Dissipation in Non-Level Running. *J Biomech*. 2008; 41(16):3354-3359.

15. Fenn WO. The Relation between the Work Performed and the Energy Liberated in Muscular Contraction. *J Physiol*. 1924; 58(6):373-395.

16. Fukunaga T, Kawakami Y, Kubo K, Kanehisa H. Muscle and Tendon Interaction During Human Movements. *Exerc Sport Sci Rev*. 2002; 30(3):106-110.

17. Fukunaga T, Kubo K, Kawakami Y, Fukashiro S, Kanehisa H, Maganaris CN. In Vivo Behaviour of Human Muscle Tendon During Walking. *Proc Biol Sci*. 2001; 268(1464):229-233.

18. Gordon AM, Huxley AF, Julian FJ. The Variation in Isometric Tension with Sarcomere Length in Vertebrate Muscle Fibres. *J Physiol*. 1966; 184(1):170-192.

19. Hasegawa H, Yamauchi T, Kraemer WJ. Foot Strike Patterns of Runners at the 15-Km Point During an Elite-Level Half Marathon. *J Strength Cond Res*. 2007; 21(3):888-893.

20. Heise GD, Smith JD, Martin PE. Lower Extremity Mechanical Work During Stance Phase of Running Partially Explains Interindividual Variability of Metabolic Power. *Eur J Appl Physiol*. 2011; 111(8):1777-1785.

21. Hill AV. The Heat of Shortening and the Dynamic Constants of Muscle. *Proc Royal Soc*. 1938; 126B:136-195.

22. Hof AL, Van Zandwijk JP, Bobbert MF. Mechanics of Human Triceps Surae Muscle in Walking, Running and Jumping. *Acta Physiol Scand*. 2002; 174(1):17-30.

23. Huxley AF. Muscular Contraction. *J Physiol*. 1974; 243(1):1-43.

24. Ishikawa M, Pakaslahti J, Komi PV. Medial Gastrocnemius Muscle Behavior During Human Running and Walking. *Gait Posture*. 2007; 25(3):380-384.

25. Ker RF, Bennett MB, Bibby SR, Kester RC, Alexander RM. The Spring in the Arch of the Human Foot. *Nature*. 1987; 325(7000):147-149.

26. Lichtwark GA and Wilson AM. Interactions between the Human Gastrocnemius Muscle and the Achilles Tendon During Incline, Level and Decline Locomotion. *J Exp Biol*. 2006; 209(Pt 21):4379-4388.

27. Lichtwark GA and Wilson AM. Muscle Fascicle and Series Elastic Element Length Changes Along the Length of the Human Gastrocnemius During Walking and Running. *J Biomech*. 2007a; 40(1):157-164.

28. Lieberman DE, Venkadesan M, Werbel WA, Daoud AI, D'Andrea S, Davis IS, Mang'eni RO, Pitsiladis Y. Foot Strike Patterns and Collision Forces in Habitually Barefoot Versus Shod Runners. *Nature*. 2010; 463(7280):531-535.

29. McClay I and Manal K. Three-Dimensional Kinetic Analysis of Running: Significance of Secondary Planes of Motion. *Med Sci Sports Exerc*. 1999; 31(11):1692-1737.

30. Minetti AE and Alexander RM. A Theory of Metabolic Costs for Bipedal Gaits. *J Theor Biol*. 1997; 186(4):467-476.

31. Nilsson J and Thorstensson A. Ground Reaction Forces at Different Speeds of Human Walking and Running. *Acta Physiol Scand*. 1989; 136(2):217-227.

32. Perl DP, Daoud AI, Lieberman DE. Effects of Footwear and Strike Type on Running Economy. *Med Sci Sports Exerc*. 2012; 44(7):1335-1343.

33. Pratt DJ. Mechanisms of Shock Attenuation Via the Lower Extremity During Running. *Clin Biomech (Bristol, Avon)*. 1989; 4(1):51-57.

34. Rall JA. Energetic Aspects of Skeletal Muscle Contraction: Implications of Fiber Types. *Exerc Sport Sci Rev*. 1985; 13:33-74.

35. Riener R and Edrich T. Identification of Passive Elastic Joint Moments in the Lower Extremities. *J Biomech*. 1999; 32(5):539-544.

36. Roberts TJ, Kram R, Weyand PG, Taylor CR. Energetics of Bipedal Running. I. Metabolic Cost of Generating Force. *J Exp Biol*. 1998; 201(Pt 19):2745-2751.

37. Roberts TJ, Marsh RL, Weyand PG, Taylor CR. Muscular Force in Running Turkeys: The Economy of Minimizing Work. *Science*. 1997; 275(5303):1113-1115.

38. Sasaki K, Neptune RR, Kautz SA. The Relationships between Muscle, External, Internal and Joint Mechanical Work During Normal Walking. *J Exp Biol*. 2009; 212(Pt 5):738-744.

39. Scholz MN, Bobbert MF, van Soest AJ, Clark JR, van Heerden J. Running Biomechanics: Shorter Heels, Better Economy. *J Exp Biol*. 2008; 211(Pt 20):3266-3271.

40. Sellers WI, Dennis LA, Crompton RH. Predicting the Metabolic Energy Costs of Bipedalism Using Evolutionary Robotics. *J Exp Biol*. 2003; 206(Pt 7):1127-1136.

41. Stefanyshyn DJ and Nigg BM. Dynamic Angular Stiffness of the Ankle Joint During Running and Sprinting. *J App Biomech*. 1998; 14(3):292-299.

42. Umberger BR and Rubenson J. Understanding Muscle Energetics in Locomotion: New Modeling and Experimental Approaches. *Exerc Sport Sci Rev*. 2011; 39(2):59-67.

43. van Soest AJ and Bobbert MF. The Contribution of Muscle Properties in the Control of Explosive Movements. *Biol Cybern*. 1993; 69(3):195-204.

44. Winter DA. Moments of Force and Mechanical Power in Jogging. *Journal of Biomechanics*. 1983; 16(1):91-97.

45. Winter DA, Sidwall HG, Hobson DA. Measurement and Reduction of Noise in Kinematics of Locomotion. *Journal of Biomechanics*. 1974; 7(2):157-159.

CHAPTER 7

IMPACT CHARACTERISTICS AND SHOCK ATTENUATION BETWEEN FOOTFALL PATTERNS IN RUNNING

Abstract

The initial impact peak within the vertical ground reaction force (GRF) component that occurs with the rearfoot (RF) running pattern has been implicated as the cause of many running injuries. For this reason, the forefoot (FF) running pattern, which does not result in this initial impact peak, has been advocated to reduce the risk of running injuries. However, the differences in vertical GRF profile in the time domain suggests that the frequency content of the vertical GRF, and thereby the frequency content of the impact shock and how impact shock is attenuated, may also differ. Therefore, the purposes of this study were to: 1) determine the difference in impact shock wave attenuation between footfall patterns; 2) determine if there is an advantage of altering footfall pattern to improve impact shock attenuation; and 3) determine if there may be difference in impact shock attenuation mechanisms between footfall patterns. Twenty natural RF runners and twenty natural FF runners performed treadmill and over-ground running with the RF and FF patterns at 3.5 $m \cdot s^{-1}$ ± 5%. Tibial and head accelerometer data was recorded during treadmill running and used to determine impact shock attenuation by using a transfer function of the power spectral density of each signal. Vertical GRF data was recorded during the over-ground conditions and transformed into the frequency domain with a discrete Fourier transform. A mixed-factor ANOVA was used to determine the difference in impact shock attenuation and GRF

amplitude at frequencies 1 – 50 Hz ($\alpha = 0.05$). RF running resulted in significantly greater shock attenuation for most frequencies 6 – 48 Hz ($p < 0.05$). Additionally, FF running resulted in greater vertical GRF amplitudes at frequencies 1 – 16 Hz whereas RF running resulted in greater amplitudes at frequencies 18 – 43 Hz ($p < 0.05$). The RF pattern resulted in greater shock attenuation as a result of greater tibial loading. Greater head power at frequencies 3 – 8 Hz despite less energy to be attenuated with the FF pattern suggests that this pattern may result in a reduced capacity for shock attenuation. The difference in vertical GRF amplitudes suggests that each footfall pattern may rely on different mechanisms in order to attenuate impact shock.

Introduction

Rearfoot (RF) running footfall pattern results in the presence of an initial impact peak (IMP) in the vertical ground reaction force (GRF) component (Cavanagh and Lafortune, 1980; Dickinson et al., 1985; Munro et al., 1987). This vertical IMP is the main source of the shock wave transmitted into the foot and through the rest of the body (Nigg et al., 1981; Shorten and Winslow, 1992; Voloshin et al., 1985). Consequently, the vertical IMP and tibial shock have been implicated in the development of overuse injuries from running (Davis et al., 2010; Grimston et al., 1991; Hreljac et al., 2000; James et al., 1978; Milner et al., 2006; Paul et al., 1978; Radin et al., 1973; Voloshin and Wosk, 1982; Zifchock et al., 2006).

It has been suggested that reducing the magnitude of the vertical IMP and tibial shock may be beneficial for preventing injury (Cavanagh and Lafortune, 1980; Davis et al., 2010; James et al., 1978). Reducing the magnitude of the vertical IMP can be

accomplished by changing the position and acceleration of the foot and leg at ground contact. For example, a smaller dorsiflexion angle and a more vertically oriented leg when using a RF pattern will decrease the magnitude of the IMP (Gerritsen et al., 1995). Changes in segmental position and acceleration can also be achieved by modifying running speed, stride length and stride frequency (Bobbert et al., 1991; Clarke et al., 1985; Derrick et al., 1998; Hamill et al., 1983; Hamill et al., 1995; Mercer et al., 2003; Mercer et al., 2002). Changing from an RF running footfall pattern to a forefoot (FF) running footfall pattern has been suggested as an alternative method to modify the magnitude of the IMP and reduce injury risk (Cavanagh and Lafortune, 1980; Dickinson et al., 1985; Lieberman et al., 2010; Munro et al., 1987).

The RF and FF patterns differ with respect to the initial portion of the foot that makes contact with the ground. In addition, the vertical IMP seen in the time domain with the RF pattern does not typically exist with the FF pattern. The absence of the vertical impact peak has led some to speculate that FF running is beneficial for injury prevention (Davis et al., 2010; Laughton et al., 2003; Lieberman et al., 2010; Oakley and Pratt, 1988; Pratt, 1989; Williams et al., 2000). Although RF running results in an initial impact peak, FF running results in greater peak vertical active GRF (Cavanagh and Lafortune, 1980; Laughton et al., 2003; McClay and Manal, 1995b; Oakley and Pratt, 1988). The resulting joint loads from the active force can be 3 – 5 times greater than the loads resulting from the impact peak (Burdett, 1982; Harrison et al., 1986; Scott and Winter, 1990). Therefore, these high forces generated during push-off may also be a significant contributor to running injury mechanisms (Dickinson et al., 1985; Messier et al., 1991; Nigg, 2011; Radin, 1972; Winter, 1983).

Inherent differences in kinematics between the RF and FF footfall patterns not only dictate the vertical GRF profile but may also contribute to differences in the frequency content of the vertical GRF and the impact shock wave. Previous investigations have indicated that the initial GRF impact peak has a frequency content of between 10 – 20 Hz (Derrick et al., 1998; Nigg et al., 1981; Nigg and Wakeling, 2001). The resulting impact shock measured at the tibia also has a frequency content of 12 – 20 Hz (Hamill et al., 1995; Shorten and Winslow, 1992). Therefore, frequency components from the vertical GRF or impact shock wave in this range may have lower power during FF running due to the absence of the impact peak. Vertical GRF frequency components below 8 Hz are associated to the active force (Potthast et al., 2010; Shorten and Mientjes, 2003) and resulting impact shock measured at the tibia also has a frequency content of 4 – 8 Hz (Hamill et al., 1995; Shorten and Winslow, 1992). The difference in active peak magnitude between footfall patterns suggests the vertical GRF and tibial acceleration frequency components may have greater power and amplitude in the 4 – 8 Hz range with FF running.

Appropriate attenuation of the impact shock wave is necessary to maintain the visual field and head stabilization for adequate vestibular functioning (Pozzo et al., 1991). A difference in frequency content of the GRF and impact shock between patterns may alter how impact shock is attenuated by the body tissues and the ability to maintain head stabilization. In order to prevent injury to the tissues and maintain head stability, the body must be able to respond to a greater impact shock wave by increasing the amount of attenuation that occurs.

Shock attenuation occurs by absorption of the impact shock wave by the body tissues and kinematic adjustments (Bobbert et al., 1992; Chu et al., 1986; Denoth, 1986; Nigg et al., 1981; Voloshin et al., 1985). The body is able to dynamically respond to increased impact magnitudes by increasing the reliance of attenuation among the various mechanisms. Passive mechanisms, such as deformation of the heel fat pad, the running shoe, ligaments, bone and articular cartilage are responsible for attenuating the high frequency waveforms generated at initial ground contact (Chu et al., 1986; Lafortune et al., 1996; Nigg et al., 1981; Paul et al., 1978; Voloshin et al., 1985; Williams and Cavanagh, 1987). Previous investigations have found that the heel fat pad has been shown to attenuate all frequencies and bone attenuates frequencies greater than 18 Hz (Paul et al., 1978). Although the there is a fat pad under the metatarsal heads, it has not as thick as the fat pad under the heel and its shock attenuation properties have yet to be investigated. Because the FF pattern does not take advantage of the heel fat pad or shoe cushioning in the heel to attenuate impacts, high frequency components must be attenuated by other passive tissues or by active mechanisms.

Active shock attenuation mechanisms include eccentric muscle contractions, increased muscle activation, changes in segment geometry and adjustments in joint stiffness (Bobbert et al., 1992; Cole et al., 1996a; Denoth, 1986; Derrick et al., 1998; Gerritsen et al., 1995; McMahon et al., 1987). Active mechanisms are responsible for attenuating lower frequency components because muscle latency is too slow to elicit muscular reactions during the short impact phase despite pre-activation in late swing to prepare for impact (Nigg, 1986; Nigg, 2011; Nigg et al., 1981). Because muscle latency is approximately 30 – 75 ms (Nigg et al., 1981; Simon et al., 1981), active muscle

contractions that are specifically responding to an impact stimulus may only be effective at attenuating frequencies below 10 Hz (Paul et al., 1978). The FF pattern may have a greater reliance on active shock attenuation mechanisms since the active force peak is greater compared to the RF pattern.

Differences in impact characteristics between footfall patterns may affect which mechanisms are responsible for attenuating impacts, how much attenuation occurs and the degree of stress placed on different tissues. RF running may rely more on passive mechanisms such as footwear, cartilage and bone deformation, whereas FF running may rely more on active mechanisms such as eccentric contractions of the plantar flexors (Pratt, 1989; Williams and Cavanagh, 1987). The difference in how the body attenuates impacts during RF and FF running may subject different tissues to injury and may also affect the total amount of attenuation that occurs. Potential differences in how the body attenuates impacts between footfall patterns, and not just the difference in impact characteristics, may allow for the ability to assess the potential for FF running at preventing injury.

Since some investigations have found a relationship between time domain vertical impact peak variables and the risk of developing running injuries whereas others have not (Azevedo et al., 2009; Bredeweg, 2011; McCrory et al., 1999; Pohl et al., 2008; Scott and Winter, 1990), examining the frequency content of impact characteristics may identify the mechanisms responsible for shock attenuation between footfall patterns and may be a better indicator of injury risk than traditional loading characteristics. Therefore, the purposes of this study were to: 1) determine the difference in impact shock wave attenuation between footfall patterns; 2) determine if there is an advantage of altering

footfall pattern to improve impact shock attenuation; and 3) determine if there may be difference in impact shock attenuation mechanisms between footfall patterns. It was hypothesized that RF running would result in greater shock attenuation between the tibia and the head than FF running as indicated by reduced power of the frequencies contained in the head acceleration signal. Secondly, RF running takes advantage of the heel fat pad and shoe cushioning to attenuate impacts. Therefore, it was also hypothesized that if RF running results in greater shock attenuation, natural RF runners would not increase the amount of impact shock attenuation when switching to a FF pattern whereas natural FF runners would increase the amount of impact shock attenuated when switching to a RF pattern. The third hypothesis was that the RF pattern would rely more on passive shock attenuation mechanisms (e.g. frequencies greater than 10 Hz) whereas the FF pattern would rely more on active shock attenuation mechanisms (e.g. frequencies below 10 Hz).

Methodology

Participant Selection

A list of acronyms and abbreviations used in this study are listed in Table 7.1. Twenty natural RF runners and twenty natural FF runners participated in this study (Table 7.2). All male and female participants where healthy, experienced runners and did not have a history of cardiovascular or neurological problems. Inclusion criteria required that participants completed at least 16 km per week at a minimum preferred running speed of 3.5 $m \bullet s^{-1}$ and had not developed an injury to the lower extremity or back within the past year. Participants were divided into a RF runners group or a FF runners group

based on the footfall pattern habitually performed when distance running. Habitual footfall pattern was determined by recording vertical GRFs and high speed video as each participant ran over a force platform at his or her preferred speed. RF running was defined as making initial contact with the heel. FF running was defined as making initial contact on the ball of the foot and preventing the heel from touching the ground. If a participant was classified as a midfoot runner, they were placed in the RF group if they made contact with a semi-dorsiflexed or flat foot position (approximately zero degrees of dorsiflexion or greater) and generated an initial IMP within the vertical GRF component (n = 5). Midfoot runners were classified into the FF group if they landed with a plantar flexed foot position but allowed the heel to touch the ground and did not generate an initial impact peak (n = 6). All participants read and completed an informed consent document and questionnaires approved by the University of Massachusetts Amherst Institutional Review Board before participating.

Table 7.1: Acronyms and abbreviations for each variable.

ActP	vertical ground reaction force active peak	MF	midfoot
BW	units of body weight	PPTA	peak positive tibial acceleration
CT	contact time	PSD	power spectral density
FF	forefoot	RF	rearfoot
GRF	ground reaction force	RPA	rate of positive tibial acceleration
HP1	first head acceleration peak	SL	stride length
HP2	second head acceleration peak	SF	stride frequency
IMP	vertical ground reaction force impact peak	VLR	vertical ground reaction force loading rate

Table 7.2: Mean ± SD participant characteristics of the rearfoot group (RF) and the forefoot group (FF) for the participants included in Study 4. Differences between groups were assessed with a student's t-test (α = 0.05).

	Males/Females (#)	Age (yrs)	Height (m)	Mass (kg)	Pref. Speed ($m \cdot s^{-1}$)	Distance/week (km)
RF group	13/7	26.3 ± 6.2	1.76 ± 0.09	69.89 ± 9.78	3.49 ± 0.88	46.34 ± 32.28
FF group (treadmill)	14/5	25.4 ± 6.2	1.76 ± 0.10	68.78 ± 9.51	3.73 ± 0.24	53.18 ± 25.53
p-value	-	0.702	.0726	1.000	0.374	0.662
FF group (over-ground)	15/5	25.6 ± 6.1	1.76 ± 0.10	70.27 ± 10.66	3.65 ± 0.34	47.02 ± 26.91
p-value	-	0.702	0.822	0.906	0.453	0.942

Experimental Setup

Three-dimensional kinematics of the right leg and foot were recorded with an eight-camera Qualisys Oqus 3-Series optical motion capture system (Qualisys, Inc., Gothenberg, Sweden) sampling at 240 Hz. Motion of retro-reflective markers placed on the foot and leg were used to monitor the footfall pattern performed by each participant (Appendix B). Calibration markers included the medial and lateral femoral condyles, medial and lateral malleoli, and the heads of the first and fifth metatarsals. Tracking markers included a rigid plate with three non-collinear markers placed on the lower leg and the posterior calcaneus. Participants wore form-fitting clothing and neutral racing flat shoes provided by the laboratory (RC 550, New Balance, Brighton, MA, USA).

The cameras surrounded an AMTI force platform (OR6-5, AMTI Inc., Watertown, MA, USA) mounted flush with the floor surface. The force platform was located in the center of a 25 m runway. GRFs and center of pressure were recorded at a sampling frequency of 1200 Hz and were synchronized with the motion capture data. Running speed was monitored with photoelectric sensors (Lafayette Instrument Company, Lafayette, IN) placed 3 m before and after the force platform.

For collecting the accelerometer data, a treadmill was placed in the center of the motion capture space in order for continuous accelerometer data to be captured synchronously with kinematics. A low-mass (<4 grams), uniaxial, piezoelectric accelerometers (ICP®, PCB Piezotronics, Depew, NY, USA) were placed in accordance with the methods of Valiant et al. (1987). The head accelerometer was attached to the center of the frontal bone and the tibial accelerometer was attached to the anteromedial aspect of the distal tibia (Hamill et al., 1995). Each attachment site was chosen to reduce the effects of soft tissue vibration (Valiant et al., 1987; Wosk and Voloshin, 1981). The axis of each accelerometer was aligned with the vertical axis of the laboratory coordinate system. The accelerometers were sampled at 1200 Hz and voltage was amplified by a factor of 10.

Protocol

GRFs and kinematics were recorded while the participants ran over the force platform at 3.5 $m \cdot s^{-1}$ ± 5%. Ten trials of each condition were performed. Conditions included RF and FF running. The order of the conditions was randomized. For the FF running condition, the participants were instructed to land on the ball of the foot and prevent the heel from making contact with the ground.

After the over-ground conditions were performed, accelerometers were secured to the head and anteromedial distal tibia by rubber straps tightened to participant tolerance. Participants were then asked to run on a treadmill at 3.5 $m \cdot s^{-1}$ ± 5% with each footfall pattern condition. The order of conditions performed on the treadmill was also randomized. Participants practiced running on the treadmill with each footfall pattern for

several minutes before data was collected. After sufficient practice was performed, participants ran for two minutes on the treadmill before data was collected for each condition. Accelerometer data was collected for 15 seconds during the last minute of each condition.

Data Reduction

Motion capture, GRF and accelerometer data were exported in .C3D format for processing with Visual 3D software (C-Motion, Inc, Rockville, MD, USA). Raw kinematic data was filtered with a 4^{th} order, zero-lag Butterworth digital low-pass filter with a cutoff frequency of 12 (Winter et al., 1974). Joint angles were calculated using a rotation matrix of the distal segment with respect to proximal segment with a Cardan rotation sequence of x (flexion/extension; dorsiflexion/plantar flexion) – y (abduction/adduction; inversion/eversion) – z (axial rotation) (Cole et al., 1993). The sagittal plane ankle angles during the stance phase of each condition were analyzed in order to confirm the footfall pattern performed during each condition. Kinematic data were interpolated from heel-strike to toe-off to 101 data points, with each point representing 1% of the stance phase. Ground contact time was calculated as the time from initial ground contact to toe-off.

Sagittal plane ankle joint and leg segment angles were also determined from the motion capture data collected during the treadmill conditions using the same procedures as with the over ground data. Stride frequency (SF; strides per minute) was determined from the treadmill conditions by multiplying the number of strides occurring during the 15 second recording of each treadmill condition by four. Stride length (SL; m) was

calculated by dividing the running speed set on the treadmill by the SF. Contact time (CT) was calculated for both the over ground and treadmill conditions as the time between initial ground contact and toe-off.

Time domain and frequency parameters from the vertical GRF and tibia and head accelerometers were calculated using a custom MATLAB program (Mathworks, Inc., Natick, MA). Data were filtered with a second order Butterworth low-pass filter with a cut-off frequency of 50 Hz. In the time domain, impact peak (IMP) and active peak (ActP) of the vertical GRF (in units of body weights, BW) was determined during the stance phase of over-ground running. Since the FF pattern does not result in an impact peak, IMP during the FF pattern was calculated by determining the magnitude of the vertical GRF at 25 ms of the stance phase. The selected timing of the impact peak was based on previous studies investigating vertical GRF characteristics at a similar running speed (Bobbert et al., 1992; Cavanagh and Lafortune, 1980; Munro et al., 1987). The active peak was calculated by determining the maximum of the vertical GRF across the stance phase. Vertical GRF loading rate (VLR) was calculated from the slope of the line between 20-80% of the time before the first peak of the GRF was reached during the RF pattern. VLR during the FF pattern was calculated between 20 – 80% of the first 25 ms of the stance phase (Bobbert et al., 1992; Cavanagh and Lafortune, 1980; Munro et al., 1987).

Time domain parameters from the tibia and head accelerometers were determined from 15 stance phases in each condition during treadmill running. A least-squares best fit line was subtracted from the raw data of each signal to remove any linear trend (Shorten and Winslow, 1992). Data where then filtered with a second order Butterworth low-pass

filter with a cut-off frequency of 60 Hz (Hennig and Lafortune, 1991). The first (HP1) and second (HP2) peak of the head acceleration signal were identified as the peak between 1 – 30% of stance and 31 – 101% of stance, respectively. Impact shock characteristics were determined by calculating peak positive tibial acceleration (PPTA) and rate of positive tibial acceleration (RPA). RPA was calculated from the slope of line between 10-90% of the time before peak acceleration is reached (Lafortune, 1991).

The frequency content of the vertical GRF, tibia acceleration and head acceleration was determined by expressing the signal in the frequency domain (Shorten and Winslow, 1992). Unfiltered, detrended were zero padded data to 2048 data points then transformed into the frequency domain by a discrete Fourier Transform (DFT). A DFT was performed on each trial or stance phase then normalized to 1 Hz bins. The amplitude at each frequency 1 – 50 Hz was averaged across all stance phases and participants. The criteria for differentiating between passive and active shock attenuation mechanisms were based on suggestions from previous studies (Derrick et al., 1998). This criteria was that GRF frequencies above 10 Hz indicated impact was attenuated by passive mechanisms and frequencies below 10 Hz indicated impact was attenuated by active mechanisms.

The degree of shock attenuation occurring during the stance phase with each footfall pattern was calculated by first using the frequency data of the tibia and head acceleration to determine the power spectral density (PSD) at frequencies 0 to the Nyquist frequency (Nyquist, F_N = one half of sampling rate, therefore F_N = 600) (Derrick et al., 1998; Hamill et al., 1995). Powers from each stance phase were normalized into 1 Hz bins (Winter, 1997). After binning, the PSD was normalized in order for the sum of

the powers from 0 to F_N to be equal to the mean squared amplitude of the data in the time domain. Normalizing allowed for a group average to be calculated for each frequency bin. A transfer function was then calculated to determine the degree of shock attenuation occurring between the tibia to the head by:

$$\text{Shock Attenuation} = 10 \cdot \log_{10}(PSD_{head}/PSD_{tibia}) \quad (7.1).$$

For each frequency, the transfer function calculated the gain or attenuation, in decibels, between the tibia and head signals. Positive values indicated a gain, or increase in signal strength between signals, and negative values indicated attenuation, or decrease in signal strength (Derrick et al., 1998; Hamill et al., 1995; Shorten and Winslow, 1992).

Statistical Analysis

Differences in each of the following variables were assessed between footfall from the over-ground running conditions: sagittal plane ankle and knee joint angle at initial contact, CT, IMP, ActP, VLR and the amplitude of the vertical GRF in the frequency domain from frequencies 1-50 Hz. Additionally, the differences between footfall patterns in the following variables were assessed from the treadmill conditions: sagittal plane ankle joint and leg segment angles at initial contact, SF, SL, CT, HP1, HP2, PPTA, RPA, tibia and head acceleration in the frequency domain from frequencies 1-50 Hz and the transfer function between the tibia and head. Each variable was subjected to a mixed model analysis of variance with footfall pattern and group as fixed variables and subject nested within group as a random variable. The differences between footfall patterns (2 levels) and between groups (2 levels) and the interaction of footfall pattern

and group were assessed with a significance level of $\alpha = 0.05$. When a significant group by pattern interaction was observed, a post-hoc assessment was performed by partitioning the interaction by group and by pattern. Partitioning by group determined the significance between each footfall pattern within each group. Partitioning by pattern determined the significance between groups within each footfall pattern. Effect sizes were also calculated to determine if the differences between footfall pattern and groups were biologically meaningful. An effect size (d) greater than 0.3 indicated a small effect, an effect size greater than 0.5 indicated a moderate effect and an effect size greater than 0.8 indicated a large effect (Cohen, 1992).

Results

Treadmill Running Conditions

Kinematics

A significant group by pattern interaction was observed for the sagittal plane ankle angle at touchdown meaning that the RF and FF groups did not have a consistent change between patterns ($p = 0.015$) (Table 7.3). Partitioning the interaction by pattern revealed that the RF group had a greater dorsiflexion angle during the RF pattern and a greater plantar flexion angle during the FF pattern compared to the FF group, although the differences between groups within each footfall pattern were not significant (RF pattern: $p = 0.077$, $d = 0.7$; FF pattern: $p = 0.082$, $d = 0.4$). Partitioning the interaction by group revealed that the sagittal plane ankle angle was significantly different between patterns within each group (RF group: $p < 0.001$, $d = 4.8$; FF group: $p < 0.001$, $d = 4.2$).

Characteristically, the RF pattern resulted in a dorsiflexion angle at touchdown whereas the FF pattern resulted in a plantar flexion angle (Table 7.3).

There was no significant group by pattern interaction ($p = 0.456$) or significant group main effect for sagittal plan leg angle at initial contact. A significant pattern main effect indicated that the leg was oriented more vertically at touchdown during the FF pattern in both groups ($p < 0.001$; $d = 0.9$) (Table 7.3).

Table 7.3: Mean ± SD for the kinematic parameters measured from the treadmill conditions when performing the rearfoot (RF) and forefoot (FF) patterns. Parameters include the sagittal plane ankle angle at touchdown (Ankle), the sagittal plane leg angle at touchdown (Leg), stride length (SL), stride frequency (SF) and contact time (CT). Listed statistics include the p-value for the group by pattern interaction (GxP) and the p-value (*d*) for the group main effect (G) and the pattern main effect (P) if the interaction was not significant.

	RF Group		FF Group		GxP	G	P
	RF	FF	RF	FF			
Ankle (deg)	10.20 ± 3.23	-10.39 ± 5.25	7.94 ± 2.98	-8.16 ± 4.69	0.015	-	-
Leg (deg)	-9.82 ± 2.23	-7.09 ± 3.17	-8.28 ± 2.57	-6.08 ± 2.75	0.456	0.125 (0.5)	0.001 (0.9)
SL (m)	2.47 ± 0.17	2.43 ± 0.16	2.47 ± 0.16	2.50 ± 0.22	0.029	-	-
SF (strides/s)	85.50 ± 5.66	86.95 ± 5.73	85.81 ± 5.14	85.80 ± 6.29	0.066	0.816 (0.1)	0.072 (0.1)
CT (s)	0.25 ± 0.02	0.23 ± 0.01	0.24 ± 0.02	0.22 ± 0.02	0.631	0.237 (0.4)	0.001 (1.0)

There was a significant group by pattern interaction for SL ($p = 0.029$) (Table 7.3). Partitioning the interaction by group revealed no significant differences in SL between patterns within the RF or FF groups (RF group: $p = 0.081$, $d = 0.3$; FF group: $p = 0.160$, $d = 0.2$). Partitioning the interaction by pattern revealed that there was no significant difference in SL between groups when performing the RF pattern ($p = 0.905$, $d < 0.1$). However, a significant difference between groups was observed during the FF

pattern ($p = 0.004$, $d = 0.4$). The RF group decreased SL when performing the FF pattern compared to the RF pattern whereas the FF group increased SL with the FF pattern. There were no significant main effects or interactions observed for SF ($p > 0.05$, $d = 0.1$).

No significant group by pattern interaction ($p = 0.631$) or main effect of group ($p = 0.237$; $d = 0.4$) was observed for CT (Table 7.3). A significant pattern main effect revealed CT was greater during the RF pattern compared to the FF pattern ($p < 0.001$; $d = 1.0$).

Table 7.4: Mean ± SD for the accelerometer characteristics measured from the treadmill conditions when performing the rearfoot (RF) and forefoot (FF) patterns. Parameters include the first (HP1) and second (HP2) peak of the head acceleration signal, peak positive tibial acceleration (PPTA) and rate of positive tibial acceleration (RPA). Listed statistics include the p-value for the group by pattern interaction (GxP) and the p-value (*d*) for the group main effect (G) and the pattern main effect (P) if the interaction was not significant.

	RF Group		FF Group		GxP	G	P
	RF	FF	RF	FF			
HP1 (g)	0.51 ± 0.28	0.40 ± 0.19	0.52 ± 0.22	0.47 ± 0.19	0.425	0.886 (0.2)	0.344 (0.4)
HP2 (g)	1.01 ± 0.24	1.00 ± 0.23	1.01 ± 0.25	1.06 ± 0.26	0.055	0.494 (0.1)	0.054 (0.1)
PPTA (g)	5.07 ± 1.46	4.53 ± 1.21	5.31 ± 1.35	3.87 ± 1.36	0.020	0.550 (0.2)	<0.001 (0.7)
RPA (g)	220.16 ± 86.66	219.74 ± 81.16	206.08 ± 66.53	196.24 ± 97.77	0.644	0.375 (0.2)	0.661 (0.1)

Head and Tibial Acceleration in the Time Domain

No significant interactions or main effects were observed for HP1, HP2, and RPA ($p>0.05$) (Table 7.4) (Figure 7.1). A significant group by pattern interaction was observed for PPTA ($p = 0.020$). Partitioning the interaction by group revealed that RF running resulted in significantly greater PPTA compared to FF running within the RF group ($p=0.046$, $d=0.4$) and FF group ($p< 0.001$, $d=1.1$) (Table 7.4) (Figure 7.1C). Partitioning the interaction by pattern showed that the PPTA resulting from each footfall

pattern did not differ between groups when performing the RF pattern (p=0.362, d=0.2) but was significantly greater in the RF group compared to the FF group when performing the FF pattern (p=0.016, d=0.5) (Figure 7.1C & D).

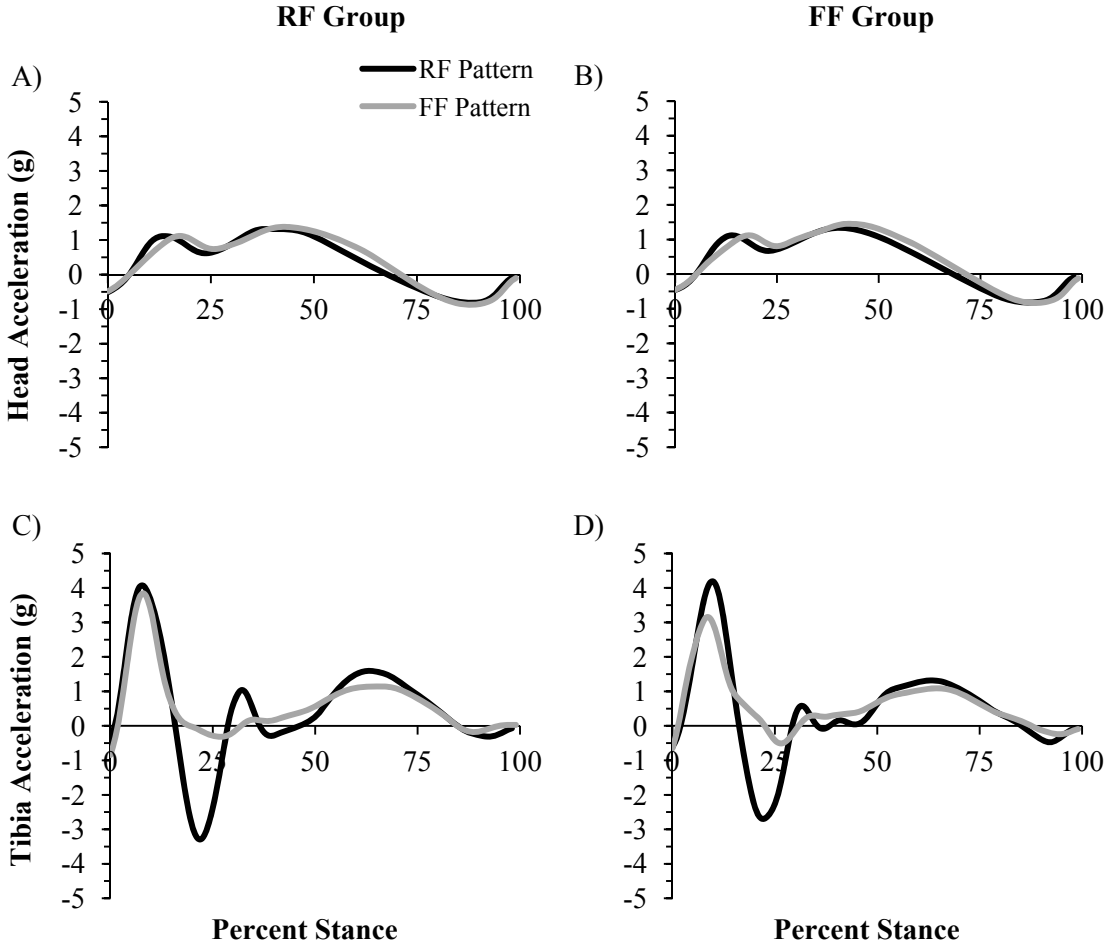

Figure 7.1: Group mean time series of the head and tibial accelerometer data from the rearfoot (RF) and forefoot (FF) groups performing the RF and FF patterns.

Head and Tibial Acceleration FFT Results

A significant group by pattern interaction was observed for head acceleration amplitude at 31 Hz (p = 0.021) but at no other frequencies (p > 0.05) (Figure 7.2A & B). Partitioning the interaction by group revealed RF running resulted in greater head

acceleration amplitude at this frequency in the RF group ($p = 0.013$, $d = 0.8$) (Figure 7.2A) but there was no difference between patterns in the FF group ($p = 0.425$, $d = 0.3$) (Figure 7.2B). Partitioning the interaction by pattern revealed no significant differences between groups within each pattern that this frequency ($p > 0.05$, $d < 0.6$).

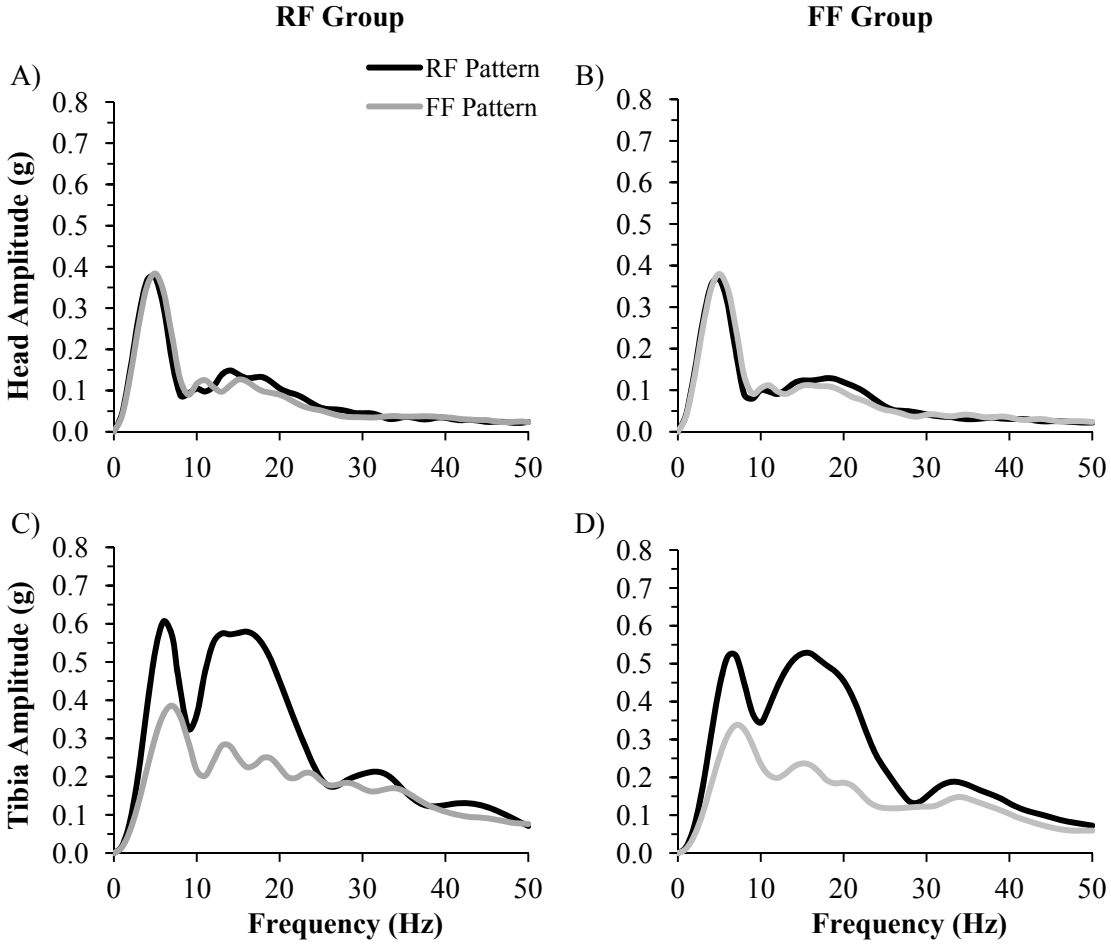

Figure 7.2: Group mean amplitude spectra of the head and tibia acceleration signal in the frequency domain compared between the rearfoot (RF) and forefoot (FF) patterns performed by the RF and FF groups

No significant group main effects were observed for the head acceleration signal amplitude for frequencies between 1 – 50 Hz ($p > 0.05$, $d < 0.2$) (Figure 7.2A & B). However, a significant pattern main effect was observed for head acceleration amplitude

at frequencies 1 – 3, 6 – 8, 11, 13, 14, 17 – 24, 27 – 29, 34, 35, 44, 45 and 49 Hz ($p <$ 0.05). The pattern main effect was not significant at all other frequencies ($p > 0.05$). The frequencies at which a significant pattern main effect was observed indicated that RF running resulted in greater head acceleration amplitude for frequencies 1 – 4 Hz and 12 – 32 Hz whereas FF running resulted in greater head acceleration amplitude for frequencies 5 – 11 Hz and 33 – 50 Hz. Large biological significance was observed at 7 and 8 Hz ($d >$ 0.8) but the difference was moderate or low for all other frequencies ($d < 0.7$).

A significant group by pattern interaction was observed for tibial acceleration amplitude at frequencies 12 and 23 – 26 Hz ($p < 0.05$) whereas no other frequencies resulted in a significant interaction ($p > 0.05$) (Figure 7.2C & D). Partitioning the interaction by group revealed that in the RF group, RF running resulted in significantly greater tibial acceleration amplitude for frequencies 12 and 23 Hz ($p < 0.05$, d: 0.8 – 2.5) but not 24 – 26 Hz ($p > 0.05$, d: 0.0 – 0.3) (Figure 7.2C). In the FF group, RF running resulted in significantly greater tibial acceleration amplitude for each of these frequencies ($p < 0.05$, d: 1.2 – 2.1) (Figure 7.2D). Partitioning the interaction by pattern revealed that, during RF running, the FF group had greater tibial acceleration amplitude at 12 Hz compared to the RF group ($p < 0.05$, $d = 0.8$) but the differences were not significant for 23 – 26 Hz ($p < 0.05$, d: 0.2 – 0.3). During FF running, the RF group had significantly greater tibial acceleration amplitude compared to the FF group at 23 – 26 Hz ($p < 0.05$, d: 1.1 – 1.4) but not at 12 Hz ($p > 0.05$, $d = 0.4$) (Figure 7.2C & D).

Significant group main effects were observed for the tibial acceleration amplitude for frequencies 27 – 30, 46, and 47 Hz ($p < 0.05$, d: 0.6 – 0.9) (Figure 7.2C & D). The RF group had greater tibial acceleration amplitudes for these frequencies compared to the

FF group ($p < 0.05$, $d = 0.6 – 0.9$). No significant group main effects were observed at any other frequency ($p > 0.05$). Significant pattern main effects were observed for tibial acceleration amplitude for frequencies 1 – 22, 30 – 33, and 41 – 48 Hz ($p < 0.05$). The RF pattern resulted in greater tibial acceleration amplitudes compared to the FF pattern at these frequencies. Large biological significance was observed for frequencies 2 – 8 Hz and 10 – 24 Hz (d: 0.8 – 2.3) whereas all other frequencies that showed a significant pattern main effect had moderate or low biological significance (d: 0.4 – 0.7). All other frequencies did not result in a significant pattern main effect ($p > 0.05$). Additionally, no significant interaction or pattern main effects were observed for tibial acceleration amplitude at 34 – 40 and 49 – 50 Hz ($p > 0.05$).

Head and Tibial Acceleration PSD Results

The PSD analysis of the head acceleration signal revealed a significant group by pattern interaction at 17, 30, 34 and 43 Hz ($p < 0.05$) but at no other frequency ($p > 0.05$) (Figure 7.3A & B). Partitioning the interaction by group revealed that the RF group had greater head acceleration power at 17 and 30 Hz during RF running compared to FF running ($p < 0.003$, d: 0.7 – 1.0) but no differences between patterns were observed at 34 and 43 Hz ($p > 0.05$; d: 0.1 – 0.2) (Figure 7.3A). For the FF group, the opposite was observed: no significant difference between patterns was observed at 17 and 30 Hz ($p > 0.05$, $d = 0.1 – 0.3$) but FF running resulted in greater head acceleration power at 34 and 43 Hz ($p < 0.001$, $d = 1.1 – 1.3$) (Figure 7.3B). Partitioning the interaction by pattern revealed no significant difference between groups when performing the RF pattern ($p > 0.05$, d: 0.2 – 0.6). However, when performing the FF pattern, the FF group had greater head acceleration power at 17, 34 and 43 Hz ($p < 0.035$, d: 0.5 – 07). However, no

difference was observed between groups at 30 Hz despite a large biological significance at 30 Hz ($p = 0.077$, $d = 0.9$).

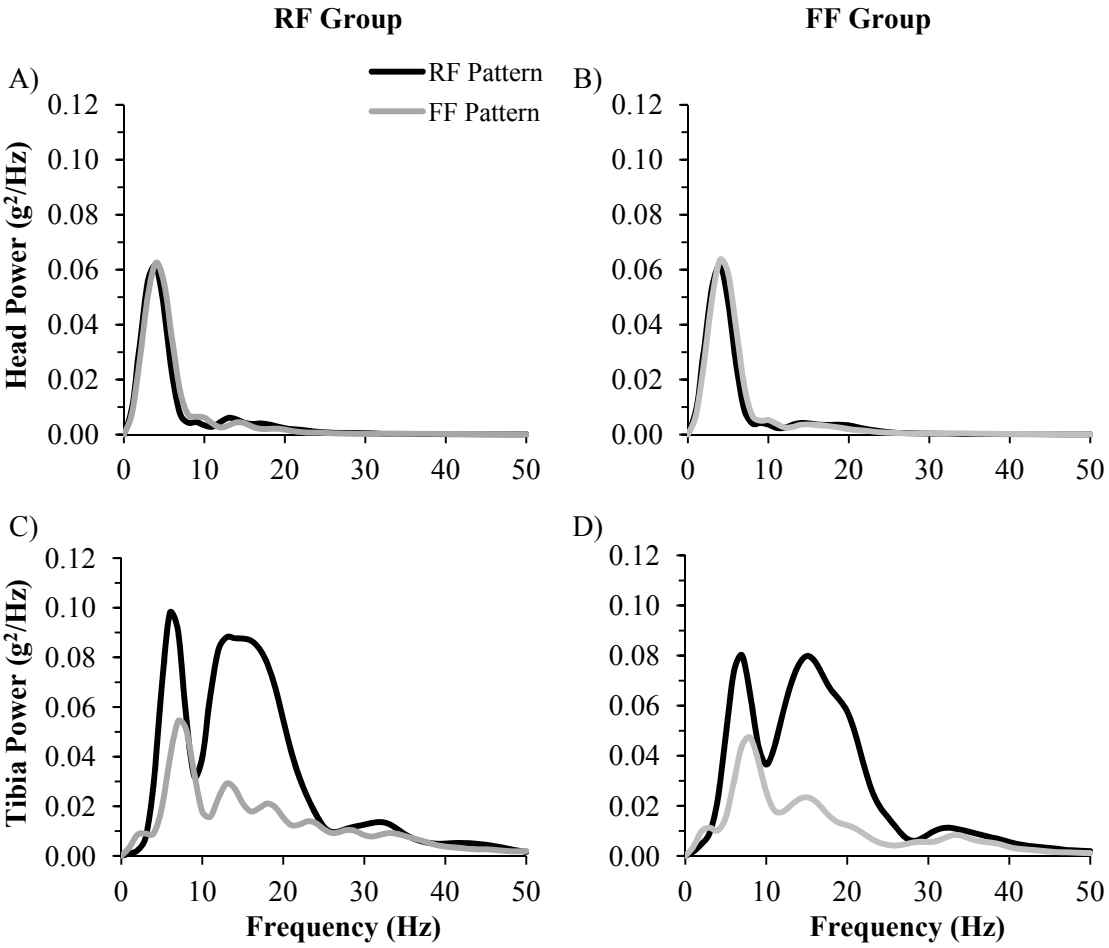

Figure 7.3: Group mean power spectra of the head and tibia acceleration signals in the frequency domain compared between the rearfoot (RF) and forefoot (FF) patterns performed by the RF and FF groups.

For frequencies at which no significant interaction was found, the PSD analysis of the head acceleration signal revealed a significant group main effect at 13 Hz ($p = 0.036$, $d = 0.5$) but at no other frequency ($p > 0.05$, $d < 0.4$) (Figure 7.3A & B). At this frequency, RF group had greater head acceleration power than the FF group. Significant pattern main effects for head acceleration power were observed for frequencies 1 – 3, 5 –

11, 13, 18, 20 – 23, 33 – 39, 42 – 44 and 46 – 48 Hz ($p < 0.013$, d: 0.2 – 1.1) but at no other frequency ($p > 0.05$). RF running resulted in greater head acceleration power at frequencies 1 – 3, 13, 18, and 20 – 23 Hz whereas FF running resulted in greater head acceleration power at frequencies 5 – 11, 33 – 39, 42 – 44 and 46 – 48 Hz. Large biological significance was observed at 6 – 8, 10, 37 and 38 Hz (d: 0.8 – 1.1).

PSD analysis of the tibia acceleration signal revealed a significant group by pattern interaction at 5, 6, 11, 12, 24 and 25 Hz ($p < 0.05$) (Figure 7.3C & D). Partitioning the interaction by group revealed that both groups had significantly greater tibial acceleration power when running with a RF pattern compared to the FF pattern for frequencies 5, 6, 11, and 12 Hz ($p < 0.001$, d: 1.2 – 2.1). However, no significant difference between patterns was observed in the RF group for frequencies 24 and 25 Hz ($p > 0.05$, d: 0.1 – 0.3) (Figure 7.3C) whereas the RF pattern resulted in greater tibial acceleration power in the FF group at these frequencies ($p = 0.001$, $d = 1.3$) (Figure 7.3D). Partitioning the interaction by pattern revealed the RF group had greater tibial acceleration power compared to the FF group for frequencies 5, 6, 11, and 12 Hz when performing the RF pattern ($p < 0.002$, d: 0.6 – 0.8) but no significant difference was observed between groups when performing the RF pattern for frequencies 24 and 25 Hz ($p > 0.05$, $d = 0.2 – 0.3$). During the FF pattern, there was no significant difference between groups in tibial acceleration power at 5, 6, 11, and 12 Hz ($p > 0.05$, $d = 0.1$- 0.4) but the RF group had significantly greater tibial acceleration power compared to the FF group at 24 and 25 Hz ($p < 0.044$, $d = 1.4$).

For frequencies at which no significant interaction was found, PSD analysis of the tibia acceleration signal revealed group main effects at 27 – 29 Hz ($p < 0.05$, d: 0.6 –

0.7). The RF group had greater tibial acceleration power at these frequencies compared to the FF group (Figure 7.3C). No significant group main effects were observed at any other frequency ($p > 0.05$). A significant pattern main effect was observed for tibial acceleration power at frequencies 1, 2, 4, 7, 8, 10, 13 – 23, 26, 30 – 32 and 41 – 48 Hz ($p < 0.033$, d: 0.4 – 2.2). Large biological significance was observed for frequencies 1, 2, 4, 7, and 13 - 23 Hz (d: 0.8 – 2.2) whereas moderate to small biological significance was observed for frequencies 8, 10, 26, 30 – 32 and 41 – 48 Hz (d: 0.4 – 0.7). The RF pattern resulted in greater tibial acceleration power for all frequencies in which a significant pattern main effect was found except 1 and 2 Hz in which the FF pattern resulted in greater tibial acceleration power.

Impact Shock Attenuation

For both running patterns, there was a gain in the head signal relative to the tibia for frequencies below approximately 6 Hz and all other frequencies showed attenuation in the head signal relative to the tibia (Figure 7.4). However, the first frequency at which attenuation in the signal was observed differed between running patterns and groups. In the RF group, attenuation began at 5 Hz during RF running but began at 6 Hz during FF running (Figure 7.4A). In the FF group, attenuation began at 6 Hz during RF running and 7 Hz during FF running (Figure 7.4B).

A significant group by pattern interaction was observed for the transfer function at frequencies 13, 23, 26, 34, 35 and 49 Hz ($p < 0.05$). Partitioning the interaction by group revealed no significant difference in shock attenuation between patterns in the RF group at these frequencies ($p > 0.05$, $d < 0.5$) (Figure 7.4A) whereas the FF group had greater shock attenuation when performing the RF pattern compared to the FF pattern ($p < 0.05$,

d: 0.7 – 1.2) (Figure 7.4B). Partitioning the interaction by pattern revealed no significant difference between groups when performing the RF pattern at frequencies at these frequencies ($p > 0.05$, *d*: 0.0 – 0.6). However, when performing the FF pattern, the RF group had greater shock attenuation then the FF group at these frequencies ($p < 0.05$, *d*: 0.5 – 1.2) except at 35 Hz in which no difference was found ($p > 0.05$, $d = 0.5$).

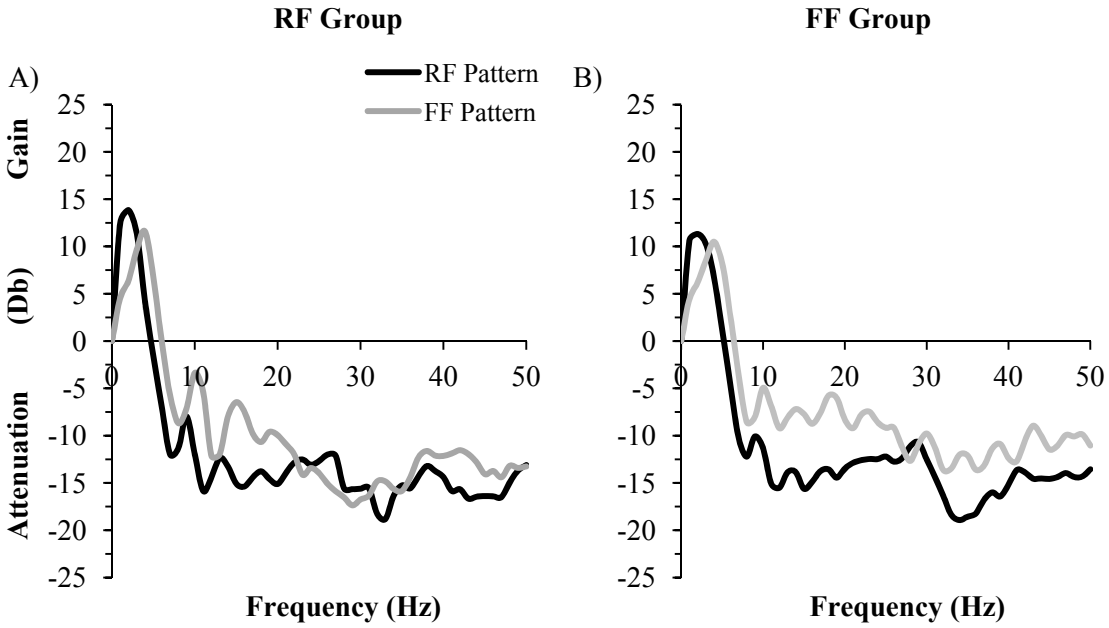

Figure 7.4: Group mean transfer function between leg and head accelerometers compared between the rearfoot (RF) and forefoot (FF) patterns performed by the RF and FF groups.

For frequencies at which no significant interaction was found, a significant group main effect was observed for the transfer function at frequencies 24, 28 – 31 and 47 Hz ($p < 0.05$, *d*: 0.4 – 0.9) but at no other frequency ($p > 0.05$, $d < 0.5$). The RF group had greater shock attenuation at these frequencies compared to the FF group (Figure 7.4A & B). A significant group main effect was not observed for the transfer function at any other frequency ($p > 0.05$). A significant pattern main effect was observed for frequencies 1, 2, 4 – 8, 10 – 12, 14 – 22, 32, 33, 36, 38 – 40, 42 – 48 Hz ($p < 0.05$, *d*: 0.4

– 1.1). RF running resulted in a greater gain in the head signal relative to the tibia for frequencies 1 and 2 Hz whereas FF running resulted in a greater gain for frequencies 4 – 6 Hz. Additionally, RF running resulted in greater attenuation in the head signal relative to the tibia for all frequencies above 6 Hz in which a significant pattern main effect was found.

Over-ground Running Conditions

Kinematics

During the over-ground running conditions, no significant group by pattern interactions or group main effects were observed for the sagittal plane ankle and knee joint angles at touchdown ($p > 0.05$, $d < 0.2$). These results indicate that both groups were able to successfully replicate the kinematics of the alternative pattern (Table 7.5). A significant pattern main effect was observed for both sagittal plane ankle ($p < 0.001$, $d = 6.1$) and knee ($p < 0.001$, $d = 0.5$) joint angles at touchdown. Characteristically, the RF pattern resulted in a dorsiflexed position at touchdown whereas the FF pattern resulted in a plantar flexed position. FF running resulted in a greater knee flexion angle at touchdown compared to RF running, but with only moderate biological significance ($d = 0.5$).

No significant group main effects or group by pattern interactions were found for contact time during the over ground conditions ($p > 0.05$, $d = 0.5$) (Table 7.5). However, a significant pattern main effect was observed with large biological significance ($p < 0.001$, $d = 0.8$). RF running resulted in a longer contact time compared to FF running.

Table 7.5: Mean ± SD for the kinematic parameters measured from the over-ground running conditions when performing the rearfoot (RF) and forefoot (FF) patterns. Parameters include the ankle angle at touchdown (Ankle), knee angle at touchdown (Knee) and contact time (CT). Listed statistics include the p-value for the group by pattern interaction (GxP) and the p-value (*d*) for the group main effect (G) and the pattern main effect (P) if the interaction was not significant.

	RF Group		FF Group		GxP	G	P
	RF	FF	RF	FF			
Ankle (deg)	15.18 ± 3.28	-12.35 ± 4.63	15.04 ± 4.61	-10.66 ± 4.98	0.210	0.422 (0.2)	<0.001 (6.1)
Knee (deg)	13.81 ± 4.61	17.28 ± 5.85	13.97 ± 3.48	15.53 ± 4.40	0.076	0.623 (0.2)	<0.001 (0.5)
CT (s)	0.24 ± 0.02	0.23 ± 0.01	0.23 ± 0.02	0.22 ± 0.02	0.545	0.111 (0.5)	<0.001 (0.8)

Vertical Ground Reaction Force Characteristics

The IMP only occurred during the RF pattern condition (Figure 7.5). No significant group by pattern interaction ($p = 0.986$) or a group main effect ($p = 0.068$, $d = 0.4$) was observed for the IMP (Table 7.6). However, a significant pattern main effect was observed reflecting that RF running resulted in a greater IMP compared to FF running ($p < 0.001$, $d = 3.1$).

Table 7.6: Mean ± SD for the vertical ground reaction force (GRF) characteristics measured from the over-ground running conditions when performing the rearfoot (RF) and forefoot (FF) patterns. Parameters include the magnitude of the impact (IMP) and active (ActP) peaks and the vertical loading rate (VLR). Listed statistics include the p-value for the group by pattern interaction (GxP) and the p-value (*d*) for the group main effect (G) and the pattern main effect (P) if the interaction was not significant.

	RF Group		FF Group		GxP	G	P
	RF	FF	RF	FF			
IMP (BW)	1.71 ± 0.29	0.95 ± 0.23	1.82 ± 0.23	1.06 ± 0.23	0.986	0.068 (0.4)	<0.001 (3.1)
ActP (BW)	2.44 ± 0.17	2.55 ± 0.20	2.52 ± 0.21	2.70 ± 0.22	0.126	0.044 (0.6)	<0.001 (0.7)
VLR (BW/s)	67.91 ± 20.21	38.11 ± 8.89	70.06 ± 15.63	41.92 ± 8.21	0.737	0.307 (0.2)	<0.001 (2.2)

No significant group by pattern interaction was observed for the ActP ($p = 0.126$). However, a significant group main effect was observed ($p = 0.044$, $d = 0.6$) (Figure 7.5) (Table 7.6). The ActP was greater in the FF group compared to the RF group. A significant pattern main effect was also observed for ActP reflecting that the ActP was greater during with the FF pattern ($p < 0.001$, $d = 0.7$).

No significant group by pattern interaction ($p = 0.737$) or a group main effect ($p = 0.307$, $d = 0.2$) were observed for VLR (Table 7.6). However, RF running resulted in a greater VLR compared to FF running as reflected by a significant pattern main effect ($p < 0.001$, $d = 2.2$).

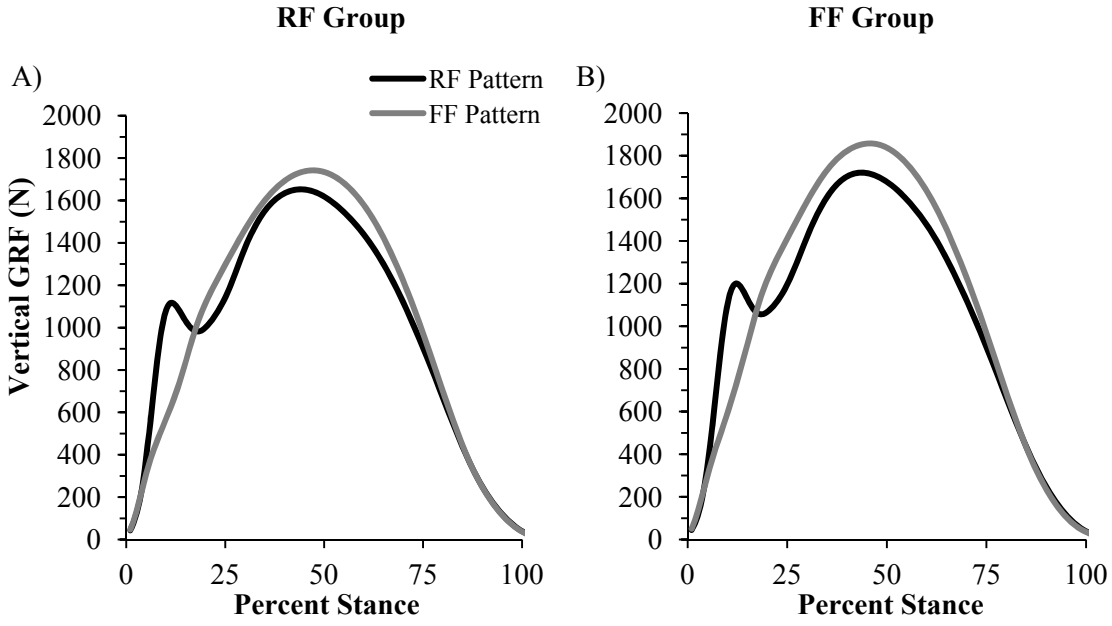

Figure 7.5: Group mean vertical ground reaction force (GRF) of the vertical ground reaction force in the time domain compared between the rearfoot (RF) and forefoot (FF) patterns performed by the RF and FF groups.

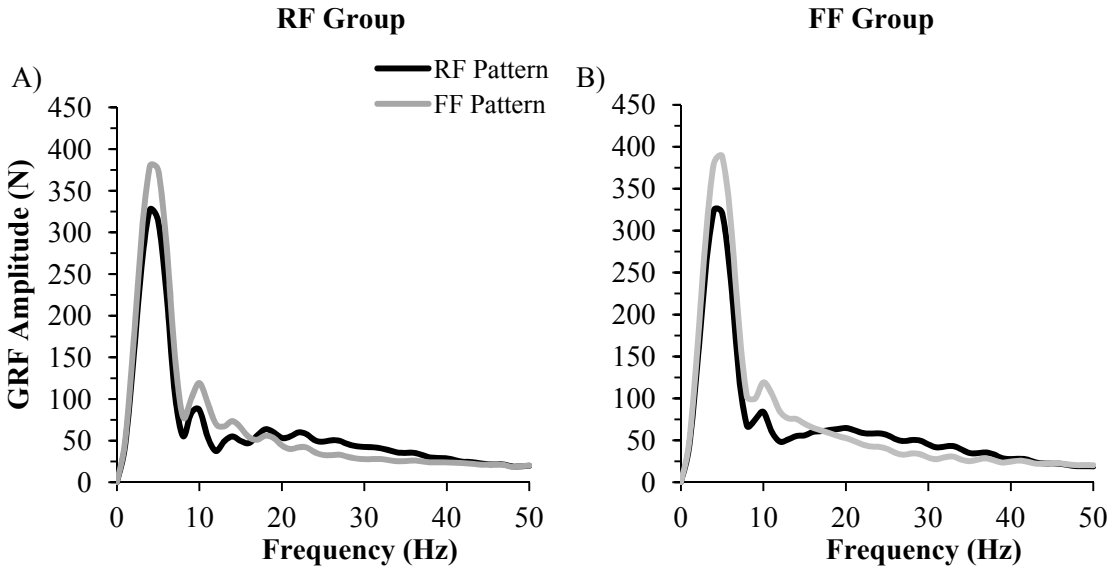

Figure 7.6: Group mean amplitude spectra of the vertical ground reaction force (GRF) in the frequency domain compared between the rearfoot (RF) and forefoot (FF) patterns performed by the RF and FF groups.

Vertical Ground Reaction Force in the Frequency Domain

A significant group by pattern interaction was only observed at the vertical GRF amplitude in the frequency domain at 8 Hz ($p = 0.034$) (Figure 7.6). No other frequencies had a significant group by pattern interaction ($p > 0.05$). Partitioning the interaction by group revealed FF running resulted in greater vertical GRF amplitude compared to RF running in both groups at this frequency ($p < 0.001$, $d > 0.8$). Partitioning the interaction by pattern revealed the FF group had greater vertical GRF amplitude at 8 Hz during both the RF pattern ($p = 0.020$, $d = 0.5$) and FF pattern compared to the RF group ($p < 0.001$, $d = 0.8$). At the frequencies in which no significant interaction was observed, a significant group main effect was observed for the vertical GRF amplitude for frequencies of 12, 16, 20 and 25 Hz ($p < 0.05$, $d = 0.7$) (Figure 7.6). At these frequencies, the FF group had greater amplitudes compared to the RF group. A significant pattern main effect was observed for frequencies 1 – 43 Hz

except for 17 Hz ($p < 0.05$, d: 0.3 – 1.9). FF running resulted in greater vertical GRF amplitudes for frequencies 1 – 16 Hz compared to RF running; however, RF running resulted in greater amplitudes for frequencies 18 – 43 Hz compared to FF running. Differences between patterns with the largest biological significance (i.e. $d > 1.0$) included 5 – 8, 10 – 14, and 22 – 36 Hz.

Discussion

The first purpose of this study was to determine the difference in impact shock attenuation between footfall patterns. The first hypothesis, that RF running would result in greater shock attenuation between the tibia and the head than FF running, was supported. RF running resulted in greater shock attenuation of most frequencies between 6 – 26 Hz and 32 – 49 Hz. A greater degree of shock attenuation during RF running may be a result of the body responding to an increased foot-ground impact (Derrick et al., 1998; Hamill et al., 1995; Shorten and Winslow, 1992). Tibial acceleration and amplitude were greater at nearly all frequencies with the RF pattern, which may reflect a greater impact load on the system with this footfall pattern. However, RF running resulted in greater PPTA of the tibia, which may only explain the increased tibia acceleration amplitude and powers at frequencies between 12 – 20 Hz (Hamill et al., 1995; Shorten and Winslow, 1992). Frequencies below 8 Hz, representing the active peak (Derrick et al., 1998; Shorten and Winslow, 1992), had greater tibial amplitude and power with the RF pattern despite the FF pattern resulting in greater ActP. Therefore, differences in leg segment motion may explain why the RF pattern had greater tibial amplitude and power at frequencies lower than 8 Hz (Clarke et al., 1985; Derrick et al.,

1998; Hamill et al., 1995; Shorten and Winslow, 1992). Interestingly, tibial acceleration amplitude and power were not different between footfall patterns for frequencies between 34 – 40 Hz yet RF running resulted in greater attenuation of the frequencies in this range. The source of tibial acceleration frequencies between 20 – 60 Hz has not been well documented thus it is unknown why these frequencies had different amplitudes and powers between footfall patterns. However, studies have shown that kinematic adjustments and muscular contractions may be responsible for attenuating these frequencies (Boyer and Nigg, 2007; Lafortune et al., 1995; Lafortune et al., 1996; Nigg et al., 1981; Voloshin et al., 1985). Therefore, the RF pattern may result in greater attenuation by these mechanisms since attenuation was greater with this pattern for frequencies 32 – 49 Hz.

The RF pattern uses the heel of the shoe and the shoe fat pad for attenuating some impact shock. Therefore, the second purpose of this study was to determine impact shock attenuation was improved if natural FF runners performed the RF pattern. It was hypothesized that natural FF runners would increase the amount of impact shock attenuation when switching to a RF pattern and natural RF runners would not increase the amount of impact shock attenuation when switching to a FF pattern. In both groups, RF running resulted in greater shock attenuation of frequencies 6 – 26 Hz and 32–49 Hz, which supports this hypothesis. However, the natural RF and FF groups did not have a consistent response in shock attenuation between patterns for the frequencies of 13, 23, 26, 34, 35 and 49 Hz. At these frequencies, the FF group had greater shock attenuation with large a large effect size, and thus a large biological relevance, when performing the RF pattern compared to the FF pattern. However, the RF group did not have a significant

difference in shock attenuation between patterns at these frequencies but moderate effect size was observed, suggesting the differences may have some biological relevance. Additionally, significant differences between groups within a single footfall pattern occurred with six or less individual head or tibial frequencies between 1–50 Hz. However, both groups were able to successfully replicate the alternate footfall pattern as indicated from the ankle joint angle. The kinematic similarities suggest that these differences may be a result of normal variation between participants and groups. Identifying differences in frequency ranges may be more meaningful than examining individual frequencies.

Previous investigations have shown that shock attenuation increases with greater impact magnitudes in order to maintain head stabilization (Derrick et al., 1998; Hamill et al., 1995; Shorten and Winslow, 1992). In the present study, the RF pattern resulted in greater head acceleration power and amplitude at frequencies of 13 – 24 Hz frequencies, which represent the impact peak (Derrick et al., 1998; Hamill et al., 1995; Nigg et al., 1981; Nigg and Wakeling, 2001; Shorten and Winslow, 1992). Increased amplitude and power at these frequencies may be a result of greater PPTA with the RF pattern. However, the difference in head acceleration in the frequency domain between patterns had a small to moderate effect size in this frequency range. A low effect size suggests that the statistical differences observed in head acceleration in the time and frequency domains may not be biologically meaningful. Additionally, HP1, which occurred with a similar time course as the PPTA, was not different between footfall patterns. This finding suggests that the differences between footfall patterns in head acceleration for frequencies representing the impact peak may not be biologically meaningful. Therefore,

the increased amount of attenuation occurring with the RF pattern may be sufficient to compensate for greater loading of the tibia and maintain adequate head acceleration as a result of the impact phase.

HP2 was also not different between footfall patterns although FF running resulted in greater head acceleration powers in the 5 – 11 Hz range, most with a large effect size. This frequency range spans those that represent the active peak and active movement of the leg during stance (Bobbert et al., 1991; Hamill et al., 1995; Shorten and Winslow, 1992). Greater head acceleration powers in this range may be a result of greater vertical GRF active peak generated with FF running (Laughton et al., 2003; Oakley and Pratt, 1988). Although head acceleration power was greater with the FF pattern between 5 – 11 Hz, the degree of shock attenuation was greater with the RF pattern in this range because of the relative difference in tibia and head acceleration signal power. Therefore, RF running resulted in greater shock attenuation because tibial acceleration power was also greater with this pattern. Findings from previous studies have suggested the body may have a reduced capacity for attenuating frequencies between 3 – 8 Hz (Derrick et al., 1998; Lafortune et al., 1996). Despite RF running resulting in greater tibial acceleration power of frequencies in this range, head acceleration power in this range was decreased compared to the FF pattern. These findings may suggest that FF running may not be as effective at attenuating these low frequency components and reducing head acceleration as a result of greater active GRFs. Alternatively, attenuation of frequencies between 3 – 8 Hz may have been lower with the FF pattern because the tibial acceleration power in this range was also lower.

The tibial acceleration results support previous findings that the RF pattern results in increased tibial acceleration in the time domain (Laughton et al., 2003; Oakley and Pratt, 1988). The present study demonstrated that there is an increase in shock attenuation with the RF pattern in order to compensate for the increased tibial load to prevent excessive head acceleration. However, the mechanisms used to attenuate the impact shock may be different between footfall patterns. Therefore, the third purpose of this study was to determine if there was a difference in impact shock attenuation mechanisms between footfall patterns. The present study examined the frequency content of the vertical GRF for this purpose because the impact shock wave, and thus the frequencies that must be attenuated, depends on the magnitude and timing of the GRF (Lafortune et al., 1995). It was hypothesized that the RF pattern would have a greater reliance on passive shock attenuation mechanisms whereas the FF pattern would have a greater reliance on active shock attenuation mechanisms. RF running resulted in greater vertical GRF amplitudes at frequencies 18 – 43 Hz. These higher frequency components are believed to be attenuated by passive mechanisms such as deformation of the shoe and body tissues such as the heel fat pad, ligaments, bone and articular cartilage (Chu et al., 1986; Paul et al., 1978). Therefore, RF running may have an increased reliance on these passive mechanisms to attenuate vertical GRFs and impact shock. Conversely, FF pattern resulted in greater vertical GRF amplitudes at frequencies between 1 – 16 Hz. Active mechanisms, such as muscle activity and joint position, may be responsible for attenuating low frequency components (Paul et al., 1978). Therefore, FF running may have an increased reliance on muscle actions to attenuate vertical GRF frequencies,

especially those in the 4 – 8 Hz range, which are generated by active forces (Nigg et al., 1981; Potthast et al., 2010; Shorten and Mientjes, 2003).

Both footfall patterns resulted in high amplitudes above 10 Hz, which was used to discriminate between shock attenuation mechanisms. A combination of active and passive mechanisms will be used for shock attenuation with both footfall patterns. However, the RF pattern may result in a greater reliance on passive mechanisms because it resulted in greater amplitudes of frequencies above 18 Hz. Conversely, the FF pattern may have an increased reliance on active mechanisms because it resulted in greater GRF amplitudes of frequencies below 10 Hz, despite it also resulting in greater amplitudes for frequencies between 10 – 16 Hz. These differences in frequency amplitude between footfall patterns may affect how specific tissues adapt or are injured with each footfall pattern.

Previous studies have indicated that bone is responsible for absorbing frequencies above 18 Hz (Paul et al., 1978). Bone may be more susceptible to higher frequency accelerations because movement of rigid structures occurs over a shorter time interval then other tissues such as muscle. Bone is subjected to high accelerations at impact while absorption of lower frequencies through movement of soft tissue is delayed (Nigg, 2011). The forces generated from running impact loads result in increased bone mass (Carter et al., 1981; Frost, 1986; Martin and Burr, 1989; Nigg, 2011). However, strain rate and signal frequency may be a stronger predictor of bone mass than impact magnitude (Nigg, 2011; O'Connor et al., 1982; Qin et al., 1998; Rubin et al., 2001). In particular, loading from frequencies greater than 15 Hz may be required to maintain adequate bone density (McLeod and Rubin, 1990). Therefore, RF running may be superior for bone health

because impact magnitude, vertical loading rate, and the amplitude of vertical GRF frequencies above 18 Hz were found to be greater with RF running whereas FF running resulted in greater amplitudes for frequencies below 16 Hz.

Despite the beneficial adaptations of loading, increased attenuation will result in injury if a tissue is overloaded (Voloshin and Wosk, 1982; Voloshin et al., 1981). Although bone strain due to impact forces generated with RF running is typically below cortical bone failure limits (Burr et al., 1996; Milgrom et al., 2000; Milgrom et al., 2002; Nigg, 2011), some studies have found that greater loading may be related to tibial stress fracture (Edwards et al., 2008; Grimston et al., 1991; Milner et al., 2006). However, loading has not been related to tibial stress fracture in all studies (Bennell et al., 2004; Crossley et al., 1999). Both RF and FF patterns generate frequencies that will cause the micro-damage required for increasing bone density. However, neither footfall pattern will prevent bone injury if sufficient time for remodeling between bouts is not given.

The bones at which the impact shock is initially applied may also affect injury mechanisms and shock wave transmission because of bone size, density, and elastic properties (Kinsler and Frey, 1950; Radin and Paul, 1970). In RF running, plantar pressure is applied to the heel fat pad and calcaneus at initial ground contact and shifts to under the metatarsal heads during push-off. Metatarsal stress fractures from running are more common than calcaneus stress fractures (Fourchet et al., 2011; Fredericson et al., 2006), likely as a result of the metatarsal heads experience greater plantar pressures during the push-off phase of RF running compared to the pressures applied to the calcaneus at impact (Maiwald et al., 2008). Conversely, in FF running, high plantar pressure is applied to the metatarsal pad and metatarsal heads throughout the stance

phase. Although metatarsal plantar pressure at impact has yet to be investigated in FF running, the amount of time at which force is applied to the metatarsals during the stance phase is much longer than with RF running. Therefore, the small bones of the metatarsals may not be able to withstand the strain caused by both impact and push-off which may lead to an increase in metatarsal injury rates with FF running.

Other passive mechanisms that attenuate impact shock include deformation of the shoe, heel fat pad, ligaments, synovial fluid and articular cartilage (Chu et al., 1986; Paul et al., 1978; Radin and Paul, 1970). The heel is a significant contributor to shock attenuation in RF running because it absorbs approximately 85% of the energy resulting from impact and may attenuate all frequencies (Cavanagh et al., 1984; Paul et al., 1978). The material properties of shoe cushioning in the heel are also able to reduce impact acceleration by up to 38% and substantially reduces loading compared to RF running when barefoot running (De Wit et al., 2000; Frederick et al., 1984; Light et al., 1980; MacLellan and Vyvyan, 1981; Oakley and Pratt, 1988). The FF pattern cannot take advantage of the heel fat pad or shoe cushioning in the heel to reduce impact shock which will result in increased attenuation by other tissues. Preventing heel contact may be a contributing factor to the reduced shock attenuation occurring with FF running compared to RF running in the present study. Therefore, reduced loading with the FF pattern may not necessarily result in injury prevention compared to RF running.

In addition to passive mechanisms, active shock attenuation mechanisms such as muscle contractions may also responsible for attenuating large amounts of impact shock (Radin and Paul, 1970). Muscle contractions that specifically responded to an impact stimulus may only be effective at attenuating frequencies below 10 Hz (Paul et al., 1978)

and thus may have a greater role in attenuating shock in FF running. However, the intensity, timing and frequency of muscle activation will vary before and after impact to change the material properties and increase damping of impact shock wave frequencies greater than 40 or 50 Hz (Boyer and Nigg, 2007). These variations in muscle activation will affect the stiffness amount of joint stiffness during running and the capacity to perform negative work and attenuate impact shock (Hamill et al., 2000). Reduced leg or joint stiffness results in an increase in shock attenuation (McMahon et al., 1987). Results from previous studies on leg and joint stiffness in RF and FF running suggest that a compliant ankle is responsible for active shock attenuation during FF running and a compliant knee is responsible for active shock attenuation during RF running (Hamill et al., 2000; Laughton et al., 2003). The knee has a greater capacity for shock absorption because of its wide range of possible joint positions as well as having more shock absorbing structural components compared to the ankle (Christiansen et al., 2008; Radin and Paul, 1970). These observations from previous studies may explain the greater shock attenuation occurring with the RF pattern in the present study. Previous studies have also found that increased stiffness may result in bony injuries whereas increased compliance may result in soft tissue injuries (Butler et al., 2003; Milner et al., 2006; Milner et al., 2007). Together with the present study, these findings suggest that the FF pattern may not reduce the risk of developing injuries more so than the RF pattern. However, prospective studies relating joint stiffness and injury have yet to be performed.

Kinematic adjustments are an additional active shock attenuation mechanism, particularly for frequencies above 5 Hz (Clarke et al., 1984; Derrick et al., 1998; Lafortune et al., 1996a; Lafortune et al., 1996; Winter, 1983). Different segment and

joint positions can also affect the transmissibility of the impact shock (Griffin, 1990; Lafortune et al., 1996). Greater dorsiflexion and knee flexion angles at initial contact in RF running have been shown to decrease the magnitude of the impact peak and increase shock absorption by increasing eccentric activity of the tibialis anterior and quadriceps, respectively (Derrick et al., 1998; Gerritsen et al., 1995; Lafortune et al., 1996a; Lafortune et al., 1996). Although shock attenuation was not measured during the over-ground conditions in the present study, FF running resulted in a greater knee flexion angle at touchdown. If the knee is too extended, the knee extensor muscles cannot contribute to shock attenuation which may result in a greater reliance or overload of passive mechanisms, especially in the hip or back (Derrick et al., 1998; Voloshin and Wosk, 1982). It has been suggested that increasing knee flexion may shift the amount of shock attenuation from passive tissue to muscular contractions (Edwards et al., In Press). Therefore, the FF pattern may utilize knee flexion angles at impact to attenuate impact shock, but decreased knee stiffness resulting from the knee range of motion and joint moments may result in the RF pattern having a greater capacity for shock attenuation.

Previous studies have shown that increased stride length results in greater knee flexion angles and greater shock attenuation (Bobbert et al., 1991; Bobbert et al., 1992; Clarke et al., 1985; Derrick et al., 1998; Hamill et al., 1995; Mercer et al., 2003). In the present study, stride length and stride frequency measured during the treadmill conditions were not statistically different between footfall patterns, which is consistent with previous studies (Ardigo et al., 1995). Similar stride parameters between footfall patterns suggests that the differences in frequency components of the vertical GRF and acceleration measures were a result of the footfall pattern specifically rather than a consequential

change in stride length or stride frequency. It may also be unlikely that the differences in shock attenuation between footfall patterns can be attributed to the small and non-significant differences in stride parameters.

Regardless of the mechanism, an over-reliance on one mechanism or tissue for attenuation may lead to inadequate shock absorption and tissue damage (Derrick et al., 1998; Voloshin and Wosk, 1982; Wosk and Voloshin, 1981). Varying amounts of shock attenuation between footfall patterns suggests that the body has the capacity to manage a range of impulsive loads in order to protect the head from excessive acceleration. It is possible that the increased requirement of the body tissues to attenuate greater impulsive loads may be detrimental. It is also possible that the tissues adapt to greater impulsive loads in a beneficial manner; similar to skeletal muscle adaptation to high intensity resistance training. In addition to increased bone density, other tissues, such as muscle and tendon, have also been shown to adapt beneficially to loading from running (Rosager et al., 2002; Stone et al., 1996). However, the threshold between injury and adaptation is currently unknown.

Previous literature has focused on impact related variables as a major contributor to running injuries. The absence of the vertical IMP with FF running is the basis for the argument promoting that this pattern is beneficial for injury prevention (Cavanagh and Lafortune, 1980; Davis et al., 2010; Laughton et al., 2003; Lieberman et al., 2010; Oakley and Pratt, 1988; Pratt, 1989; Williams et al., 2000). However, results from the present study showed that the frequencies representative of the IMP were present in both footfall patterns. This result suggests that the FF pattern contains an IMP that is not visible in the time domain. Therefore, claims that suggest FF running may prevent

injuries due to the absence of the impact peak may be unjustified. It is more likely that the difference in time domain impact variables between patterns do not result in one pattern being more injurious than another, but that the injuries each pattern may be susceptible to may be different.

Frequencies representing the impact peak span 10 – 20 Hz because the magnitude and timing of the impact peak can change with running speed, stride frequency and joint position (Bobbert et al., 1992; Cavanagh and Lafortune, 1980; Clarke et al., 1985; Gerritsen et al., 1995; Hamill et al., 1983). Greater amplitudes at the low end of the 10 – 20 Hz range in FF running may suggest that the time course and magnitude of the impact peak may be reduced compared to the RF pattern. Greater amplitudes at the high end of this range in RF may be due to greater IMP and VLR observed with RF running in the present study. These results must be interpreted cautiously because the timing of the IMP during FF running was estimated to occur at approximately 25 ms (Bobbert et al., 1992; Cavanagh and Lafortune, 1980; Munro et al., 1987). Although this estimation was similar to the time-to-peak IMP observed during RF running, the GRF frequency data from the present study suggest that the timing and amplitude of the IMP was different between footfall patterns. A previous study calculated IMP and VLR from a small shift in the IMP observed in FF running and found no significant differences compared to the RF pattern (Laughton et al., 2003). This shift in the impact peak is further evidence that the IMP is present in FF running but observing this shift may not be possible with every trial. Therefore, calculating VLR from the summated vertical GRF profile may not be accurate or meaningful. Decomposing the vertical GRF profile into its separate

waveform components may be necessary to accurately identify the true timing and magnitude of the IMP in FF running.

It may be argued that FF running remains a preventative technique for running injuries because it resulted in reduced IMP and VLR compared to RF running. Although several human studies have suggested tibial shock and impact peak magnitude or loading rate are related to developing running injuries (Davis et al., 2010; Hreljac et al., 2000; Milner et al., 2006; Voloshin and Wosk, 1982; Zifchock et al., 2006), several other studies have not identified this relationship (Azevedo et al., 2009; Bredeweg, 2011; McCrory et al., 1999; Nigg, 1997; Pohl et al., 2008; Scott and Winter, 1990). Additionally, in some studies reporting a relationship between IMP or VLR and injury reported differences in IMP of less than 0.5 body-weights (Davis et al., 2010; Hreljac et al., 2000; Milner et al., 2006). In other words, a non-injured individual may have the same impact related characteristics as an injured individual. It is likely that running injuries are a result of many interrelated variables such as loading magnitude, loading rate, and the total dose (Edwards et al., 2008; Milner et al., 2006). Although impact forces are claimed to be the main contributor to running injuries, injuries are more likely due to a combination of anatomical and biomechanical abnormalities (Hreljac, 2004). Impact forces may only result in injury when combined with abnormal anatomy, kinematics and training errors such as excessive duration or inadequate rest (Derrick, 2004).

Other loading parameters seem to be ignored in the running injury literature. Joint loading resulting from the active peak can be 3 – 5 times greater than the loads resulting from the impact peak (Burdett, 1982; Harrison et al., 1986; Scott and Winter,

1990). Additionally, nearly 75% of running injuries, including shin splints, stress fractures, plantar fasciitis and chondromalacia, may occur because of the large forces generated during propulsion when the joint forces across the knee and ankle are greatest (Dickinson et al., 1985; Winter, 1983). These findings suggest the active vertical GRF may also be a significant contributor to running injury mechanisms (Dickinson et al., 1985; Messier et al., 1991; Nigg, 2011; Radin, 1972; Winter, 1983) which may have greater implications with FF running compared to RF running. Therefore, the FF pattern may not be as beneficial for preventing running injuries as previously suggested. It is likely that injury from repetitive loading is a function of the method or effectiveness of shock absorption rather than the magnitude or rate of the load itself. Despite the mechanical or anatomical parameter investigated, there is currently no consensus as to what will prevent or cause a running injury (Hreljac, 2004).

Conclusion

Although greater impact force characteristics and tibial shock were found with the RF pattern in the present study, greater amplitudes of low frequency components with the FF pattern suggest that it may result in a greater reliance of active shock attenuation mechanisms. Conversely, greater amplitudes of high frequency components with the RF pattern suggest that it may result in a greater reliance of passive shock attenuation mechanisms. Therefore, it is possible that injury from repetitive impact loading is a function of the method or effectiveness of shock absorption rather than the magnitude or rate of the load itself.

References

1. Ardigo LP, Lafortuna C, Minetti AE, Mognoni P, Saibene F. Metabolic and Mechanical Aspects of Foot Landing Type, Forefoot and Rearfoot Strike, in Human Running. *Acta Physiol Scand*. 1995; 155(1):17-22.

2. Azevedo LB, Lambert MI, Vaughan CL, O'Connor CM, Schwellnus MP. Biomechanical Variables Associated with Achilles Tendinopathy in Runners. *Br J Sports Med*. 2009; 43(4):288-292.

3. Bennell K, Crossley K, Jayarajan J, Walton E, Warden S, Kiss ZS, Wrigley T. Ground Reaction Forces and Bone Parameters in Females with Tibial Stress Fracture. *Med Sci Sports Exerc*. 2004; 36(3):397-404.

4. Bobbert MF, Schamhardt HC, Nigg BM. Calculation of Vertical Ground Reaction Force Estimates During Running from Positional Data. *J Biomech*. 1991; 24(12):1095-1105.

5. Bobbert MF, Yeadon MR, Nigg BM. Mechanical Analysis of the Landing Phase in Heel-Toe Running. *J Biomech*. 1992; 25(3):223-234.

6. Boyer KA and Nigg BM. Changes in Muscle Activity in Response to Different Impact Forces Affect Soft Tissue Compartment Mechanical Properties. *J Biomech Eng*. 2007; 129(4):594-602.

7. Bredeweg S. No Relationship between Running Related Injuries and Kinetic Variables. *Br J Sports Med*. 2011; 45(4):328.

8. Burdett RG. Forces Predicted at the Ankle During Running. *Med Sci Sports Exerc*. 1982; 14(4):308-316.

9. Burr DB, Milgrom C, Fyhrie D, Forwood M, Nyska M, Finestone A, Hoshaw S, Saiag E, Simkin A. In Vivo Measurement of Human Tibial Strains During Vigorous Activity. *Bone*. 1996; 18(5):405-410.

10. Butler RJ, Crowell HP, 3rd, Davis IM. Lower Extremity Stiffness: Implications for Performance and Injury. *Clin Biomech (Bristol, Avon)*. 2003; 18(6):511-517.

11. Carter DR, Caler WE, Spengler DM, Frankel VH. Fatigue Behavior of Adult Cortical Bone: The Influence of Mean Strain and Strain Range. *Acta Orthop Scand*. 1981; 52(5):481-490.

12. Cavanagh PR and Lafortune MA. Ground Reaction Forces in Distance Running. *J Biomech*. 1980; 13(5):397-406.

13. Cavanagh PR, Valiant GA, Miserich KW. Biological Aspects of Modelling Shoe/Foot Interactions During Running. In: *Sports Shoes and Playing Surfaces*. Frederick EC (Ed.). Human Kinetics, Champaign, Illinois, 1984. 24-46.

14. Christiansen BA, Bayly PV, Silva MJ. Constrained Tibial Vibration in Mice: A Method for Studying the Effects of Vibrational Loading of Bone. *J Biomech Eng*. 2008; 130(4):044502.

15. Chu ML, Yazdani-Ardakani S, Gradisar IA, Askew MJ. An in Vitro Simulation Study of Impulsive Force Transmission Along the Lower Skeletal Extremity. *J Biomech*. 1986; 19(12):979-987.

16. Clarke TE, Cooper LB, Hamill CL, Clark DE. The Effect of Varied Stride Rate Upon Shank Deceleration in Running. *J Sports Sci*. 1985; 3(1):41-49.

17. Clarke TE, Frederick EC, Hamill CL. The Study of Rearfoot Movement in Running. In: *Sports Shoes and Playing Surfaces*. Frederick EC (Ed.). Human Kinetics, Champaign, IL, 1984. 166-189.

18. Cohen J. A Power Primer. *Psychol Bull*. 1992; 112(1):155-159.

19. Cole GK, Nigg BM, Ronsky JL, Yeadon MR. Application of the Joint Coordinate System to Three-Dimensional Joint Attitude and Movement Representation: A Standardization Proposal. *J Biomech Eng*. 1993; 115(4A):344-349.

20. Cole GK, Nigg BM, van Den Bogert AJ, Gerritsen KG. The Clinical Biomechanics Award Paper 1995 Lower Extremity Joint Loading During Impact in Running. *Clin Biomech (Bristol, Avon)*. 1996a; 11(4):181-193.

21. Crossley K, Bennell KL, Wrigley T, Oakes BW. Ground Reaction Forces, Bone Characteristics, and Tibial Stress Fracture in Male Runners. *Med Sci Sports Exerc*. 1999; 31(8):1088-1093.

22. Davis IS, Bowser B, Mullineaux DR. Do Impacts Cause Running Injuries? A Prospective Investigation. Proceedings of the Annual Meeting of the American Society of Biomechanics. 2010.

23. De Wit B, De Clercq D, Aerts P. Biomechanical Analysis of the Stance Phase During Barefoot and Shod Running. *J Biomech*. 2000; 33(3):269-278.

24. Denoth J. Load on the Locomotor System and Modelling. In: *Biomechanics of Running Shoes*. Nigg BM (Ed.). Human Kinetics, Champaign, Illinois, 1986. 63-116.

25. Derrick TR. The Effects of Knee Contact Angle on Impact Forces and Accelerations. *Med Sci Sports Exerc*. 2004; 36(5):832-837.

26. Derrick TR, Hamill J, Caldwell GE. Energy Absorption of Impacts During Running at Various Stride Lengths. *Med Sci Sports Exerc*. 1998; 30(1):128-135.

27. Dickinson JA, Cook SD, Leinhardt TM. The Measurement of Shock Waves Following Heel Strike While Running. *J Biomech*. 1985; 18(6):415-422.

28. Edwards WB, Derrick TR, Hamill J. Musculoskeletal Attenuation of Impact Shock in Response to Knee Angle Manipultion. *J App Biomech*. In Press.

29. Edwards WB, Gillette JC, Thomas JM, Derrick TR. Internal Femoral Forces and Moments During Running: Implications for Stress Fracture Development. *Clin Biomech (Bristol, Avon)*. 2008; 23(10):1269-1278.

30. Fourchet F, Kelly L, Horobeanu C, Loepelt H, Taiar R, Millet GP. Comparison of Plantar Pressure Distribution in Adolescent Runners at Low Vs. High Running Velocity. *Gait Posture*. 2011.

31. Frederick EC, Clarke TE, Hamill CL. The Effect of Running Shoe Design on Shock Attenuation. In: *Sports Shoes and Playing Surfaces*. Frederick EC (Ed.). Human Kinetics, Champaign, IL, 1984. 190-198.

32. Fredericson M, Jennings F, Beaulieu C, Matheson GO. Stress Fractures in Athletes. *Top Magn Reson Imaging*. 2006; 17(5):309-325.

33. Frost HM. Intermediary Organization of the Skeleton. CRC Press, Boca Raton, FL, 1986.

34. Gerritsen KG, van den Bogert AJ, Nigg BM. Direct Dynamics Simulation of the Impact Phase in Heel-Toe Running. *J Biomech*. 1995; 28(6):661-668.

35. Griffin MJ. Handbook of Human Vibration. Academic Press, New York, NY, 1990.

36. Grimston SK, Engsberg JR, Kloiber R, Hanley DA. Bone Mass, External Loads, and Stress Fracture in Female Runners. *International Journal of Sport Biomechanics*. 1991; 7(3):293-302.

37. Hamill J, Bates BT, Knutzen KM, Sawhill JA. Variations in Ground Reaction Force Parameters at Different Running Speeds. *Human Movement Science*. 1983; 2(1-2):47-56.

38. Hamill J, Derrick TR, Holt KG. Shock Attenuation and Stride Frequency During Running. *Human Movement Science*. 1995; 14:45-60.

39. Hamill J, Derrick TR, McClay I. Joint Stiffness During Running with Different Footfall Patterns. XIth Congress of the Canadian Society of Biomechanics. 2000.

40. Harrison RN, Lees A, McCullagh PJ, Rowe WB. A Bioengineering Analysis of Human Muscle and Joint Forces in the Lower Limbs During Running. *J Sports Sci*. 1986; 4(3):201-218.

41. Hennig EM and Lafortune MA. Relationships between Ground Reaction Force and Tibial Bone Acceleration Parameters. *Int J Sports Biomech*. 1991; 7:303-309.

42. Hreljac A. Impact and Overuse Injuries in Runners. *Med Sci Sports Exerc*. 2004; 36(5):845-849.

43. Hreljac A, Marshall RN, Hume PA. Evaluation of Lower Extremity Overuse Injury Potential in Runners. *Med Sci Sports Exerc*. 2000; 32(9):1635-1641.

44. James SL, Bates BT, Osternig LR. Injuries to Runners. *Am J Sports Med*. 1978; 6(2):40-50.

45. Kinsler LE and Frey AR. In: *Fundamentals of Acoustics*. John Wiley & Sons, Inc., New York, NY, 1950. Chapters 1-3.

46. Lafortune MA. Three-Dimensional Acceleration of the Tibia During Walking and Running. *J Biomech*. 1991; 24(10):877-886.

47. Lafortune MA, Hennig EM, Lake MJ. Dominant Role of Interface over Knee Angle for Cushioning Impact Loading and Regulating Initial Leg Stiffness. *J Biomech*. 1996a; 29(12):1523-1529.

48. Lafortune MA, Lake MJ, Hennig E. Transfer Function between Tibial Acceleration and Ground Reaction Force. *J Biomech*. 1995; 28(1):113-117.

49. Lafortune MA, Lake MJ, Hennig EM. Differential Shock Transmission Response of the Human Body to Impact Severity and Lower Limb Posture. *J Biomech*. 1996; 29(12):1531-1537.

50. Laughton CA, Davis IS, Hamill J. Effect of Strike Pattern and Orthotic Intervention on Tibial Shock During Running. *J App Biomech*. 2003; 19:153-168.

51. Lieberman DE, Venkadesan M, Werbel WA, Daoud AI, D'Andrea S, Davis IS, Mang'eni RO, Pitsiladis Y. Foot Strike Patterns and Collision Forces in Habitually Barefoot Versus Shod Runners. *Nature*. 2010; 463(7280):531-535.

52. Light LH, McLellan GE, Klenerman L. Skeletal Transients on Heel Strike in Normal Walking with Different Footwear. *J Biomech*. 1980; 13(6):477-480.

53. MacLellan GE and Vyvyan B. Management of Pain beneath the Heel and Achilles Tendonitis with Visco-Elastic Heel Inserts. *Br J Sports Med*. 1981; 15(2):117-121.

54. Maiwald C, Grau S, Krauss I, Mauch M, Axmann D, Horstmann T. Reproducibility of Plantar Pressure Distribution Data in Barefoot Running. *J Appl Biomech*. 2008; 24(1):14-23.

55. Martin RB and Burr DB. Structure, Function and Adaptation of Compact Bone. Raven Press, New York, NY, 1989.

56. McClay I and Manal K. Lower Extremity Kinetic Comparisons between Forefoot and Rearfoot Strikers. 19th Annual Meeting of the American Society of Biomechanics. 1995b. 213-214.

57. McCrory JL, Martin DF, Lowery RB, Cannon DW, Curl WW, Read HM, Jr., Hunter DM, Craven T, Messier SP. Etiologic Factors Associated with Achilles Tendinitis in Runners. *Med Sci Sports Exerc*. 1999; 31(10):1374-1381.

58. McLeod KJ and Rubin CT. Frequency Specific Modulation of Bone Adaptation by Induced Electric Fields. *J Theor Biol*. 1990; 145(3):385-396.

59. McMahon TA, Valiant G, Frederick EC. Groucho Running. *J Appl Physiol*. 1987; 62(6):2326-2337.

60. Mercer JA, Devita P, Derrick TR, Bates BT. Individual Effects of Stride Length and Frequency on Shock Attenuation During Running. *Med Sci Sports Exerc*. 2003; 35(2):307-313.

61. Mercer JA, Vance J, Hreljac A, Hamill J. Relationship between Shock Attenuation and Stride Length During Running at Different Velocities. *Eur J Appl Physiol*. 2002; 87(4-5):403-408.

62. Messier SP, Davis SE, Curl WW, Lowery RB, Pack RJ. Etiologic Factors Associated with Patellofemoral Pain in Runners. *Med Sci Sports Exerc*. 1991; 23(9):1008-1015.

63. Milgrom C, Finestone A, Levi Y, Simkin A, Ekenman I, Mendelson S, Millgram M, Nyska M, Benjuya N, Burr D. Do High Impact Exercises Produce Higher Tibial Strains Than Running? *Br J Sports Med*. 2000; 34(3):195-199.

64. Milgrom C, Finestone A, Sharkey N, Hamel A, Mandes V, Burr D, Arndt A, Ekenman I. Metatarsal Strains Are Sufficient to Cause Fatigue Fracture During Cyclic Overloading. *Foot Ankle Int*. 2002; 23(3):230-235.

65. Milner CE, Ferber R, Pollard CD, Hamill J, Davis IS. Biomechanical Factors Associated with Tibial Stress Fracture in Female Runners. *Med Sci Sports Exerc*. 2006; 38(2):323-328.

66. Milner CE, Hamill J, Davis I. Are Knee Mechanics During Early Stance Related to Tibial Stress Fracture in Runners? *Clin Biomech (Bristol, Avon)*. 2007; 22(6):697-703.

67. Munro CF, Miller DI, Fuglevand AJ. Ground Reaction Forces in Running: A Reexamination. *J Biomech*. 1987; 20(2):147-155.

68. Nigg BM. Biomechanical Aspects of Running. In: *Biomechanics of Running Shoes*. Nigg BM (Ed.). Human Kinetics, Champaign, IL, 1986. 15-19.

69. Nigg BM. Impact Forces in Running. *Current Opinion in Orthopedics*. 1997; 8(6):43-47.

70. Nigg BM. Impact Forces. In: *Biomechanics of Sport Shoes*. Nigg BM (Ed.). Univeristy of Calgary Press, Calgary, 2011. 1-35.

71. Nigg BM, Denoth J, Neukomm PA. Quantifying the Load on the Human Body: Problems and Some Possible Solutions. In: *Biomechanics Vii*. Morecki A et al. (Eds.). University Park Press, Baltimore, MD, 1981. 88-89.

72. Nigg BM and Wakeling JM. Impact Forces and Muscle Tuning: A New Paradigm. *Exerc Sport Sci Rev*. 2001; 29(1):37-41.

73. O'Connor JA, Lanyon LE, MacFie H. The Influence of Strain Rate on Adaptive Bone Remodelling. *J Biomech*. 1982; 15(10):767-781.

74. Oakley T and Pratt DJ. Skeletal Transients During Heel and Toe Strike Running and the Effectiveness of Some Materials in Their Attenuation. *Clin Biomech (Bristol, Avon)*. 1988; 3(3):159-165.

75. Paul IL, Munro MB, Abernethy PJ, Simon SR, Radin EL, Rose RM. Musculo-Skeletal Shock Absorption: Relative Contribution of Bone and Soft Tissues at Various Frequencies. *J Biomech*. 1978; 11(5):237-239.

76. Pohl MB, Mullineaux DR, Milner CE, Hamill J, Davis IS. Biomechanical Predictors of Retrospective Tibial Stress Fractures in Runners. *J Biomech*. 2008; 41(6):1160-1165.

77. Potthast W, Bruggemann GP, Lundberg A, Arndt A. The Influences of Impact Interface, Muscle Activity, and Knee Angle on Impact Forces and Tibial and Femoral Accelerations Occurring after External Impacts. *J Appl Biomech*. 2010; 26(1):1-9.

78. Pozzo T, Berthoz A, Lefort L, Vitte E. Head Stabilization During Various Locomotor Tasks in Humans. Ii. Patients with Bilateral Peripheral Vestibular Deficits. *Exp Brain Res*. 1991; 85(1):208-217.

79. Pratt DJ. Mechanisms of Shock Attenuation Via the Lower Extremity During Running. *Clin Biomech (Bristol, Avon)*. 1989; 4(1):51-57.

80. Qin YX, Rubin CT, McLeod KJ. Nonlinear Dependence of Loading Intensity and Cycle Number in the Maintenance of Bone Mass and Morphology. *J Orthop Res*. 1998; 16(4):482-489.

81. Radin EL. The Physiology and Degeneration of Joints. *Semin Arthritis Rheum*. 1972; 2(3):245-257.

82. Radin EL, Parker HG, Pugh JW, Steinberg RS, Paul IL, Rose RM. Response of Joints to Impact Loading. 3. Relationship between Trabecular Microfractures and Cartilage Degeneration. *J Biomech*. 1973; 6(1):51-57.

83. Radin EL and Paul IL. Does Cartilage Compliance Reduce Skeletal Impact Loads? The Relative Force-Attenuating Properties of Articular Cartilage, Synovial Fluid, Periarticular Soft Tissues and Bone. *Arthritis Rheum*. 1970; 13(2):139-144.

84. Rosager S, Aagaard P, Dyhre-Poulsen P, Neergaard K, Kjaer M, Magnusson SP. Load-Displacement Properties of the Human Triceps Surae Aponeurosis and Tendon in Runners and Non-Runners. *Scand J Med Sci Sports*. 2002; 12(2):90-98.

85. Rubin C, Turner AS, Bain S, Mallinckrodt C, McLeod K. Anabolism. Low Mechanical Signals Strengthen Long Bones. *Nature*. 2001; 412(6847):603-604.

86. Scott SH and Winter DA. Internal Forces of Chronic Running Injury Sites. *Med Sci Sports Exerc*. 1990; 22(3):357-369.

87. Shorten M and Mientjes M. The Effects of Shoe Cushioning on Impact Force During Running. 6th symposium on footwear biomechanics. 2003.

88. Shorten MR and Winslow DS. Spectral Analysis of Impact Shock During Running. *Int J Sports Biomech*. 1992; 8:288-304.

89. Simon SR, Paul IL, Mansour J, Munro M, Abernethy PJ, Radin EL. Peak Dynamic Force in Human Gait. *J Biomech*. 1981; 14(12):817-822.

90. Stone J, Brannon T, Haddad F, Qin A, Baldwin KM. Adaptive Responses of Hypertrophying Skeletal Muscle to Endurance Training. *J Appl Physiol*. 1996; 81(2):665-672.

91. Valiant GA, McMahon TA, Frederick EC. A New Test to Evaluate the Cushioning Properties of Athletic Shoes. In: *Biomechanics X-B*. Jonsson BE (Ed.). Human Kinetics, Champaign, IL, 1987. 937-941.

92. Voloshin A and Wosk J. An in Vivo Study of Low Back Pain and Shock Absorption in the Human Locomotor System. *J Biomech*. 1982; 15(1):21-27.

93. Voloshin A, Wosk J, Brull M. Force Wave Transmission through the Human Locomotor System. *J Biomech Eng*. 1981; 103(1):48-50.

94. Voloshin AS, Burger CP, Wosk J, Arcan M. An in Vivo Evaluation of the Leg's Shock Absorbing Capacity. In: *Biomechanics Ix-B* Winter D et al. (Eds.). Human Kinetics, Champaign, IL:, 1985. 112-116.

95. Williams DS, McClay IS, Manal KT. Lower Extremity Mechanics in Runners with a Converted Forefoot Strike Pattern. *J App Biomech*. 2000; 16(2):210-218.

96. Williams KR and Cavanagh PR. Relationship between Distance Running Mechanics, Running Economy, and Performance. *J Appl Physiol*. 1987; 63(3):1236-1245.

97. Winter DA. Moments of Force and Mechanical Power in Jogging. *Journal of Biomechanics*. 1983; 16(1):91-97.

98. Winter DA. Frequency Domain Analysis. In: *Singal Processing and Linear Systems for the Movement Sciences*. Winter DAand Patla AE (Eds.). Graphic Services, University of Waterloo, Waterloo, Ont., 1997. 51-76.

99. Winter DA, Sidwall HG, Hobson DA. Measurement and Reduction of Noise in Kinematics of Locomotion. *Journal of Biomechanics*. 1974; 7(2):157-159.

100. Wosk J and Voloshin A. Wave Attenuation in Skeletons of Young Healthy Persons. *J Biomech*. 1981; 14(4):261-267.

101. Zifchock RA, Davis IS, Hamill J. Kinetic Asymmetry in Female Runners with and without Retrospective Tibial Stress Fractures. *J Biomech*. 2006; 39(15):2792-2797.

CHAPTER 8

SUMMARY AND FUTURE DIRECTIONS

Summary

The forefoot (FF) running footfall pattern has been advocated to improve running economy and reduce the risk of developing running related injuries (Cavanagh and Lafortune, 1980; Davis et al., 2010; Hasegawa et al., 2007; Lieberman et al., 2010; Pratt, 1989). The fastest competitive runners in short and middle distance events tend to land on the anterior portion of the foot suggesting that FF running may enhance performance by improving running economy or running speed (Hasegawa et al., 2007; Payne, 1983). It has been suggested that the FF pattern improves running economy compared to the rearfoot (RF) footfall pattern as a result of increased elastic energy storage (Ardigo et al., 1995; Hasegawa et al., 2007; Lieberman et al., 2010; Perl et al., 2012). However, the RF pattern results in gait mechanics found to be related to more economical runners (Heise et al., 2011; Williams and Cavanagh, 1987). Previous studies have not found overwhelming evidence to support one footfall pattern as being more economical than the other (Ardigo et al., 1995; Cunningham et al., 2010; Perl et al., 2012; Slavin, 1992). Additionally, the mechanisms that may explain why one footfall pattern is more economical have not been identified.

The RF running pattern results in an initial impact peak transient which is thought to be related to the development of running overuse injuries (Cavanagh and Lafortune, 1980; Davis et al., 2010; Hreljac et al., 2000; Milner et al., 2006; Zifchock et al., 2006). However, this finding has not been supported by all studies (Azevedo et al., 2009;

Bredeweg, 2011; McCrory et al., 1999; Nigg, 1997; Pohl et al., 2008; Scott and Winter, 1990). Differences in the vertical ground reaction force (GRF) component between footfall patterns suggest there may also be a difference in the vertical GRF frequency content and the frequency content of the impact shock wave which travels through the body. Altering the frequency content may overload tissues responsible for attenuation and result in injury (Voloshin and Wosk, 1982; Voloshin et al., 1981). Conflicting evidence exists regarding the damaging effects of the impact transient. Examining frequency domain variables, rather than time domain variables, may provide more insight to the mechanisms of developing running related injuries.

Study 1

The first study of this dissertation found that, when comparing each group performing their natural footfall pattern at each speed, no differences in rate of oxygen consumption or cost of transport existed. Additionally, it was found that RF running was more economical than FF running in a group of natural RF runners. Natural FF runners, however, did not have a significant difference in rate of oxygen consumption or cost of transport between footfall patterns at the slow and medium speeds. At the fast speed, RF running resulted in lower rates of oxygen consumption and cost of transport across both groups. In the RF group, the differences in running economy variables were large enough to suggest that training with the FF pattern would not ultimately result in it becoming more economical than the RF pattern. However, task novelty may explain why no differences in running economy were observed in the FF group and that training with the RF pattern may improve economy in this group. Additionally, there may be an

optimal speed in which one footfall pattern becomes more economical than the other. Since both groups were trained runners with their respective footfall patterns, this finding suggests that there may not be an economical benefit of either RF or FF running patterns.

Study 2

The second study aimed to identify if the static Achilles tendon (AT) moment arm or the difference in dynamic AT moment arm length related to running economy. Only weak to moderate relationships were found between AT moment arm length and running economy variables. Less than 25% of the variance in running economy was explained by either static or dynamic AT moment arm. Previous studies have suggested that a shorter AT moment arm may improve running economy by requiring greater force production but more elastic energy storage by the triceps surae muscle tendon complex (Scholz et al., 2008). However, a consequence of greater force transmission through the AT is an increased risk of injury due to increased tendon stress. The second study also found that FF running results in significantly greater AT forces, and thus a greater risk of tendon injury, compared to the RF pattern.

Study 3

The third study used a muscle model to examine the triceps surae muscle-tendon interactions and effects of elastic energy utilization in RF and FF running. It was found that FF running resulted in greater elastic energy recoil in the gastrocnemius (GA) and the soleus (SO) compared to RF running. However, greater elastic energy recoil did not result in decreased metabolic cost. In the GA, the contractile element work ($W_{CE\text{-}GA}$) and

GA metabolic cost was similar between footfall patterns. These results can be explained by the difference in force production and contractile velocities between footfall patterns. The RF pattern resulted in higher shortening velocities which resulted in lower force generation capacity but at a greater metabolic cost. Conversely, the FF pattern resulted in slower shortening velocities as well as a period of isometric contraction, both of which result in a lower metabolic cost and greater force production capability than high shortening velocities. The differences in contraction velocity, which dictated the force production and metabolic cost, resulted in no difference in GA metabolic cost between footfall patterns. The increased force generation during FF running negated any metabolic benefit of more optimal contractile velocities. In the SO, the RF pattern resulted in isometric contractions during mid-stance and a lower force production; therefore, overall $W_{CE\text{-}SO}$ and SO metabolic cost was significantly decreased in the RF pattern compared to the FF pattern. However, the difference in overall $W_{CE\text{-}SO}$ between footfall patterns did not fully explain the differences in metabolic cost. The FF pattern required greater SO muscle-tendon work ($W_{MT\text{-}SO}$) during the second half of stance compared to RF running. Greater $W_{MT\text{-}SO}$ was accomplished by an increase in both and series elastic element work ($W_{SEE\text{-}SO}$) and $W_{CE\text{-}SO}$. Although FF running resulted in greater elastic recoil indicated by greater positive $W_{SEE\text{-}SO}$, greater $W_{CE\text{-}SO}$ resulted in an increase in SO metabolic cost in FF running compared to RF running.

Study 4

The fourth study examined the frequency content of the vertical GRF and the degree of shock attenuation between RF and FF running. RF running resulted in greater

amplitudes and powers of GRF frequencies that represent the impact peak whereas the FF pattern resulted in greater amplitudes and powers of GRF frequencies that represent the active peak. These differences in frequency content may suggest that different tissues act as the primary shock attenuators with each footfall pattern. For example, bone is responsible for attenuating high frequency components (Paul et al., 1978), thus it may be the primary tissue attenuating shock with the RF pattern. Conversely, muscle and joint actions may be the primary mechanism for shock attenuation in FF running because they attenuate lower frequency components (Derrick et al., 1998; Lafortune et al., 1996; Paul et al., 1978). It was also found that RF running resulted in greater attenuation of frequency components of the tibia relative to the head compared to FF running. Greater impact shock attenuation with RF running was a result of a peak positive tibial acceleration and greater amplitude and power of the tibial acceleration signal. It is currently unknown whether the increased shock attenuation occurring with RF running is detrimental or increases the risk of injury. Unlike the FF pattern, RF running uses the heel fat pad and shoe cushioning in the heel to attenuate impacts. Therefore the increased attenuation occurring with the RF pattern may be compensated by using these additional mechanisms. In FF running, the frequencies that would otherwise be absorbed by the shoe or heel fat pad must be absorbed by other mechanisms. If the impact shock wave is not appropriately attenuated, then a tissue may become overloaded (Voloshin et al., 1981). However, subjecting a tissue to a greater stimulus may also result in beneficial tissue adaptation (McLeod et al., 1998; Rosager et al., 2002; Stone et al., 1996). However, the threshold between tissue injury and tissue adaptation is currently unknown.

Summary of Dissertation Results

These four studies provide empirical evidence related to the efficacy of switching footfall patterns in order to improve running performance and decrease injury risk. Contrary to previous speculation, these studies have shown that the FF running footfall pattern was not more economical than the RF pattern. Additionally, the absence of the initial impact peak transient in the time domain does not lead to protection against developing running related injuries. Rather, the differences in vertical ground reaction force frequency components may suggest that different tissues have the potential to be overloaded with each footfall pattern. It is unlikely that one footfall pattern is more protective against developing injury than the other, but that each footfall pattern results in a different susceptibility to different injuries. Therefore, the present study does not support recommendations for one to alter footfall pattern in hopes of improving performance or preventing running injury.

Future Directions

Further research is needed to identify the mechanisms for running economy and injury with each footfall pattern. The present study incorporated both natural RF and natural FF runners in which each group can be a surrogate for training with the alternate footfall pattern. Although this was the first step in determining the efficacy for altering footfall pattern, longitudinal training studies may be needed to investigate if training with an alternate footfall pattern results in an improvement in running economy. The present study hypothesized that the FF group would improve economy by training with the RF pattern. However, a training study is needed in order to support or refute this hypothesis.

It is currently unknown why individuals naturally select a specific footfall pattern. Future studies should examine the morphological considerations for why one may naturally select a specific footfall pattern. Morphological characteristics such as tendon stiffness, muscle moment arms, and others may cause on individual to naturally select a specific footfall pattern. As suggested in study 2, the muscle forces required by the FF pattern may result in tendon adaptations such as increased cross sectional area. Identifying morphological characteristics and adaptations may provide additional evidence for the factors relating to running economy and risk of developing different types of injuries. Future research should examine different mechanical aspects of each footfall pattern such as muscle mechanical advantage, elastic energy storage of other muscles, and gear ratios. Additionally, there are currently no studies investigating the neuromuscular aspects of each footfall pattern. Mechanical, neuromuscular, and morphological considerations together will provide understanding for the mechanisms of selecting a footfall pattern and their potential benefits.

Longitudinal prospective studies are also needed to identify the injuries resulting from each footfall pattern. Several of the participants of the present study anecdotally reported that habituating to the FF pattern eliminated symptoms of ilio-tibial band syndrome. Additionally, emerging evidence has found that the FF pattern may increase the risk of developing metatarsal stress fractures (Giuliani et al., 2011). Therefore, each footfall pattern may result in the risk of different types of injuries.

The present study investigated several differences between RF and FF running footfall patterns. However, a third footfall pattern, the midfoot (MF) pattern, also exists. The MF pattern is considered an intermediate between the RF and FF patterns and could

incorporate the benefits of the other footfall patterns. For example, the metabolic benefits of increased elastic energy storage resulting from the FF pattern were negated as a result of high muscle force demands. The MF pattern may utilize the increased elastic energy storage of the FF pattern but the low force demands of the RF pattern. Additionally, some ambiguity exists for the definitions of each footfall pattern. Some researchers differentiate between MF and FF running by whether or not the heel contacts the ground. Other definitions of the MF pattern have described it as an initial midfoot contact with either the whole foot making ground contact at nearly the same time or a slight delay between midfoot and heel contact. These seemingly insignificant differences between definitions may have functional implications. Therefore, studies investigating the variation in each of the three footfall patterns are needed.

References

1. Ardigo LP, Lafortuna C, Minetti AE, Mognoni P, Saibene F. Metabolic and Mechanical Aspects of Foot Landing Type, Forefoot and Rearfoot Strike, in Human Running. *Acta Physiol Scand*. 1995; 155(1):17-22.

2. Azevedo LB, Lambert MI, Vaughan CL, O'Connor CM, Schwellnus MP. Biomechanical Variables Associated with Achilles Tendinopathy in Runners. *Br J Sports Med*. 2009; 43(4):288-292.

3. Bredeweg S. No Relationship between Running Related Injuries and Kinetic Variables. *Br J Sports Med*. 2011; 45(4):328.

4. Cavanagh PR and Lafortune MA. Ground Reaction Forces in Distance Running. *J Biomech*. 1980; 13(5):397-406.

5. Cunningham CB, Schilling N, Anders C, Carrier DR. The Influence of Foot Posture on the Cost of Transport in Humans. *J Exp Biol*. 2010; 213(5):790-797.

6. Davis IS, Bowser B, Mullineaux DR. Do Impacts Cause Running Injuries? A Prospective Investigation. Proceedings of the Annual Meeting of the American Society of Biomechanics. 2010.

7. Derrick TR, Hamill J, Caldwell GE. Energy Absorption of Impacts During Running at Various Stride Lengths. *Med Sci Sports Exerc*. 1998; 30(1):128-135.

8. Giuliani J, Masini B, Alitz C, Owens BD. Barefoot-Simulating Footwear Associated with Metatarsal Stress Injury in 2 Runners. *Orthopedics*. 2011; 34(7):e320-323.

9. Hasegawa H, Yamauchi T, Kraemer WJ. Foot Strike Patterns of Runners at the 15-Km Point During an Elite-Level Half Marathon. *J Strength Cond Res*. 2007; 21(3):888-893.

10. Heise GD, Smith JD, Martin PE. Lower Extremity Mechanical Work During Stance Phase of Running Partially Explains Interindividual Variability of Metabolic Power. *Eur J Appl Physiol*. 2011; 111(8):1777-1785.

11. Hreljac A, Marshall RN, Hume PA. Evaluation of Lower Extremity Overuse Injury Potential in Runners. *Med Sci Sports Exerc*. 2000; 32(9):1635-1641.

12. Lafortune MA, Lake MJ, Hennig EM. Differential Shock Transmission Response of the Human Body to Impact Severity and Lower Limb Posture. *J Biomech*. 1996; 29(12):1531-1537.

13. Lieberman DE, Venkadesan M, Werbel WA, Daoud AI, D'Andrea S, Davis IS, Mang'eni RO, Pitsiladis Y. Foot Strike Patterns and Collision Forces in Habitually Barefoot Versus Shod Runners. *Nature*. 2010; 463(7280):531-535.

14. McCrory JL, Martin DF, Lowery RB, Cannon DW, Curl WW, Read HM, Jr., Hunter DM, Craven T, Messier SP. Etiologic Factors Associated with Achilles Tendinitis in Runners. *Med Sci Sports Exerc*. 1999; 31(10):1374-1381.

15. McLeod KJ, Rubin CT, Otter MW, Qin YX. Skeletal Cell Stresses and Bone Adaptation. *The American Journal of the Medical Sciences*. 1998; 316(3):176-183.

16. Milner CE, Ferber R, Pollard CD, Hamill J, Davis IS. Biomechanical Factors Associated with Tibial Stress Fracture in Female Runners. *Med Sci Sports Exerc*. 2006; 38(2):323-328.

17. Nigg BM. Impact Forces in Running. *Current Opinion in Orthopedics*. 1997; 8(6):43-47.

18. Paul IL, Munro MB, Abernethy PJ, Simon SR, Radin EL, Rose RM. Musculo-Skeletal Shock Absorption: Relative Contribution of Bone and Soft Tissues at Various Frequencies. *J Biomech*. 1978; 11(5):237-239.

19. Payne AH. Foot to Ground Contact Forces of Elite Runners. In: *Biomechanics Viii-B*. Matsui Hand Kobayashi K (Eds.). Human Kinetics, Champaign, IL, 1983. 748-753.

20. Perl DP, Daoud AI, Lieberman DE. Effects of Footwear and Strike Type on Running Economy. *Med Sci Sports Exerc*. 2012; 44(7):1335-1343.

21. Pohl MB, Mullineaux DR, Milner CE, Hamill J, Davis IS. Biomechanical Predictors of Retrospective Tibial Stress Fractures in Runners. *J Biomech*. 2008; 41(6):1160-1165.

22. Pratt DJ. Mechanisms of Shock Attenuation Via the Lower Extremity During Running. *Clin Biomech (Bristol, Avon)*. 1989; 4(1):51-57.

23. Rosager S, Aagaard P, Dyhre-Poulsen P, Neergaard K, Kjaer M, Magnusson SP. Load-Displacement Properties of the Human Triceps Surae Aponeurosis and Tendon in Runners and Non-Runners. *Scand J Med Sci Sports*. 2002; 12(2):90-98.

24. Scholz MN, Bobbert MF, van Soest AJ, Clark JR, van Heerden J. Running Biomechanics: Shorter Heels, Better Economy. *J Exp Biol*. 2008; 211(Pt 20):3266-3271.

25. Scott SH and Winter DA. Internal Forces of Chronic Running Injury Sites. *Med Sci Sports Exerc*. 1990; 22(3):357-369.

26. Slavin MM. The Effects of Foot Strike Pattern Alteration on Efficiency in Skilled Runners. M.S. thesis, University of Massachusetts, Amherst, MA, 1992.

27. Stone J, Brannon T, Haddad F, Qin A, Baldwin KM. Adaptive Responses of Hypertrophying Skeletal Muscle to Endurance Training. *J Appl Physiol*. 1996; 81(2):665-672.

28. Voloshin A and Wosk J. An in Vivo Study of Low Back Pain and Shock Absorption in the Human Locomotor System. *J Biomech*. 1982; 15(1):21-27.

29. Voloshin A, Wosk J, Brull M. Force Wave Transmission through the Human Locomotor System. *J Biomech Eng*. 1981; 103(1):48-50.

30. Williams KR and Cavanagh PR. Relationship between Distance Running Mechanics, Running Economy, and Performance. *J Appl Physiol*. 1987; 63(3):1236-1245.

31. Zifchock RA, Davis IS, Hamill J. Kinetic Asymmetry in Female Runners with and without Retrospective Tibial Stress Fractures. *J Biomech*. 2006; 39(15):2792-2797.

APPENDIX A

INFORMED CONSENT DOCUMENTS

PROJECT DESCRIPTION:

Biomechanical differences between rearfoot and forefoot landing patterns in running.

The study of forefoot (FF) and rearfoot (RF) strike patterns in running has included ground reaction force and metabolic cost differences between individuals with different strike patterns (Cavangh and LaFortune, 1980; Ardigo, et al., 1995; Cunningham et al., 2010). Some running experts and elite running coaches believe the forefoot running pattern will improve running economy and reduce the risk of overuse injuries. Many have speculated that the FF pattern may reduce the risk of impact related injury due to the lack of the impact transient and reductions in vertical tibial acceleration and loading rates (Oakley & Pratt, 1988; Williams et al., 2000). Because of differences in kinematic patterns between RF and FF running, impact shock attenuation may be controlled through different mechanisms (Pratt, 1989; Williams & Cavanagh, 1987). Williams and Cavanagh (1987) found lower strike index was associated with running economy. They speculate economy is lower in RF running because of the reliance of footwear to attenuate impact forces whereas FF running must rely on muscular contractions. However, a recent study has looked at the effect of forefoot and rearfoot strike patterns on race performance (Hasegawa, Yamauchi, & Kraemer, 2007). These researchers examined 283 runners at the 15 km point during a half marathon and determined 74.9% of all analyzed runners were rearfoot strikers, 23.7% were midfoot strikers, and 1.4% were forefoot strikers. When the runners were divided into groups of 50 based on placement order, it was observed that the percentage of rearfoot runners decreased and the percentage of midfoot runners increased as placement order increased. Inversion of the foot was observed in 42% of all runners; however the midfoot runners had the greatest within group percentage of inversion compared to the other strike patterns. The decreased inversion was shown to be coupled with a shorter contact time, leading the researchers to conclude that these two factors may contribute to running economy. While previous research has typically observed subjects' natural running patterns, the purpose of this study is to examine the effect of altering running footfall patterns on kinematic and kinetic parameters as well as metabolic cost, impact shock and electromyography (EMG) in healthy runners.

Thirty healthy young adult males and females between the ages of 18-45 yrs will participate in this study. All subjects will be healthy runners and have not experienced an injury or surgery to the lower extremity or back in the last year. Additional exclusion criteria include cardiovascular or neurological problems or disease, diabetes, and smoking. Each subject will be asked to participate in two testing sessions, lasting approximately 2 hours each. At the beginning of the first test session, the subject will complete: 1) an informed consent form; 2) a Physical Activity Readiness Questionnaire; and 3) a demographic information form. The session will begin with measurements of body mass and height. During the first testing session, reflective markers will be placed on the subjects' foot, leg, thigh, and hip in order to record gait kinematics. Motion analysis cameras will record the position of the reflective markers as the subjects perform each condition. A force plate in the center of the collection volume of the cameras will measure ground reaction forces. Subjects will be asked to run across the floor and

over a force plate under each footfall condition: 1) rearfoot and 2) forefoot. Both conditions will be performed at three different running speeds (3.0, 3.5 and 4.0 m/s). Ten trials of each condition performed at each of the three speeds will be completed. Subjects will be able to rest ad libitum between each trial. The order of speeds and conditions will be randomized. Kinematic and kinetic variables will be compared between subjects to determine the differences in ground reaction forces and running mechanics between footfall conditions.

For the second testing session, subjects will be asked to repeat each of the footfall and speed combinations on a treadmill. The order of the conditions will be randomized. Reflective markers will be placed on the heel and toe of each foot to determine touchdown and toe-off of each stance phase. Electromyography (EMG) data will be recorded by measuring the amount of muscle activity in both legs during running. Muscle activity will be recorded by placing surface electrodes on several muscles of the leg, including: tibialis anterior, medial and lateral heads of the gastrocnemius, soleus, vastus medialis and lateralis, rectus femoris, biceps femoris, and gluteus maximus. A metabolic cart will be used to measure oxygen consumption while running. An accelerometer will be placed on the midfoot on the outside of the shoe, on the lower leg and on the head. The accelerometer will measure impact shock at each location. Subjects will perform each speed and footfall condition for 5-10 minutes. EMG, accelerometer data and metabolic cost of each condition will be compared within and between subjects to better understand the differences between the two footfall patterns.

Participant Number_____

INFORMED CONSENT FORM
Biomechanics Laboratory, Department of Kinesiology
University of Massachusetts
Amherst, MA 01003

Title: Biomechanical differences between rearfoot and forefoot landing patterns in running.

Principal Investigator: Allison Gruber, M.A.; Joseph Hamill, Ph.D.

Purpose: To identify the effect of altering running footfall patterns on running mechanics, oxygen consumption, the force of impact and muscle activity in healthy runners.

Requirements: You have been asked to participate in this study because you are a healthy and active male or female of age 18-45 yrs, have not suffered any injuries or surgery to the lower extremity in the past year, do not wear orthotics, or have any cardiovascular problems. You should also have not eaten a meal during the period of 2 hours preceding a data collection.

Study Duration: You will be required to make a minimum of two (2) visits to the testing laboratory, lasting approximately 2 hours each. The total time that you are expected to be enrolled in the study is approximately two (2) days.

General Testing Procedures:

Visit 1:

1. You will be asked to read and sign this Informed Consent Form, Modified Physical Activity Readiness Questionnaire, and Demographic Questionnaire.

2. If, after all questionnaires have been completed, you are deemed qualified to participate, you will be asked to participate in one testing session, lasting approximately 2 hours.

3. The testing session will begin with measurements of body mass and height.

4. To be prepared for data collection, you will be asked to change into form fitting clothing and running shoes provided by the laboratory.

Participant's initials_____

5. Next, reflective markers will be placed on your feet legs, thighs, and hips in order to record 3-D gait kinematics. The position of the reflective markers will be recorded by high-speed infrared cameras circling the data collection space you will run through.

6. Once markers have been placed, you will be asked to stand in the data collection space to record a standing calibration trial of the markers. The standing calibration trial will be used to create a computer model of you on which data analysis will be performed.

7. Next, you will be instructed on how to run through the data collection volume at the appropriate speed and so your right leg will land on the force platform in the center of the collection volume. You will be able to practice several times before data collection begins.

8. Once you are comfortable running through the collection volume, you will be asked to run through the data collection volume with either a rearfoot footfall pattern or a forefoot footfall pattern at each of three different speeds (3.0, 3.5 and 4.0 m/s). The order of the conditions will be determined randomly.

9. You will perform ten successful trials for each condition and speed combination. A successful trial means that your running speed is within +/-5% of the target speed and your right foot lands completely on the force platform without targeting or adjusting your stride. You will be allowed to rest between trials for as long as necessary.

10. After you complete all conditions, all of the equipment will be removed and a staff member will inform you of your next appointment time

Visit 2:

1. You will arrive at the study facility as instructed and will be asked about any changes in your health. All changes to your health will be recorded.

2. Next, you will be prepared for data collection by first placing an accelerometer onto the middle of your foot, on your lower leg and on your head. The accelerometers will be secured with a rubber strap which will be tightened but so that you are still comfortable.

3. Small electrodes will be placed on the surface of your skin in order to measure muscle activity while you run. The electrodes will be placed on several muscles of your lower leg (tibialis anterior, medial and lateral heads of the gastrocnemius, soleus) and several muscles of your thigh and hip (vastus medialis and lateralis, rectus femoris, biceps femoris, and gluteus maximus).

4. Reflective markers will be placed on your toe and heel in order to record when your foot lands on the treadmill and when it is lifted off of the treadmill while running.

5. You will be asked to breathe into a mouth piece while you are running. The mouth piece is similar to a rubber mouth guard and you will be able to breathe normally. The mouth piece allows you to breathe-in air from the room but it will send the air you breathe-out into a tube connected to a machine. The machine will measure the amount of air you breathed-out. A foam clip will be placed on your noise to make sure the air you breathe is only going into and out of your mouth.

6. To begin the data collection, a baseline measurement of your oxygen consumption will be taken while you stand quietly for 3-5 minutes. During this measurement, a mask will be placed over your nose and mouth area.

7. Next, you will be asked to perform either a rearfoot footfall pattern or a forefoot footfall pattern at each of three different speeds (3.0, 3.5 and 4.0 m/s). The order of the conditions will be determined randomly. Each footfall and speed condition will be performed for 5-10 minutes.

8. After you complete all conditions, all of the equipment will be removed and you will then be dismissed from the study.

9. You may be asked to return to the laboratory to repeat testing procedures if necessary. You are not required to return for additional testing if you do not wish.

Additional Costs: There are no costs for participation in this study.

Females of Childbearing Potential: You may not participate in this study if you are pregnant.

Benefits: You may not directly benefit from this research; however, we hope that your participation in this study may help in the understanding of the effects of speed on the mechanics of running and oxygen consumption.

Participant's initials_____

Participant Number_____

Expected Risks or Discomforts: During any type of exercise there are slight health risks. These include the possibility of fatigue and muscle soreness. However, any health risks are small in subjects who have no prior history of cardiovascular, respiratory or musculoskeletal disease or injury. Any ordinary fatigue or muscle soreness is temporary. In the unlikely event that medical treatment is required as a result of this study, study personnel will assist you in getting treatment. The University of Massachusetts does not have a program for compensation subjects for injury or complications related to human subjects' research.

Compensation: The University of Massachusetts does not have a program for compensation subjects for injury or complications related to human subjects' research but the study personnel will assist you in getting treatment. There is no monetary compensation for participating in this study.

Alternative Procedures: There are no reasonable alternatives for this procedure. These procedures are standard for this type of equipment and these measures.

Confidentiality: Information concerning you that is obtained in connection with this study will be kept confidential by the testing facility. The records will be coded to protect your identity. In addition, the Investigational Review Board may inspect the records of this study. Information obtained in the study may be used for medical or scientific publication, but your identity will remain confidential. Data will be stored in a locked filing cabinet in a locked office. Only staff involved in this study will have access to the data.

Informing of New Findings: You will be informed of any new findings concerning this study that could directly affect you.

Questions and Answers: Any questions concerning testing procedures, risks, benefits, or participant's rights will be answered by investigators.

Subject Enrollment: It is expected that 30 male and female subjects aged 18-40 will take part in this study. The study is expected to last three months but your participation will only be for about 60 – 90 minutes for two days of testing.

Participation/Withdrawal: You are under no obligation to participate in this project. You are free to withdrawal your consent and participation at any time, for any reason.

Participant's initials_____

Participant Number_____

Additional Information: Should you have any questions about your treatment or any other matter relative to your participation in this project or if you experience a research related injury at any time during this study you may contact Dr. Joseph Hamill via email (jhamill@kin.umass.edu). If you would like to discuss your rights as a participant in a research study or to speak with someone not directly involved with this study, you may contact the office of Research Affairs at the University of Massachusetts via email (humansubjects@ora.umass.edu); by telephone (413-545-3428); or by mail (Office of Research Affairs, Research Administration Building, University of Massachusetts Amherst, 70 Butterfield Terrace, Amherst, MA 01003.)

Participant's initials_____

Participant Number_____

Statement and Participant Signature (study copy)

The investigators have read and understood the General Guidelines for the Right and Welfare of Human Subjects (Sen. Doc. 79-012) and agree to fulfill these guidelines to the best of their ability.

Investigator signature _____ Date _____

When signing this form, I am agreeing to voluntarily enter this study. I understand that, by signing this document, I do not waive any of my legal rights. I have read and understood the Informed Consent Document and it was explained to me in a language that I use and understand. I have had the opportunity to ask questions and have received satisfactory answers. A copy of this document has been given to me.

Participant Name _____

Participant Signature _____ Date _____

Address _____

_____

Telephone _____

Witness Name _____

Witness Signature _____

Participant's initials_____

Participant Number_____

Statement and Participant Signature (participant copy)

The investigators have read and understood the General Guidelines for the Right and Welfare of Human Subjects (Sen. Doc. 79-012) and agree to fulfill these guidelines to the best of their ability.

Investigator signature _____ Date _____

When signing this form, I am agreeing to voluntarily enter this study. I understand that, by signing this document, I do not waive any of my legal rights. I have read and understood the Informed Consent Document and it was explained to me in a language that I use and understand. I have had the opportunity to ask questions and have received satisfactory answers. A copy of this document has been given to me.

Participant Name _____

Participant Signature _____ Date _____

Address _____

_____

Telephone _____

Witness Name _____

Witness Signature _____

Participant's initials_____

Participant Number_____

Modified Physical Activity Readiness Questionnaire

Date _____

Please answer the following questions to the best of your knowledge (circle YES or NO)

YES NO Has a doctor ever said you have a heart condition and recommended only medically supervised activity?

YES NO Do you ever suffer pains in your chest brought on by physical activity

YES NO Have you developed chest pain in the last month?

YES NO Do you ever feel faint or have spells of severe dizziness, passed out, Palpitations or rapid heart beat?

YES NO Has the doctor ever told you that your blood pressure was too high? (systolic $\geq$ 160 mm Hg or diastolic $\geq$ 90 mm Hg on at least two separate occasions?)

YES NO Do you smoke cigarettes?

YES NO Do you have a bone or joint that could be aggravated by the proposed physical activity?

YES NO Do you have diabetes?

YES NO Do you have a family history of coronary or other atherosclerotic disease in parents or siblings prior to age 55?

YES NO Has your serum cholesterol ever been elevated?

YES NO Is there any physical reason not mentioned hee why you should not follow an activity program even if you wanted to?

Please provide an explanation below for any of the questions to which you answered YES:

Participant's initials _____

Participant Number_____

Demographic Questionnaire

Date _____

Age (in years) _____

Gender (circle one) M F

Height _____ feet _____ inches or _____cm

Weight _____ lbs or _____ kg

Please circle one:

Do you use any specialized insoles or foot orthotics? YES NO

Do you have any injuries that may affect the way you walk or run? YES NO

If YES, please describe the injury, and when it happened:

_____

_____

_____

Did you injure your lower extremity in the last year? YES NO

If YES, please describe the injury and when it happened:

_____

_____

_____

Participant's initials_____

APPENDIX B

DIAGRAM OF REFLECTIVE MARKER PLACEMENT

Calibration Markers Location

- Right and left iliac crest
- Right and left greater trochanter
- Medial and lateral knee joint line
- Medial and lateral malleoli
- 1st Metatarsal head
- 5th Metatarsal head

Tracking Markers

- Right and left anterior superior iliac spine
- 5th Lumbar vertebrae/1st sacral vertebrae
- Thigh plate
- Leg plate
- Foot plate
- Heel plate
- Toe

Marker placement is based on McClay and Manal (1999).

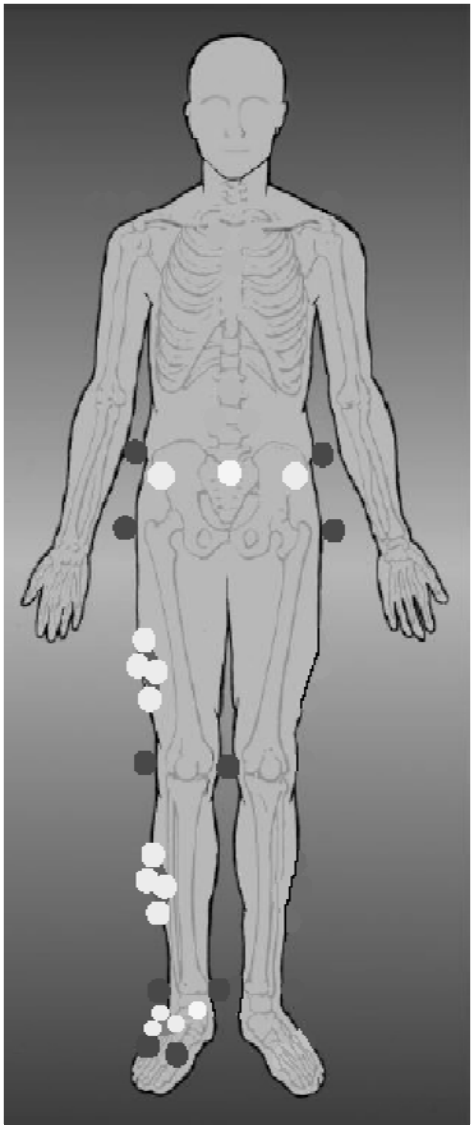

APPENDIX C

DETAILED STATISTICAL TABLES FOR THE RESULTS FROM STUDY 1

Table C.1: *P*-value (*d*) for each partition of the interaction for the rate of oxygen consumption ($\dot{V}O_2$) at the slow and medium speeds (interaction at the fast speed was not significant). Mean ± SD and percent difference are given for the rearfoot (RF) and forefoot (FF) patterns performed by each group. Negative percent difference indicates larger magnitudes when performing the FF pattern.

Speed	Partition	Group	Pattern	Net $\dot{V}O_2$ $L \cdot min^{-1}$	Net $\dot{V}O_2$ $ml \cdot kg^{-1} \cdot min^{-1}$	Gross $\dot{V}O_2$ $L \cdot min^{-1}$	Gross $\dot{V}O_2$ $ml \cdot kg^{-1} \cdot min^{-1}$
Slow		RF	RF	2.09 ± 0.36	29.60 ± 1.80	2.42 ± 0.40	34.19 ± 1.93
			FF	2.21 ± 0.36	31.27 ± 1.83	2.53 ± 0.41	35.86 ± 1.99
	Group		RF vs. FF	<0.001(0.3)	<0.001(0.9)	<0.001(0.3)	<0.001(0.9)
			%	-5.4	-5.5	-4.7	-4.8
		FF	RF	2.02 ± 0.36	29.36 ± 2.53	2.34 ± 0.40	33.95 ± 2.71
			FF	2.03 ± 0.34	29.49 ± 2.56	2.35 ± 0.38	34.08 ± 2.71
	Group		RF vs. FF	0.731(0.0)	0.663(0.1)	0.736(0.0)	0.663(0.0)
			%	-0.4	-0.4	-0.3	-0.4
	Pattern	RF vs. FF	RF	0.003(0.2)	0.431(0.1)	0.001(0.2)	0.424(0.1)
	Pattern	RF vs. FF	FF	<0.001(0.5)	<0.001(0.8)	<0.001(0.5)	0.001(0.8)
Med.		RF	RF	2.44 ± 0.38	34.79 ± 1.85	2.76 ± 0.42	39.36 ± 2.00
			FF	2.53 ± 0.42	36.05 ± 1.80	2.85 ± 0.46	40.62 ± 2.02
	Group		RF vs. FF	<0.001(0.2)	<0.001(0.7)	<0.001(0.2)	<0.001(0.6)
			%	-3.7	-3.6	-3.3	-3.2
		FF	RF	2.32 ± 0.38	33.66 ± 2.39	2.63 ± 0.42	38.25 ± 2.61
			FF	2.34 ± 0.39	33.93 ± 2.51	2.65 ± 0.43	38.51 ± 2.63
	Group		RF vs. FF	0.245(0.1)	0.255(0.1)	0.239(0.0)	0.255(0.1)
			%	-0.9	-0.8	-0.8	-0.7
	Pattern	RF vs. FF	RF	<0.001(0.3)	<0.001(0.5)	<0.001(0.3)	<0.001(0.5)
	Pattern	RF vs. FF	FF	<0.001(0.5)	<0.001(1.0)	<0.001(0.4)	<0.001(0.9)

Table C.2: *P*-value (*d*) for each partition of the interaction for the cost of transport (COT) at the slow and medium speeds (interactions at the fast speed were not significant). Mean ± SD and percent difference are given for the rearfoot (RF) and forefoot (FF) patterns performed by each group. Negative percent difference indicates larger magnitudes when performing the FF pattern.

Speed	Partition	group	pattern	Net COT $J \cdot m^{-1}$	Net COT $J \cdot m^{-1} \cdot kg^{-1}$	Gross COT $J \cdot m^{-1}$	Gross COT $J \cdot m^{-1} \cdot kg^{-1}$
Slow		RF	RF	237.3 ± 39.9	3.36 ± 0.20	274.0 ± 45.0	3.88 ± 0.22
			FF	251.7 ± 41.2	3.56 ± 0.22	288.5 ± 46.6	4.09 ± 0.24
	Group		RF vs. FF	<0.001(0.4)	<0.001(1.0)	<0.001(0.3)	<0.001(0.9)
			%	-5.9	-5.9	-5.2	-5.2
		FF	RF	231.1 ± 41.4	3.36 ± 0.29	267.1 ± 46.3	3.88 ± 0.31
			FF	231.2 ± 39.1	3.36 ± 0.29	267.2 ± 44.0	3.89 ± 0.31
	Group		RF vs. FF	0.955(0.0)	0.835(0.0)	0.974(0.0)	0.856(0.0)
			%	-0.1	-0.2	< -0.1	-0.2
	Pattern	RF vs. FF	RF	0.028(0.2)	0.970(0.0)	0.018(0.2)	0.950(0.0)
	Pattern	RF vs. FF	FF	<0.001(0.5)	<0.001(0.8)	<0.001(0.5)	<0.001(0.7)
Med.		RF	RF	241.3 ± 36.1	3.45 ± 0.20	273.1 ± 40.6	3.90 ± 0.22
			FF	251.2 ± 40.1	3.58 ± 0.18	283.0 ± 44.8	4.03 ± 0.21
	Group		RF vs. FF	<0.001(0.3)	<0.001(0.7)	<0.001(0.2)	<0.001(0.6)
			%	-4.0	-3.8	-3.6	-3.4
		FF	RF	229.2 ± 37.4	3.33 ± 0.24	260.4 ± 41.8	3.79 ± 0.26
			FF	231.1 ± 38.3	3.36 ± 0.26	262.4 ± 42.4	3.82 ± 0.27
	Group		RF vs. FF	0.272(0.1)	0.239(0.1)	0.269(0.0)	0.232(0.1)
			%	-0.9	-0.9	-0.8	-0.8
	Pattern	RF vs. FF	RF	<0.001(0.3)	<0.001(0.5)	<0.001(0.3)	<0.001(0.5)
	Pattern	RF vs. FF	FF	<0.001(0.5)	<0.001(1.0)	<0.001(0.5)	<0.001(0.9)

Table C.3: Statistical results for the rate of oxygen consumption ($\dot{V}O_2$) and cost of transport (COT) at the fast speed. Mean ± SD (percent difference) are given for the rearfoot (RF) and forefoot (FF) patterns performed by each group. Negative percent difference indicates larger magnitudes when performing the FF pattern. Listed ANOVA results include the *p*-value for the group by pattern interaction (GxP), the p-value (*d*) for the group main effect (G) and the pattern main effect (P).

	RF Group		FF Group		GxP	G	P
	RF	FF	RF	FF			
Net $\dot{V}O_2$ $L \cdot min^{-1}$	2.88 ± 0.46	2.95 ± 0.45	2.70 ± 0.42	2.76 ± 0.45	0.670	0.402 (0.4)	<0.001 (0.1)
	-2.3%		-1.9%				
Net $\dot{V}O_2$ $ml \cdot kg^{-1} \cdot min^{-1}$	40.19 ± 2.13	41.12 ± 1.86	38.80 ± 2.25	39.54 ± 2.67	0.641	0.102 (0.7)	<0.001 (0.4)
	-2.3%		-1.9%				
Gross $\dot{V}O_2$ $L \cdot min^{-1}$	3.21 ± 0.50	3.28 ± 0.50	3.03 ± 0.47	3.08 ± 0.49	0.667	0.450 (0.4)	<0.001 (0.1)
	-2.0%		-1.7%				
Gross $\dot{V}O_2$ $ml \cdot kg^{-1} \cdot min^{-1}$	44.77 ± 2.26	45.71 ± 1.96	43.42 ± 2.48	44.15 ± 2.87	0.641	0.150 (0.6)	<0.001 (0.3)
	-2.1%		-1.7%				
Net COT $J \cdot m^{-1}$	253.8 ± 38.6	260.3 ± 37.7	237.8 ± 36.4	242.8 ± 39.1	0.585	0.358 (0.4)	<0.001 (0.2)
	-2.5%		-2.1%				
Net COT $J \cdot m^{-1} \cdot kg^{-1}$	3.54 ± 0.18	36.4 ± 0.16	3.43 ± 0.19	3.49 ± 0.23	0.527	0.089 (0.7)	<0.001 (0.4)
	-2.6%		-2.0%				
Gross COT $J \cdot m^{-1}$	282.7 ± 42.3	289.2 ± 41.4	266.1 ± 40.0	271.1 ± 42.6	0.578	0.401 (0.4)	<0.001 (0.1)
	-2.3%		-1.9%				
Gross COT $J \cdot m^{-1} \cdot kg^{-1}$	3.95 ± 0.20	4.04 ± 0.17	3.83 ± 0.21	3.90 ± 0.24	0.518	0.130 (0.6)	<0.001 (0.4)
	-2.3%		-1.8%				

Table C.4: *P*-value (*d*) for each partition of the interaction for the absolute (gCHO) and relative (%CHO) rates of carbohydrate oxidation at the slow and medium speeds. Results for the medium and fast speeds are presented in Table C.5. Mean ± SD and percent difference are given for the rearfoot (RF) and forefoot (FF) patterns performed by each group. Negative percent difference indicates larger magnitudes when performing the FF pattern.

Speed	Partition	group	pattern	gCHO $g \cdot hr^{-1}$	%CHO %
Slow		RF	RF	88.89 ± 23.41	51.3 ± 12.7
			FF	104.68 ± 31.53	56.7 ± 13.1
	Group		RF vs. FF	0.001(0.6)	0.009(0.4)
			%	-16.3%	-10.0%
		FF	RF	104.67 ± 25.78	61.1 ± 10.5
			FF	100.23 ± 21.76	58.5 ± 8.3
	Group		RF vs. FF	0.313(0.2)	0.191(0.3)
			%	4.3%	4.4%
	Pattern	RF vs. FF	RF	0.001(0.6)	<0.001(0.8)
	Pattern	RF vs. FF	FF	0.312(0.2)	0.359(0.2)
Med.		RF	RF	131.17 ± 39.65	
			FF	144.28 ± 43.76	
	Group		RF vs. FF	<0.001(0.3)	
			%	-9.5%	
		FF	RF	137.18 ± 31.61	
			FF	140.08 ± 33.00	
	Group		RF vs. FF	0.371(0.1)	
			%	-2.1%	
	Pattern	RF vs. FF	RF	0.064(0.2)	
	Pattern	RF vs. FF	FF	0.191(0.1)	

Table C.5: Statistical results for the absolute carbohydrate oxidation (gCHO) at the fast speed and relative carbohydrate oxidation (%CHO) at the medium and fast speeds. Mean ± SD (percent difference) are given for the rearfoot (RF) and forefoot (FF) patterns performed by each group. Negative percent difference indicates larger magnitudes when performing the FF pattern. Listed ANOVA results include the *p*-value for the group by pattern interaction (GxP), the p-value (*d*) for the group main effect (G) and the pattern main effect (P).

	RF Group		FF Group		GxP	G	P
	RF	FF	RF	FF			
gCHO $g \cdot hr^{-1}$ (fast speed)	187.87 ± 58.05	199.99 ± 60.16	178.85 ± 37.92	186.12 ± 39.82	0.552	0.710 (0.2)	0.028 (0.2)
	-6.2%		-4.0%				
%CHO % (fast speed)	77.9 ± 16.8	80.8 ± 16.9	79.1 ± 11.8	80.9 ± 11.8	0.730	0.893 (0.0)	0.114 (0.2)
	-3.6%		-2.3%				
%CHO % (med. speed)	64.7 ± 15.5	68.5 ± 14.9	70.4 ± 10.3	71.3 ± 11.4	0.153	0.326 (0.3)	0.022 (0.2)
	-5.7%		-1.3%				

APPENDIX D

COMPLETE CORRELATION TABLES FOR THE RESULTS FROM STUDY 2

The aims of Study 2 (Chapter 5) was to determine the Achilles tendon (AT) moment arm length during the stance phase of running, to investigate the relationship between moment arm length and running economy, and to determine the difference in AT force between rearfoot (RF) and forefoot (FF) running patterns in natural RF and natural FF runners.

The results presented in the tables are the correlation results between the following variables: net and gross rate of oxygen consumption ($\dot{V}O_2$), the net and gross cost of transport (COT), the static AT moment arm measured during standing (dmt_0), the dynamic AT moment arm (dmt_{10}), AT force (AT_{10}), active ankle joint moment (AM_{10}), and the ankle joint moment found by the inverse dynamics procedure ($InvM_{10}$). dmt_0, dmt_{10}, AT_{10}, AM_{10}, and $InvM_{10}$ were determined by taking the average of each variable over the period of stance in which the AT force was greater than ±10% of the maximum.

Tables B.1 and B.2 list the results for the absolute (not normalized) variables in the RF group and the FF group, respectively. Tables B.3 and B.4 list the results for the relative (mass normalized) variables in the RF group and the FF group, respectively.

Table B.1: Correlation tables for absolute data of the RF group when performing the (A) RF pattern and the (B) FF pattern.

(A)		Net $\dot{V}O_2$ $L \cdot min^{-1}$	Gross $\dot{V}O_2$ $L \cdot min^{-1}$	Net COT $J \cdot m^{-1}$	Gross COT $J \cdot m^{-1}$	dmt_0 cm	dmt_{10} cm	AM_{10} N•m	AT_{10} N	$InvM_{10}$ N•m
Net $\dot{V}O_2$ $L \cdot min^{-1}$	r	1.000	0.998	0.988	0.985	0.483	0.484	-0.849	0.560	-0.876
	p		<.0001	<.0001	<.0001	0.036	0.036	<.0001	0.013	<.0001
Gross $\dot{V}O_2$ $L \cdot min^{-1}$	r	0.998	1.000	0.987	0.988	0.489	0.488	-0.847	0.553	-0.875
	p	<.0001		<.0001	<.0001	0.034	0.034	<.0001	0.014	<.0001
Net COT $J \cdot m^{-1}$	r	0.988	0.987	1.000	0.998	0.426	0.431	-0.837	0.588	-0.861
	p	<.0001	<.0001		<.0001	0.069	0.066	<.0001	0.008	<.0001
Gross COT $J \cdot m^{-1}$	r	0.985	0.988	0.998	1.000	0.432	0.434	-0.834	0.580	-0.859
	p	<.0001	<.0001	<.0001		0.065	0.064	<.0001	0.009	<.0001
dmt_0 cm	r	0.483	0.489	0.426	0.432	1.000	0.981	-0.529	-0.244	-0.557
	p	0.036	0.034	0.069	0.065		<.0001	0.020	0.314	0.013
dmt_{10} cm	r	0.484	0.488	0.431	0.434	0.981	1.000	-0.569	-0.216	-0.567
	p	0.036	0.034	0.066	0.064	<.0001		0.011	0.374	0.011
AM_{10} N•m	r	-0.849	-0.847	-0.837	-0.834	-0.529	-0.569	1.000	-0.672	0.986
	p	<.0001	<.0001	<.0001	<.0001	0.020	0.011		0.002	<.0001
AT_{10} N	r	0.560	0.553	0.588	0.580	-0.244	-0.216	-0.672	1.000	-0.663
	p	0.013	0.014	0.008	0.009	0.314	0.374	0.002		0.002
$InvM_{10}$ N•m	r	-0.876	-0.875	-0.861	-0.859	-0.557	-0.567	0.986	-0.663	1.000
	p	<.0001	<.0001	<.0001	<.0001	0.013	0.011	<.0001	0.002	

(B)		Net $\dot{V}O_2$ $L \cdot min^{-1}$	Gross $\dot{V}O_2$ $L \cdot min^{-1}$	Net COT $J \cdot m^{-1}$	Gross COT $J \cdot m^{-1}$	dmt_0 cm	dmt_{10} cm	AM_{10} N•m	AT_{10} N	$InvM_{10}$ N•m
Net $\dot{V}O_2$ $L \cdot min^{-1}$	r	1.000	0.999	0.991	0.988	0.466	0.452	-0.934	0.655	-0.944
	p		<.0001	<.0001	<.0001	0.045	0.052	<.0001	0.002	<.0001
Gross $\dot{V}O_2$ $L \cdot min^{-1}$	r	0.999	1.000	0.991	0.991	0.471	0.458	-0.937	0.653	-0.947
	p	<.0001		<.0001	<.0001	0.042	0.049	<.0001	0.002	<.0001
Net COT $J \cdot m^{-1}$	r	0.991	0.991	1.000	0.999	0.421	0.412	-0.939	0.691	-0.950
	p	<.0001	<.0001		<.0001	0.073	0.079	<.0001	0.001	<.0001
Gross COT $J \cdot m^{-1}$	r	0.988	0.991	0.999	1.000	0.425	0.417	-0.940	0.688	-0.951
	p	<.0001	<.0001	<.0001		0.070	0.075	<.0001	0.001	<.0001
dmt_0 cm	r	0.466	0.471	0.421	0.425	1.000	0.982	-0.488	-0.258	-0.481
	p	0.045	0.042	0.073	0.070		<.0001	0.034	0.286	0.037
dmt_{10} cm	r	0.452	0.458	0.412	0.417	0.982	1.000	-0.503	-0.260	-0.477
	p	0.052	0.049	0.079	0.075	<.0001		0.028	0.282	0.039
AM_{10} N•m	r	-0.934	-0.937	-0.939	-0.940	-0.488	-0.503	1.000	-0.696	0.995
	p	<.0001	<.0001	<.0001	<.0001	0.034	0.028		0.001	<.0001
AT_{10} N	r	0.655	0.653	0.691	0.688	-0.258	-0.260	-0.696	1.000	-0.714
	p	0.002	0.002	0.001	0.001	0.286	0.282	0.001		0.001
$InvM_{10}$ N•m	r	-0.944	-0.947	-0.950	-0.951	-0.481	-0.477	0.995	-0.714	1.000
	p	<.0001	<.0001	<.0001	<.0001	0.037	0.039	<.0001	0.001	

Table B.2: Correlation tables for absolute data of FF group when performing the (A) RF pattern and the (B) FF pattern.

(A)		Net $\dot{V}O_2$ $L \cdot min^{-1}$	Gross $\dot{V}O_2$ $L \cdot min^{-1}$	Net COT $J \cdot m^{-1}$	Gross COT $J \cdot m^{-1}$	dmt_0 cm	dmt_{10} cm	AM_{10} N•m	AT_{10} N	$InvM_{10}$ N•m
Net $\dot{V}O_2$ $L \cdot min^{-1}$	r	1.000	0.994	0.996	0.994	0.070	-0.099	-0.560	0.611	-0.600
	p		<.0001	<.0001	<.0001	0.784	0.695	0.016	0.007	0.009
Gross $\dot{V}O_2$ $L \cdot min^{-1}$	r	0.994	1.000	0.987	0.996	0.137	-0.050	-0.600	0.631	-0.639
	p	<.0001		<.0001	<.0001	0.589	0.843	0.008	0.005	0.004
Net COT $J \cdot m^{-1}$	r	0.996	0.987	1.000	0.994	0.028	-0.138	-0.517	0.580	-0.559
	p	<.0001	<.0001		<.0001	0.912	0.584	0.028	0.012	0.016
Gross COT $J \cdot m^{-1}$	r	0.994	0.996	0.994	1.000	0.094	-0.090	-0.559	0.602	-0.600
	p	<.0001	<.0001	<.0001		0.711	0.722	0.016	0.008	0.009
dmt_0 cm	r	0.070	0.137	0.028	0.094	1.000	0.916	-0.392	0.077	-0.352
	p	0.784	0.589	0.912	0.711		<.0001	0.108	0.761	0.152
dmt_{10} cm	r	-0.099	-0.050	-0.138	-0.090	0.916	1.000	-0.253	-0.100	-0.175
	p	0.695	0.843	0.584	0.722	<.0001		0.310	0.692	0.488
AM_{10} N•m	r	-0.560	-0.600	-0.517	-0.559	-0.392	-0.253	1.000	-0.932	0.993
	p	0.016	0.008	0.028	0.016	0.108	0.310		<.0001	<.0001
AT_{10} N	r	0.611	0.631	0.580	0.602	0.077	-0.100	-0.932	1.000	-0.953
	p	0.007	0.005	0.012	0.008	0.761	0.692	<.0001		<.0001
$InvM_{10}$ N•m	r	-0.600	-0.639	-0.559	-0.600	-0.352	-0.175	0.993	-0.953	1.000
	p	0.009	0.004	0.016	0.009	0.152	0.488	<.0001	<.0001	

(B)		Net $\dot{V}O_2$ $L \cdot min^{-1}$	Gross $\dot{V}O_2$ $L \cdot min^{-1}$	Net COT $J \cdot m^{-1}$	Gross COT $J \cdot m^{-1}$	dmt_0 cm	dmt_{10} cm	AM_{10} N•m	AT_{10} N	$InvM_{10}$ N•m
Net $\dot{V}O_2$ $L \cdot min^{-1}$	r	1.000	0.994	0.997	0.994	0.011	-0.140	-0.675	0.677	-0.677
	p		<.0001	<.0001	<.0001	0.966	0.579	0.002	0.002	0.002
Gross $\dot{V}O_2$ $L \cdot min^{-1}$	r	0.994	1.000	0.988	0.997	0.083	-0.092	-0.705	0.687	-0.709
	p	<.0001		<.0001	<.0001	0.744	0.718	0.001	0.002	0.001
Net COT $J \cdot m^{-1}$	r	0.997	0.988	1.000	0.994	-0.028	-0.172	-0.661	0.675	-0.664
	p	<.0001	<.0001		<.0001	0.912	0.495	0.003	0.002	0.003
Gross COT $J \cdot m^{-1}$	r	0.994	0.997	0.994	1.000	0.042	-0.125	-0.692	0.687	-0.697
	p	<.0001	<.0001	<.0001		0.867	0.621	0.002	0.002	0.001
dmt_0 cm	r	0.011	0.083	-0.028	0.042	1.000	0.908	-0.209	-0.107	-0.196
	p	0.966	0.744	0.912	0.867		<.0001	0.405	0.671	0.437
dmt_{10} cm	r	-0.140	-0.092	-0.172	-0.125	0.908	1.000	0.019	-0.356	0.055
	p	0.579	0.718	0.495	0.621	<.0001		0.940	0.147	0.828
AM_{10} N•m	r	-0.675	-0.705	-0.661	-0.692	-0.209	0.019	1.000	-0.936	0.997
	p	0.002	0.001	0.003	0.002	0.405	0.940		<.0001	<.0001
AT_{10} N	r	0.677	0.687	0.675	0.687	-0.107	-0.356	-0.936	1.000	-0.947
	p	0.002	0.002	0.002	0.002	0.671	0.147	<.0001		<.0001
$InvM_{10}$ N•m	r	-0.677	-0.709	-0.664	-0.697	-0.196	0.055	0.997	-0.947	1.000
	p	0.002	0.001	0.003	0.001	0.437	0.828	<.0001	<.0001	

Table B.3: Correlation tables for relative data of RF group when performing the (A) RF pattern and the (B) FF pattern.

(A)		Net $\dot{V}O_2$ ml•kg^{-1} •min^{-1}	Gross $\dot{V}O_2$ ml•kg^{-1} •min^{-1}	Net COT J•m^{-1} •kg^{-1}	Gross COT J•m^{-1} •kg^{-1}	dmt_0 cm	dmt_{10} cm	AM_{10} N•m •kg^{-1}	AT_{10} N•kg^{-1}	$InvM_{10}$ N•m •kg^{-1}
Net $\dot{V}O_2$ ml•kg^{-1} •min^{-1}	r	1.000	0.983	0.921	0.904	-0.042	-0.043	0.030	-0.006	-0.006
	p		<.0001	<.0001	<.0001	0.866	0.862	0.903	0.980	0.981
Gross $\dot{V}O_2$ ml•kg^{-1} •min^{-1}	r	0.983	1.000	0.901	0.914	-0.029	-0.038	-0.005	0.015	0.009
	p	<.0001		<.0001	<.0001	0.906	0.877	0.983	0.953	0.972
Net COT J·m^{-1}•kg^{-1}	r	0.921	0.901	1.000	0.986	-0.219	-0.205	0.221	-0.026	-0.033
	p	<.0001	<.0001		<.0001	0.368	0.400	0.364	0.915	0.892
Gross COT J·m^{-1}•kg^{-1}	r	0.904	0.914	0.986	1.000	-0.214	-0.206	0.196	-0.010	-0.022
	p	<.0001	<.0001	<.0001		0.380	0.397	0.421	0.968	0.929
dmt_0 cm	r	-0.042	-0.029	-0.219	-0.214	1.000	0.981	-0.737	-0.378	-0.387
	p	0.866	0.906	0.368	0.380		<.0001	0.000	0.110	0.102
dmt_{10} cm	r	-0.043	-0.038	-0.205	-0.206	0.981	1.000	-0.702	-0.455	-0.409
	p	0.862	0.877	0.400	0.397	<.0001		0.001	0.050	0.082
AM_{10} N•m•kg^{-1}	r	0.030	-0.005	0.221	0.196	-0.737	-0.702	1.000	-0.297	-0.300
	p	0.903	0.983	0.364	0.421	0.000	0.001		0.217	0.212
AT_{10} N•kg^{-1}	r	-0.006	0.015	-0.026	-0.010	-0.378	-0.455	-0.297	1.000	0.944
	p	0.980	0.953	0.915	0.968	0.110	0.050	0.217		<.0001
$InvM_{10}$ N•m•kg^{-1}	r	-0.006	0.009	-0.033	-0.022	-0.387	-0.409	-0.300	0.944	1.000
	p	0.981	0.972	0.892	0.929	0.102	0.082	0.212	<.0001	

(B)		Net $\dot{V}O_2$ ml•kg^{-1} •min^{-1}	Gross $\dot{V}O_2$ ml•kg^{-1} •min^{-1}	Net COT J•m^{-1} •kg^{-1}	Gross COT J•m^{-1} •kg^{-1}	dmt_0 cm	dmt_{10} cm	AM_{10} N•m •kg^{-1}	AT_{10} N•kg^{-1}	$InvM_{10}$ N•m •kg^{-1}
Net $\dot{V}O_2$ ml•kg^{-1} •min^{-1}	r	1.000	0.985	0.915	0.896	0.008	0.025	0.230	-0.436	-0.458
	p		<.0001	<.0001	<.0001	0.974	0.919	0.344	0.062	0.048
Gross $\dot{V}O_2$ ml•kg^{-1} •min^{-1}	r	0.985	1.000	0.904	0.914	0.016	0.034	0.217	-0.436	-0.465
	p	<.0001		<.0001	<.0001	0.947	0.891	0.372	0.062	0.045
Net COT J·m^{-1}•kg^{-1}	r	0.915	0.904	1.000	0.987	-0.161	-0.119	0.366	-0.429	-0.454
	p	<.0001	<.0001		<.0001	0.511	0.628	0.124	0.067	0.051
Gross COT J·m^{-1}•kg^{-1}	r	0.896	0.914	0.987	1.000	-0.154	-0.111	0.353	-0.428	-0.458
	p	<.0001	<.0001	<.0001		0.530	0.650	0.138	0.068	0.049
dmt_0 cm	r	0.008	0.016	-0.161	-0.154	1.000	0.982	-0.741	-0.334	-0.293
	p	0.974	0.947	0.511	0.530		<.0001	0.000	0.163	0.224
dmt_{10} cm	r	0.025	0.034	-0.119	-0.111	0.982	1.000	-0.722	-0.388	-0.318
	p	0.919	0.891	0.628	0.650	<.0001		0.001	0.101	0.185
AM_{10} N•m•kg^{-1}	r	0.230	0.217	0.366	0.353	-0.741	-0.722	1.000	-0.336	-0.395
	p	0.344	0.372	0.124	0.138	0.000	0.001		0.159	0.094
AT_{10} N•kg^{-1}	r	-0.436	-0.436	-0.429	-0.428	-0.334	-0.388	-0.336	1.000	0.980
	p	0.062	0.062	0.067	0.068	0.163	0.101	0.159		<.0001
$InvM_{10}$ N•m•kg^{-1}	r	-0.458	-0.465	-0.454	-0.458	-0.293	-0.318	-0.395	0.980	1.000
	p	0.048	0.045	0.051	0.049	0.224	0.185	0.094	<.0001	

Table B.4: Correlation tables for relative data of the FF group when performing the (A) RF pattern and the (B) FF pattern.

(A)		Net $\dot{V}O_2$ ml•kg^{-1} •min^{-1}	Gross $\dot{V}O_2$ ml•kg^{-1} •min^{-1}	Net COT J•m^{-1} •kg^{-1}	Gross COT J•m^{-1} •kg^{-1}	dmt_0 cm	dmt_{10} cm	AM_{10} N•m •kg^{-1}	AT_{10} N•kg^{-1}	$InvM_{10}$ N•m •kg^{-1}
Net $\dot{V}O_2$ ml•kg^{-1} •min^{-1}	r	1.000	0.971	0.994	0.979	-0.274	-0.449	-0.221	0.473	0.389
	p		<.0001	<.0001	<.0001	0.271	0.061	0.379	0.048	0.110
Gross $\dot{V}O_2$ ml•kg^{-1} •min^{-1}	r	0.971	1.000	0.952	0.993	-0.124	-0.346	-0.180	0.375	0.290
	p	<.0001		<.0001	<.0001	0.623	0.160	0.476	0.125	0.243
Net COT J·m^{-1}•kg^{-1}	r	0.994	0.952	1.000	0.973	-0.338	-0.494	-0.246	0.516	0.431
	p	<.0001	<.0001		<.0001	0.170	0.037	0.326	0.028	0.074
Gross COT J·m^{-1}•kg^{-1}	r	0.979	0.993	0.973	1.000	-0.199	-0.401	-0.209	0.429	0.341
	p	<.0001	<.0001	<.0001		0.430	0.099	0.404	0.076	0.166
dmt_0 cm	r	-0.274	-0.124	-0.338	-0.199	1.000	0.916	-0.072	-0.378	-0.312
	p	0.271	0.623	0.170	0.430		<.0001	0.776	0.122	0.207
dmt_{10} cm	r	-0.449	-0.346	-0.494	-0.401	0.916	1.000	-0.217	-0.280	-0.166
	p	0.061	0.160	0.037	0.099	<.0001		0.387	0.260	0.510
AM_{10} N•m•kg^{-1}	r	-0.221	-0.180	-0.246	-0.209	-0.072	-0.217	1.000	-0.872	-0.911
	p	0.379	0.476	0.326	0.404	0.776	0.387		<.0001	<.0001
AT_{10} N•kg^{-1}	r	0.473	0.375	0.516	0.429	-0.378	-0.280	-0.872	1.000	0.982
	p	0.048	0.125	0.028	0.076	0.122	0.260	<.0001		<.0001
$InvM_{10}$ N•m•kg^{-1}	r	0.389	0.290	0.431	0.341	-0.312	-0.166	-0.911	0.982	1.000
	p	0.110	0.243	0.074	0.166	0.207	0.510	<.0001	<.0001	

(B)		Net $\dot{V}O_2$ ml•kg^{-1} •min^{-1}	Gross $\dot{V}O_2$ ml•kg^{-1} •min^{-1}	Net COT J•m^{-1} •kg^{-1}	Gross COT J•m^{-1} •kg^{-1}	dmt_0 cm	dmt_{10} cm	AM_{10} N•m •kg^{-1}	AT_{10} N•kg^{-1}	$InvM_{10}$ N•m •kg^{-1}
Net $\dot{V}O_2$ ml•kg^{-1} •min^{-1}	r	1.000	0.970	0.993	0.969	-0.381	-0.439	0.099	0.185	0.157
	p		<.0001	<.0001	<.0001	0.119	0.068	0.696	0.462	0.535
Gross $\dot{V}O_2$ ml•kg^{-1} •min^{-1}	r	0.970	1.000	0.958	0.992	-0.237	-0.350	0.096	0.134	0.098
	p	<.0001		<.0001	<.0001	0.344	0.155	0.706	0.595	0.698
Net COT J·m^{-1}•kg^{-1}	r	0.993	0.958	1.000	0.972	-0.444	-0.492	0.134	0.173	0.141
	p	<.0001	<.0001		<.0001	0.065	0.038	0.596	0.493	0.577
Gross COT J·m^{-1}•kg^{-1}	r	0.969	0.992	0.972	1.000	-0.312	-0.413	0.135	0.123	0.084
	p	<.0001	<.0001	<.0001		0.207	0.089	0.594	0.626	0.741
dmt_0 cm	r	-0.381	-0.237	-0.444	-0.312	1.000	0.908	-0.364	-0.101	-0.070
	p	0.119	0.344	0.065	0.207		<.0001	0.138	0.691	0.783
dmt_{10} cm	r	-0.439	-0.350	-0.492	-0.413	0.908	1.000	-0.585	0.116	0.178
	p	0.068	0.155	0.038	0.089	<.0001		0.011	0.647	0.480
AM_{10} N•m•kg^{-1}	r	0.099	0.096	0.134	0.135	-0.364	-0.585	1.000	-0.869	-0.893
	p	0.696	0.706	0.596	0.594	0.138	0.011		<.0001	<.0001
AT_{10} N•kg^{-1}	r	0.185	0.134	0.173	0.123	-0.101	0.116	-0.869	1.000	0.991
	p	0.462	0.595	0.493	0.626	0.691	0.647	<.0001		<.0001
$InvM_{10}$ N•m•kg^{-1}	r	0.157	0.098	0.141	0.084	-0.070	0.178	-0.893	0.991	1.000
	p	0.535	0.698	0.577	0.741	0.783	0.480	<.0001	<.0001	

APPENDIX E

DESCRIPTION OF MUSCULOSKELETAL & ENERGETICS MODELS

Musculoskeletal Model

The musculoskeletal model that was used in Study 3 was adapted from those used in similar studies investigating triceps surae muscle function in running or jumping (Bobbert et al., 1986a; Hof et al., 2002; van Soest and Bobbert, 1993). The metabolic work used a previously published model (Minetti and Alexander, 1997; Sellers et al., 2003). The muscle parameter A_{REL} took muscle fiber type into consideration thereby improving the representation of the power capability of the muscles (Umberger et al., 2003; Umberger et al., 2006). The model consisted of three rigid segments representing the foot, leg and thigh (Figure E.1). Inputs to the model included the experimental ankle joint moment, ankle and knee joint angles and static Achilles tendon moment arm lengths calculated from the data in Study 2. All variables determined by the model were calculated for the gastrocnemius (GA) and soleus (SO) individually as well as each participant individually. Muscle parameter values specific to the GA and SO are listed in Table E.1. Refer to Appendix F for a list of all abbreviations used in the model.

Table E.1: Parameter values used to determine muscle properties. Maximum isometric force production at optimum fiber length (F_0) was taken from Hof et al. (2002). Optimum fiber length (L_0) was taken from Out et al. (1996). Tendon slack length (L_S) and physiological cross sectional area (PCSA) were taken from Arnold et al. (2010). Maximum length range for force production relative to L_0 (w) and percent fast twitch muscle fibers (%FT) were taken from Umberger et al. (2006). The normalized Hill constant a (A_{REL}) was calculated from %FT. The normalized Hill constant b (B_{REL}) was calculated from A_{REL} and a maximum shortening velocity of 15 $L_0 \cdot s^{-1}$.

	F_0 (N)	L_0 (cm)	L_S (cm)	PSCA (cm)	w	%FT	A_{REL}	B_{REL}
GA	2900	4.9	39.1	31.3	0.56	50	0.30	4.50
SO	7500	4.3	27.9	58.8	0.56	20	0.18	2.75

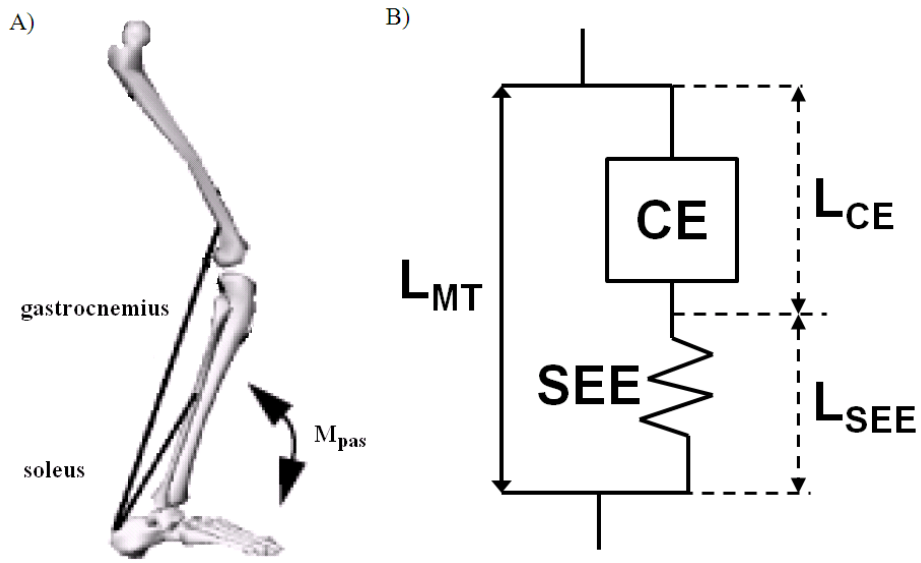

Figure E.1: A) Link segment model representing the foot, leg, thigh, gastrocnemius, soleus, and passive moment (M_{pas}) (Adapted from Nagano et al., 2001). B) Elements of the Hill-type model representing each muscle.

The moment arm length (d_{MT}) of each muscle was based on the generic model described by Arnold et al. (2010) and was expressed as a function of joint angle (θ) (Grieve et al., 1978). A plot of d_{MT} as a function of joint angle was created for the GA and SO from the Arnold et al. (2010) data. The model data were fit to a second-order polynomial by a custom MATLAB program (Mathworks, Inc., Natick, MA) and used to determine the polynomial coefficients. A second-order polynomial was the lowest order that adequately fit the moment arm data, based on an assessment of the root mean square error between the polynomial prediction and the data. The polynomials representing the relationship between d_{MT} and θ which took the form:

$$d_{MT\text{-}GA} = a_0 + a_1\theta_{ank} + a_2\theta_{ank}^2 \quad \text{(E1)}$$

$$d_{MT\text{-}SO} = a_0 + a_1\theta_{ank} + a_2\theta_{ank}^2 + a_3\theta_{ank}^3 \quad \text{(E2)}$$

The zeroth-order polynomial coefficient was scaled for each subject individually by the static Achilles tendon moment arm measurement. Equations E1 and E2 were integrated with respect to the knee and ankle joint angle, thus creating third-order polynomials for GA and SO muscle tendon length (L_{MT}) as a function θ:

$$L_{MT\text{-}GA} = c_0 - a_0\theta_{ank} + \frac{a_1\theta_{ank}^2}{2} + \frac{a_2\theta_{ank}^3}{3} + b_0\theta_{kn} + \frac{b_1\theta_{kn}^2}{2} + \frac{b_2\theta_{kn}^3}{3} \quad \text{(E3)}$$

$$L_{MT\text{-}SO} = c_0 - a_0\theta_{ank} + \frac{a_1\theta_{ank}^2}{2} + \frac{a_2\theta_{ank}^3}{3} \quad \text{(E4)}$$

where c_0 was the L_{MT} when the ankle and knee angles were zero (Arnold et al., 2010). L_{MT} was defined as the length between the muscle origin and insertion, and was expressed as a function of the joint angle (θ) (Grieve et al., 1978). The zeroth-order coefficients for the L_{MT} polynomials were scaled based on the participant's static leg length. Equations E3 and E4 were differentiated with respect to time to determine the muscle velocity (V_{MT}) as a function of θ:

$$V_{MT\text{-}GA} = -a_0\theta_{ank} - b_0\theta_{kn} - 2b_1\theta_{ank}\theta_{ank} - 2b_1\theta_{kn}\theta_{kn} - 3a_2\theta_{ank}^2\theta_{ank} - 3b_2\theta_{kn}^2\theta_{kn} \quad \text{(E5)}$$

$$V_{MT\text{-}SO} = -1(a_0 + 2\,a_1\theta_{ank} + 3a_2\theta_{ank}^2\theta_{ank}) \quad \text{(E6).}$$

The force produced in each muscle was determined from the ankle joint moment (M_A), determined by inverse dynamics procedure from Study 2. M_A was defined as the

net sum of the active plantar flexor muscles and all passive structures acting about the ankle joint. A passive moment (M_{pas}) was used to represent the passive resistance by the muscle fascia, ligaments, joint capsule and joint contact forces (Hatze, 1997). M_{pas} was a function of the ankle and knee joint angles (Riener and Edrich, 1999) and was equal to:

$$M_{pas} = -\exp(2.1016 + 0.0843\varphi_A - 0.0176\varphi_K) - \exp(-7.9763 - 0.1949\varphi_A + 0.0008\varphi_K) - 1.792 \quad \text{(E7)}$$

where φ_A and φ_K are the ankle and knee joints, respectively. Therefore, the active contribution (M_{act}) to the ankle joint moment was calculated by:

$$M_{act} = M_A - M_{pas} \quad \text{(E8).}$$

The active contribution to the ankle joint moment was used to calculate the force generated by the triceps surae as a sum of the forces produced by the GA (F_{GA}) and SO (F_{SO}).

$$M_{act} = F_{GA} \bullet d_{MT\text{-}GA} + F_{SO} \bullet d_{MT\text{-}SO} \quad \text{(E9)}$$

where the force generated by the GA and SO was a proportion of each muscle's physiological cross sectional area (PCSA) to the PCSA of the triceps surae. The ratio between GA and SO PCSA 1.8786:1, therefore the force produced by each muscle was:

$$1.8786F_{GA} = F_{SO} \quad \text{(E10).}$$

The force produced by each muscle-tendon complex (F_{MT}) was equal to the force generated by the contractile element (F_{CE}). F_{CE} is transmitted completely through the series elastic element (SEE), therefore the F_{CE} and the F_{SEE} are equal and must satisfy the equation:

$$F_{MT} = F_{CE} = F_{SEE} \quad \text{(E11).}$$

The length of the SEE (L_{SEE}) was calculated from F_{SEE}, which is modeled as a nonlinear spring (van Soest and Bobbert, 1993). The amount of force that the SEE can produce depends on the L_{SEE}. The SEE can only produce force when L_{SEE} is greater than the slack length (L_S), which is the minimum length the SEE can transmit force. When $L_{SEE} \geq L_S$, then:

$$L_{SEE} = L_s + \frac{(F_{SEE})^{0.5}}{(K_{SEE})^{0.5}} \quad \text{(E12)}$$

where

$$K_{SEE} = \frac{F_0}{(U_{MAX} \cdot L_S)^2} \cdot U_{MAX} \quad \text{(E13)}$$

and where K_{SEE} was the stiffness and U_{MAX} was the relative elongation of the SEE at F_0 which was equal to 0.04 (Ettema and Huijing, 1989); and F_0 was the maximum isometric

force produced at optimal CE length (L_0). The length of the L_{SEE} and contractile element length (L_{CE}) were constrained to equal the L_{MT} found for each muscle. Therefore, L_{CE} was found by:

$$L_{CE} = L_{MT} - L_{SEE} \quad \text{(E14)},$$

and thus L_{CE} and L_{SEE} are dependent on the force within each element.

Muscle contraction dynamics of the force-length relationship was used to calculate the length of the CE (L_{CE}) for each muscle. The force-length relationship simulates the amount of force production capability based on muscle length and was calculated as:

$$F_{ISOM} = c \cdot \left(\frac{L_{CE}}{L_0}\right)^2 - 2c \cdot \left(\frac{L_{CE}}{L_0}\right) + c + 1 \quad \text{(E15)}$$

where

$$c = \frac{-1}{w^2} \quad \text{(E16)}$$

and where F_{IOSM} was the force relative to F_0 that would be produced isometrically at any length of the CE relative to L_0; and *w* was the maximum length range for force production relative to L_0 (van Soest and Bobbert, 1993). The variable *w* was equal to 0.61 for the GA and 0.80 for the SO (Umberger et al., 2006) (Table E.1). L_{CE} was between $(1 - w)\cdot L_0$ and $(1 + w)\cdot L_0$ (van Soest and Bobbert, 1993).

The velocity of each SEE of each muscle (V_{SEE}) was determined by differentiating L_{SEE} with respect to time (t):

$$V_{SEE} = \frac{d(L_{SEE})}{d(t)} \tag{E17}$$

The velocity of the CE (V_{CE}) can then be calculated by:

$$V_{CE} = V_{MT} - V_{SEE} \tag{E18}.$$

The power produced by each muscle (P_{MT}) was the product of the muscle force and muscle velocity:

$$P_{MT} = F_{MT} \cdot V_{MT} \tag{E19}$$

$$P_{CE} = F_{CE} \cdot V_{CE} \tag{E20}$$

$$P_{SEE} = F_{SEE} \cdot V_{SEE} \tag{E21}.$$

The amount of mechanical work produced by the MT, CE, and SEE were calculated by trapezoidal numerical integration of the power generation with respect to t during the stance phase:

$$\int P \bullet dt \tag{E22}$$

Net mechanical work was the sum of all mechanical work produced during the stance phase. Positive mechanical work indicated energy generation and was the total of the positive area of the power-time curve. Similarly, negative work, indicating energy absorption, was the total of the negative area of the power-time curve.

The amount of muscle force generation was dependent on the level of muscle activation (ACT) as well as the kinematic state of the muscle. Therefore, ACT can be calculated by first determining the force potential of the muscle given its kinematic state. The calculation of ACT began with determining the dynamic force (F_{dyn}) production if $L_{CE} = L_0$ given the instantaneous V_{CE} (Epstein and Herzog, 1998) by the following equation representing the Hill (1938) force-velocity relationship:

$$F_{dyn} = \begin{cases} 0 & \text{if } V_{CE} \le -V_0 \\ F_0 b + \dfrac{V_{CE} a}{-V_{CE} + b} & \text{if } V_{CE} > -V_0 \text{ and } V_{CE} \le 0 \\ F_0 F_{asympt} - 0.5\left[\dfrac{F_0 b' - V_{CE} a'}{V_{CE} + b}\right] & \text{if } V_{CE} > 0 \text{ and } V_{CE} \le F_0 \dfrac{b'}{a'} \\ F_0 F_{asympt} & \text{if } V_{CE} > F_0 \dfrac{b'}{a'} \end{cases} \quad \text{(E23)}$$

where a and b were the Hill constants, a' = 0.1a, b' = 0.1b, V_0 was the magnitude of the maximum CE velocity, F_0 was the maximum isometric force production at L_0, and F_{asympt} was the asymptotic maximum force value in the eccentric phase (relative to F_0). F_{asympt} was equal 1.5 (Joyce and Rack, 1969; van Soest and Bobbert, 1993). The shape of the force-velocity curve and the magnitude of the V_0 where dictated by the value of A_{REL} and B_{REL} (Umberger et al., 2003). A_{REL} and B_{REL} were the normalized Hill constants a and b (van Soest and Bobbert, 1993). Due to slow twitch muscle fibers being recruited at low activation levels and their low force generation capability, A_{REL} and B_{REL} were adjusted

to account for fiber type composition (Umberger et al., 2003; Winters and Stark, 1988) by the following equations:

$$A_{REL} = 0.1 + 0.4(\%FT/100) \quad \text{(E24)}$$

$$B_{REL} = A_{REL}\tilde{V}_0 \quad \text{(E25)}$$

where

$$\tilde{V}_{CE} = V_{CE}/L_0 \quad \text{(E26)}$$

and where %FT was the percentage of fast twitch muscle fibers in the muscle and $\tilde{V}_0$was V_0 expressed relative to L_0 with units $L_0 \bullet s^{-1}$. A_{REL} was equal to 0.3 and 0.18 for the GA and SO respectively (Umberger et al., 2006) and B_{REL} was equal to 4.5 and 2.75 for the GA and SO respectively (Table D1). Therefore, $\tilde{V}_0$ was equal to 15 $L_0 \bullet s^{-1}$ in this model. Previous simulations of human muscle have used maximum shortening velocities of between 8 -14 $L_0 \bullet s^{-1}$ (Epstein and Herzog, 1998; Lichtwark and Wilson, 2006). After determining F_{dyn}, ACT could then be calculated from the instantaneous F_{CE} relative to F_{dyn}:

$$ACT = \frac{F_{CE}}{F_{potential}} \quad \text{(E27)}$$

where

$$F_{potential} = F_{dyn} \bullet F_{ISOM} \quad \text{(E28).}$$

where $F_{potential}$ was F_{dyn} adjusted by F_{ISOM}. As described above, F_{dyn} was the dynamic force production if $L_{CE} = L_0$ given the instantaneous V_{CE}, and F_{IOSM} was the force relative to F_0 that would be produced isometrically at any length of the CE relative to L_0.

Muscle Energy Expenditure Model

The muscle energy expenditure model that was used for Study 3 was adapted from previous studies (Minetti and Alexander, 1997; Sellers et al., 2003). Energy expenditure from the GA and SO was calculated separately for each individual participant.

ACT was used to determine the metabolic power of the muscle for each instant of the stance phase. Metabolic power was expended when the muscle fibers were activated and generated force. The amount of metabolic power/energy consumption was dependent on ACT and V_{CE}. Therefore, the amount of metabolic power (P_{MET}) can be determined as a function of activation (ACT), maximum isometric force production (F_0), and relative V_{CE} (V_{CE}/V_0) (Minetti and Alexander, 1997; Sellers et al., 2003):

$$P_{MET} = ACT\ F_0 V_0 \Phi \left(\frac{V_{CE}}{V_0}\right) \tag{E29}$$

where

$$\Phi\left(\frac{V_{CE}}{V_0}\right) = \frac{0.054 + 0.506\left(-\frac{V_{CE}}{V_0}\right) + 2.46\left(-\frac{V_{CE}}{V_0}\right)^2}{1 - 1.13\left(-\frac{V_{CE}}{V_0}\right) + 12.8\left(-\frac{V_{CE}}{V_0}\right)^2 - 1.64\left(-\frac{V_{CE}}{V_0}\right)^3} \tag{E30}$$

.

Equation E29 was found by Minetti and Alexander (1997) who fit an algebraic equation to the data from Ma and Zahalak (1991). The data by Ma and Zahalak (1991) were experimental values of P_{MET} as a function of relative CE velocity (V_{CE}/V_0). CE metabolic energy expenditure was then calculated by integrating P_{MET} with respect to time.

$$\int P_{MET} \bullet dt \tag{E31}$$

References

1. Arnold EM, Ward SR, Lieber RL, Delp SL. A Model of the Lower Limb for Analysis of Human Movement. **Ann Biomed Eng**. 2010; 38(2):269-279.

2. Bobbert MF, Huijing PA, van Ingen Schenau GJ. A Model of the Human Triceps Surae Muscle-Tendon Complex Applied to Jumping. **J Biomech**. 1986a; 19(11):887-898.

3. Epstein M and Herzog W. Theoretical Models of Skeletal Muscle: Biological and Mathematical Considerations. John Wiley & Sons, 1998.

4. Ettema GJC and Huijing PA. Properties of Tendinous Structures and Series Elastic Componets of Edl Muscle Tendon Complex of the Rat. **J Biomech**. 1989; 22(1209-1215.

5. Grieve DW, Pheasant S, Cavanagh PR. Prediction of Gastrocnemius Length from Knee and Ankle Joint Posture. Biomechanics Vi-A. E. Asmussen, K. Jorgensen and (Eds.). University Park Press, Baltimore,,1978. 405-412.

6. Hatze H. A Three-Dimensional Multivariate Model of Passive Human Joint Torques and Articular Boundaries. **Clin Biomech (Bristol, Avon)**. 1997; 12(2):128-135.

7. Hill AV. The Heat of Shortening and the Dynamic Constants of Muscle. **Proc Royal Soc**. 1938; 126B(136-195.

8. Hof AL, Van Zandwijk JP, Bobbert MF. Mechanics of Human Triceps Surae Muscle in Walking, Running and Jumping. **Acta Physiol Scand**. 2002; 174(1):17-30.

9. Joyce GC and Rack PM. Isotonic Lengthening and Shortening Movements of Cat Soleus Muscle. **J Physiol**. 1969; 204(2):475-491.

10. Lichtwark GA and Wilson AM. Interactions between the Human Gastrocnemius Muscle and the Achilles Tendon During Incline, Level and Decline Locomotion. **J Exp Biol**. 2006; 209(Pt 21):4379-4388.

11. Ma SP and Zahalak GI. A Distribution-Moment Model of Energetics in Skeletal Muscle. **J Biomech**. 1991; 24(1):21-35.

12. Minetti AE and Alexander RM. A Theory of Metabolic Costs for Bipedal Gaits. **J Theor Biol**. 1997; 186(4):467-476.

13. Out L, Vrijkotte TG, van Soest AJ, Bobbert MF. Influence of the Parameters of a Human Triceps Surae Muscle Model on the Isometric Torque-Angle Relationship. **J Biomech Eng**. 1996; 118(1):17-25.

14. Sellers WI, Dennis LA, Crompton RH. Predicting the Metabolic Energy Costs of Bipedalism Using Evolutionary Robotics. **J Exp Biol**. 2003; 206(Pt 7):1127-1136.

15. Umberger BR, Gerritsen KG, Martin PE. A Model of Human Muscle Energy Expenditure. **Comput Methods Biomech Biomed Engin**. 2003; 6(2):99-111.

16. Umberger BR, Gerritsen KG, Martin PE. Muscle Fiber Type Effects on Energetically Optimal Cadences in Cycling. **J Biomech**. 2006; 39(8):1472-1479.

17. van Soest AJ and Bobbert MF. The Contribution of Muscle Properties in the Control of Explosive Movements. **Biol Cybern**. 1993; 69(3):195-204.

18. Winters JM and Stark L. Estimated Mechanical Properties of Synergistic Muscles Involved in Movements of a Variety of Human Joints. **J Biomech**. 1988; 21(12):1027-1041.

APPENDIX F

MODEL ABBREVIATIONS

a	Hill constant
ACT	muscle active state; activation level
A_{REL}	normalized Hill constant a
b	Hill constant
B_{REL}	normalized Hill constant b
CE	contractile element
d_{MT}	Moment arm of the muscle-tendon complex
E_{CE}	Metabolic energy expenditure
F	Force generated given the instantaneous muscle length and velocity
F_{CE}	force produced by the contractile element
F_0	Maximum isometric force production at optimal contractile element length
F_{GA}	force produced by the gastrocnemius muscle
F_{asympt}	Asymptotic maximum eccentric force in the force-velocity relation
Fdyn	Dynamic force production if LCE = L_0 and the instantaneous V_{CE}
F_{ISOM}	Force relative to the maximum isometric force that can be produced isometrically given the relative length of the contractile element
F_{MT}	force produced by the muscle-tendon complex
F_{SEE}	force produced by the series elastic element
F_{SO}	force produced by the soleus muscle
FT	Fast twitch muscle fibers
GA	gastrocnemius muscle
K_{SEE}	Relative elongation of the SEE at F_0
L_{CE}	length of the contractile element
L_{MT}	length of the muscle-tendon complex
L_{SEE}	length of the series elastic element
L_S	Series elastic element slack length
L_0	Optimal length of the contractile element for maximal isometric force production
M_A	Ankle joint moment
M_{act}	Moment produced by active forces of the triceps surae
M_{pas}	Moment produced by passive structures and forces
MT	Muscle-tendon complex
P	Muscle mechanical power
P_{CE}	Power produced by the contractile element
PCSA	Physiological cross-sectional area
P_{MET}	Muscle metabolic power

P_{MT}	Power produced by each muscle-tendon complex
P_{SEE}	Power produced by the series elastic element
φ	Ankle or knee joint angle used in the passive joint moment equation
SEE	series elastic element
SO	soleus muscle
θ	Joint angle
U_{MAX}	Relative elongation of SEE at F_0
$\widetilde{V}$	Velocity relative to L_0
V_{CE}	velocity of the contractile element
V_{MT}	velocity of the muscle-tendon complex
V_0	Maximum contractile element velocity
V_{SEE}	velocity of the series elastic element
w	Maximum length range for force production relative to L_0; Width of the parabola for the force-length relationship relative to L_0

BIBLIOGRAPHY

1. Albracht K and Arampatzis A. Influence of the Mechanical Properties of the Muscle-Tendon Unit on Force Generation in Runners with Different Running Economy. *Biol Cybern*. 2006; 95(1):87-96.

2. Albracht K, Arampatzis A, Baltzopoulos V. Assessment of Muscle Volume and Physiological Cross-Sectional Area of the Human Triceps Surae Muscle in Vivo. *J Biomech*. 2008; 41(10):2211-2218.

3. Alexander RM. Elastic Energy Stores in Running Vertebrates. *American Zoologist*. 1984; 24(1):85-94.

4. Anderson FC and Pandy MG. Storage and Utilization of Elastic Strain Energy During Jumping. *J Biomech*. 1993; 26(12):1413-1427.

5. Anderson T. Biomechanics and Running Economy. *Sports Med*. 1996; 22(2):76-89.

6. Arampatzis A, De Monte G, Karamanidis K, Morey-Klapsing G, Stafilidis S, Bruggemann GP. Influence of the Muscle-Tendon Unit's Mechanical and Morphological Properties on Running Economy. *J Exp Biol*. 2006; 209(Pt 17):3345-3357.

7. Ardigo LP, Lafortuna C, Minetti AE, Mognoni P, Saibene F. Metabolic and Mechanical Aspects of Foot Landing Type, Forefoot and Rearfoot Strike, in Human Running. *Acta Physiol Scand*. 1995; 155(1):17-22.

8. Arendse RE, Noakes TD, Azevedo LB, Romanov N, Schwellnus MP, Fletcher G. Reduced Eccentric Loading of the Knee with the Pose Running Method. *Med Sci Sports Exerc*. 2004; 36(2):272-277.

9. Arnold EM, Ward SR, Lieber RL, Delp SL. A Model of the Lower Limb for Analysis of Human Movement. *Ann Biomed Eng*. 2010; 38(2):269-279.

10. Azevedo LB, Lambert MI, Vaughan CL, O'Connor CM, Schwellnus MP. Biomechanical Variables Associated with Achilles Tendinopathy in Runners. *Br J Sports Med*. 2009; 43(4):288-292.

11. Bahler AS. Series Elastic Component of Mammalian Skeletal Muscle. *Am J Physiol*. 1967; 213(6):1560-1564.

12. Bates BT, James SL, Osternig LR. Foot Function During the Support Phase of Running. *Running*. 1978; Fall:24-31.

13. Belli A and Bosco C. Influence of Stretch-Shortening Cycle on Mechanical Behaviour of Triceps Surae During Hopping. *Acta Physiol Scand*. 1992; 144(4):401-408.

14. Bennell K, Crossley K, Jayarajan J, Walton E, Warden S, Kiss ZS, Wrigley T. Ground Reaction Forces and Bone Parameters in Females with Tibial Stress Fracture. *Med Sci Sports Exerc*. 2004; 36(3):397-404.

15. Biewener AA. Muscle-Tendon Stresses and Elastic Energy Storage During Locomotion in the Horse. *Comp Biochem Physiol B Biochem Mol Biol*. 1998; 120(1):73-87.

16. Biewener AA. Biomechanical Consequences of Scaling. *J Exp Biol*. 2005; 208(Pt 9):1665-1676.

17. Biewener AA, Farley CT, Roberts TJ, Temaner M. Muscle Mechanical Advantage of Human Walking and Running: Implications for Energy Cost. *J Appl Physiol*. 2004; 97(6):2266-2274.

18. Biewener AA and Roberts TJ. Muscle and Tendon Contributions to Force, Work, and Elastic Energy Savings: A Comparative Perspective. *Exerc Sport Sci Rev*. 2000; 28(3):99-107.

19. Bobbert MF, Huijing PA, van Ingen Schenau GJ. A Model of the Human Triceps Surae Muscle-Tendon Complex Applied to Jumping. *J Biomech*. 1986a; 19(11):887-898.

20. Bobbert MF, Schamhardt HC, Nigg BM. Calculation of Vertical Ground Reaction Force Estimates During Running from Positional Data. *J Biomech*. 1991; 24(12):1095-1105.

21. Bobbert MF and van Ingen Schenau GJ. Isokinetic Plantar Flexion: Experimental Results and Model Calculations. *J Biomech*. 1990; 23(2):105-119.

22. Bobbert MF, Yeadon MR, Nigg BM. Mechanical Analysis of the Landing Phase in Heel-Toe Running. *J Biomech*. 1992; 25(3):223-234.

23. Bohm H, Cole GK, Bruggemann GP, Ruder H. Contribution of Muscle Series Elasticity to Maximum Performance in Drop Jumping. *J Appl Biomech*. 2006; 22(1):3-13.

24. Bonacci J, Green D, Saunders PU, Blanch P, Franettovich M, Chapman AR, Vicenzino B. Change in Footstrike Position Is Related to Alterations in Running Economy in Triathletes. International Symposium on Biomechanics in Sports: Conference Proceedings Archive. 2010. 1-2.

25. Boyer KA and Nigg BM. Muscle Activity in the Leg Is Tuned in Response to Impact Force Characteristics. *J Biomech*. 2004; 37(10):1583-1588.

26. Boyer KA and Nigg BM. Changes in Muscle Activity in Response to Different Impact Forces Affect Soft Tissue Compartment Mechanical Properties. *J Biomech Eng*. 2007; 129(4):594-602.

27. Bredeweg S. No Relationship between Running Related Injuries and Kinetic Variables. *Br J Sports Med*. 2011; 45(4):328.

28. Brisswalter J and Legros P. Daily Stability in Energy Cost of Running, Respiratory Parameters and Stride Rate among Well-Trained Middle Distance Runners. *Int J Sports Med*. 1994; 15(5):238-241.

29. Brooks GA, Fahey TD, Baldwin KM. Exercise Physiology: Human Bioenergetics and Its Applications. McGraw-Hill, New York, NY, 2004.

30. Burdett RG. Forces Predicted at the Ankle During Running. *Med Sci Sports Exerc*. 1982; 14(4):308-316.

31. Burr DB, Milgrom C, Fyhrie D, Forwood M, Nyska M, Finestone A, Hoshaw S, Saiag E, Simkin A. In Vivo Measurement of Human Tibial Strains During Vigorous Activity. *Bone*. 1996; 18(5):405-410.

32. Butler RJ, Crowell HP, 3rd, Davis IM. Lower Extremity Stiffness: Implications for Performance and Injury. *Clin Biomech (Bristol, Avon)*. 2003; 18(6):511-517.

33. Carter DR, Caler WE, Spengler DM, Frankel VH. Fatigue Behavior of Adult Cortical Bone: The Influence of Mean Strain and Strain Range. *Acta Orthop Scand*. 1981; 52(5):481-490.

34. Cavagna GA. Storage and Utilization of Elastic Energy in Skeletal Muscle. *Exerc Sport Sci Rev*. 1977a; 5:89-129.

35. Cavagna GA, Heglund NC, Taylor CR. Mechanical Work in Terrestrial Locomotion: Two Basic Mechanisms for Minimizing Energy Expenditure. *Am J Physiol*. 1977b; 233(5):R243-261.

36. Cavagna GA and Kaneko M. Mechanical Work and Efficiency in Level Walking and Running. *J Physiol*. 1977c; 268(2):467--481.

37. Cavagna GA and Margaria R. [Mechanics of the Contraction of Muscle Previously Exposed to Stretching]. *Boll Soc Ital Biol Sper*. 1964; 40(24):Suppl:2051-2054.

38. Cavagna GA, Saibene FP, Margaria R. Mechanical Work in Running. *J Appl Physiol*. 1964; 19:249-256.

39. Cavanagh PR and Kram R. Mechanical and Muscular Factors Affecting the Efficiency of Human Movement. *Med Sci Sports Exerc*. 1985; 17(3):326-331.

40. Cavanagh PR and Lafortune MA. Ground Reaction Forces in Distance Running. *J Biomech*. 1980; 13(5):397-406.

41. Cavanagh PR, Valiant GA, Miserich KW. Biological Aspects of Modelling Shoe/Foot Interactions During Running. In: *Sports Shoes and Playing Surfaces*. Frederick EC (Ed.). Human Kinetics, Champaign, Illinois, 1984. 24-46.

42. Cavanagh PR and Williams KR. The Effect of Stride Length Variation on Oxygen Uptake During Distance Running. *Med Sci Sports Exerc*. 1982; 14(1):30-35.

43. Christiansen BA, Bayly PV, Silva MJ. Constrained Tibial Vibration in Mice: A Method for Studying the Effects of Vibrational Loading of Bone. *J Biomech Eng*. 2008; 130(4):044502.

44. Chu ML, Yazdani-Ardakani S, Gradisar IA, Askew MJ. An in Vitro Simulation Study of Impulsive Force Transmission Along the Lower Skeletal Extremity. *J Biomech*. 1986; 19(12):979-987.

45. Clarke TE, Cooper LB, Hamill CL, Clark DE. The Effect of Varied Stride Rate Upon Shank Deceleration in Running. *J Sports Sci*. 1985; 3(1):41-49.

46. Clarke TE, Frederick EC, Hamill CL. The Study of Rearfoot Movement in Running. In: *Sports Shoes and Playing Surfaces*. Frederick EC (Ed.). Human Kinetics, Champaign, IL, 1984. 166-189.

47. Cohen J. Statistical Power Analysis for the Behavioral Sciences. Lawrence Erlbaum Associates, Hillsdale (NJ), 1988.

48. Cohen J. A Power Primer. *Psychol Bull*. 1992; 112(1):155-159.

49. Cole GK, Nigg BM, Ronsky JL, Yeadon MR. Application of the Joint Coordinate System to Three-Dimensional Joint Attitude and Movement Representation: A Standardization Proposal. *J Biomech Eng*. 1993; 115(4A):344-349.

50. Cole GK, Nigg BM, van Den Bogert AJ, Gerritsen KG. The Clinical Biomechanics Award Paper 1995 Lower Extremity Joint Loading During Impact in Running. *Clin Biomech (Bristol, Avon)*. 1996a; 11(4):181-193.

51. Cole GK, van den Bogert AJ, Herzog W, Gerritsen KG. Modelling of Force Production in Skeletal Muscle Undergoing Stretch. *J Biomech*. 1996b; 29(8):1091-1104.

52. Coyle EF, Coggan AR, Hemmert MK, Ivy JL. Muscle Glycogen Utilization During Prolonged Strenuous Exercise When Fed Carbohydrate. *J Appl Physiol*. 1986; 61(1):165-172.

53. Crossley K, Bennell KL, Wrigley T, Oakes BW. Ground Reaction Forces, Bone Characteristics, and Tibial Stress Fracture in Male Runners. *Med Sci Sports Exerc*. 1999; 31(8):1088-1093.

54. Crowninshield RD and Brand RA. The Prediction of Forces in Joint Structures; Distribution of Intersegmental Resultants. *Exerc Sport Sci Rev*. 1981; 9:159-181.

55. Cunningham CB, Schilling N, Anders C, Carrier DR. The Influence of Foot Posture on the Cost of Transport in Humans. *J Exp Biol*. 2010; 213(5):790-797.

56. Daniels JT. A Physiologist's View of Running Economy. *Med Sci Sports Exerc*. 1985; 17(3):332-338.

57. Daoud AI, Geissler GJ, Wang F, Saretsky J, Daoud YA, Lieberman DE. Foot Strike and Injury Rates in Endurance Runners: A Retrospective Study. *Med Sci Sports Exerc*. 2012a; 44(7):1325-1334.

58. Daoud AI, Geissler GJ, Wang F, Saretsky J, Daoud YA, Lieberman DE. Foot Strike and Injury Rates in Endurance Runners: A Retrospective Study. *Med Sci Sports Exerc*. 2012b.

59. Davies MJ, Mahar MT, Cunningham LN. Running Economy: Comparison of Body Mass Adjustment Methods. *Res Q Exerc Sport*. 1997; 68(2):177-181.

60. Davis IS, Bowser B, Mullineaux DR. Do Impacts Cause Running Injuries? A Prospective Investigation. Proceedings of the Annual Meeting of the American Society of Biomechanics. 2010.

61. De Wit B, De Clercq D, Aerts P. Biomechanical Analysis of the Stance Phase During Barefoot and Shod Running. *J Biomech*. 2000; 33(3):269-278.

62. Denoth J. Load on the Locomotor System and Modelling. In: *Biomechanics of Running Shoes*. Nigg BM (Ed.). Human Kinetics, Champaign, Illinois, 1986. 63-116.

63. Derrick TR. The Effects of Knee Contact Angle on Impact Forces and Accelerations. *Med Sci Sports Exerc*. 2004; 36(5):832-837.

64. Derrick TR, Hamill J, Caldwell GE. Energy Absorption of Impacts During Running at Various Stride Lengths. *Med Sci Sports Exerc*. 1998; 30(1):128-135.

65. Devita P, Janshen L, Rider P, Solnik S, Hortobagyi T. Muscle Work Is Biased toward Energy Generation over Dissipation in Non-Level Running. *J Biomech*. 2008; 41(16):3354-3359.

66. di Prampero PE, Fusi S, Sepulcri L, Morin JB, Belli A, Antonutto G. Sprint Running: A New Energetic Approach. *J Exp Biol*. 2005; 208(Pt 14):2809-2816.

67. Dickinson JA, Cook SD, Leinhardt TM. The Measurement of Shock Waves Following Heel Strike While Running. *J Biomech*. 1985; 18(6):415-422.

68. Divert C, Mornieux G, Freychat P, Baly L, Mayer F, Belli A. Barefoot-Shod Running Differences: Shoe or Mass Effect? *Int J Sports Med*. 2008; 29(6):512-518.

69. Donelan JM, Kram R, Kuo AD. Mechanical and Metabolic Determinants of the Preferred Step Width in Human Walking. *Proc Biol Sci*. 2001; 268(1480):1985-1992.

70. Duchateau J, Semmler JG, Enoka RM. Training Adaptations in the Behavior of Human Motor Units. *J Appl Physiol*. 2006; 101(6):1766-1775.

71. Edwards WB, Derrick TR, Hamill J. Musculoskeletal Attenuation of Impact Shock in Response to Knee Angle Manipultion. *J App Biomech*. In Press.

72. Edwards WB, Gillette JC, Thomas JM, Derrick TR. Internal Femoral Forces and Moments During Running: Implications for Stress Fracture Development. *Clin Biomech (Bristol, Avon)*. 2008; 23(10):1269-1278.

73. Epstein M and Herzog W. Theoretical Models of Skeletal Muscle: Biological and Mathematical Considerations. John Wiley & Sons, 1998.

74. Erdemir A, McLean S, Herzog W, van den Bogert AJ. Model-Based Estimation of Muscle Forces Exerted During Movements. *Clin Biomech (Bristol, Avon)*. 2007; 22(2):131-154.

75. Ettema GJ. Muscle Efficiency: The Controversial Role of Elasticity and Mechanical Energy Conversion in Stretch-Shortening Cycles. *Eur J Appl Physiol*. 2001; 85(5):457-465.

76. Ettema GJC and Huijing PA. Properties of Tendinous Structures and Series Elastic Componets of Edl Muscle Tendon Complex of the Rat. *J Biomech*. 1989; 22:1209-1215.

77. Farris DJ, Trewartha G, McGuigan MP. Could Intra-Tendinous Hyperthermia During Running Explain Chronic Injury of the Human Achilles Tendon? *J Biomech*. 2011; 44(5):822-826.

78. Fath F, Blazevich AJ, Waugh CM, Miller SC, Korff T. Direct Comparison of in Vivo Achilles Tendon Moment Arms Obtained from Ultrasound and Mr Scans. *J Appl Physiol*. 2010; 109(6):1644-1652.

79. Fenn WO. The Relation between the Work Performed and the Energy Liberated in Muscular Contraction. *J Physiol*. 1924; 58(6):373-395.

80. Fourchet F, Kelly L, Horobeanu C, Loepelt H, Taiar R, Millet GP. Comparison of Plantar Pressure Distribution in Adolescent Runners at Low Vs. High Running Velocity. *Gait Posture*. 2011.

81. Frederick EC. Extrinsic Biomechanical Aids In: *Ergogenic Aids in Sport*. Williams M (Ed.). Human Kinetics, Champaign, IL, 1983. 323-339.

82. Frederick EC, Clarke TE, Hamill CL. The Effect of Running Shoe Design on Shock Attenuation. In: *Sports Shoes and Playing Surfaces*. Frederick EC (Ed.). Human Kinetics, Champaign, IL, 1984. 190-198.

83. Frederick EC, Clarke TE, Larsen JL, Cooper LB. The Effects of Shoe Cushioning on the Oxygen Demands of Running. In: *Biomechanical Aspects of Sports Shoes and Playing Surfaces*. Nigg Band Kerr B (Eds.). University of Calgary Printing Services, Calgary, 1983. 107-114.

84. Fredericson M, Jennings F, Beaulieu C, Matheson GO. Stress Fractures in Athletes. *Top Magn Reson Imaging*. 2006; 17(5):309-325.

85. Friederich JA and Brand RA. Muscle Fiber Architecture in the Human Lower Limb. *J Biomech*. 1990; 23(1):91-95.

86. Frost HM. Intermediary Organization of the Skeleton. CRC Press, Boca Raton, FL, 1986.

87. Fukashiro S, Komi PV, Jarvinen M, Miyashita M. In Vivo Achilles Tendon Loading During Jumping in Humans. *Eur J Appl Physiol Occup Physiol*. 1995; 71(5):453-458.

88. Fukashiro S, Kurokawa S, Hay D, Nagano A. Comparison of Muscle-Tendon Ineraction of Human M. Gastrocnemius between Ankle- and Drop-Jumping. *International Journal of Sport and Health Science*. 2005; 3:253-263.

89. Fukunaga T, Kawakami Y, Kubo K, Kanehisa H. Muscle and Tendon Interaction During Human Movements. *Exerc Sport Sci Rev*. 2002; 30(3):106-110.

90. Fukunaga T, Kubo K, Kawakami Y, Fukashiro S, Kanehisa H, Maganaris CN. In Vivo Behaviour of Human Muscle Tendon During Walking. *Proc Biol Sci*. 2001; 268(1464):229-233.

91. Gerritsen KG, van den Bogert AJ, Nigg BM. Direct Dynamics Simulation of the Impact Phase in Heel-Toe Running. *J Biomech*. 1995; 28(6):661-668.

92. Giuliani J, Masini B, Alitz C, Owens BD. Barefoot-Simulating Footwear Associated with Metatarsal Stress Injury in 2 Runners. *Orthopedics*. 2011; 34(7):e320-323.

93. Gordon AM, Huxley AF, Julian FJ. The Variation in Isometric Tension with Sarcomere Length in Vertebrate Muscle Fibres. *J Physiol*. 1966; 184(1):170-192.

94. Grieve DW, Pheasant S, Cavanagh PR. Prediction of Gastrocnemius Length from Knee and Ankle Joint Posture. In: *Biomechanics Vi-A*. Asmussen Eand Jorgensen K (Eds.). University Park Press, Baltimore,, 1978. 405-412.

95. Griffin MJ. Handbook of Human Vibration. Academic Press, New York, NY, 1990.

96. Griffin TM, Roberts TJ, Kram R. Metabolic Cost of Generating Muscular Force in Human Walking: Insights from Load-Carrying and Speed Experiments. *J Appl Physiol*. 2003; 95(1):172-183.

97. Grimston SK, Engsberg JR, Kloiber R, Hanley DA. Bone Mass, External Loads, and Stress Fracture in Female Runners. *International Journal of Sport Biomechanics*. 1991; 7(3):293-302.

98. Gutmann AK, Jacobi B, Butcher MT, Bertram JE. Constrained Optimization in Human Running. *J Exp Biol*. 2006; 209(Pt 4):622-632.

99. Hamill J, Bates BT, Knutzen KM, Sawhill JA. Variations in Ground Reaction Force Parameters at Different Running Speeds. *Human Movement Science*. 1983; 2(1-2):47-56.

100. Hamill J, Derrick TR, Holt KG. Shock Attenuation and Stride Frequency During Running. *Human Movement Science*. 1995; 14:45-60.

101. Hamill J, Derrick TR, McClay I. Joint Stiffness During Running with Different Footfall Patterns. XIth Congress of the Canadian Society of Biomechanics. 2000a.

102. Hamill J, Gruber AH, Russell EM, Miller RH, Van Emmerik REA. Does Changing Footfall Pattern Alter Running Performance? Proceedings of the 6th World Congress of Biomechanics. 2010. 238.

103. Hamill J, Haddad JM, McDermott WJ. Issues in Quantifying Variability from a Dynamical Systems Perspective. *J App Biomech*. 2000b; 16(4):407-418.

104. Hanavan EP, Jr. A Mathematical Model of the Human Body. Amrl-Tr-64-102. *AMRL TR*. 1964:1-149.

105. Harrison RN, Lees A, McCullagh PJ, Rowe WB. A Bioengineering Analysis of Human Muscle and Joint Forces in the Lower Limbs During Running. *J Sports Sci*. 1986; 4(3):201-218.

106. Hasegawa H, Yamauchi T, Kraemer WJ. Foot Strike Patterns of Runners at the 15-Km Point During an Elite-Level Half Marathon. *J Strength Cond Res*. 2007; 21(3):888-893.

107. Hatze H. A Three-Dimensional Multivariate Model of Passive Human Joint Torques and Articular Boundaries. *Clin Biomech (Bristol, Avon)*. 1997; 12(2):128-135.

108. Heise GD and Martin PE. Are Variations in Running Economy in Humans Associated with Ground Reaction Force Characteristics? *Eur J Appl Physiol*. 2001; 84(5):438-442.

109. Heise GD, Smith JD, Martin PE. Lower Extremity Mechanical Work During Stance Phase of Running Partially Explains Interindividual Variability of Metabolic Power. *Eur J Appl Physiol*. 2011; 111(8):1777-1785.

110. Hennig EM and Lafortune MA. Relationships between Ground Reaction Force and Tibial Bone Acceleration Parameters. *Int J Sports Biomech*. 1991; 7:303-309.

111. Hill AV. The Heat of Shortening and the Dynamic Constants of Muscle. *Proc Royal Soc*. 1938; 126B:136-195.

112. Hof AL, Geelen BA, Van den Berg J. Calf Muscle Moment, Work and Efficiency in Level Walking; Role of Series Elasticity. *J Biomech*. 1983; 16(7):523-537.

113. Hof AL, Van Zandwijk JP, Bobbert MF. Mechanics of Human Triceps Surae Muscle in Walking, Running and Jumping. *Acta Physiol Scand*. 2002; 174(1):17-30.

114. Holt KG, Hamill J, Andres RO. Predicting the Minimal Energy Costs of Human Walking. *Med Sci Sports Exerc*. 1991; 23(4):491-498.

115. Hreljac A. Impact and Overuse Injuries in Runners. *Med Sci Sports Exerc*. 2004; 36(5):845-849.

116. Hreljac A, Marshall RN, Hume PA. Evaluation of Lower Extremity Overuse Injury Potential in Runners. *Med Sci Sports Exerc*. 2000; 32(9):1635-1641.

117. Huxley AF. Muscular Contraction. *J Physiol*. 1974; 243(1):1-43.

118. Ishikawa M, Komi PV, Grey MJ, Lepola V, Bruggemann GP. Muscle-Tendon Interaction and Elastic Energy Usage in Human Walking. *J Appl Physiol*. 2005; 99(2):603-608.

119. Ishikawa M, Pakaslahti J, Komi PV. Medial Gastrocnemius Muscle Behavior During Human Running and Walking. *Gait Posture*. 2007; 25(3):380-384.

120. James SL, Bates BT, Osternig LR. Injuries to Runners. *Am J Sports Med*. 1978; 6(2):40-50.

121. Joyce GC and Rack PM. Isotonic Lengthening and Shortening Movements of Cat Soleus Muscle. *J Physiol*. 1969; 204(2):475-491.

122. Ker RF, Bennett MB, Bibby SR, Kester RC, Alexander RM. The Spring in the Arch of the Human Foot. *Nature*. 1987; 325(7000):147-149.

123. Ker RF, Wang XT, Pike AV. Fatigue Quality of Mammalian Tendons. *J Exp Biol*. 2000; 203(Pt 8):1317-1327.

124. Kerr BA, Beauchamp L, Fisher V, Neil R. Footstrike Patterns in Distance Running. In: *Biomechanical Aspects of Sport Shoes and Playing Surfaces*. Nigg BMand Kerr B (Eds.). University of Calgary Press, Calgary, 1983.

125. Kinsler LE and Frey AR. In: *Fundamentals of Acoustics*. John Wiley & Sons, Inc., New York, NY, 1950. Chapters 1-3.

126. Klein Horsman MD, Koopman HF, van der Helm FC, Prose LP, Veeger HE. Morphological Muscle and Joint Parameters for Musculoskeletal Modelling of the Lower Extremity. *Clin Biomech (Bristol, Avon)*. 2007; 22(2):239-247.

127. Kram R. Muscular Force or Work: What Determines the Metabolic Energy Cost of Running? *Exerc Sport Sci Rev*. 2000; 28(3):138-143.

128. Kram R and Taylor CR. Energetics of Running: A New Perspective. *Nature*. 1990; 346(6281):265-267.

129. Kurokawa S, Fukunaga T, Fukashiro S. Behavior of Fascicles and Tendinous Structures of Human Gastrocnemius During Vertical Jumping. *J Appl Physiol*. 2001; 90(4):1349-1358.

130. Lafortune MA. Three-Dimensional Acceleration of the Tibia During Walking and Running. *J Biomech*. 1991; 24(10):877-886.

131. Lafortune MA, Hennig EM, Lake MJ. Dominant Role of Interface over Knee Angle for Cushioning Impact Loading and Regulating Initial Leg Stiffness. *J Biomech*. 1996a; 29(12):1523-1529.

132. Lafortune MA, Lake MJ, Hennig E. Transfer Function between Tibial Acceleration and Ground Reaction Force. *J Biomech*. 1995; 28(1):113-117.

133. Lafortune MA, Lake MJ, Hennig EM. Differential Shock Transmission Response of the Human Body to Impact Severity and Lower Limb Posture. *J Biomech*. 1996; 29(12):1531-1537.

134. Larson P, Higgins E, Kaminski J, Decker T, Preble J, Lyons D, McIntyre K, Normile A. Foot Strike Patterns of Recreational and Sub-Elite Runners in a Long-Distance Road Race. *J Sports Sci*. 2011; 29(15):1665-1673.

135. Laughton CA, Davis IS, Hamill J. Effect of Strike Pattern and Orthotic Intervention on Tibial Shock During Running. *J App Biomech*. 2003; 19:153-168.

136. Leadbetter WB. Cell-Matrix Response in Tendon Injury. *Clin Sports Med*. 1992; 11(3):533-578.

137. Lichtwark GA and Wilson AM. A Modified Hill Muscle Model That Predicts Muscle Power Output and Effeciency During Sinusoidal Length Changes. *J Exp Biol*. 2005a; 208(Pt 15):2831-2843.

138. Lichtwark GA and Wilson AM. Effects of Series Elasticity and Activation Conditions on Muscle Power Output and Effeciency. *J Exp Biol*. 2005b; 208(Pt 15):2845-2853.

139. Lichtwark GA and Wilson AM. Muscle Fascicle and Series Elastic Element Length Changes Along the Length of the Human Gastrocnemius During Walking and Running. *J Biomech*. 2005d,2007; 40:157-164.

140. Lichtwark GA and Wilson AM. Interactions between the Human Gastrocnemius Muscle and the Achilles Tendon During Incline, Level and Decline Locomotion. *J Exp Biol*. 2006; 209(Pt 21):4379-4388.

141. Lichtwark GA and Wilson AM. Muscle Fascicle and Series Elastic Element Length Changes Along the Length of the Human Gastrocnemius During Walking and Running. *J Biomech*. 2007a; 40(1):157-164.

142. Lichtwark GA and Wilson AM. Is Achilles Tendon Compliance Optimised for Maximum Muscle Efficiency During Locomotion? *J Biomech*. 2007b; 40(8):1768-1775.

143. Lichtwark GA and Wilson AM. Optimal Muscle Fascicle Length and Tendon Stiffness for Maximising Gastrocnemius Efficiency During Human Walking and Running. *J Theor Biol*. 2008; 252(4):662-673.

144. Lieberman DE, Venkadesan M, Werbel WA, Daoud AI, D'Andrea S, Davis IS, Mang'eni RO, Pitsiladis Y. Foot Strike Patterns and Collision Forces in Habitually Barefoot Versus Shod Runners. *Nature*. 2010; 463(7280):531-535.

145. Light LH, McLellan GE, Klenerman L. Skeletal Transients on Heel Strike in Normal Walking with Different Footwear. *J Biomech*. 1980; 13(6):477-480.

146. Luethi SM, Denoth J, Kaelin X, Stacoff A. The Influence of Shoe and Foot Movement and Shock Attenuation in Running. In: *Biomechanics X-B*. Jonsson B (Ed.). Human Kinetics, Champaign, IL:, 1987. 921-935.

147. Lundberg A, Svensson OK, Nemeth G, Selvik G. The Axis of Rotation of the Ankle Joint. *J Bone Joint Surg Br*. 1989; 71(1):94-99.

148. Ma SP and Zahalak GI. A Distribution-Moment Model of Energetics in Skeletal Muscle. *J Biomech*. 1991; 24(1):21-35.

149. MacLean CL, Davis IS, Hamill J. Short- and Long-Term Influences of a Custom Foot Orthotic Intervention on Lower Extremity Dynamics. *Clin J Sport Med*. 2008; 18(4):338-343.

150. MacLellan GE and Vyvyan B. Management of Pain beneath the Heel and Achilles Tendonitis with Visco-Elastic Heel Inserts. *Br J Sports Med*. 1981; 15(2):117-121.

151. Maganaris CN, Baltzopoulos V, Sargeant AJ. Changes in Achilles Tendon Moment Arm from Rest to Maximum Isometric Plantarflexion: In Vivo Observations in Man. *J Physiol*. 1998; 510 (Pt 3):977-985.

152. Maganaris CN, Baltzopoulos V, Sargeant AJ. In Vivo Measurement-Based Estimations of the Human Achilles Tendon Moment Arm. *Eur J Appl Physiol*. 2000; 83(4 -5):363-369.

153. Magnusson SP, Aagaard P, Dyhre-Poulsen P, Kjaer M. Load-Displacement Properties of the Human Triceps Surae Aponeurosis in Vivo. *J Physiol*. 2001; 531(Pt 1):277-288.

154. Magnusson SP and Kjaer M. Region-Specific Differences in Achilles Tendon Cross-Sectional Area in Runners and Non-Runners. *Eur J Appl Physiol*. 2003; 90(5-6):549-553.

155. Maiwald C, Grau S, Krauss I, Mauch M, Axmann D, Horstmann T. Reproducibility of Plantar Pressure Distribution Data in Barefoot Running. *J Appl Biomech*. 2008; 24(1):14-23.

156. Marti B, Vader JP, Minder CE, Abelin T. On the Epidemiology of Running Injuries. The 1984 Bern Grand-Prix Study. *Am J Sports Med*. 1988; 16(3):285-294.

157. Martin DE and Cole PN. Better Training for Distance Runners. Human Kinetics, Champaign, IL, 1991.

158. Martin PE and Morgan DW. Biomechanical Considerations for Economical Walking and Running. *Med Sci Sports Exerc*. 1992; 24(4):467-474.

159. Martin RB and Burr DB. Structure, Function and Adaptation of Compact Bone. Raven Press, New York, NY, 1989.

160. Mason B. Unpublished doctoral dissertation, University of Oregon, Eugene, Oregon, 1980.

161. McArdle WD, Katch FI, Katch VL. Exercise Physiology. Lippincott, Williams & Wilkins, Philadelphia, PA, 2001.

162. McClay I and Manal K. Lower Extremity Kinematic Comparisons between Forefoot and Rearfoot Strikers. 19th Annual Meeting of the American Society of Biomechanics. 1995a. 211-212.

163. McClay I and Manal K. Lower Extremity Kinetic Comparisons between Forefoot and Rearfoot Strikers. 19th Annual Meeting of the American Society of Biomechanics. 1995b. 213-214.

164. McClay I and Manal K. Three-Dimensional Kinetic Analysis of Running: Significance of Secondary Planes of Motion. *Med Sci Sports Exerc*. 1999; 31(11):1692-1737.

165. McCrory JL, Martin DF, Lowery RB, Cannon DW, Curl WW, Read HM, Jr., Hunter DM, Craven T, Messier SP. Etiologic Factors Associated with Achilles Tendinitis in Runners. *Med Sci Sports Exerc*. 1999; 31(10):1374-1381.

166. McLeod KJ and Rubin CT. Frequency Specific Modulation of Bone Adaptation by Induced Electric Fields. *J Theor Biol*. 1990; 145(3):385-396.

167. McLeod KJ, Rubin CT, Otter MW, Qin YX. Skeletal Cell Stresses and Bone Adaptation. *The American Journal of the Medical Sciences*. 1998; 316(3):176-183.

168. McMahon TA and Green PR. The Influence of Track Compliance of Running. In: *Sports Shoes and Playing Surfaces*. Frederick EC (Ed.). Human Kinetics, Champaign, IL, 1984. 138-162.

169. McMahon TA, Valiant G, Frederick EC. Groucho Running. *J Appl Physiol*. 1987; 62(6):2326-2337.

170. McNeill Alexander R. Energetics and Optimization of Human Walking and Running: The 2000 Raymond Pearl Memorial Lecture. *Am J Hum Biol*. 2002; 14(5):641-648.

171. Mercer JA, Devita P, Derrick TR, Bates BT. Individual Effects of Stride Length and Frequency on Shock Attenuation During Running. *Med Sci Sports Exerc*. 2003; 35(2):307-313.

172. Mercer JA, Vance J, Hreljac A, Hamill J. Relationship between Shock Attenuation and Stride Length During Running at Different Velocities. *Eur J Appl Physiol*. 2002; 87(4-5):403-408.

173. Messier SP, Davis SE, Curl WW, Lowery RB, Pack RJ. Etiologic Factors Associated with Patellofemoral Pain in Runners. *Med Sci Sports Exerc*. 1991; 23(9):1008-1015.

174. Milgrom C, Finestone A, Levi Y, Simkin A, Ekenman I, Mendelson S, Millgram M, Nyska M, Benjuya N, Burr D. Do High Impact Exercises Produce Higher Tibial Strains Than Running? *Br J Sports Med*. 2000; 34(3):195-199.

175. Milgrom C, Finestone A, Sharkey N, Hamel A, Mandes V, Burr D, Arndt A, Ekenman I. Metatarsal Strains Are Sufficient to Cause Fatigue Fracture During Cyclic Overloading. *Foot Ankle Int*. 2002; 23(3):230-235.

176. Miller RH and Hamill J. Footfall Pattern Selection for the Performance of Various Running Tasks. *J App Biomech*. 2012; In Review XX(X):XX-XX.

177. Milner CE, Ferber R, Pollard CD, Hamill J, Davis IS. Biomechanical Factors Associated with Tibial Stress Fracture in Female Runners. *Med Sci Sports Exerc*. 2006; 38(2):323-328.

178. Milner CE, Hamill J, Davis I. Are Knee Mechanics During Early Stance Related to Tibial Stress Fracture in Runners? *Clin Biomech (Bristol, Avon)*. 2007; 22(6):697-703.

179. Minetti AE and Alexander RM. A Theory of Metabolic Costs for Bipedal Gaits. *J Theor Biol*. 1997; 186(4):467-476.

180. Minetti AE, Moia C, Roi GS, Susta D, Ferretti G. Energy Cost of Walking and Running at Extreme Uphill and Downhill Slopes. *J Appl Physiol*. 2002; 93(3):1039-1046.

181. Morgan DW, Craib MW, Krahenbuhl GS, Woodall K, Jordan S, Filarski K, Burleson C, Williams T. Daily Variability in Running Economy among Well-Trained Male and Female Distance Runners. *Res Q Exerc Sport*. 1994a; 65(1):72-77.

182. Morgan DW, Martin P, Craib M, Caruso C, Clifton R, Hopewell R. Effect of Step Length Optimization on the Aerobic Demand of Running. *J Appl Physiol*. 1994b; 77(1):245-251.

183. Morgan DW, Martin PE, Krahenbuhl GS. Factors Affecting Running Economy. *Sports Med*. 1989; 7(5):310-330.

184. Munro CF, Miller DI, Fuglevand AJ. Ground Reaction Forces in Running: A Reexamination. *J Biomech*. 1987; 20(2):147-155.

185. Nevill AM, Ramsbottom R, Williams C. Scaling Physiological Measurements for Individuals of Different Body Size. *Eur J Appl Physiol Occup Physiol*. 1992; 65(2):110-117.

186. Nigg BM. External Force Measurements with Sport Shoes and Playing Surfaces. In: *Biomechanical Aspects of Sport Shoes and Playing Surfaces*. Nigg BMand Kerr B (Eds.). Univeristy of Calgary Press, Calgary, 1983. 11-23.

187. Nigg BM. Biomechanical Aspects of Running. In: *Biomechanics of Running Shoes*. Nigg BM (Ed.). Human Kinetics, Champaign, IL, 1986. 15-19.

188. Nigg BM. Impact Forces in Running. *Current Opinion in Orthopedics*. 1997; 8(6):43-47.

189. Nigg BM. The Role of Impact Forces and Foot Pronation: A New Paradigm. *Clin J Sport Med*. 2001; 11(1):2-9.

190. Nigg BM. Impact Forces. In: *Biomechanics of Sport Shoes*. Nigg BM (Ed.). Univeristy of Calgary Press, Calgary, 2011. 1-35.

191. Nigg BM, Bahlsen HA, Luethi SM, Stokes S. The Influence of Running Velocity and Midsole Hardness on External Impact Forces in Heel-Toe Running. *J Biomech*. 1987; 20(10):951-959.

192. Nigg BM, Cole GK, Bruggemann GP. Impact Forces During Heel Toe Running. *J Appl Biomech*. 1995; 11:407-432.

193. Nigg BM, Denoth J, Kerr B, Luethi S, Smith D, Stacoff A. Load Sport Shoes and Playing Surfaces. In: *Sports Shoes and Playing Surfaces*. Frederick EC (Ed.). Human Kinetics, Champaign, IL, 1984. 1-23.

194. Nigg BM, Denoth J, Neukomm PA. Quantifying the Load on the Human Body: Problems and Some Possible Solutions. In: *Biomechanics Vii*. Morecki A et al. (Eds.). University Park Press, Baltimore, MD, 1981. 88-89.

195. Nigg BM and Wakeling JM. Impact Forces and Muscle Tuning: A New Paradigm. *Exerc Sport Sci Rev*. 2001; 29(1):37-41.

196. Nilsson J and Thorstensson A. Ground Reaction Forces at Different Speeds of Human Walking and Running. *Acta Physiol Scand*. 1989; 136(2):217-227.

197. Novacheck TF. The Biomechanics of Running. *Gait Posture*. 1998; 7(1):77-95.

198. O'Connor JA, Lanyon LE, MacFie H. The Influence of Strain Rate on Adaptive Bone Remodelling. *J Biomech*. 1982; 15(10):767-781.

199. Oakley T and Pratt DJ. Skeletal Transients During Heel and Toe Strike Running and the Effectiveness of Some Materials in Their Attenuation. *Clin Biomech (Bristol, Avon)*. 1988; 3(3):159-165.

200. Out L, Vrijkotte TG, van Soest AJ, Bobbert MF. Influence of the Parameters of a Human Triceps Surae Muscle Model on the Isometric Torque-Angle Relationship. *J Biomech Eng*. 1996; 118(1):17-25.

201. Paul IL, Munro MB, Abernethy PJ, Simon SR, Radin EL, Rose RM. Musculo-Skeletal Shock Absorption: Relative Contribution of Bone and Soft Tissues at Various Frequencies. *J Biomech*. 1978; 11(5):237-239.

202. Payne AH. Foot to Ground Contact Forces of Elite Runners. In: *Biomechanics Viii-B*. Matsui Hand Kobayashi K (Eds.). Human Kinetics, Champaign, IL, 1983. 748-753.

203. Pereira MA and Freedson PS. Intraindividual Variation of Running Economy in Highly Trained and Moderately Trained Males. *Int J Sports Med*. 1997; 18(2):118-124.

204. Perl DP, Daoud AI, Lieberman DE. Effects of Footwear and Strike Type on Running Economy. *Med Sci Sports Exerc*. 2012; 44(7):1335-1343.

205. Pohl MB, Mullineaux DR, Milner CE, Hamill J, Davis IS. Biomechanical Predictors of Retrospective Tibial Stress Fractures in Runners. *J Biomech*. 2008; 41(6):1160-1165.

206. Potthast W, Bruggemann GP, Lundberg A, Arndt A. The Influences of Impact Interface, Muscle Activity, and Knee Angle on Impact Forces and Tibial and Femoral Accelerations Occurring after External Impacts. *J Appl Biomech*. 2010; 26(1):1-9.

207. Pozzo T, Berthoz A, Lefort L, Vitte E. Head Stabilization During Various Locomotor Tasks in Humans. Ii. Patients with Bilateral Peripheral Vestibular Deficits. *Exp Brain Res*. 1991; 85(1):208-217.

208. Pratt DJ. Mechanisms of Shock Attenuation Via the Lower Extremity During Running. *Clin Biomech (Bristol, Avon)*. 1989; 4(1):51-57.

209. Qin YX, Rubin CT, McLeod KJ. Nonlinear Dependence of Loading Intensity and Cycle Number in the Maintenance of Bone Mass and Morphology. *J Orthop Res*. 1998; 16(4):482-489.

210. Queen RM, Gross MT, Liu HY. Repeatability of Lower Extremity Kinetics and Kinematics for Standardized and Self-Selected Running Speeds. *Gait Posture*. 2006; 23(3):282-287.

211. Radin EL. The Physiology and Degeneration of Joints. *Semin Arthritis Rheum*. 1972; 2(3):245-257.

212. Radin EL, Parker HG, Pugh JW, Steinberg RS, Paul IL, Rose RM. Response of Joints to Impact Loading. 3. Relationship between Trabecular Microfractures and Cartilage Degeneration. *J Biomech*. 1973; 6(1):51-57.

213. Radin EL and Paul IL. Does Cartilage Compliance Reduce Skeletal Impact Loads? The Relative Force-Attenuating Properties of Articular Cartilage, Synovial Fluid, Periarticular Soft Tissues and Bone. *Arthritis Rheum*. 1970; 13(2):139-144.

214. Rall JA. Energetic Aspects of Skeletal Muscle Contraction: Implications of Fiber Types. *Exerc Sport Sci Rev*. 1985; 13:33-74.

215. Riener R and Edrich T. Identification of Passive Elastic Joint Moments in the Lower Extremities. *J Biomech*. 1999; 32(5):539-544.

216. Roberts TJ. The Integrated Function of Muscles and Tendons During Locomotion. *Comp Biochem Physiol A Mol Integr Physiol*. 2002; 133(4):1087-1099.

217. Roberts TJ, Kram R, Weyand PG, Taylor CR. Energetics of Bipedal Running. I. Metabolic Cost of Generating Force. *J Exp Biol*. 1998; 201(Pt 19):2745-2751.

218. Roberts TJ, Marsh RL, Weyand PG, Taylor CR. Muscular Force in Running Turkeys: The Economy of Minimizing Work. *Science*. 1997; 275(5303):1113-1115.

219. Romanov N. Pose Method of Running. Pose Tech Corporation, Coral Gables, FL, 2002.

220. Rosager S, Aagaard P, Dyhre-Poulsen P, Neergaard K, Kjaer M, Magnusson SP. Load-Displacement Properties of the Human Triceps Surae Aponeurosis and Tendon in Runners and Non-Runners. *Scand J Med Sci Sports*. 2002; 12(2):90-98.

221. Rubin C, Turner AS, Bain S, Mallinckrodt C, McLeod K. Anabolism. Low Mechanical Signals Strengthen Long Bones. *Nature*. 2001; 412(6847):603-604.

222. Sasaki K, Neptune RR, Kautz SA. The Relationships between Muscle, External, Internal and Joint Mechanical Work During Normal Walking. *J Exp Biol*. 2009; 212(Pt 5):738-744.

223. Saunders PU, Pyne DB, Telford RD, Hawley JA. Factors Affecting Running Economy in Trained Distance Runners. *Sports Med*. 2004a; 34(7):465-485.

224. Saunders PU, Pyne DB, Telford RD, Hawley JA. Reliability and Variability of Running Economy in Elite Distance Runners. *Med Sci Sports Exerc*. 2004b; 36(11):1972-1976.

225. Scholz MN, Bobbert MF, van Soest AJ, Clark JR, van Heerden J. Running Biomechanics: Shorter Heels, Better Economy. *J Exp Biol*. 2008; 211(Pt 20):3266-3271.

226. Scott SH and Winter DA. Internal Forces of Chronic Running Injury Sites. *Med Sci Sports Exerc*. 1990; 22(3):357-369.

227. Sellers WI, Dennis LA, Crompton RH. Predicting the Metabolic Energy Costs of Bipedalism Using Evolutionary Robotics. *J Exp Biol*. 2003; 206(Pt 7):1127-1136.

228. Shorten M and Mientjes M. The Effects of Shoe Cushioning on Impact Force During Running. 6th symposium on footwear biomechanics. 2003.

229. Shorten MR and Winslow DS. Spectral Analysis of Impact Shock During Running. *Int J Sports Biomech*. 1992; 8:288-304.

230. Shorter F. Running for Peak Performance. Dorling Kindersley Publishing, New York, NY, 2005.

231. Sih BL and Stuhmiller JH. The Metabolic Cost of Force Generation. *Med Sci Sports Exerc*. 2003; 35(4):623-629.

232. Simon SR, Paul IL, Mansour J, Munro M, Abernethy PJ, Radin EL. Peak Dynamic Force in Human Gait. *J Biomech*. 1981; 14(12):817-822.

233. Simon SR, Radin EL, Paul IL, Rose RM. The Response of Joints to Impact Loading. Ii. In Vivo Behavior of Subchondral Bone. *J Biomech*. 1972; 5(3):267-272.

234. Slavin M and Hamill J. Alterations in Footstrike Pattern in Distance Running. The Xth Symposium of the International Society of Biomechanics In Sports. 1992. 53-57.

235. Slavin MM. The Effects of Foot Strike Pattern Alteration on Efficiency in Skilled Runners. M.S. thesis, University of Massachusetts, Amherst, MA, 1992.

236. Sparrow W and Newell K. Metabolic Energy Expenditure and the Regulation of Movement Economy. *Psychonomic Bulletin & Review*. 1998; 5(2):173-196.

237. Squadrone R and Gallozzi C. Biomechanical and Physiological Comparison of Barefoot and Two Shod Conditions in Experienced Barefoot Runners. *J Sports Med Phys Fitness*. 2009; 49(1):6-13.

238. Stackhouse CL, Davis IM, Hamill J. Orthotic Intervention in Forefoot and Rearfoot Strike Running Patterns. *Clin Biomech (Bristol, Avon)*. 2004; 19(1):64-70.

239. Stefanyshyn DJ and Nigg BM. Dynamic Angular Stiffness of the Ankle Joint During Running and Sprinting. *J App Biomech*. 1998; 14(3):292-299.

240. Stephens BR, Cole AS, Mahon AD. The Influence of Biological Maturation on Fat and Carbohydrate Metabolism During Exercise in Males. *Int J Sport Nutr Exerc Metab*. 2006; 16(2):166-179.

241. Stone J, Brannon T, Haddad F, Qin A, Baldwin KM. Adaptive Responses of Hypertrophying Skeletal Muscle to Endurance Training. *J Appl Physiol*. 1996; 81(2):665-672.

242. Umberger BR, Gerritsen KG, Martin PE. A Model of Human Muscle Energy Expenditure. *Comput Methods Biomech Biomed Engin*. 2003; 6(2):99-111.

243. Umberger BR, Gerritsen KG, Martin PE. Muscle Fiber Type Effects on Energetically Optimal Cadences in Cycling. *J Biomech*. 2006; 39(8):1472-1479.

244. Umberger BR and Rubenson J. Understanding Muscle Energetics in Locomotion: New Modeling and Experimental Approaches. *Exerc Sport Sci Rev*. 2011; 39(2):59-67.

245. Valiant GA, McMahon TA, Frederick EC. A New Test to Evaluate the Cushioning Properties of Athletic Shoes. In: *Biomechanics X-B*. Jonsson BE (Ed.). Human Kinetics, Champaign, IL, 1987. 937-941.

246. van den Bogert AJ, Gerritsen KG, Cole GK. Human Muscle Modelling from a User's Perspective. *J Electromyogr Kinesiol*. 1998; 8(2):119-124.

247. van Soest AJ and Bobbert MF. The Contribution of Muscle Properties in the Control of Explosive Movements. *Biol Cybern*. 1993; 69(3):195-204.

248. Voloshin A and Wosk J. An in Vivo Study of Low Back Pain and Shock Absorption in the Human Locomotor System. *J Biomech*. 1982; 15(1):21-27.

249. Voloshin A, Wosk J, Brull M. Force Wave Transmission through the Human Locomotor System. *J Biomech Eng*. 1981; 103(1):48-50.

250. Voloshin AS, Burger CP, Wosk J, Arcan M. An in Vivo Evaluation of the Leg's Shock Absorbing Capacity. In: *Biomechanics Ix-B* Winter D et al. (Eds.). Human Kinetics, Champaign, IL:, 1985. 112-116.

251. Wakeling JM, Von Tscharner V, Nigg BM, Stergiou P. Muscle Activity in the Leg Is Tuned in Response to Ground Reaction Forces. *J Appl Physiol*. 2001b; 91(3):1307-1317.

252. Ward SR, Eng CM, Smallwood LH, Lieber RL. Are Current Measurements of Lower Extremity Muscle Architecture Accurate? *Clin Orthop Relat Res*. 2009; 467(4):1074-1082.

253. Weir JB. New Methods for Calculating Metabolic Rate with Special Reference to Protein Metabolism. *J Physiol*. 1949; 109(1-2):1-9.

254. Wickiewicz TL, Roy RR, Powell PL, Edgerton VR. Muscle Architecture of the Human Lower Limb. *Clin Orthop Relat Res*. 1983; (179):275-283.

255. Wickler SJ, Hoyt DF, Cogger EA, Hirschbein MH. Preferred Speed and Cost of Transport: The Effect of Incline. *J Exp Biol*. 2000; 203(Pt 14):2195-2200.

256. Wilkie DR. The Relation between Force and Velocity in Human Muscle. *J Physiol*. 1950; 110:249-280.

257. Williams DS, McClay IS, Manal KT. Lower Extremity Mechanics in Runners with a Converted Forefoot Strike Pattern. *J App Biomech*. 2000; 16(2):210-218.

258. Williams KR. Relationship between Distance Running Biomechanics and Running Economy. In: *Biomechanics of Distance Running*. Cavanagh PR (Ed.). Human Kinetics, Champaign, IL, 1990. 271-306.

259. Williams KR and Cavanagh PR. Relationship between Distance Running Mechanics, Running Economy, and Performance. *J Appl Physiol*. 1987; 63(3):1236-1245.

260. Winter DA. Moments of Force and Mechanical Power in Jogging. *Journal of Biomechanics*. 1983; 16(1):91-97.

261. Winter DA. Frequency Domain Analysis. In: *Singal Processing and Linear Systems for the Movement Sciences*. Winter DAand Patla AE (Eds.). Graphic Services, University of Waterloo, Waterloo, Ont., 1997. 51-76.

262. Winter DA, Sidwall HG, Hobson DA. Measurement and Reduction of Noise in Kinematics of Locomotion. *Journal of Biomechanics*. 1974; 7(2):157-159.

263. Winters JM and Stark L. Estimated Mechanical Properties of Synergistic Muscles Involved in Movements of a Variety of Human Joints. *J Biomech*. 1988; 21(12):1027-1041.

264. Wosk J and Voloshin A. Wave Attenuation in Skeletons of Young Healthy Persons. *J Biomech*. 1981; 14(4):261-267.

265. Wright IC, Neptune RR, van Den Bogert AJ, Nigg BM. Passive Regulation of Impact Forces in Heel-Toe Running. *Clin Biomech (Bristol, Avon)*. 1998; 13(7):521-531.

266. Yessis M. Explosive Running. McGraw-Hill, Columbus, OH, 2000.

267. Zajac FE. Muscle and Tendon: Properties, Models, Scaling, and Application to Biomechanics and Motor Control. *Crit Rev Biomed Eng*. 1989; 17(4):359-411.

268. Zifchock RA, Davis IS, Hamill J. Kinetic Asymmetry in Female Runners with and without Retrospective Tibial Stress Fractures. *J Biomech*. 2006; 39(15):2792-2797.